UNIVERSITY OF SOUTHAMPTON

FACULTY OF ENGINEERING, SCIENCE AND MATHEMATICS

SCHOOL OF CHEMISTRY

AN INVESTIGATION INTO THE MOLECULAR RECOGNITION, STRUCTURAL AND EXTRACTION PROPERTIES OF HYDROGEN BONDING ANION RECEPTORS.

By

Gareth William Bates

Thesis for the degree of Doctor of Philosophy

February 2008

UNIVERSITY OF SOUTHAMPTON

ABSTRACT

FACULTY OF ENGINEERING, SCIENCE AND MATHEMATICS
SCHOOL OF CHEMISTRY

Doctor of Philosophy

AN INVESTIGATION INTO THE MOLECULAR RECOGNITION, STRUCTURAL AND EXTRACTION PROPERTIES OF HYDROGEN BONDING ANION RECEPTORS.

By Gareth William Bates

This thesis reports the synthesis and study of the molecular recognition properties of a variety of synthetic organic receptors. An investigation into the ion-pair recognition properties of calix[4]pyrrole derivatives has been carried out with a number of organic salts. Crystallographic studies revealed that the anion induced cavity of the calix[4]pyrrole derivatives were able to accommodate cationic species within it. Proton NMR titrations were performed with *meso*-octacalix[4]pyrrole and a variety of organic chloride and bromide salts in dichloromethane-d_2. The results show that the chloride and bromide stability constants increase with a change of cation (tetrabutylammonium < imidazolium < pyridinium). This effect was not observed in DMSO-d_6/0.5% water solution.

Two cleft-like bis-indole anion receptors have been synthesised and their anion binding studies showed a high selectivity for fluoride in DMSO-water solutions. X-ray crystallography showed that the receptors cavity is able to encapsulate the fluoride anion whereas the larger chloride anion is too large and perches above the plane of the cavity. A series of 2,7-functionalized indoles have been synthesized with appended amide and/or urea or thiourea groups. Anion complexation studies show a marked difference in the mode of interaction of carboxylates with indole-ureas vs indole-amides.

A number of simple receptors have been synthesised and investigated as potential sulfuric acid extraction ligands for the hydrometallurgical extraction of nickel(II) sulfate by a dual-host system. Liquid-liquid solvent extraction experiments showed that the dual-host systems containing an isophthalamide based ligand extracted ~90% of nickel(II) sulfate at pH 4.9 which corresponds well to pH values likely in nickel extraction circuits.

DECLARATION OF AUTHORSHIP

I, Gareth William Bates declare that the thesis entitled

An investigation into the molecular recognition, structural and extraction properties of hydrogen bonding anion receptors.

and the work presented in the thesis are both my own, and have been generated by me as the result of my own original research. I confirm that:

- this work was done wholly or mainly while in candidature for a research degree at this University;
- where any part of this thesis has previously been submitted for a degree or any other qualification at this University or any other institution, this has been clearly stated;
- where I have consulted the published work of others, this is always clearly attributed;
- where I have quoted from the work of others, the source is always given. With the exception of such quotations, this thesis is entirely my own work;
- I have acknowledged all main sources of help;
- where the thesis is based on work done by myself jointly with others, I have made clear exactly what was done by others and what I have contributed myself;
- parts of this work have been published as:

Calix[4]pyrrole: An Old yet New Ion-Pair Receptor. R. Custelcean, L.H. Delmau, B.A. Moyer, J.L. Sessler, W.-S. Cho, D. Gross, G.W. Bates, S,J. Brooks, M.E. Light, P.A. Gale, *Angew. Chem. Int. Ed.* **2005**, 44, 2537 –2542

Calix[4]pyrrole as a Chloride Anion Receptor: Solvent andCountercation Effects. J.L. Sessler, D. Gross, W.-S. Cho, V.M. Lynch, F.P. Schmidtchen, G.W. Bates, M.E. Light, P.A. Gale, *J. Am. Chem. Soc.* **2006**, 128, 12281-12288

Ionic liquid–calix[4]pyrrole complexes: pyridinium inclusion in the calixpyrrole cup. G.W. Bates, M.E. Light, P.A. Gale, *CrystEngComm*, **2006**, 8, 300–302

Organic salt inclusion: the first crystal structures of anion complexes of N-confused calix[4]pyrrole. G.W. Bates, M. Kostermans, W. Dehaen, P.A. Gale, M.E. Light, *CrystEngComm*, **2006**, 8, 444–447

Isophthalamides and 2,6-dicarboxamidopyridines with pendant indole groups: a 'twisted' binding mode for selective fluoride recognition. G.W. Bates, M.E. Light, P.A. Gale, *Chem. Commun.*, **2007**, 2121-2123

2,7-Functionalized Indoles as New Receptors for Anions. Gareth. W. Bates, Triyanti, Mark. E. Light, Markus Albrecht, and Philip. A. Gale, *J. Org. Chem.*, **2007**, 72, 8921-8927

An introduction to anion receptors based on organic frameworks. G. W. Bates, P.A. Gale, *Struct. Bonding.* In press **2007**, DOI 10.1007/430_2007_069

Interactions of organic halide and nitrate salts with meso-octamethylcalix[4]pyrrole. G.W. Bates, M.E. Light, P.A. Gale, *Supramol. Chem.* In press **2007**

Signed: GBatS

Date: 13/02/2008

ABBREVIATIONS

Ar	Aryl
br	Broad resonance (NMR)
bu	Butyl
°C	degrees celcius
calc.	Calculated
CD_2Cl_2	Dichloromethane-d_2
$CDCl_3$	Chloroform-d_1
COSY	Correlation Spectroscopy
d	Doublet (NMR)
DCM	Dichloromethane
DMAP	4-Dimethylaminopyridine
DMF	Dimethylformamide
DMSO	Dimethylsulfoxide
eq	Equivalents
Et	Ethyl
ES	Electrospray
EYPC	Egg Yolk Phosphocholine
^1H	Proton
HRMS	High resolution mass spectrometry
Hz	Hertz
ICP-OES	Inductively Coupled Plasma – Optical Emission Spectrometry
K	Kelvin
m	Multiplet
M	Molarity
Me	Methyl
mol	Mole(s)
m.p.	Melting point

m/z	Mass to charge ratio (mass spectrometry)
NMR	Nuclear Magnetic Resonance
Ph	Phenyl
ppm	Parts per million
q	Quartet (NMR)
R	rectus (enantiomer)
S	sinister (enantiomer)
s	Singlet (NMR)
t	triplet (NMR)
TBA	Tetrabutylammonium
TEA	Tetraethylammonium
TMA	Tetramethylammonium
TPA	Tetrapropylammonium
TMACl	Tetramethylammonium Chloride
TMABr	Tetramethylammonium Bromide
TMAF	Tetramethylammonium Fluoride
UV-vis	Ultra Violet – visible (spectroscopic technique)

CONTENTS

AKNOWLEDGEMENTS

I would like to thank my supervisor Professor Philip A. Gale for all his support, encouragement and guidance over the past three years. I would also like to thank members of the Gale group past (Simon, Louise, Ismael, Roberto and Josep) and present (Mathew, Claudia, Jo, Sergio, Peter and Jen). Additionally I would like to thank the visitors to the Gale group (Marta, Tomas, Somchai and Luis).

I would like to thank Professor Peter Tasker and his group (in particular Vesna, Jy, Christine and Ross) from the University of Edinburgh for their help and expertise. Additionally I would like to thank Dr. Markus Albrecht, Professor Wim Dehaen and their students Triyanti and Maarten for help and contribution to my work.

I would like to thank the University of Southampton, the EPSRC and Crystal Faraday for funding and the NMR, MS and stores at Southampton for all their assistance.

I would like to thank Dr Mark E. Light and the EPSRC crystallographic services for the expertise and time dedicated to solving the x-ray crystal structures outlined in this thesis.

Special thanks go to my family for their constant support and encouragement throughout the past three years. Finally I would like to thank Nicola for everything.

CHAPTER 1 - INTRODUCTION

1.1 SUPRAMOLECULAR CHEMSITRY

Supramolecular chemistry is the study of molecular systems that are reversibly held together *via* intermolecular forces much weaker than a covalent bond. Jean Marie-Lehn has described the field of supramolecular chemistry as "chemistry beyond the molecule"[1] and he also comments, "Beyond molecular chemistry based on the covalent bond there lies the field of supramolecular chemistry, whose goal it is to gain control over the intermolecular bond".[2]

A supermolecule can be considered as an organized system consisting of two or more chemical species and the intermolecular interactions between them. Generally the system is described as the binding of a host (usually the larger component) with a guest (which can be ionic or neutral in nature). The intermolecular forces between the components result in the formation of stable complexes both in solution and in solid state.

There are a number of intermolecular forces that contribute to the host/guest complex stability. These include:

1. Electrostatic interactions (ion-ion, ion-dipole and dipole-dipole), which are the Coulombic attraction between opposite charges (**Figure 1.1**). Bond energies are in the range of 100 - 350 kJ mol^{-1}, 50 - 200 kJ mol^{-1} and 5 - 50 kJ mol^{-1} for ion-ion, ion-dipole and dipole-dipole interactions respectively.

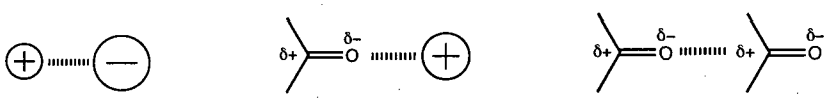

Ion-Ion Ion-Dipole Dipole-Dipole

Figure 1.1: Representations of the different types of electrostatic interactions

2. Hydrogen bonds are a particular type of dipole-dipole interaction in which a hydrogen atom attached to an electronegative atom (or electron withdrawing group) interacts with a neighbouring dipole on an adjacent molecule. These interactions are highly directional with optimum interactions at a bond angle of 180°. These interactions have energies between 4 - 120 kJ mol^{-1}.

3. π-π stacking interactions. These occur between aromatic rings and have energies between 1 - 50 kJ mol^{-1}. There are two general types of π-π stacking interactions: face-to-face and edge-to-face, although a wide range of other geometries have been observed. The edge-to-face interaction is more favourable as the π-cloud of the face is electron rich and the σ-skeleton of the edge is electron deficient. This interaction is driven by electrostatic interactions.

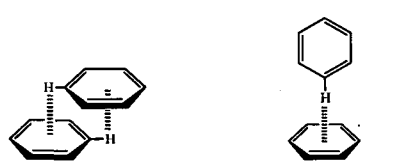

Face-to-face Edge-to-Face

Figure 1.2: π-π stacking interactions

4. Dispersion and induction forces (van der Waals forces) occur from the polarization of an electron cloud by the proximity of an adjacent nucleus. The individual bond energies for these interaction are weak at <5 kJ mol^{-1} but cumulatively they may contribute to a significant interaction.

5. Hydrophobic or solvatophobic effects. These effects are thermodynamically driven and can be split into enthalpic and entropic terms.

1.2 ANION RECOGNITION

The importance of anions throughout the natural world is often overlooked. However anions are involved in important biochemical operations, such as the formation of enzyme-substrate and enzyme-cofactor complexes and interactions between proteins, RNA and DNA. Anions are therefore critical to the maintenance of life.[3]

Compared to the design of receptors for cationic species designing synthetic receptors for anion recognition is challenging as anions have a lower charge to radius ratio compared to isoelectronic cations and as a result binding interactions are less effective. Additionally anions have a wide range of geometries and require a higher degree of receptor design in order for the anion to be selectively recognised by a receptor. For these reasons the development of new anion receptors based on organic frameworks is currently an area attracting considerable research effort and as result of the relative complexity required in design of an anion receptor a wide variety of systems have been published in the last ten years with both macrocyclic and acyclic systems functioning as effective and selective anion receptors.[4-6]

1.3 NEUTRAL SYNTHETIC ANION RECEPTORS

1.3.1 ACYCLIC AMIDE AND SULFONAMIDE BASED RECEPTORS

Secondary amides are versatile and highly accessible hydrogen bond donors that have been used in numerous synthetic receptors. In the biological arena, there are many examples of proteins that employ amide NH···anion interactions to bind negatively charged guests. The first example of a synthetic amide containing receptor, published in 1986 by Pascal and co-workers, was a crytpand-like tris-amide that was shown to interact with fluoride in DMSO-d_6.[7]

In 1993, Reinhoudt and co-workers described the synthesis and binding properties of a series of tris-amides and tris-sulfonamides based upon the tren skeleton.[8] These receptors proved to be selective for phosphate in acetonitrile solution and demonstrated, arguably for the first time, that anion receptor systems need not be difficult to make but rather that simple organic compounds could function as very effective receptors. Stability constants were calculated by conductivity experiments and showed that receptor **1.1f** bound dihydrogenphosphate with the highest affinity (14 200 M^{-1}) in acetonitrile presumably due to the preorganisation of the receptor *via* π-π interactions between the naphthyl groups.

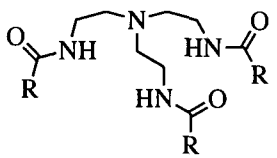

1.1a R = CH_2Cl
1.1b R= $(CH_2)_4CH_3$
1.1c R= C_6H_5
1.1d R= 4-$MeOC_6H_5$

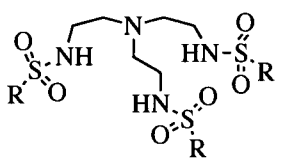

1.1e R = 4-MeC_6H_5
1.1f R= 2-naphthyl

Four years later, in 1997, Crabtree and co-workers reported that simple isophthalamide receptors e.g. **1.2** can bind anions in organic solution.[9] These receptors, even simpler than Reinhoudt's tren-based anion binders, were found to bind smaller halides selectively in dichloromethane solution.

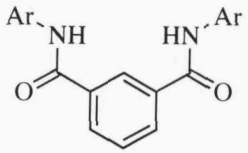

1.2a Ar= Ph
1.2b Ar= *p*-(n-Bu)C_6H_4

The X-ray crystal structure of the bromide complex of **1.2a** shows the receptor adopting the *syn-syn* conformation with the bromide anion coordinated to the amide NH's with N···Br distances of 3.44 and 3.64 Å (**Figure 1.3**). The crystal structure also reveals that the bromide anion is positioned above the plane of the central aryl ring. Solution studies revealed that receptors **1.2a** and **1.2b** have high affinity for halide anions and form complexes with exclusively 1:1 host/guest stoichiometry. Stability constants for **1.2b** were determined by ^{1}H NMR titration studies and found to be 6.1 × 10^4 M^{-1} for chloride, 7.1 × 10^3 M^{-1} for bromide and 4.6 × 10^2 M^{-1} for iodide in dichloromethane-d_2.

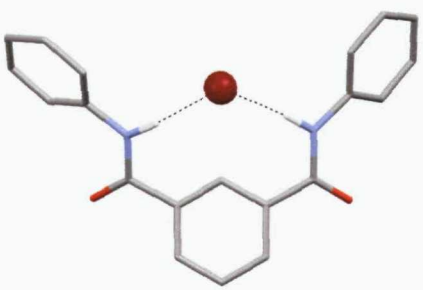

Figure 1.3: X-ray crystal structure of the bromide complex of **1.2**

Almost contemporaneously, B.D. Smith and co-workers reported the use of functionalized isophthalamide receptors for the coordination of anions.[10] Smith appended boronate groups to the peripheral aryl groups in order to form interactions between the Lewis acidic boron with the carbonyl oxygens of the amides therefore 'pre-organising' the receptor into the *syn-syn* conformation (preferable for anion coordination) and presumably increasing the acidity of the NH group. Proton COSY and NOE difference experiments indicated that the receptor did indeed adopt the desired *syn-syn* conformation in DMSO-d_6. NMR titration experiments in DMSO-d_6 at 295K

showed that receptor **1.3** bound acetate with a stability constant of 2.1×10^3 M^{-1} as compared to 1.1×10^2 M^{-1} found with the non-preorganised receptor **1.2a** and acetate.

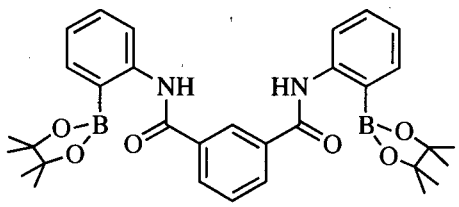

1.3

Recently J.T. Davis, Gale, Quesada and co-workers have shown that appended hydroxy groups on the central aryl ring of an isophthalamide can pre-organise the receptor into the *syn-syn* conformation and again presumably increase the acidity of the amide NH groups, which increases the receptor's ability to bind chloride (**Figure 1.4**).[11] The preorganisation occurs due to intramolecular hydrogen bonds between the hydroxy groups and carbonyl oxygen of the amides.

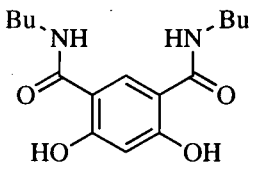

1.4

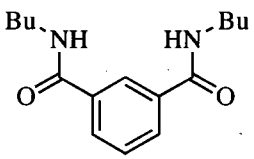

1.5

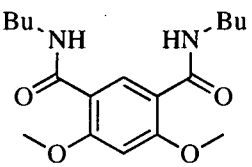

1.6

Proton NMR titration experiments in CD_3CN at 298K revealed that receptor **1.4** bound chloride most strongly with an stability constant of 5230 M^{-1}, whereas a stability constant of 195 M^{-1} was obtained for the unfunctionalised cleft **1.5**. Model compound **1.6** contains methoxy groups in the 4- and 6-positions and functions as a control. In this system the intramolecular hydrogen bonds form between the amide NH groups and the methoxy oxygens and consequently the compound does not interact with chloride (**Figure 1.4**). Most interestingly, it was shown that compound **1.4** functions as a highly efficient chloride transport agent across EYPC lipid bilayers whilst the analogous isophthalamide **1.5**, and model compound **1.6** show no transport ability. Compound **1.4** seems to be the simplest synthetic lipid bilayer transport agent for chloride studied so far. The origin of this ability is currently being investigated.

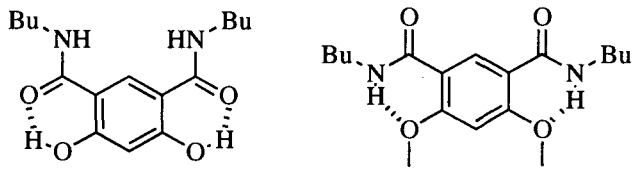

Figure 1.4: Hydrogen bonding interactions in **1.4** and **1.6**

Thordarson *et al.* have studied the aggregation of pyromellitamide **1.7** and its response to anions. It was found that compound **1.7** aggregates in non-polar solvent by the formation of one-dimensional intermolecular hydrogen-bonding networks.[12] Upon the introduction of anions the aggregation of **1.7** is disturbed. Proton NMR titration experiments in d_6-acetone at 300 K revealed that compound **1.7** bound a range of anions with 2:1 anion/receptor stoichiometry. Although compound **1.7** has two discrete binding sites the anions were found to bind with negative cooperativity with the strength of anion binding to **1.7** decreasing in the order $Cl^- < CH_3CO_2^- < Br^- < NO_3^- \approx I^-$.

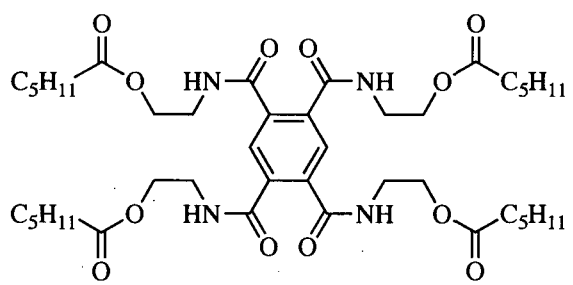

1.7

Prohens and co-workers have synthesized compounds **1.8a** and **1.8b**, simple squaramido-based receptors and investigated their ability to coordinate carboxylate anion in competitive solvents.[13] The amide NH groups of the squaramide form a more open cleft (similar to ureas) than the isophthalamides. Receptors **1.8a** and **1.8b** therefore adopt a more suitable geometry for the coordination of bidentate anions, such as carboxylate anions, through two approximately linear hydrogen bonds. Proton NMR titration experiments revealed association constants of 217 M^{-1} and 1980 M^{-1} for the binding of acetate by **1.8a** and **1.8b** respectively in DMSO-d_6 at 295K.

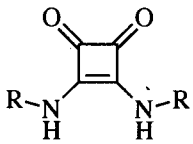

1.8a R= ^{t}Bu
1.8b R= Ph

A.P. Davis and co-workers have designed a number of acyclic receptors using the steroid cholic acid as a scaffold upon which they appended sulfonamide and carbamate amide groups.[14] The inflexibility of the fused ring system and the axial conformation of the functional groups in the 7α and 12α positions results in the formation of a convergent hydrogen-bonding array, ideal for anion binding.

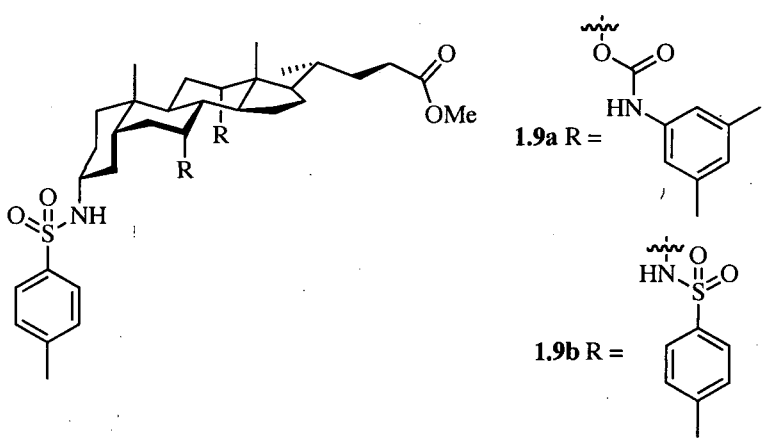

Both the structural rigidity and the shape of the receptor result in the formation of a relatively small, well defined binding site that shows selectivity for halide anions with particularly high affinities observed for fluoride with receptor **1.9a** (15400 M^{-1} association constants were determined by ^{1}H NMR titration experiments in $CDCl_3$ at 298K). In the case of compound **1.9b** the association constant for fluoride was too high to be determined however, association constants for chloride and bromide were found to be much higher than for compound **1.9a**.

1.3.2 MACROCYCLIC AMIDE RECEPTORS

Macrocyclic receptors often possess a higher degree of selectivity than acyclic systems. Hamilton and Choi have described the synthesis and anion binding properties of a family of cyclic triamides **1.10a** and **1.10b**.[15] These C_3 symmetric receptors were found to be selective for oxo-anions such as tosylate with association constants of 2.6×10^5 M^{-1} and 2.1×10^5 M^{-1} obtained for compounds **1.10a** and **1.10b** respectively in $CDCl_3$/2% dimethylsulfoxide at 296 K. Hamilton also studied the binding ability of an acyclic analogue (**1.11**) and found significantly lower stability constants for the anion complexes formed. For example, in the case of nitrate, a stability constant of 620 M^{-1} was calculated for compound **1.11** whereas a stability constant of $4.6 \times 10^5 M^{-1}$ ($K_2 = 2.1 \times 10^3 M^{-1}$) was found with compound **1.10a**.

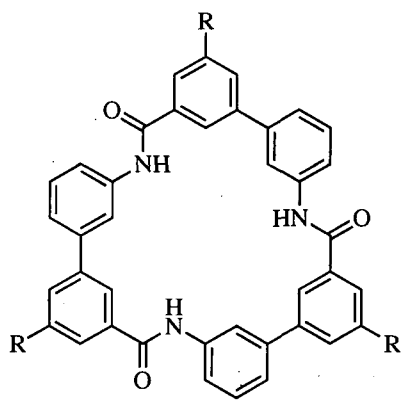

1.10a R= CO_2Et
1.10b R= NHBoc

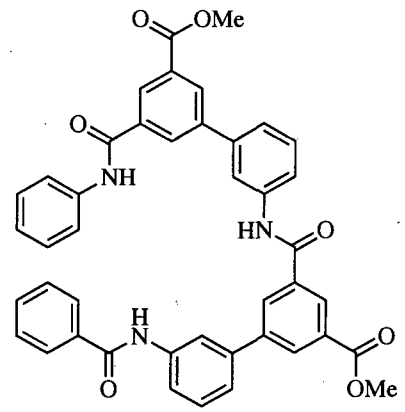

1.11

Interestingly, the NMR data led the authors to suggest that receptor **1.10b** forms a 2:1 host/anion 'sandwich' complex at low concentrations of iodide (as evidenced by an initial up-field shift of the NH resonances until *ca.* 0.5 equivalents of iodide) then switching to a 1:1 complex at higher concentrations of iodide (down-field shift of NH resonances after ca 0.5 equivalents of iodide). Titrations with **1.10a** and **1.10b** in $CDCl_3$/2% DMSO-d_6 mixture displayed complex binding behaviour, thus titration experiments were conducted in 100% DMSO-d_6 at 296K to simplify the equilibria occurring in solution. All data for receptor **1.10b** were fitted to a 1:1 binding model and

again the macrocycle was found to be oxo-anion selective with the highest stability constants being found with dihydrogen phosphate and hydrogen sulfate ($1.5\times 10^4\ M^{-1}$ and $1.7\times 10^3\ M^{-1}$ respectively).

Chmielewski and Jurczak have reported a series of extended tetra-amide macrocycles containing two pyridine-2,6-dicarboxamide 'caps' linked *via* short aliphatic chains.[16,17] The macrocycles possess a well-defined cavity with all the amide NH groups directed inwards.

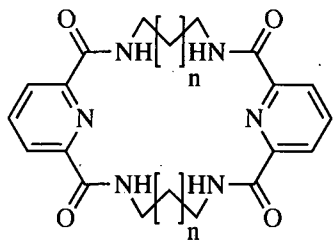

1.12a $n = 0$
1.12b $n = 1$
1.12c $n = 3$

Proton NMR titrations in DMSO-d_6 at 298K were conducted in order to determine the stability constants of receptors **1.12a**, **1.12b** and **1.12c** with a range of anions, added as their tetrabutylammonium salts. The strongest association constants were obtained for the 20-membered macrocycle **1.12b** with the most significant increase in affinity between the macrocycles being observed in the binding of chloride. Enlargement from the 18-membered macrocycle **1.12a** to the 20-membered macrocycle **1.12b** results in a 30-fold increase in the association constant for chloride (65 M^{-1} for **1.12a** against 1930 M^{-1}) whereas further enlargement to the 24-membered macrocycle **1.12c** results in the reduction of the association constant by two orders of magnitude (1930 M^{-1} against 18 M^{-1}). This suggests that the 20-membered macrocycle **1.12b** has good size complementarity with the chloride anion. Although the 24-membered macrocycle **1.12c** was designed with a large enough cavity to accommodate two oxygen atoms from oxo-anionic guests, the stability constants obtained were the lowest of the receptors tested. This is evidence that the additional flexibility introduced into the macrocycle *via* the longer aliphatic chain has a detrimental effect on the anion binding ability of the receptor.

More recently the same authors have studied the anion binding ability of similar macrocyclic systems based on isophthalamides.[18] The isophthalamide moieties were introduced as previous studies have shown isophthalamide derivatives bind anions more strongly than the analogous pyridine-2,6- dicarboxamides.[19,20]

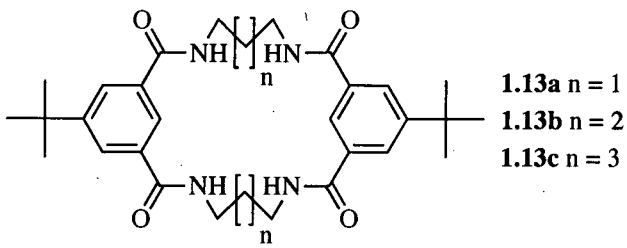

Stability constants were obtained for receptors **1.13a**, **1.13b** and **1.13c** using analogous conditions to those employed for receptors **1.12a**, **1.12b** and **1.12c**. As with the pyridine-2,6-dicarboxamide macrocycles, the stability constants for the isophthalamide macrocycles appear to be influenced by the size and flexibility of the system with the higher constants observed in the 20-memebered receptor **1.13a** with notable decreases in the association constants with the 22- and 24-membered receptors **1.13b** and **1.13c**. The greatest decreases where observed in the stability constants obtained with the carboxylate anions. In the case of acetate the constants decreased from 3130 M^{-1} for **1.13a** to 552 M^{-1} and 205 M^{-1} for **1.13b** and **1.13c** respectively. In the case of benzoate a constant of 601 M^{-1} was calculated for **1.13a** decreasing to 302 M^{-1} and 82 M^{-1} for **1.13b** and **1.13c** respectively. Unexpectedly lower binding constants were obtained for the isophthalamide macrocycles (**1.13a – 1.13c**) compared to the pyridine-2,6-dicarboxamide macrocycles (**1.12a – 1.12c**), a result rationalised in terms of the competition between the formation of intramolecular hydrogen bonds (arising from the preferred *syn-anti* conformation of the isophthalamide in solution) and complexation of the anion (**Scheme 1.1**).

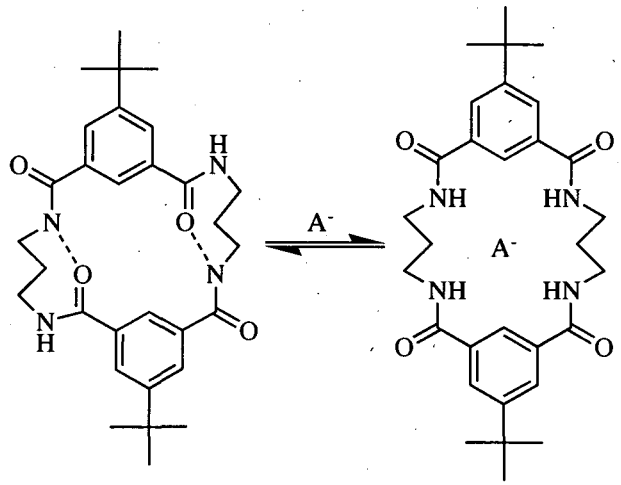

Scheme 1.1: Intramolecular hydrogen-bonding *vs* anion binding in **1.13a**

Bowman-James and co-workers have designed polyamide cryptand-type systems based on triamines, such as tren (e.g. **1.14**) and trpn (e.g. **1.15**), and shown that they bind anions.[21] The crystal structure of the hydrochloric acid and fluoride complexes of **1.14** reveal that the anions are encapsulated within the cavity of the amidocryptand and bound to the six-amide NH groups. In contrast the hydrochloric acid structure of the expanded trpn-based amidocryptand **1.15** shows the encapsulation of two chloride anions within the cryptand, bridged by a water molecule. Each chloride is bound to the water molecule as well as a protonated bridgehead amine and two hydrogen bonds from the amides groups.

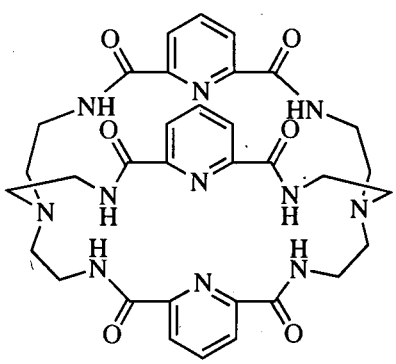

1.14

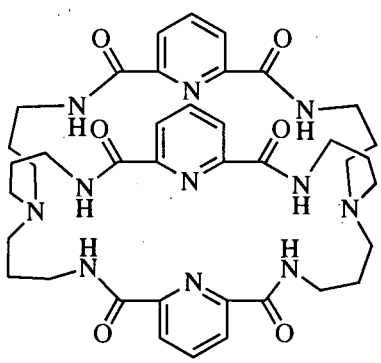

1.15

Stability constants for **1.14** and **1.15** with different anions (added as their tetrabutylammonium salts) were obtained by ^{1}H NMR titrations in DMSO-d_6. In both

cases, a slow equilibrium was observed in the titrations with fluoride with stability constants $>10^5$ M^{-1}. The expansion of the cavity from receptor **1.14** to **1.15** results in a significant change in the binding and selectivity for anions. In the smaller receptor, **1.14**, chloride is bound much more strongly (3000 M^{-1}) as compared to **1.15** (180 M^{-1}) whereas the receptor **1.15** has a much higher affinity for hydrogen sulfate with a stability constant of 2700 M^{-1} as compared to 68 M^{-1} for **1.14**. These findings may be due to the size complementarity between the receptors and guests with **1.14** being an ideal size to encapsulate chloride and **1.15** being ideal for hydrogen sulfate, as illustrated by the crystal structures (**Figure 1.5**).

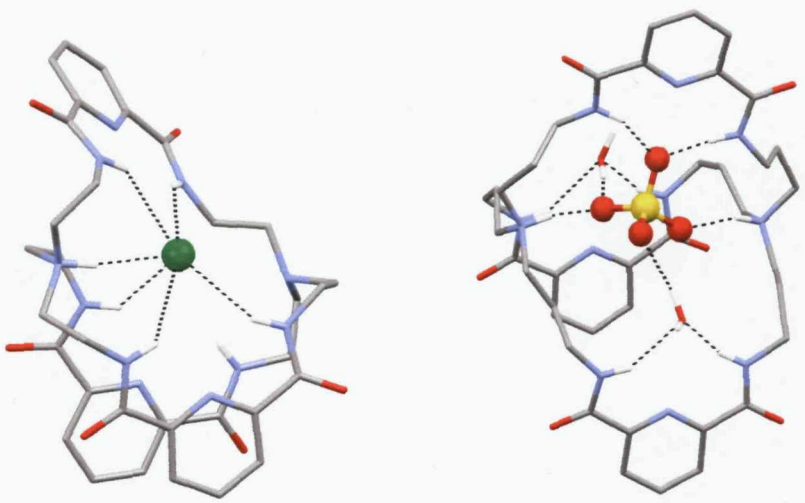

Figure 1.5: X-ray crystal structures of the chloride complex of **1.14** and the sulfate complex of **1.15** respectively

The authors have also synthesised **1.16**, a tricyclic cryptand-like receptor, and have studied its ability to bind anions.[22] Proton NMR titration experiments in DMSO-d_6 at 23 °C revealed that compound **1.16** was selective for bifluoride (FHF^-) with an association constant of 5500 M^{-1} being calculated. Dihydrogenphosphate, azide and acetate were also found to bind to **16** with stability constants of 740 M^{-1}, 340 M^{-1} and 100 M^{-1} respectively.

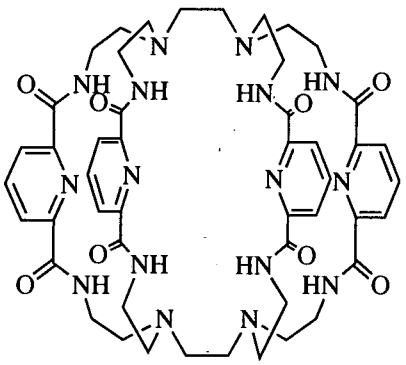

1.16

Kubik and co-workers have developed a series of highly effective anion receptors based upon cyclic peptides.[23,24] Cyclic hexapeptide receptors such as **1.17** consist of alternately linked L-proline and 6-aminopicolinic acid subunits. A 1:1 binding stoichometry for **1.17** and the sodium salt of benzenesulfonate was confirmed by a Job plot but in the case of the halide and sulfate sodium salts 2:1 host/guest complexes were found. This was confirmed by electrospray mass spectrometry and in the case of iodide a crystal structure of the 2:1 complex was obtained where the iodide was 'sandwiched' between two cyclic hexapeptide receptors.

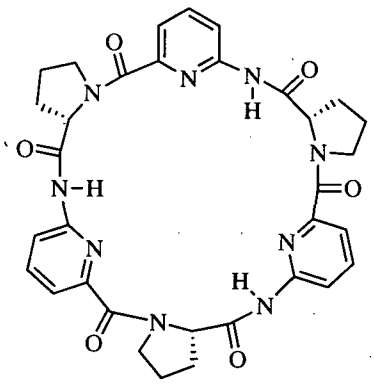

1.17

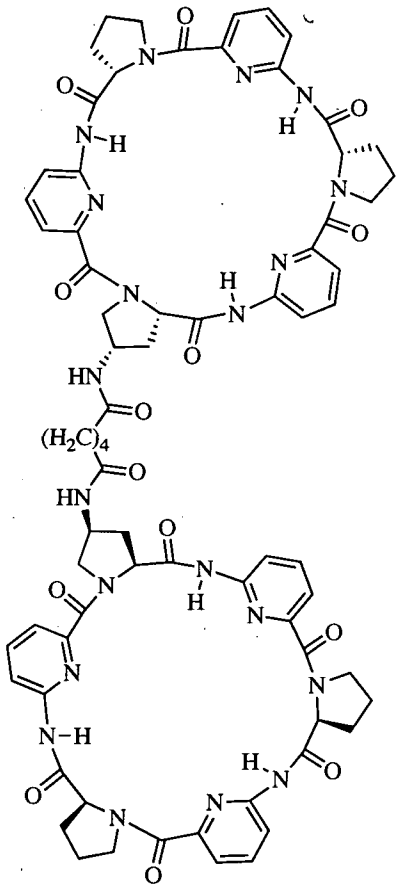

1.18

The formation of the 2:1 complexes observed in **1.17** lead the authors to design and synthesise compound **1.18** where two cyclic hexapeptides are covalently linked. The new receptor binds anions in a 1:1 stoichiometry in methanol/water mixtures efficiently, with high affinity and selectivity for sulfate being observed. Both ^{1}H NMR titrations and by ITC experiments were conducted in 50% methanol/water at 298K and stability constants (log K_a) of 5.54 and 4.55 ± 0.23 were found by ^{1}H NMR and ITC respectively for **1.18** with sulfate (added as Na_2SO_4).

1.3.3 UREA AND THIOUREA BASED RECEPTORS

Ureas and thioureas possess two parallel NH hydrogen bond donor groups and have been shown in a wide variety of receptors to function as highly efficient binding sites for 'Y-shaped' anions such as carboxylates. Thioureas are more acidic than analogous ureas and on this basis might be expected to form stronger complexes with anions. However other effects can often mask or reverse this expected trend.

There have been a number of reports of anions triggering the deprotonation neutral NH groups in anion receptor systems. This is often due, in the case of fluoride, to the formation of the stable HF_2^- anion driving the deprotonation process.[25-28] Fabbrizzi and co-workers have shown that this process can occur in urea systems containing electron-withdrawing groups.[29] The interactions between a number of anions and the simple 1,2-bis(4-nitrophenyl) urea **1.19** were investigated.[30] Oxo-anions were found to bind to the receptor with a 1:1 host/guest stoichiometry with the strength of the interaction depending on the partial negative charge located on each oxygen atom of the anion.

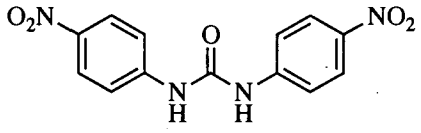

1.19

Stability constants were determined for compound **1.19** by UV-vis spectrophotometric titrations in acetonitrile at 25 °C and revealed that the association constants increased with the increasing basicity of the anion (CH_3COO^- > $C_6H_5COO^-$ > $H_2PO_4^-$ > NO_2^- > HSO_4^- > NO_3^-). Addition of fluoride appears to stabilise a strong 1:1 complex at low anion concentration, however at higher anion concentrations deprotonation of the urea subunit occurs resulting in the formation of HF_2^- (confirmed by ^{1}H NMR). This process was also characterised by the formation of a new band at 475 nm in the UV-vis spectrum upon the additions of the fluoride anion and was clearly present after the addition of two equivalents of fluoride.

Gunnlaugsson and co-workers have studied several receptors containing a thiourea group attached to an anthracence moiety.[31] These compounds were designed to behave

as fluorescent PET (photo-induced electron transfer) sensors for the detection of anionic species. Proton NMR titration experiments, conducted in DMSO-d_6, confirmed that the anions bind to the receptors through the two NH protons of the thiourea group and form a 1:1 complex. The authors demonstrated that **1.20a-1.20d** act as ideal PET sensors (only fluorescent quantum yield affected upon additions of anions) with quenching of the fluorescence being observed with the addition of fluoride, acetate and dihydrogen phosphate anions. Chloride and bromide did not induce any changes in the fluorescence spectra.

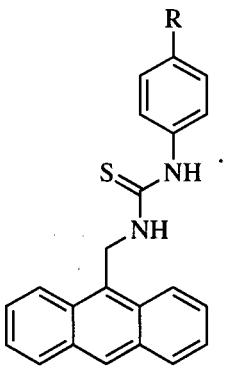

1.20a R = H
1.20b R = CF_3

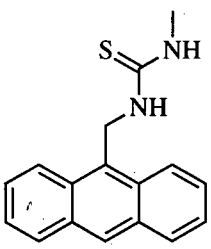

1.20c

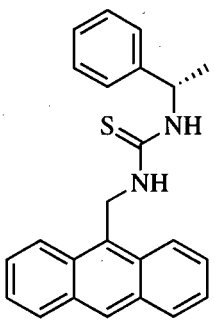

1.20d

Yoon and co-workers have reported a series of mono- and bis-functionalised anthracenes and described their colorimetric and fluorescent properties for the sensing of both fluoride and pyrophosphate anions.[32] The authors appended either a phenylurea and *p*-nitrophenylurea groups through the 1-position (for the mono-functionalised derivatives **1.21a** and **1.21b**) and the 1- and 8-position (for the bis-functionalised derivative **1.22a** and **1.22b**) of the anthracene.

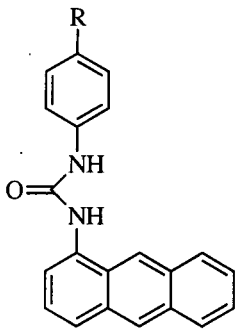

1.21a R = NO_2
1.21b R= H

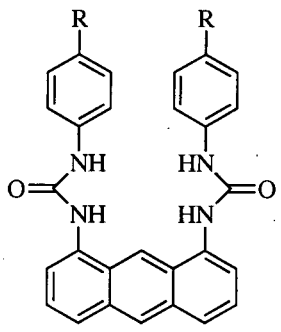

1.22a R = NO_2
1.22b R = H

Fluorescent titration experiments with receptors **1.21b** and **1.22b** were carried out in DMSO with a variety of anions, added as the tetrabutylammonium salts, in order to compare the stability constants of the mono- and bis-functionalised receptors. The strongest anion binding was observed with the bis-functionalised receptor (**1.22b**) with stability constants of 108,000, 9700 and 6000 M^{-1} calculated for fluoride, bromide and pyrophosphate respectively. For compound **1.21b** a much lower binding constant of 4000 M^{-1} was found with fluoride as compared to the strong anion complexation observed with **1.22b**, illustrating that there is a cooperative binding effect in operation with the two urea groups in receptors **1.22a** and **1.22b**. Temperature dependant ^1H NMR experiments in DMF-d_7 also revealed that the anion complex stability was enhanced by the formation of a hydrogen bond between the hydrogen atom in the 9-position and both the fluoride and pyrophosphate guests in receptors **1.22a** and **1.22b**.

Gale and co-workers have designed **23a**, a bis-urea cleft based on *o*-phenylenediamine, to selectively bind carboxylate anions.[33] The geometry of the receptors provides a convergent cleft appropriate for the binding of carboxylate anion through four hydrogen bonds. Stability constants of 3210, 1330 and 732 M^{-1} were calculated for acetate, benzoate and dihydrogen phosphate respectively after analysis of data from ^1H NMR titration experiments conducted in DMSO-d_6/ 0.5% water at 298 K. The crystal structure of the benzoate complex of compound **1.23a** is shown in Figure 1.6 revealing that the receptor binds this carboxylate *via* four hydrogen bonds in the solid state. The stability constants for compound **1.23a** were found to be greater than constants obtained with *N,N'*-diphenylurea with a 2.5 fold increase observed for **23a**

with acetate compared to the diphenylurea (3210 M^{-1} for **1.23a** and 1261 M^{-1} for diphenylurea).[34]

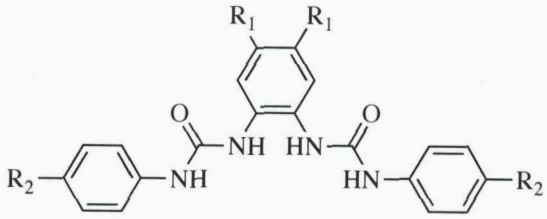

1.23a R_1, R_2 = H
1.23b R_1 = H R_2 = NO_2
1.23c R_1 = Cl, R_2 = H

The same authors appended electron-withdrawing groups onto both the central aryl ring and peripheral aryl rings of the receptor in order to increase the acidity of the urea NH groups.[35] Titration studies were conducted under the same conditions as for **1.23a** and enhanced stability constants were observed for both receptors **1.23b** and **1.23c** compared to **1.23a**. In the case of acetate the stability constant increased from 3210 M^{-1} for **1.23a**, to 4020 M^{-1} and 8080 M^{-1} for **1.23b** and **1.23c** respectively. In the case of dihydrogenphosphate there is a decrease in affinity from 732 M^{-1} for **1.23a**, to 666 M^{-1} for **1.23b** but a large increase to 4720 M^{-1} for **1.23c**. The authors proposed that the dihydrogenphosphate anion interacted most strongly with the central NH groups thus with the increased acidity of these NH groups in **1.23c**, due to the presence of the two chloro-groups, stronger complexation is observed.

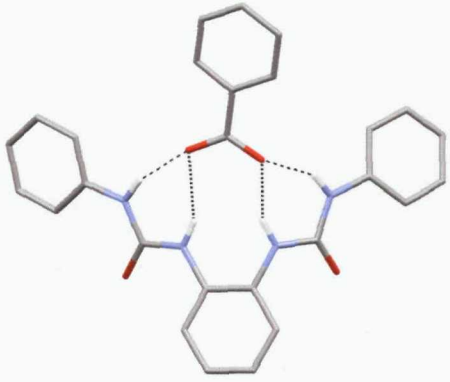

Figure 1.6: X-ray crystal structure of the benzoate complex of **1.23a**

Naphthalene and binaphthalene appended with thiourea groups (**1.24** and **1.25** respectively) have been synthesised by Kondo and co-workers in order to investigate potential cooperative binding between two thiourea groups in **1.25**.[36] This group found that 1:1 complexes were formed between **1.25** and fluoride, acetate and dihydrogen phosphate anion, which was confirmed by Job plots in acetonitrile and ESI-MS.

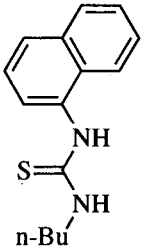

1.24

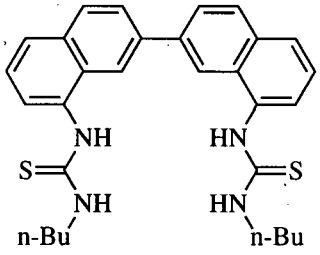

1.25

UV-vis spectroscopy titration experiments in acetonitrile solution were carried out to ascertain the anion binding properties of the receptors with acetate, dihydrogen phosphate, fluoride and chloride. The binding constants revealed that the presence of the second thiourea group in **1.25** significantly improves the receptor's affinity for anions with respect to the mono-thiourea **1.24**. The most significant differences were obtained for titration with fluoride and acetate where binding constants of 1.1×10^5 M^{-1} and 2.1×10^6 M^{-1} were elucidated for **1.25** and 3.7×10^3 and 7.7×10^3 for compound **1.24** with acetate and fluoride respectively.

Pfeffer and co-workers have described the use of a highly rigid [3]polynorbornane as a scaffold on which to append electron deficient thiourea subunits.[37]

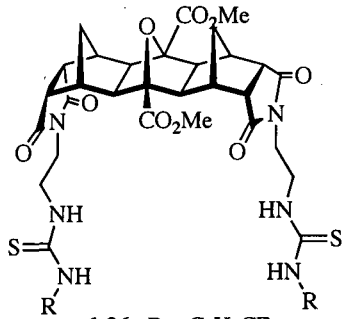

1.26a R = $C_6H_4CF_3$
1.26b R = $C_6H_4NO_2$

The anion binding abilities of **1.26a** and **1.26b** were evaluated by ^{1}H NMR titration techniques in DMSO-d_6 with CH_3COO^-, F^-, $H_2PO_4^-$ and $H_2P_2O_7^{2-}$ (added as their tetrabutylammonium salts). Additions of fluoride to the receptor resulted in a distinctive colour change attributed to deprotonation. This process was characterised by the loss of the thiourea NH proton resonances and the appearance of the HF_2^- resonance in the ^{1}H NMR during the titration. Analysis of the binding isotherms of receptors **1.26a** and **1.26b** with acetate revealed that the anions were strongly bound by both **1.26a** and **1.26b** in a 1:2 receptor-to-anion complex with each of the thiourea units binding to a single acetate anion. Binding constants (log β_1 and log β_2 values) of 3.5(±0.1) and 2.4(±0.1) were calculated for **1.26a** and 3.5(±0.1) and 3.0(±0.1) for **1.26b** with acetate. Titrations with $H_2PO_4^-$ were fitted to a 1:1 binding model and constants of 3.9(±0.1) and 3.6(±0.1) (log β values) were calculated for receptors **1.26a** and **1.26b** respectively. Pyrophosphate was then investigated to evaluate the binding ability of **1.26a** and **1.26b** with a dianion. Analysis of the titration curves for both **1.26a** and **1.26b** with pyrophosphate revealed the formation of a 2:1 receptor-to-anion stoichiometry in which each anion terminus is accommodated by two urea groups of a single receptor.

Extending their work on 'cholapods', A.P. Davis and co-workers have appended urea and thiourea groups from the 7 and 12 positions of the steroid scaffold and evaluated the ability of these receptors to bind chloride and bromide (added as their tetraethylammonium salts).[38]

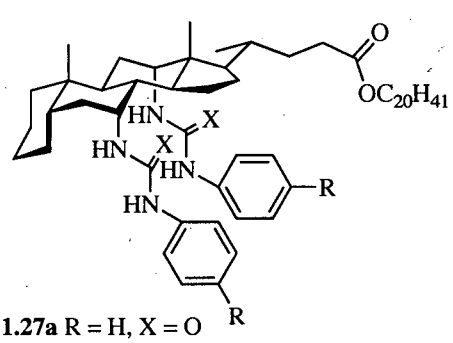

1.27a R = H, X = O
1.27b R = CF_3, X = O
1.27c R = NO_2, X = O
1.27d R = NO_2, X = S

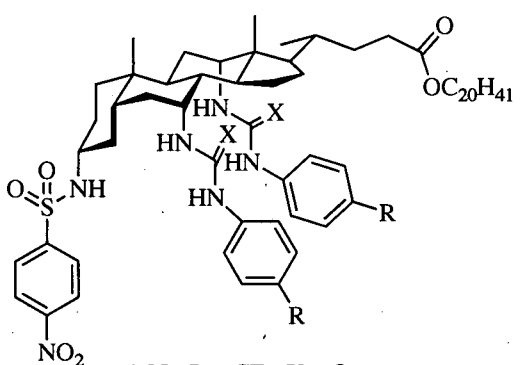

1.28a R = CF_3, X = O
1.28b R = NO_2, X = O
1.28c R = NO_2, X = S

NMR data was found to be consistent with the formation of predominantly 1:1 complexes of the receptors and anions. Stability constants were determined by Cram's extraction method in water-saturated chloroform at 30°C. Affinities for both chloride and bromide anions increased through the series **1.27a-1.27d**, reflecting the increase in acidity of the NH groups due to the electron-withdrawing aryl substituents and the change from urea to thiourea in **1.27d**. In the case of chloride the association constant for the 'unsubstituted' derivative **1.27a** was calculated to be 1.62×10^7 M^{-1}, with the nitrophenyl substituted **1.27c** the constant increased to 4.77×10^8 M^{-1} and the constant increased further to 1.05×10^9 M^{-1} with the introduction of the thiourea (**1.27d**). The addition of the nitrosulfonamide group in **1.28a-1.28c** also enhances the anion binding affinities with the largest constants being observed in the thiourea derivative **1.28c** with constants of 1.03×10^{11} M^{-1} and 2.59×10^{10} M^{-1} calculated for chloride and bromide respectively.

A further detailed study of these 'cholapod' anion receptors was conducted where the anion binding ability of several receptors with increasing numbers of hydrogen bond donor groups was investigated.[39] It was found that a combination of increasing numbers of hydrogen bonding groups and increasing acidity of the NH groups *via* electron-withdrawing substituents had a significant effect on the anion stability constants. Receptor **1.29** was found to have the highest affinities for all the anions investigated except acetate where the previously studied **1.28b** and **1.28c** had higher affinities (2.6×10^{11} M^{-1} and 2.0×10^{11} M^{-1} respectively) when compared to **1.29** (1.3×10^{11} M^{-1}). These steroid based receptors have also been studied as transport agents for anions across vesicle and cell membranes.[40] Electrochemical, NMR and fluorescence techniques were employed and revealed that the 'cholapod' receptors act as mobile carriers and facilitate the transport of chloride ions across vesicle membranes.

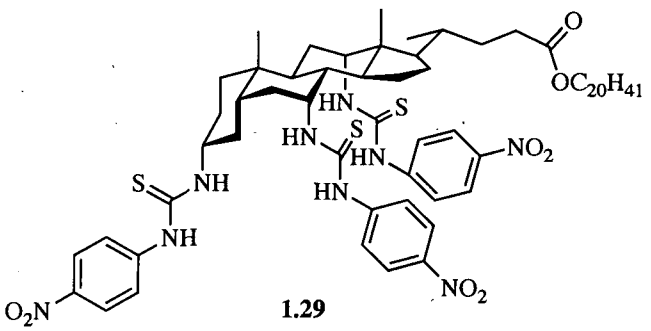

1.29

Reinhoudt and co-workers have synthesised both acyclic and cyclic receptors containing multiple urea-binding sites (e.g. **1.30** and **1.31**).[41] Anion binding studies were conducted with these systems and a variety of putative anionic guests (added as their tetrabutylammonium salts) using ^{1}H NMR titration experiments in DMSO-d_6. In the case of the cleft-like receptors dihydrogen phosphate caused the largest shift in the NH group resonances of all the receptors however an association constant could not be obtained for **1.30a** due to the complexity of the binding processes in solution. Job plot analysis of receptor **1.30b** showed the formation of an exclusive 1:2 host/guest complex with dihydrogen phosphate and an association constant of 5×10^7 M^{-2} was calculated. The thiourea functionalised **1.30c** cleft was also shown to bind dihydrogen phosphate with a 1:2 host/guest stoichiometry and chloride with 1:1 host/guest stoichiometry.

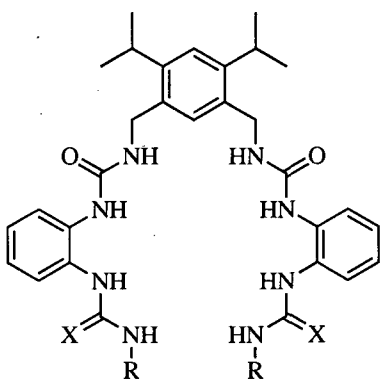

1.30a X= O, R= C_3H_7
1.30b X= O, R= Ph
1.30c X= S, R= Ph

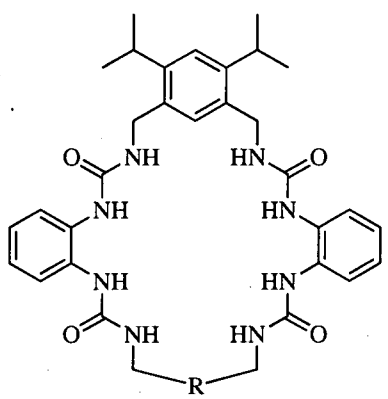

1.31a R= Ph
1.31b R= CH_2CH_2

Macrocyclic receptors **1.31a** and **1.31b** were found to bind both dihydrogen phosphate and chloride in exclusively 1:1 host/guest stoichiometries. Binding constants

were calculated for **1.31a** and **1.31b** with dihydrogen phosphate and chloride and revealed that dihydrogenphosphate was bound more strongly (2.5×10^3 M^{-1} for **1.31a** and 4.0×10^3 M^{-1} for **1.31b**) than chloride (500 M^{-1} for **1.31a** and < 50 M^{-1} for **1.31b**).

Gale and co-workers have combined urea and amide groups into a new macrocyclic motif and studied the anion complexation properties of **1.32**.[34]

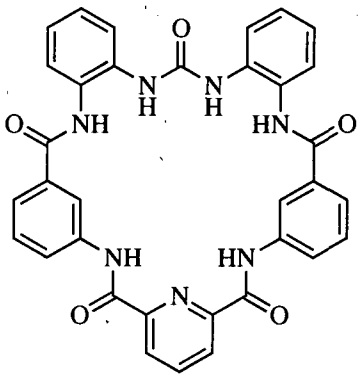

1.32

Stability constants with a variety of anionic guests were elucidated by ^1H NMR titration techniques in both DMSO-d_6/0.5% water and DMSO-d_6/5% water at 298 K. The macrocyclic receptor shows significant selectivity for carboxylate anions over dihydrogen phosphate and chloride. Titrations in DMSO-d_6/0.5% water resulted in a high stability constants for acetate (>10^4 M^{-1}) and benzoate (6430 M^{-1}) therefore the titrations were conducted in 5% water, a much more competitive media, and stability constants of 5170 M^{-1} and 1830 M^{-1} were calculated for acetate and benzoate respectively. Interestingly, a crystal structure of a carbonate complex was obtained from a crystallisation with tetrabutylammonium fluoride (**Figure 1.7**). It was presumed that carbonate was gained *via* the fixation of atmospheric CO_2 by the fluoride salt-macrocycle solution.

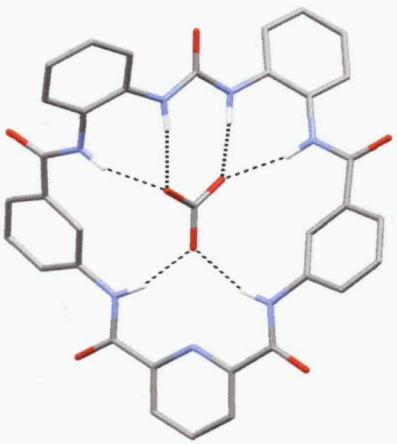

Figure 1.7: X-ray crystal structure of the carboate complex of **1.32**

In 2000 Lee and Hong synthesised tris-thiourea macrocycles **1.33a** and **1.33b** and studied their anion recognition properties by ^{1}H NMR titration experiments in DMSO-d_6 at 25 °C.[42] It was found that macrocycle **1.33a** was selective for dihydrogen phosphate (800 M^{-1}) over acetate (320 M^{-1}) and chloride (40 M^{-1}). In contrast macrocycle **1.33b** was found to be selective acetate (5300 M^{-1}) over dihydrogen phosphate (1600 M^{-1}) and chloride (95 M^{-1}).

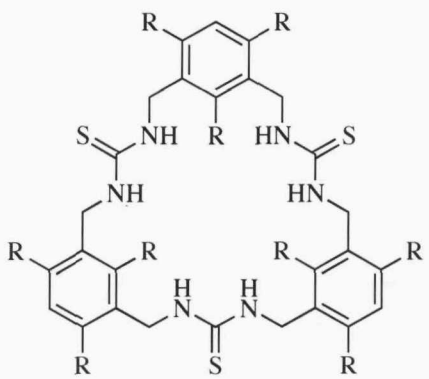

1.33a R= H
1.33b R= Et

Recently Tobe and co-workers have designed cryptand-like macrocycles based on homobenzylic tripodal thiourea and compared their anion binding properties to a series of acyclic tripod-type receptors.[43]

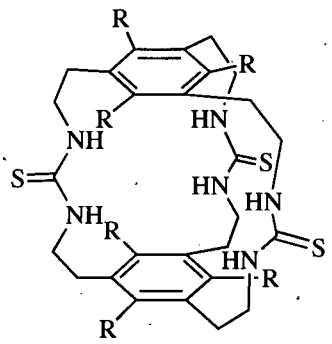

1.34a R= Me
1.34b R= $(CH_2)_2CH(CH_3)_2$

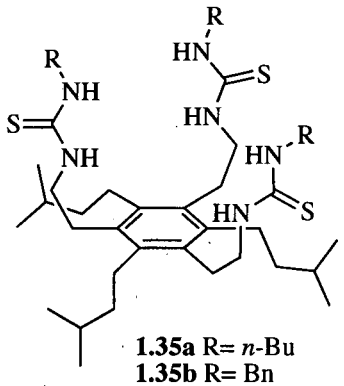

1.35a R= *n*-Bu
1.35b R= Bn
1.35c R= Ph

The proton resonances in the ^{1}H NMR spectra of cryptand-type receptor **1.34b** in various solvents were found to be very broad, possibly due to conformational changes that are slow on the NMR timescale. Therefore the complexation of **1.34b** with anionic species was evaluated by ^{1}H NMR titration experiments in $CDCl_2CDCl_2$ at 373 K. Association constants of 116 M^{-1} and 112 M^{-1} were calculated for acetate and chloride respectively and were found to be much lower than the tripodal receptor **1.35a** under the same condition (3030 M^{-1} for acetate and 3700 M^{-1} for chloride). This low binding ability of **1.34b** was attributed to strong intramolecular hydrogen bonds between the thiourea groups. Receptors **1.35a** and **1.35c** were then compared and the stability constants (obtained from ^{1}H NMR titrations in DMSO-d_6 at 303 K) revealed that **1.35a** has poor affinity towards all anionic species in DMSO solutions whereas **1.35c** has high affinity for dihydrogen phosphate and acetate.

1.4 SYNTHETIC NEUTRAL RECEPTORS CONTAINING AROMATIC NH AND OH DONOR GROUPS

1.4.1 PYRROLE BASED RECEPTORS

Sessler and co-workers have pioneered the use of the pyrrole NH hydrogen bond donor group in both charged and neutral anion receptor systems.[44] In 1992 they reported the anion binding abilities and fluoride selectivity of sapphyrin **1.36a**, a pentapyrrolic macrocycle.[45,46] Fluorescence titration experiments carried out in methanol revealed that

1:1 complexes formed between the diprotonated sapphyrin **1.36a** and halide anions and association constants of 2.8×10^5, $\sim 10^2$ and $< 10^2$ M^{-1} were calculate with fluoride, chloride and bromide respectively. Four years later Sessler reported the effective binding of phosphate by receptor **1.36b**. Phosphorus NMR titration experiments were carried out in methanol-d_4 at ambient temperature and revealed that compound **1.36b** bound both phosphoric acid and phenylphosphonic acid with affinity (1.8×10^4 and 1.3×10^4 M^{-1} for H_3PO_4 and $C_6H_7PO_3$ respectively).

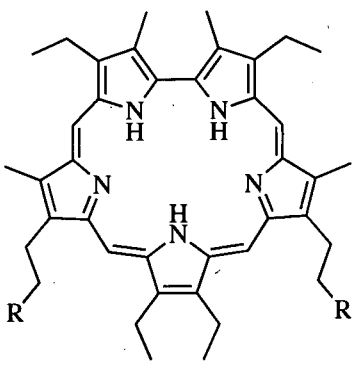

1.36a R= H
1.36b R = CH_2OH

Gale and co-workers have developed a number of receptors based on the 2,5-dicarboxamidopyrrole skeleton where the combination of a pyrrole and amide groups form convergent hydrogen-bonding arrays (e.g. **1.37a** and **1.37b**).[47]

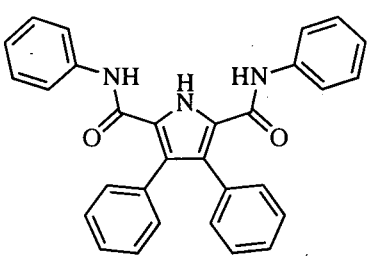

1.37a

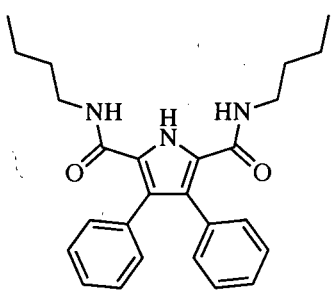

1.37b

Differences in the solubility of receptors **1.37a** and **1.37b** meant that their ability to bind anions was assessed in different solvents (DMSO-d_6/0.5% water for **1.37a** and CD_3CN for **1.37b** at 298 K). Both receptors proved to be selective for oxo-anions,

however **1.37a** bound dihydrogen phosphate most strongly (1450 M^{-1}) whereas **1.37b** bound benzoate most strongly (2500 M^{-1}).

Continuing this work, Gale and co-workers have synthesised more acidic diamidopyrrole derivatives **1.37c** and **1.37d** by including electron withdrawing nitro groups on the peripheral phenyl rings and assessed their anion binding ability compared to the unfunctionalized **1.37a**.[28] Proton NMR titrations were carried out in DMSO-d_6/0.5% water solutions at 298 K and revealed that the presence of the electron withdrawing groups in receptors **1.37c** and **1.37d** improved the systems affinity for anionic guests. In the case of benzoate the association constants increased significantly from 560 M^{-1} (obtained for **1.37a** under identical conditions) to 4150 M^{-1} for **1.37c** and 4200 M^{-1} for **1.37d**. Upon the addition of one equivalent fluoride to **1.37d** the anion appears to coordinate to the receptor. However upon further additions of fluoride deprotonation occurs (as indicated by the evolution of a blue colour in solution due to the deprotonated pyrrole). In the case of compound **1.37a** fluoride was found to bind to the receptor with a stability constant of 1245 M^{-1}.

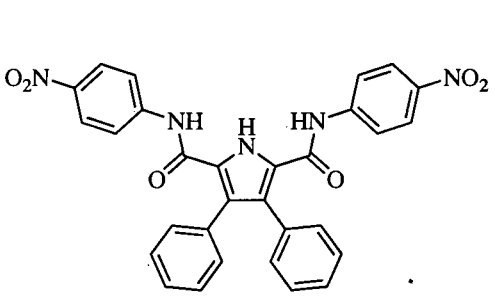

1.37c

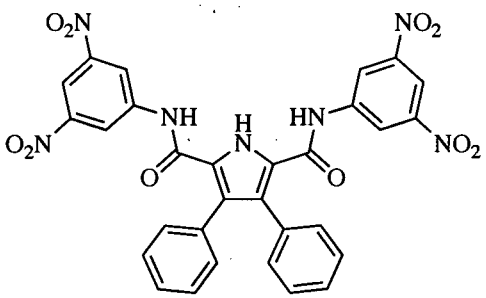

1.37d

Sessler, Gale and co-workers have further developed receptors based on the 2,5-diamidopyrroles skeleton by appending 2-aminopyrrole groups (e.g. compound **1.38**) thus increasing the number of hydrogen-bonding groups, which was hoped to increase the selectivity for oxo-anions compared to the previously studied **1.37a** and **1.37b**.[48]

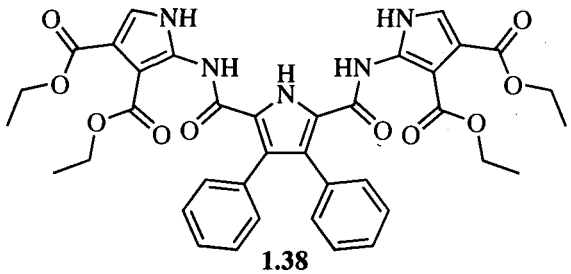

1.38

Proton NMR titration experiments were conducted in DMSO-d_6/0.5% water at 298 K to investigate the solution phase anion complexation properties of **1.38** compared to **1.37a**. The stability constants revealed that **1.38** showed enhanced selectivity for both dihydrogen phosphate and benzoate compared to **1.37a** however **1.38** was found to bind dihydrogen phosphate with higher affinity (10300 M^{-1}) than benzoate (5500 M^{-1}), the reverse selectivity observed for **1.37a**.

Recently Sessler and co-workers have appended the 2-aminopyrroles subunit onto a pyridine-2,6-dicarboxamide spacer group to afford two acyclic receptors (compound **1.39a** and **1.39b**).[49]

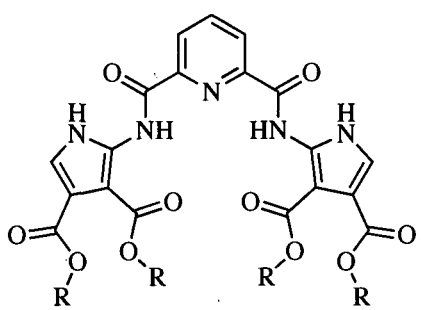

1.39a R= Et
1.39b R= $CH_2CH_2CH(CH_3)_3$

Elucidation of the solution phase anion complexation properties of receptors **1.39a** and **1.39b** (determined by UV-vis spectrophotometric titrations in dichloromethane at 298 K) revealed that **1.39b** bound only acetate with a stability constant of 13900 M^{-1} whereas strong binding was observed for benzoate, acetate, NO_2^- and CN^- with receptor **1.39a** (43000, 19000, 13000 and 5600 M^{-1} respectively).

Gale and co-workers have also investigated 5,5'-dicarboxamido-dipyrrolylmethanes as anion receptors.[50,51] These systems demonstrated a remarkable

affinity and selectivity for dihydrogen phosphate in highly competitive solvent media with stability constants of 234 M^{-1} and 20 M^{-1} being calculated (by ^1H NMR titration experiments at 298 K) for **1.40a** and **1.40b** respectively in DMSO-d_6/25% water. Receptors **1.40a** and **1.40b** were found to be unstable in solution therefore analogous compounds containing two methyl groups attached to the *meso*-carbon were synthesised (**1.41a** and **1.41b**) in the hope they would display increased stability in solution.

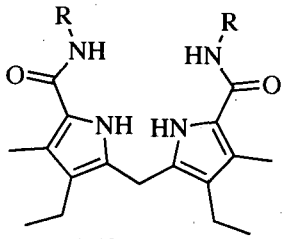

1.40a R= Ph
1.40b R= *n*-Bu

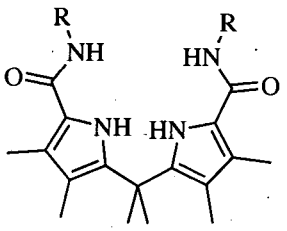

1.41a R= Ph
1.41b R= *n*-Bu

The *meso*-substituted derivatives showed lower affinities for anion compared to **1.40a** and **1.40b** however **1.41a** did display selectivity for dihydrogen phosphate over other anions with constants of 1092 M^{-1} for dihydrogen phosphate, 124 M^{-1} for fluoride and 41 M^{-1} for benzoate calculated in DMSOd_6/5% water at 298 K.

Sessler, Ustynyuk and co-workers have incorporated dipyrromethane subunits into 2,6-diamidopyridinedipyrromethane hybrid macrocyclic systems.[52] Initially **1.42** was synthesised and the anion binding ability was elucidated by UV-vis spectroscopic titrations in CH_3CN at 23 °C. Weak binding was observed for chloride, bromide, cyanide and nitrate which was rationalised by the receptor forming a deep cavity that favours the formation of well-oriented, directional NH-anion hydrogen bonds. Hydrogensulfate was found to bind strongly to the receptor in a 1:1 host/anion fashion in acetonitrile (K_a = 64,000 ± 2600 M^{-1}) presumably due to the orientation of the hydrogen bonding groups within the macrocycle being ideal for tetrahedral anions.

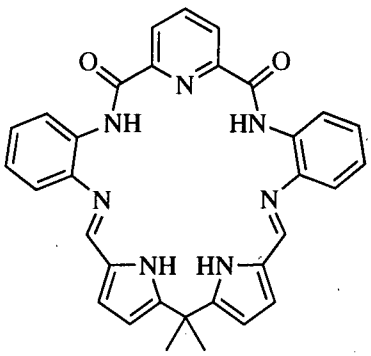

1.42

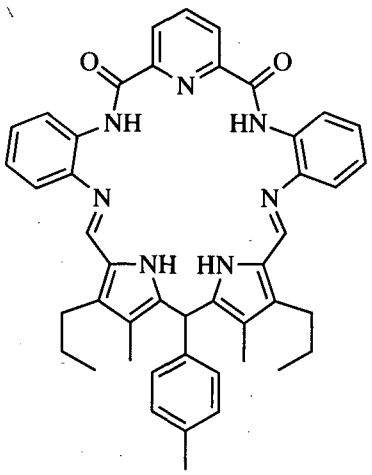

1.43

The same authors went onto 'fine tune' the anion binding properties of the pyridine-2,6-dicarboxamide-dipyrromethane-hybrid macrocyclic system and designed receptor **1.43** after DFT calculations suggested it to be more suitable for hydrogensulfate complexation.[53] The receptor's affinity for a number of anions was determined by UV-vis spectroscopic titrations in CH_3CN at 23 °C and revealed that bromide, nitrate and chloride are not bound by compound **1.43**. Acetate and dihydrogen phosphate bound with a 1:1 stoichiometry with constants of 12600 ± 450 M^{-1} and 29000 ± 1900 M^{-1} respectively. An enhanced affinity and selectivity was observed for **1.43** with hydrogen sulfate (108000 ± 17000 M^{-1}) compared to **1.42**.

Recently Katayev, Sessler and co-workers have further developed the hybrid macrocycle systems by replacing the pyridine-2,6-dicarboxamide moieties used in receptors **1.42** and **1.43** with bipyrrole and dipyrromethane subunits (compounds **1.44** and **1.45**).[54] UV-vis spectroscopic titrations in acetonitrile at 23 °C showed that the smaller macrocycle **1.44** bound hydrogensulfate with high affinity (2.7 × 10^6 M^{-1}) similar to the previously studied receptors **1.42** and **1.43** whereas the larger bis-dipyrromethane macrocycle **1.45** exhibited a different selectivity for anions with chloride being selectively bound with high affinity (281000 M^{-1}). Interestingly titrations with hydrogensulfate resulted in the lowest association constant of all the anions investigated with **1.45** (2100 M^{-1}).

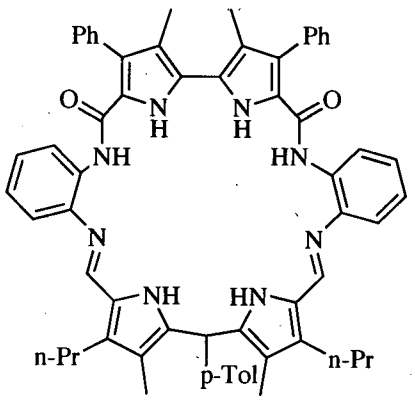

1.44

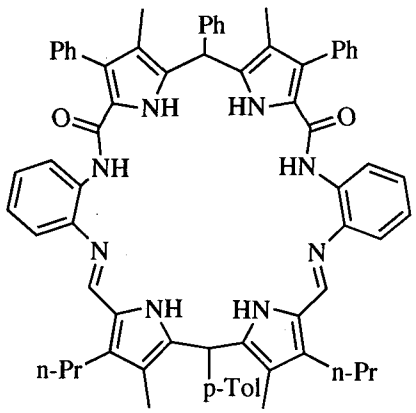

1.45

In 1996, Sessler and co-workers reported the anion complexation properties of calix[4]pyrroles e.g. **1.46**.[55] Compound **1.46** (*meso*-octamethylcalix[4]pyrrole) was originally synthesised by Baeyer in 1886 [56] and is arguably the simplest anion receptor to synthesise as it is formed in one step via the acid catalysed condensation of pyrrole and acetone. The macrocycle forms four hydrogen bonds to anionic guests and binding fluoride and chloride strongly.

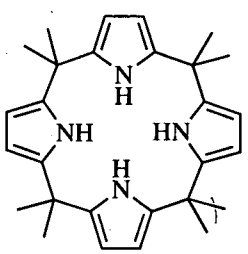

1.46

One approach to dramatically increase the affinity of calixpyrroles for anions is to introduce a 'strap' across the macrocycle containing additional hydrogen bond donor groups. For example, Lee, Sessler and co-workers have recently reported the synthesis of isophthalamide strapped calix[4]pyrroles. The authors studied the effect of varying the length of the strap on the anion complexation properties of the macrocycle and used isothermal titration calorimetry was employed to investigate the anion binding abilities of receptors **1.47a – 1.47c** (in CH_3CN at 30 °C).[57] Receptors **1.47a – 1.47c** were found to have high binding affinities toward halide anions however they failed to show an appreciable size-dependence selectivity based on the increase of strap length. This is

illustrated in the case of chloride (the most strongly bound anion) where association constants of 3.89×10^6 M^{-1}, 3.35×10^6 M^{-1} and 3.24×10^6 M^{-1} were calculated for **1.47a**, **1.47b** and **1.47c** respectively.

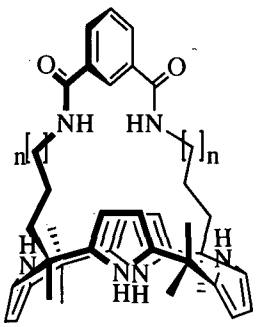

1.47a n= 0
1.47b n= 2
1.47c n= 3

Recently Lee and co-workers have shown that a binol-strapped calix[4]pyrrole (**1.48**) can be used in the enantioselective recognition of carboxylate anions.[58] Both the *R*- and *S*- enantiomers of the strapped calixpyrrole were isolated and characterised. Detailed studies of the enantioselectivety of the *S* enantiomer were carried by isothermal titration calorimetry experiments in acetonitrile with the chiral anions (*R*)-2-phenylbutyrate and (*S*)-2-phenylbutyrate. Stability constants were determined and revealed that receptor (*S*)-**1.48** shows selectivity for (*S*)-2-phenylbutyrate over (R)-2-phenylbutyrate with an order of magnitude difference in the constants ($K_a(R) = 9.8 \times 10^3$ M^{-1} and $K_a(S) = 1.0 \times 10^5$ M^{-1}).

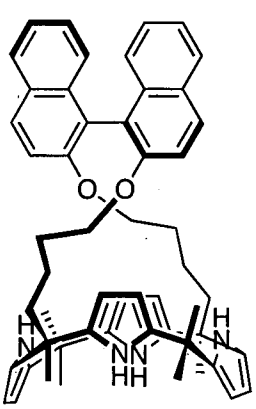

(*S*) **1.48**

In 2000 Kohnke and co-workers described the synthesis of *meso*-octamethylcalix[6]pyrrole *via* the conversion of calix[6]furan into dodecaketone, that was then treated with ammonium acetate to obtain calix[6]pyrrole **1.49**.[59,60]

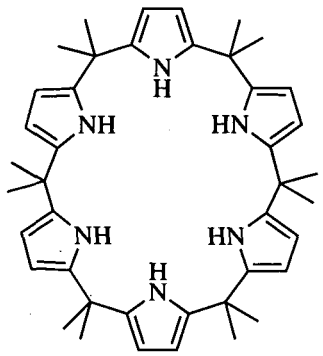

1.49

Association constants were determined by Cram extraction methods, which revealed that the macrocycle **1.49** formed a strong complex with chloride (12800 ± 1300 M^{-1}). Proton NMR titration experiments conducted in CD_2Cl_2 also revealed the size dependence selectivity of the calix[n]pyrroles where bromide was found to bind approximately seven times stronger to the larger calix[6]pyrrole compared to calix[4]pyrrole (710 ± 25 M^{-1} for **1.49** against 10 M^{-1} for **1.46**).

Recently Cafeo, Kohnke and co-workers have continued work on expanded calixpyrroles and have reported the anion binding properties of two calix[2]benzo[4]pyrroles **1.50a** and **1.50b**.[61]

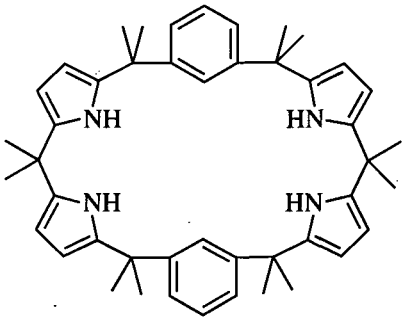

1.50a

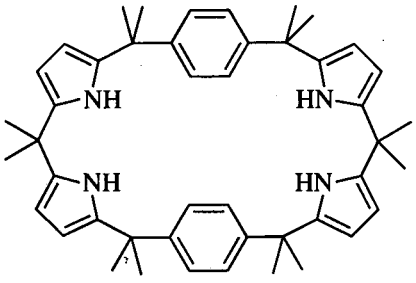

1.50b

Elucidation of the stability constants (determined by ^{1}H NMR titrations in CD_2Cl_2 at 20 °C) showed that although chemically similar the two macrocycles have significantly different anion binding properties. Receptor **1.50b** only bound fluoride and acetate to an appreciable level (2246 ± 132 M^{-1} for fluoride and 597 ± 236 M^{-1} for acetate) whereas receptor **1.50a** bound a number of anions with higher affinities. **1.50a** was found to have selectivity for fluoride with a constant of approximately 20000 M^{-1} estimated from competitive binding studies in the presence of **1.50b**. This selectivity is presumably due to good size complementarity between **1.50b** and the fluoride anion.

1.4.2 CARBAZOLE BASED RECEPTORS

Jurczak and co-workers have described 1,8-diamino-3,6-dichlorocarbazole as a building block for anion receptor construction.[62] Stability constants for receptors **1.51a** and **1.51b** with various anions, added as tetrabutylammonium salts, were calculated by ^{1}H NMR titration experiments in DMSO-d_6/0.5% water and it was found that compound **1.51b** bound anions more strongly with constants of 115 M^{-1} and 8340 M^{-1} for chloride and benzoate respectively compared to 13 M^{-1} and 1230 M^{-1} with compound **1.51a** with chloride and acetate respectively.

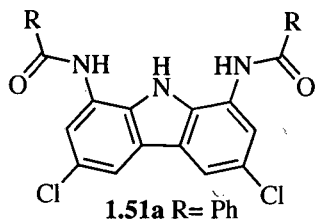

1.51a R= Ph
1.51b R= Pr

Sessler and co-workers have incorporated two carbazole subunits into expanded calixpyrrole-type macrocycle **1.52**.[63] Fluorescence titration experiments in dichloromethane at 0.5 μM concentration of host revealed that compound **1.52** shows selectivity for acetate (K_a = 229000 M^{-1}) over a number of other carboxylate-type anions (benzoate, oxalate and succinate).

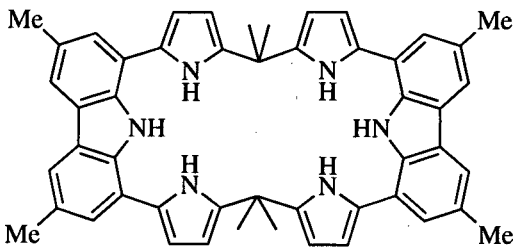

1.52

Beer and co-workers have reported the anion binding ability of a number of indolocarbazoles sensors (**1.53a–1.53c**).[64] The highest association constants were obtained with receptor **1.53c** presumably due to the presence of the electron withdrawing bromide groups increasing the acidity of the NH groups. UV-vis spectroscopic titrations in acetone at 25 °C revealed that compound **1.53c** bound benzoate most strongly (log K_a = 5.9) followed by phosphate (log K_a = 5.3) then fluoride (log K_a = 5.0) and chloride (log K_a = 4.9), a trend observed in both **1.53a** and **1.53b**.

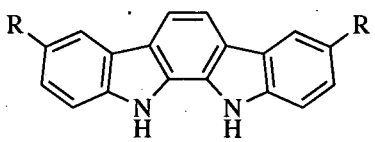

1.53a R= H
1.53b R= Me
1.53c R= Br

1.4.3 AROMATIC HYDROXY (OH) BASED RECEPTORS

In 2003, D.K. Smith showed that simple aromatic hydroxides can complex chloride anions.[65] Smith compared stability constants (obtained from NMR competition experiments in CD_3CN) of phenol, **1.54**, resorcinol, **1.55** and catechol, **1.56**, with chloride (added as its tetrabutylammonium salt) and found that **1.56** bound chloride with greater affinity than **1.54** and **1.55** (1015 M^{-1} for **1.56** against 125 M^{-1} for **1.54** and 145 M^{-1} for **1.56**).

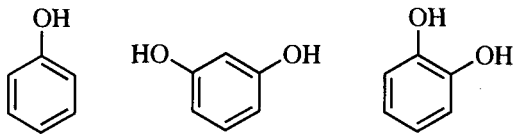

1.54 **1.55** **1.56**

Recently Smith and Winstanley have further explored aromatic hydroxides as anion receptor by studying the effect of ortho substituents on the chloride binding affinity of catechols **1.57a**, **1.57b** and **1.58**.[66] Binding constants were elucidated by proton NMR titrations in CD_3CN:DMSO-d_6 (9:1) solutions and showed that **1.58** bound chloride with the highest affinity (235 M^{-1}) presumably due to the additional hydrogen bonding provided the amide groups. Although amide groups are present in **1.57a** and **1.57b** it appeared that they were not involved in binding the anion and as results **1.57a** and **1.57b** bound chloride with lower affinities (110 M^{-1} for **1.57a** and 115 M^{-1} for **1.57b**).

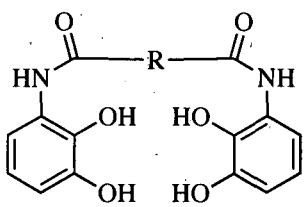

1.57a R= $(CH_2)_6$
1.58b R= $(CH_2)_8$

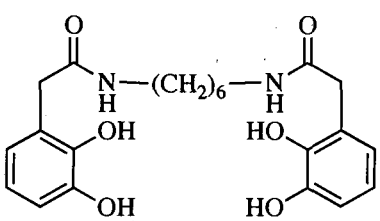

1.58

Row, Maitra and co-workers have linked two steroidal subunits to synthesise macrocycle **1.59**.[67] The fluoride binding properties of compound **1.59** were then investigated by a ^1H NMR titration experiment in $CDCl_3$ at 22 °C, which found that the receptor bound fluoride with a 1:2 receptor/anion stoichiometry (a result confirmed by Job plot analysis) and stability constants of K_1 = 1.8 (±0.1) × 10^3 M^{-1} and K_2 = 2.5 ((±0.35) × 10^2 M^{-1} were found.

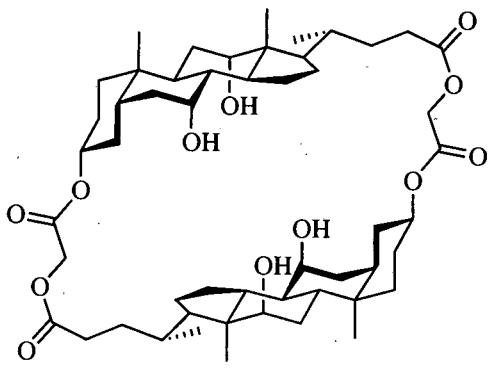

1.59

1.5 CHARGED SYNTHETIC ANION RECEPTORS

The incorporation of charged groups into receptors designed for anion recognition allows for the receptors to bind the anion with both electrostatic interaction and additional interactions dependent on the group and receptor design. In the case of imidazolium groups, the cation can stabilise the anion complex with additional CH···A$^-$ type hydrogen bonds.

1.5.1 IMIDAZOLIUM AND PYRIDINIUM BASED RECEPTORS

Kang and Kim have synthesised the fluorescent anion receptor compound **1.60** where two methylene bridged bis-imidazolium subunits are attached to a naphthalene backbone through the 1- and 8-position.[68]

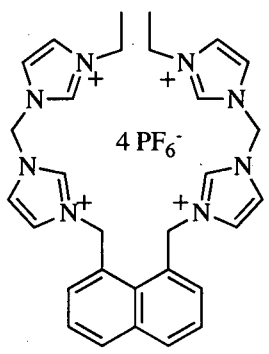

1.60

Molecular modelling showed that the receptor forms a convergent concave cavity with all the imidazolium C(2)-H's pointing inwards. Modelling studies led the authors to suggest that the shape of the cavity was predisposed for the binding of halide anions. Fluorescence titration experiments in 90:10 CH_3CN:DMSO solutions were carried out with chloride, bromide and iodide anions (added as their tetrabutylammonium salts) and stability constants were calculated that showed that compound **1.60** had highest affinity for I^- (5000±470 M^{-1}) followed by Br^- (243±15 M^{-1}) then Cl^- (185±13M^{-1}).

Yoon, Kim and co-workers have reported a highly effective fluorescent sensor for dihydrogen phosphate based on a 1,8-disubstituted-anthracene-dimer macrocycle bridged by two imidazolium subunits (**1.61**).[69]

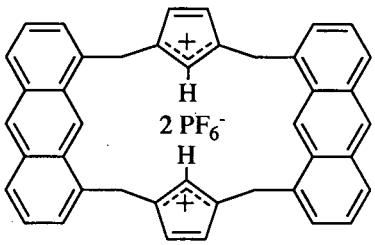

1.61

Fluorescence titration experiments were conducted in 9:1 acetonitrile:DMSO solutions in order to elucidate association constants for **1.61** with dihydrogenphosphate, fluoride, chloride and bromide. The results confirmed that compound **1.61** selectively binds to dihydrogenphosphate over the other anions tested with a stability constant >1300000 M^{-1}. Fluoride also bound to compound **1.61** with high affinity (340000 M^{-1}) and competition studies of dihydrogenphosphate and fluoride with respect to compound **1.61** clearly showed that no interference to the dihydrogenphosphate binding occurred in the presence of fluoride.

Beer and co-workers have shown how a number of tetrakis(imidazolium) macrocyclic receptors, **1.62a-1.62d**, can be used for anion binding.[70] Proton NMR titration investigations revealed that the macrocycles bind halide anions strongly with fluoride being most strongly bound by **1.62b** and **1.62c** (>10^4 M^{-1} for both **1.62b** and **1.62c**). Good size complementarity is seen for iodide with **1.62d** as it gave the highest stability constant (900 M^{-1}) compared to the other receptors (370 M, 560 and 470 M^{-1} for

1.62a, **1.62b** and **1.62c** respectively). Benzoate anions were found to bind to the receptor in a 1:2 host/anion stoichiometry a result rationalised by the relative size of the benzoate anion compared with the spherical halides, thus the anion is only partially bound within the cavity allowing a second anion to interact with the cavity.

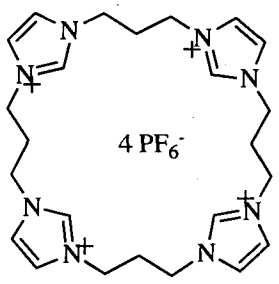

1.62a

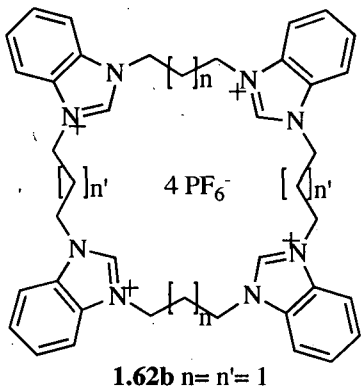

1.62b n= n'= 1
1.62c n= 1, n'= 2
1.62d n= n'= 2

Alcalde and co-workers have reported that imidazolium-based heterophanes, such as **1.63**, are capable of anion recognition.[71]

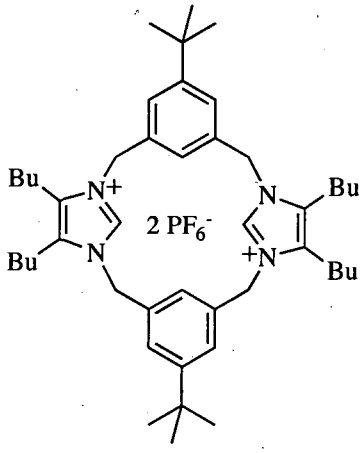

1.63

Proton NMR spectroscopy was employed in order to examine the anion-binding behavior of receptor **1.63**. Upon the addition of a number of anionic guests (added as their tetrabutylammonium salts) to compound **1.63**, significant changes in the C2 proton resonance of the imidazolium ring were observed in both CD_3CN and DMSO-d_6

solutions. Proton NMR titration experiments in DMSO-d_6 were then carried out and revealed that **1.63** binds acetate most strongly and with a 1:1 binding stoichiometry (K_a = 359 ± 42 M^{-1}).

Steed and co-workers have also utilised a tripodal backbone to construct a number of tri-pyridinium 'venus flytrap' receptors (**1.64a – 1.64c**) and investigated their anion binding and sensing properties.[72,73]

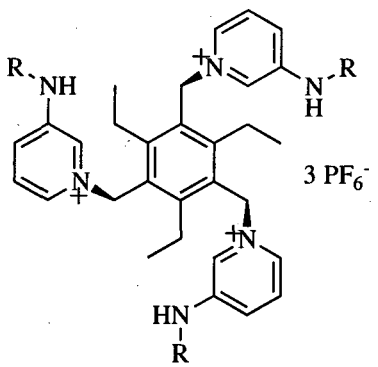

1.64a R= H

1.64b R= Bn

1.64c R=

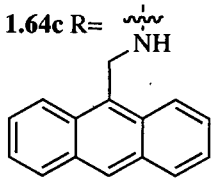

Receptors **1.64a** and **1.64b** showed similar anion binding behaviour with both receptors binding chloride most strongly (constants of >100,000 M^{-1} calculated for both receptors). In the case of compound **1.64b** reduced affinities were observed for both bromide and acetate (3953 M^{-1} and 2511 M^{-1} respectively) compared to **1.64a** (13800 M^{-1} and 10500 M^{-1} respectively) which was attributed to the increased steric bulk provided by the benzyl groups. For compound **1.64c** chloride is bound stronger than bromide (similar to **1.64a** and **1.64b**) however the affinities for halides are greatly reduced compared to **1.64a** and **1.64b** (5370 M^{-1} for chloride and 486 M^{-1} for bromide). Receptor **1.64c** was highly selective for acetate with the stability constant being almost an order of magnitude higher than the chloride constant (49000 M^{-1} against 5370 M^{-1}). Variable temperature ^{1}H NMR experiments were carried out and showed that compound **1.64c** selectively binds acetate over the spherical halide anions due to mixtures of conformers being adopted in solution through anthracene-anthracene mutual interactions. Further evidence of the conformational behaviour of compound **1.64c** and its selectivity for acetate over other anions was provided by UV spectroscopy and fluorescence studies.

Shinoda and co-workers have reported the one-step synthesis and anion binding properties of macrocycle **1.65**.[74] Proton NMR titration experiments (in D_2O) were used to determine the binding properties of **1.65** for tricarboxylate anions and revealed that the tricarboxylate **1.66** was bound with the highest affinity (log $K_a = 5.1$).

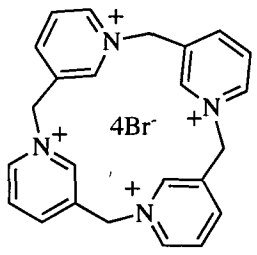

1.65

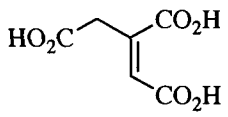

1.66

1.5.2 GUANIDINIUM BASED RECEPTORS

Guanidinium groups may be regarded as charged analogues of ureas in that they have two parallel NH groups and as a consequence often show high affinities for oxyanionic species such as carboxylates binding these anions by a combination of hydrogen bonding and electrostatic interactions. Guanidinium-carboxylate and phosphate interactions occur in many biological systems, as a guanidinium group is present in the amino acid arginine.

Schmidtchen and co-workers have described the binding of benzoate to the guanidinium based receptors **1.67a** and **1.67b**.[75] ITC titrations were carried with the iodide salts of **1.67a** and **1.67b** in acetonitrile at 30 °C with benzoate (added as its tetraethylammonium salt) and binding constants of 280,000 M^{-1} and 203,000 M^{-1} were calculated for **1.67a** and **1.67b** respectively. Receptor **1.67a** was investigated further where ITC titration experiments (under identical conditions to previous titration) were carried with **1.67a** and a variety of counter anions. It was found that the change in counter anion had significant effects upon the binding constant of benzoate observed, for example with the tetrafluoroborate anion a binding constant of 414,000 M^{-1} was calculated compared to a binding of 38,000 M^{-1} with chloride.

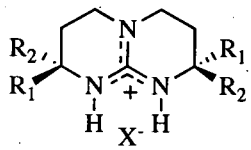

1.67a $R^1 = R^2 = CH_2CH{=}CH_2$
1.67b $R^1 = H$, $R^2 = CH_2OSi\textit{t}BuPh_2$

$X^- = Cl^-, Br^-, I^-, BF_4^-, PF_6^-$

For several years Schmuck has investigated the binding affinities of guanidinium salts appended to hydrogen bonding pyrrole-containing motifs and has shown how carboxylate anion binding is enhanced by the hybrid receptors. In 1999 Schmuck reported the binding ability of **1.68a** with various carboxylate anions in highly competitive media.[76] Proton NMR titration in DMSO-d_6/40% H_2O at 25 °C revealed that **1.68a** formed stronger complexes with acetate and Ac-L-Phe anions with binding constants of 2790 M^{-1} and 1700 M^{-1} respectively.

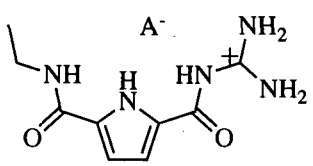

1.68a A^- = picrate

Schmuck then investigated a series of guanidinium appended pyrrole receptors and found that **1.68b** bound Ac-L-Ala-O^- more strongly than **1.68a** (1610 M^{-1} and 770 M^{-1} respectively).[77] The binding ability of **1.68b** was then assessed with a range of carboxylate anions by ^1H NMR titrations in DMSO-d_6/40% H_2O at 25 °C and showed that compound **1.68b** formed stronger complexes with the anions than **1.68a**. High affinities were observed for 2-pyrrole-COO^- and acetate (5275 M^{-1} and 3380 M^{-1}). A notable result was that compound **1.68b** displayed enantioselectivity in the case of Ac-Ala-O^- anions where a higher affinity was observed for the L-enantiomer over the D-enantiomer (1610 M^{-1} *vs.* 930 M^{-1}).

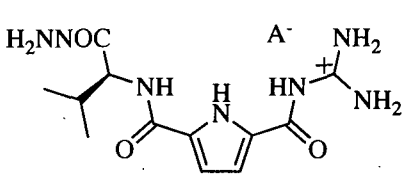

1.68b A^- = picrate

In 2005 Schmuck and Schwegmann reported the study of a tripodal 'molecular flytrap' **1.69** where the pyrrole-guanidinium moieties were appended to a triamide backbone.[78] The receptor was designed to bind tricarboxylate anions and UV and fluorescence titration experiments in water showed that **1.69** bound citrate and trimesoate with association constants $>10^5$ M^{-1}.

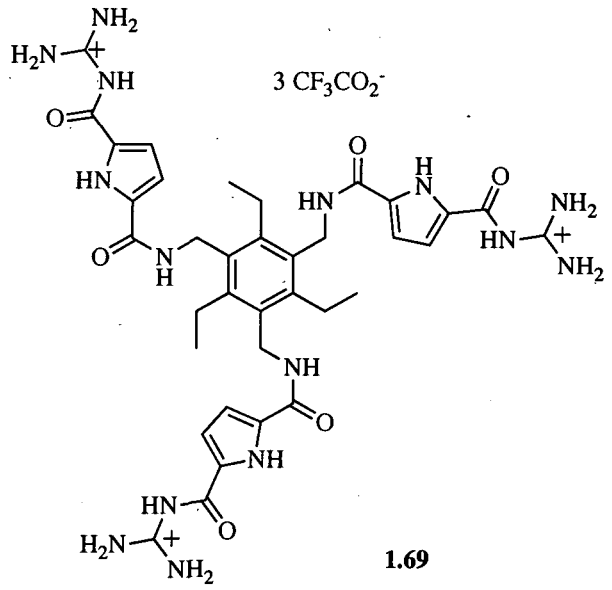

1.69

Recently de Mendoza and co-workers have reported the complexation of nitrate to an acyclic cleft and a series of macrocycles based on guanidinium.[79]

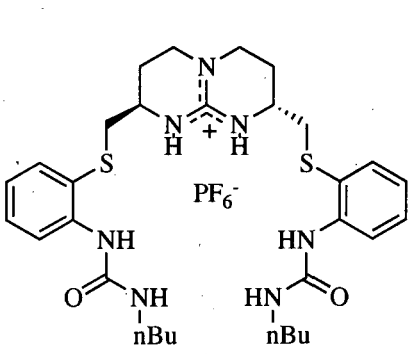

1.70

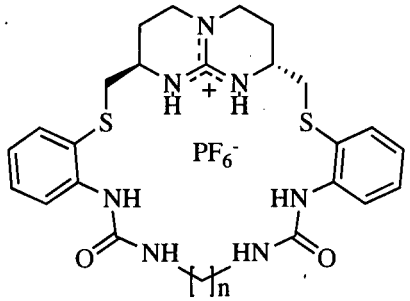

1.71a n= 4
1.71b n= 5
1.71c n= 6

Association constants were calculated by ITC titrations in acetonitrile at 303 K and it was found that the macrocyclic receptors bound the nitrate anion more strongly than

the acyclic system. The constants obtained for the macrocycles **1.71a**-**1.71c** revealed a size dependence on the binding of nitrate with the largest macrocycle **1.71c** giving rise to the highest association constant of 73.7×10^3 M^{-1}, an order of magnitude greater than the smallest macrocycle **1.71a** (7.26×10^3 M^{-1}).

1.6 AIMS OF THIS THESIS

The examples discussed in this introductory chapter provide a broad overview of the uses of synthetic organic receptors in the binding and sensing of anionic species and some recent advances in anion receptor chemistry. As the understanding of the processes and factors that influence the effective binding of anions improves there is increasing impetus to apply this knowledge to solve real-world problems.

The thesis discusses the synthesis, characterisation and molecular recognition of simple macrocyclic and acyclic systems and has been divided into the following subsections:

- Investigation into the ion-pair recognition behaviour of both *meso*-octamethylcalix[4]pyrrole and *N*-confused octamethylcalix[4]pyrrole in the solid state and in solution.
- A series of new indole based receptors have been synthesised and their anion recognition properties have been investigated in solution and in the solid state.
- The development of receptors with appended protonatable groups for the use as sulfuric acid receptors in the hydrometallurgical extraction of nickel(II)sulfate *via* a dual host strategy.

CHAPTER 2 - ION-PAIR RECOGNTION PROPERTIES OF CALIX[4]PYRROLE DERIVATIVES: SOLID STATE AND SOLUTION STUDIES

2.1 INTRODUCTION

2.1.1 DITOPIC RECEPTORS FOR ORGANIC SALTS

Within the field of supramolecular chemistry an emerging area of interest is the recognition of ion-pairs, in which a host binds both cationic and anionic guests simultaneously.[3-5] In certain instances receptors designed for this purpose may exhibit allosteric behaviour, where the binding of one ionic species induces conformational and/or electrostatic changes to the receptor that facilitates the co-ordination of the counter ion, resulting in higher association constants for the ion pair than for the single ionic species.[4]

In 2001 Pochini and co-workers described the synthesis of new receptors based on extended calix[4]arene (e.g. **2.1a** and **2.1b**) and upon the binding of a number of tetramethylammonium salts a positive allosteric effect was observed with **2.1a**.[80]

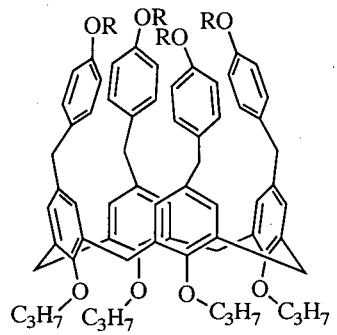

2.1a R = H
2.1b R = Me

In the case of **2.1a** the receptor was designed to bind the ion-pair *via* the encapsulation of the tetramethylammonium cation within a 'cage-like' structure induced by the binding of the anion to the pendent hydroxy groups (**Figure 2.1**). A ROESY NMR experiment with **2.1a** and TMA tosylate provided evidence for the formation of the anion induced 'cage-like' structure and the encapsulation of the tetramethylammonium cation. Association constants for the 1:1 complexation of **2.1a** with a number of tetramethylammonium salts were calculated from ^{1}H NMR titrations in $CDCl_3$ at 300 K and revealed that **2.1a** had strong affinity for TMA acetate (K_a = 10,000 M^{-1}). The stability of the complexes were found to be strongly dependent on the polarity of the solvent system where additions of polar solvent, such as CD_3OD and DMSO-d_6, to the chloroform solutions resulted in the release of the cation from the cavity. It was believed that competitive binding between the solvent and anion molecules to the hydroxy groups disrupted the anion-induced formation of the 'cage-like' structure and therefore the binding of the cation was unable to occur. Titration studies with **2.1b** showed that in the absence of hydrogen-bond donor groups the anion-induced cage was not formed and little evidence of cation binding was observed, a result providing additional evidence for the positive anion-induced allosteric effect observed in **2.1a**.

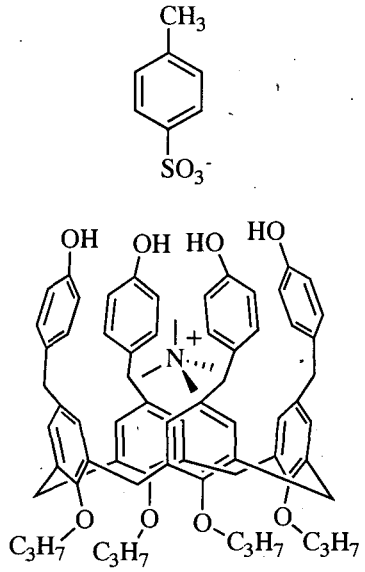

Figure 2.1: Proposed ion-pair binding of TMA tosylate in **2.1a**.

Atwood and Szumna have described a series of molecular capsules based on a modified resocin[4]arene scaffold for the encapsulating of tetramethylammonium halide salts.[81] Initially **2.2a** was synthesised and was found to encapsulate the TMA cation within a cavity through multiple CH-π interactions.

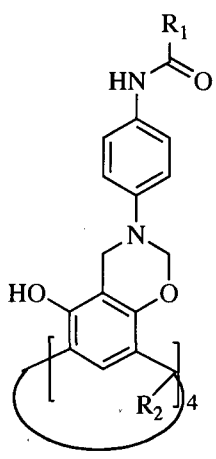

2.2a $R_1 = CH_3$, R_2 = Et
2.2b R_1 = Ph, R_2 = *i*-Bu
2.2c R_1 = Ph, R_2 = Et

An X-ray crystal structure of the TMACl complex of **2.2a** obtained from a chloroform/nitrobenzene solution revealed that the chloride anion was bound by the four

amide NH groups, however the x-ray crystal structure obtained from more polar solvents showed that the chloride anion was not bound to the amide groups presumably due to competing interactions from the polar solvent molecules (**Figure 2.2**).

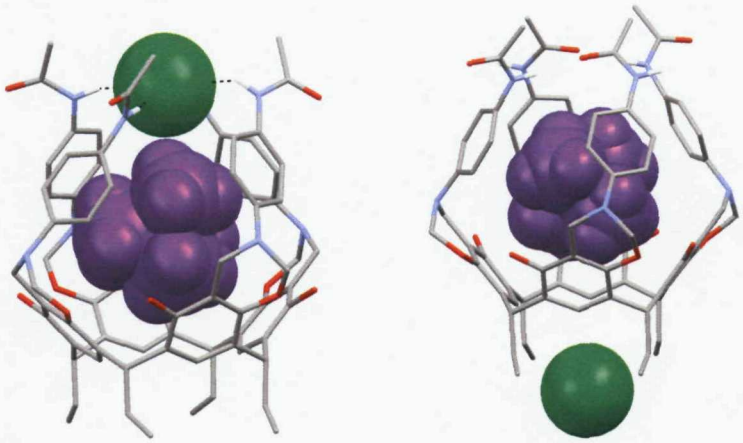

Figure 2. 2: Crystal structure TMACl complex of **2.2a** crystallised from $CHCl_3$:nitrbenzene and $CHCl_3$:MeOH respectively.

The same authors then synthesised receptors **2.2b** and **2.2c** as it was hoped that the inclusion of the phenyl amide groups would encapsulate and isolate the anion away from the polar solvent media.[82] The structural modification was shown to improve the stability of both TMACl and TMABr complexes of **2.2b** in the presence of high methanol concentrations and the crystal structure of the TMACl complex of **2.2c** revealed that the presence of the phenyl groups shield the anion from the surrounding solvent media (**Figure 2.3**).

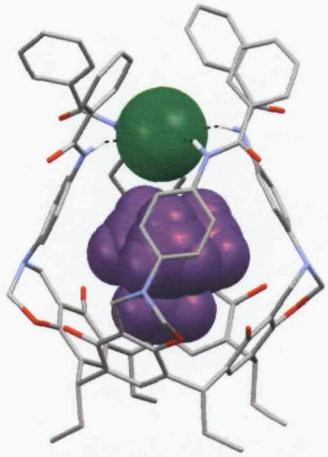

Figure 2.3: Crystal Structure of the TMACl complex of **2.2c**.

Smith and co-workers have reported the binding of alkylammonium contact ion-pairs with **2.3**, an azo-crown strapped with an isophthalamide moiety.[83] Association constants for a number of alkylammonium salts were calculated by ^{1}H NMR titration in $CDCl_3$:DMSO-d_6 85:15 solutions at 295 K and revealed that *n*-propylammonium chloride was bound with the highest affinity (K_a = 2.0 × 10^4 M^{-1}). The selectivity was attributed to the deep penetration of the ammonium cation into the receptor cavity coupled with the predisposed selective of the isophthalamide group for the chloride anion.

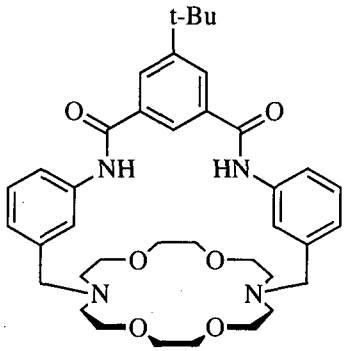

2.3

In 2003 Mandolini, Rissanen and co-workers reported the recognition of quaternary ammonium chloride salts with the uranyl-salophen based receptors **2.4a** and **2.4b**.[84] Binding constants were calculated by ^{1}H NMR titration in $CDCl_3$ at 25 °C and revealed that **2.4b** bound TMACl over two times greater than **2.4a** (28,000 ± 2000 M^{-1} and 13,600 ± 2000 M^{-1} respectively) attributed to the polarizability of the naphthalene providing stronger cation-π interactions.

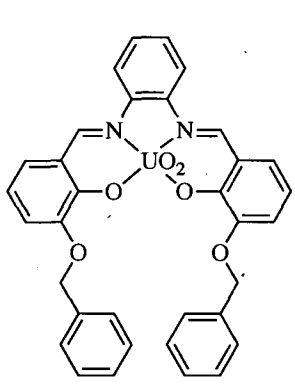

2.4a

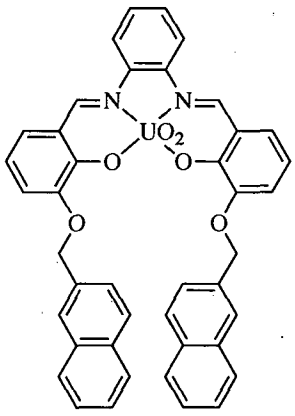

2.4b

The same authors have recently shown that **2.4a** and **2.4b** binds to more complex organic salts such as NMPI and NmiQI.[85]

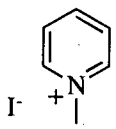

NMPI

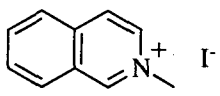

NMiQI

Binding constants calculated by ^{1}H NMR titration in $CDCl_3$ at 25 °C again revealed that the presence of the naphthalene groups in **2.4b** increased the affinity for the salts compared to **2.4a**. In the case of NMPI, **2.4b** bound the salt approximately four times higher than **2.4a** (500 M^{-1} and 130 M^{-1} respectively) and with the more aromatic cation, NmiQI, a binding constant of 800 M^{-1} was obtained with **2.4b**, approximately a seven-fold increase to that achieved with **2.4a** (110 M^{-1}).

2.2 ION-PAIR RECOGNITION PROPERTIES OF *MESO*-OCTAMETHYL CALIX[4]PYRROLE

Meso-octamethylcalix[4]pyrrole, **2.5**, was originally synthesised by Baeyer in 1886 and is arguably the simplest anion receptor to synthesise as it is formed in high yields in one step *via* the acid catalysed condensation of pyrrole and acetone.[56] In 1996 Sessler and co-workers found that the macrocycle bound anionic guests with a 1:1 stoichiometry *via* four hydrogen bond interactions and had high affinities for fluoride and chloride anions in CD_2Cl_2 solutions.[55]

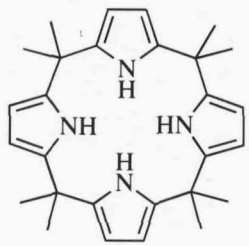

2.5

X-ray crystal structures of **2.5** revealed that the receptor adopted a 1,3-alternate conformation in the absence of anionic guestsin the solid state and, in the presence of an anionic guest **2.5**, adopted a cone-like conformation to accommodate the anion and to maximise the hydrogen bond interactions between host and guest (**Figure 2.4**).

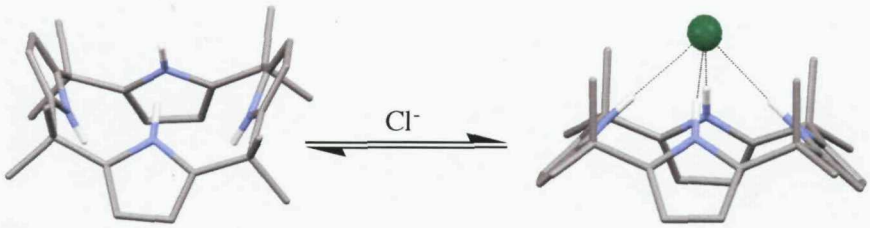

Figure 2.4: Anion induced conformation change with **2.5** in the solid state.

The anion-induced change in conformation also results in the formation of an electron rich cavity at the 'base' of the cone. However, the electron rich cup has not yet been shown to serve as a receptor for cationic guests but the possibility that **2.5** could

function as an ion-pair receptor led us to study further **2.5** in both the solid state and in solution. Initially crystallographic studies were carried out, as any potential ditpoic behaviour would be most strongly manifested in the solid state. These studies were followed by solution studies in order to ascertain if the ion-pair recognition occurs in solution and is not a phenomena observed only in the solid state.

2.2.1 TETRAALKYLAMMONIUM SALT COMPLEXES

X-ray quality crystals of all complexes were prepared by the slow evaporation of dichloromethane solutions of **2.5** in the presence of tetramethylammonium fluoride (TMAF), tetramethylammonium chloride (TMACl), tetramethylammonium bromide (TMABr), tetraethylammonium fluoride (TEAF), tetraethylammonium chloride (TEACl) and tetraethylammonium bromide (TEABr).

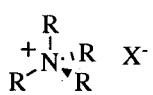

TMAF - R = Me, X = F
TMACl - R = Me, X = Cl
TMABr - R = Me, X = Br
TEAF - R = Et, X = F
TEACl - R = Et, X = Cl
TEABr - R = Et, X = Br

Complexes **2.5**·TMAF, **2.5**·TMACl and **2.5**·TMABr were found to be isostructural. In all three complexes the anions were bound by all four hydrogen bonds from the pyrrole NH's. The fluoride complex had the shortest hydrogen bond distance with a N···F distance of 2.808 Å, followed by chloride (N···Cl distances of 3.288-3.299 Å) and the bromide complex had the longest hydrogen bond distance with N···Br distances of 3.448-3.449 Å. In all three crystal structures the tetramethylammonium cations were found to be disordered but interestingly were included in the anion induced 'cup' with one methyl group pointing directly into the electron rich cavity (**Figure 2.5**).

The cation inclusion is illustrated in the space filling representation of the crystal structures (**Figure 2.6**).

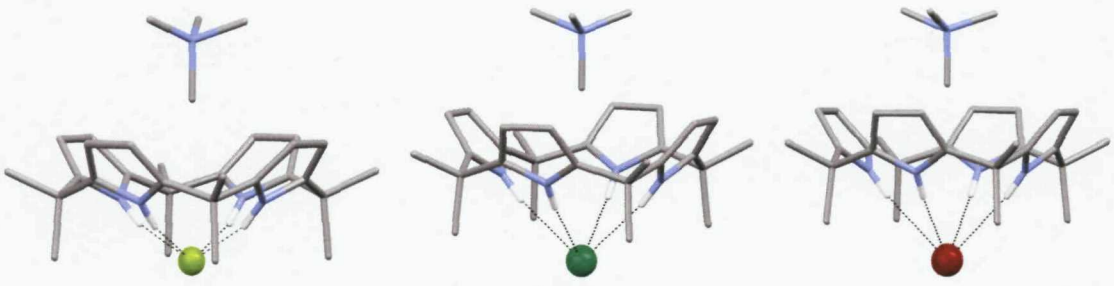

Figure 2.5: Crystal structures of complexes **2.5**·TMAF, **2.5**·TMACl and **2.5**·TMABr respectively (hydrogens omitted for clarity).

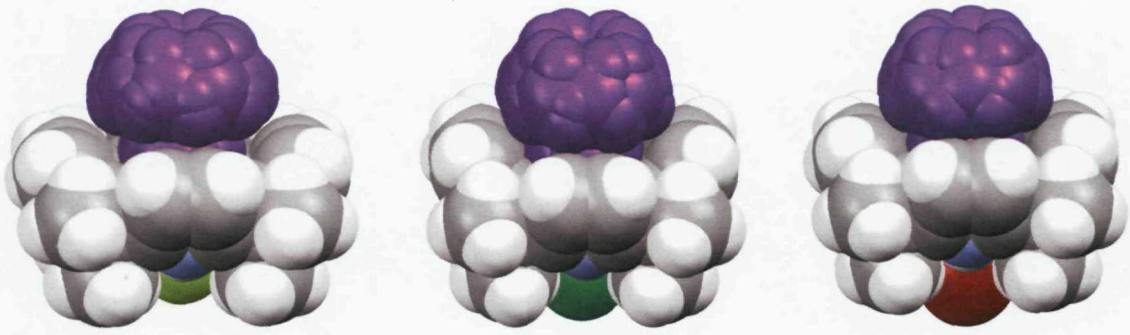

Figure 2.6: Space filling representation of complexes **2.5**·TMAF, **2.5**·TMACl and **2.5**·TMABr respectively.

Complexes **2.5**·TEAF, **2.5**·TEACl and **2.5**·TEABr were found to be isostrucutral with all three anions again being bound by four pyrrole NH hydrogen bonds with a N···F distance of 2.748(2) Å, N···Cl distances of 3.2574(18)-3.3411(18) Å and N···Br distances of 3.408(3)-3.462(3) Å. In all cases the tetraethylammonium cation was found to be included in the electron rich cavity of the calix[4]pyrrole with two of the CH_2 groups of the ethyl chain pointing into the anion induced cavity. The inclusion is illustrated in the space filling representations of the crystal structures (**Figure 2.8**).

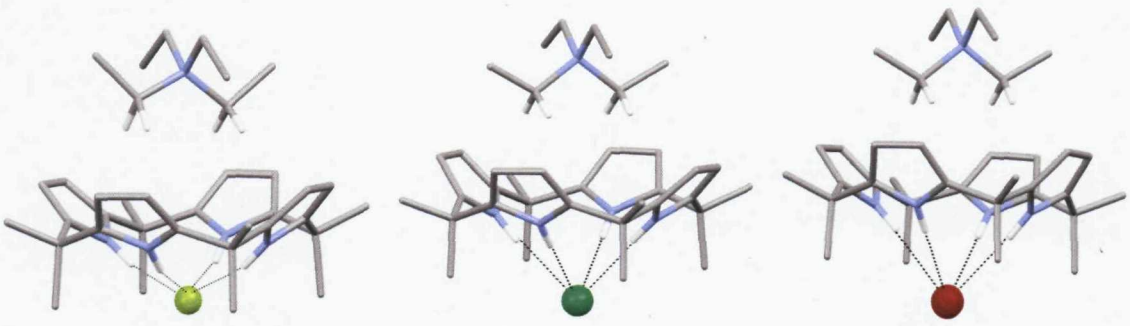

Figure 2.7: Crystal structures of complexes **2.5**·TEAF, **2.5**·TEACl and **2.5**·TEABr respectively (hydrogens omitted for clarity).

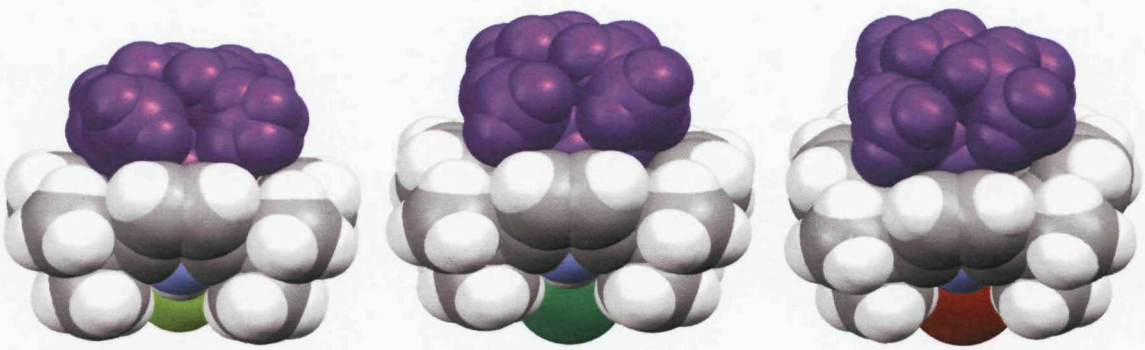

Figure 2.8: Space filling representation of complexes **2.5**·TEAF, **2.5**·TEACl and **2.5**·TEABr.

The extent of the inclusion of the cation within the anion induced cavity can be assessed to some degree by the distance between the central nitrogen atom of the cation and a centroid of the macrocycle (defined by the four nitrogens of the calix[4]pyrrole), which is shown in **Figure 2.9**. In the case of the alkylammonium chloride salts the distance increases with the increase of the size of the cation with distance of 3.906, 4.361 and 4.445 Å for the TMA, TEA and TBA cations respectively.

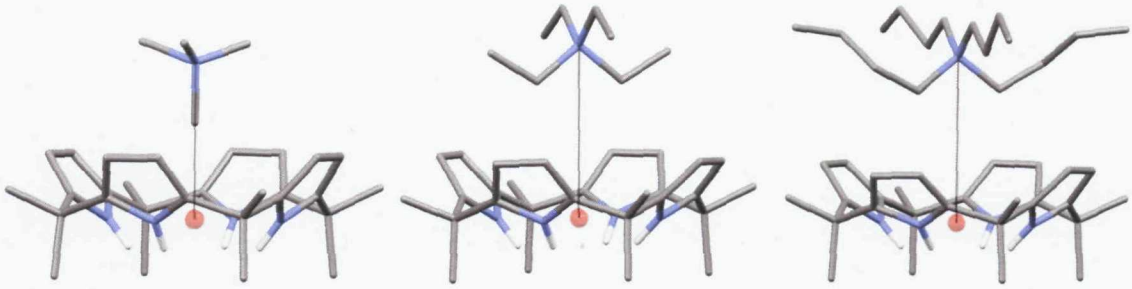

Figure 2.9: Structures of **2.5**·TMACl, **2.5**·TEACl and **2.5**·TBACl respectively showing distance from cation N atom to a centroid of **2.5** (chloride and hydrogens omitted for clarity).

2.2.2 SOLUTION STUDIES

The solid-state results prompted the study of the behaviour of calix[4]pyrrole in solution. Jonathan Sessler from the University of Texas at Austin and Franz Schimdtchen from Technische Universität München conducted ^{1}H NMR and ITC titration experiments of *meso*-octamethylcalix[4]pyrrole, **2.5**, with a variety of alkylammonium chloride salts.[86] Their results showed that when applying a simple 1:1 binding model to the data obtained from the titration experiments the association constants were greatly influenced by both the cation and solvent used in the experiments (**Table 2.1**).

Table 2.1: Stability constants (M^{-1}) of **2.5** with a number of organic chloride salts in both dichloromethane-d_2 and dimethylsulfoxide-d_6/0.5% water solutions at 298 K.

Organic Salt	DCM	DMSO	MeCN
TBACl	430	2200	25000
TEACl	3700	2300	22000
TPACl	660	-	-

The result of the ^{1}H NMR titrations in both CD_3CN and DMSO-d_6 revealed that there were insignificant differences between the chloride association constants with the different cations. However the constants obtained from dichloromethane showed that the chloride association constants were greatly affected by the counter cation present.

The results showed that as the size of the cation increased the chloride association constants decreased (TEA > TPA > TBA).

2.2.3 ORGANIC HALIDE SALT (IONIC LIQUIDS) COMPLEXES

The ion-pair recognition properties of *meso*-octamethylcalix[4]pyrrole, **2.5**, were further investigated with the commercially available dialkyl imidazolium halides salts. Similar to the studies with the alkylammonium salts crystallographic studies were initially conducted as any interaction between the anion induced electron rich cavity of **2.5** and the cation would be manifested most strongly in the solid state.

X-ray quality crystals of *N,N'*-dialkylimidazolium salts complexes were prepared by the slow evaporation of **2.5** in dichloromethane in the presence of the ionic liquids 1-butyl-3-methylimidazolium chloride (BMIMCl), 1-butyl-3-methylimidazolium bromide (BMIMBr), 1-ethyl-3-methylimidazolium chloride (EMIMCl) and 1-ethyl-3-methylimidazolium bromide (EMIMBr).

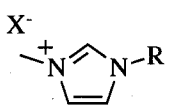

BMIMCl - R = *n*-Bu, X = Cl
BMIMBr - R = *n*-Bu, X = Br
EMIMCl - R = Et, X = Cl
EMIMBr - R = Et, X = Br

The crystal structure of complexes **2.5**·BMIMCl and **2.5**·BMIMBr were found to be isostructural with both anions being bound by all four pyrrole NH groups with N···Cl distances of 3.2934(19)-3.3499(19) Å for **2.5**·BMIMCl and N···Br distances of 3.404(9)-3.469(7) Å for **2.5**·BMIMBr. Interestingly, the imidazolium cation was found to be included in the electron rich cavity of the **2.5** *via* interactions of the 4- and 5-position protons of the imidazolium cation and the π-electron cloud of the calix[4]pyrrole (inclusion shown in space filling representations **Figure 2.11**).

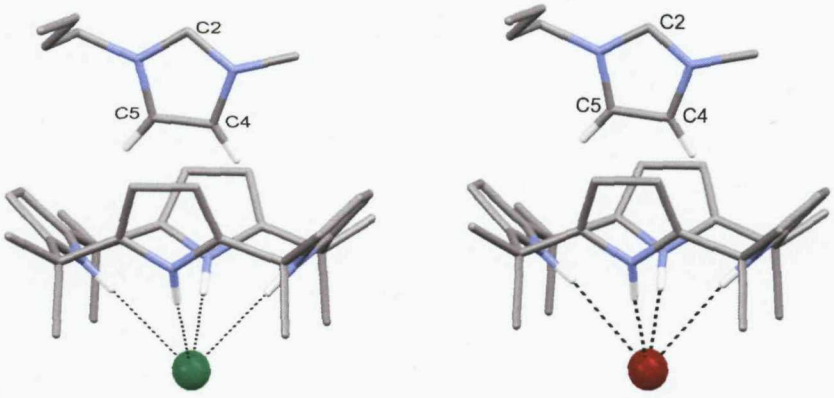

Figure 2.10: Crystal structures of complexes **2.5**·BMIMCl and **2.5**·BMIMBr (hydrogens omitted for clarity).

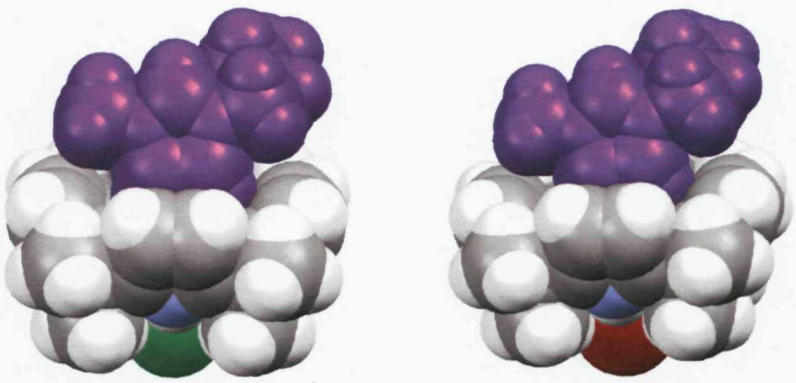

Figure 2.11: Space filling representation of complexes **2.5**·BMIMCl and **2.5**·BMIMBr.

Additional interactions between the C2-postion proton of the imidazolium cation and an adjacent anion led to the formation of one-dimensional chains in the extended crystal structures of both **2.5**·BMIMCl and **2.5**·BMIMBr (C2···Cl distance of 3.472(2) Å for **2.5**·BMIMCl and C2···Br distances of 3.513(11) Å for **2.5**·BMIMBr).

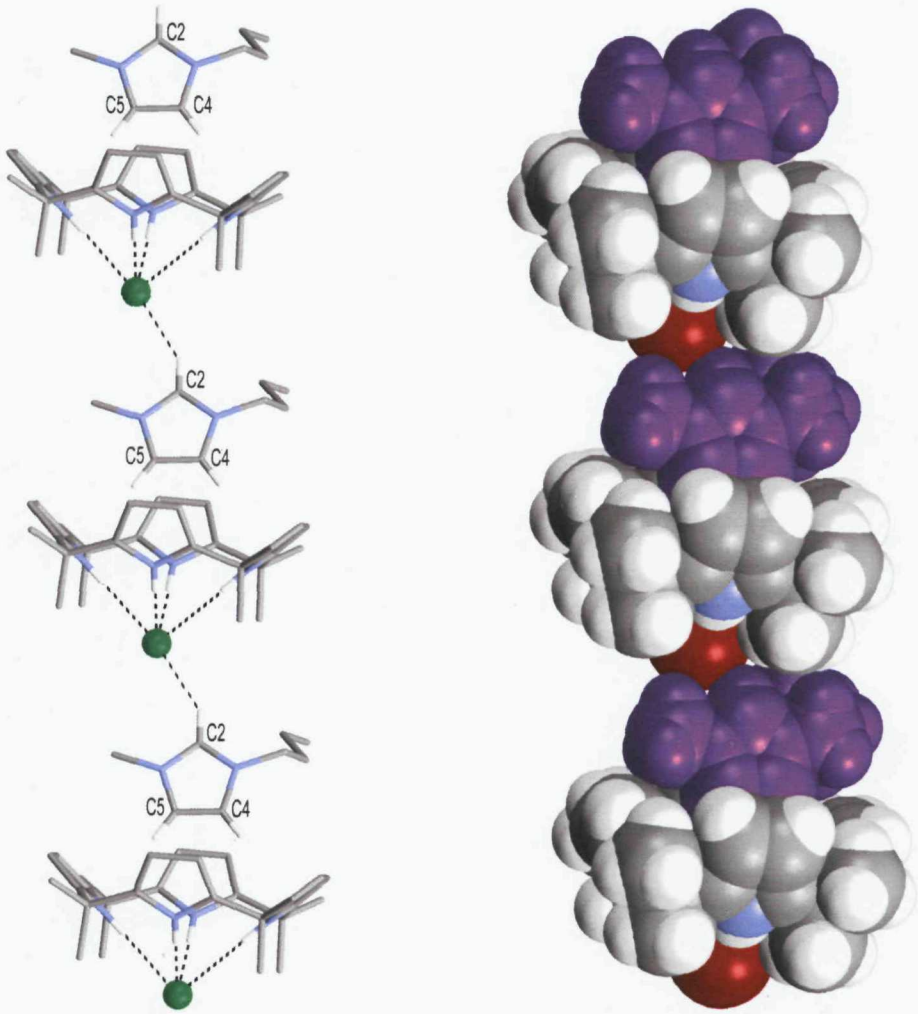

Figure 2.12: One-dimensional chain formation of complex **2.5**·BMIMCl and space filling representation of the one-dimensional chain in complex **2.5**·BMIMBr respectively.

Complexes **2.5**·EMIMCl and **2.5**·EMIMBr were found to be isostrucutral. Again both the anions were bound by the four pyrrole NH groups with N···Cl distances of 3.231(4)-3.306(5) Å for **2.5**·EMIMCl and N···Br distances of 3.398(4)-3.455(4) Å for **2.5**·EMIMBr. Similar to complexes **2.5**·BMIMCl and **2.5**·BMIMBr the imidazolium cation is included in the electron rich 'cup' with the 4- and 5- position proton of the cation pointing into the anion induced cavity (**Figure 2.13**).

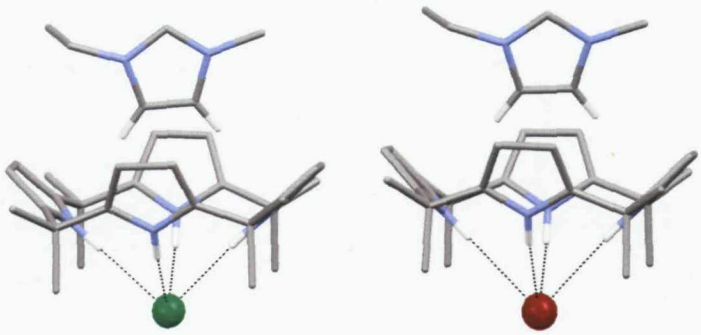

Figure 2.13: Crystal structure of complexes **2.5**·EMIMCl and **2.5**·EMIMBr respectively (hydrogens omitted for clarity).

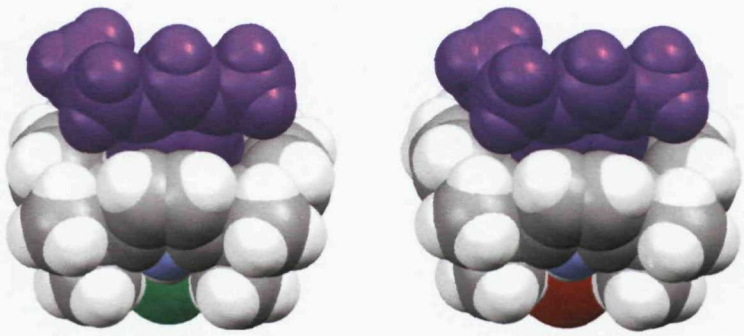

Figure 2.14: Space filling view of complexes **2.5**·EMIMCl and **2.5**·EMIMBr,

1-Butyl-3-methylimidazolium fluoride (BMIMF) and 1-ethyl-3-methylimidazolium fluoride (EMIMF) are not commercially available ionic liquids however the complexes with **2.5** were obtained by slow evaporation of dichloromethane solutions of **2.5** and 1 equivalent of tetrabutylammonium fluoride in the presence of the ionic liquids 1-butyl-3-methylimidazolium tetrafluoroborate and 1-ethyl-3-methyl imidazolium tetrafluoroborate.

The crystal structure of complex **2.5**·BMIMF revealed that the fluoride anion binds to all four pyrrole NH groups with N···F distances between 2.759(5)-2.806(5) Å (**Figure 2.15**). Similar to the analogous complexes **2.5**·BMIMCl and **2.5**·BMIMBr complex **2.5**·BMIMF forms a one-dimensional chain in the extended crystal structure *via* an additional interaction between the 2-postion CH group of the imidazolium cation and an adjacent fluoride anion with a C2···F distance of 2.902 Å (**Figure 2.16**).

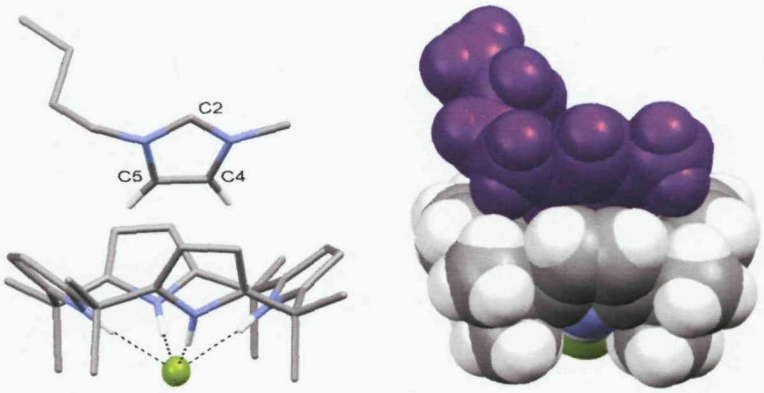

Figure 2.15: X-ray crystal structure and space filling view of **2.5**·BMIMF respectively.

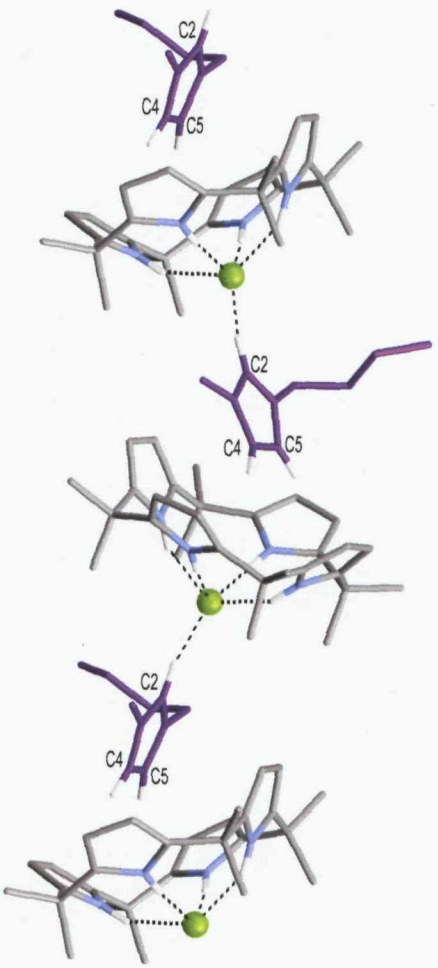

Figure 2.16: One-dimensional chain formed in the crystal of **2.5**·BMIMF.

In the crystal structure of **2.5**·EMIMF, the fluoride anion was found to interact with all four pyrrole NH groups with N···F distances between 2.765(4)-2.824(4) Å.

Unlike in the analogous **2.5**·EMIMCl and **2.5**·EMIMBr structures, the cation was found to be orientated into the cavity *via* the methyl group in the 3-position of the imidazolium ring and the 2-position CH group, orientated towards a pyrrole group.

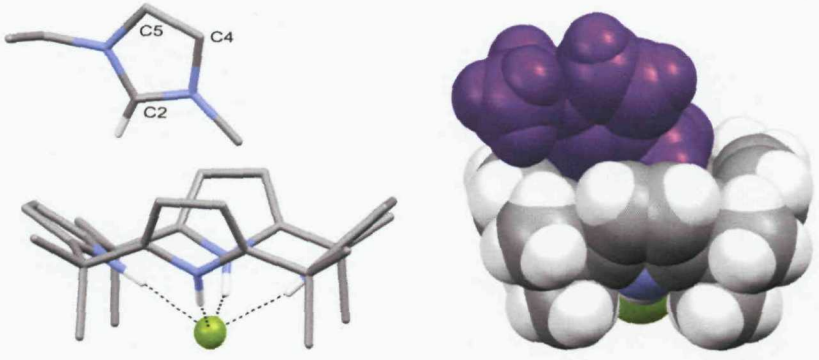

Figure 2.17: X-ray crystal structure and space-filling view of **2.5**·EMIMF.

Another class of commercially available ionic liquids are the *n*-alkylpyridinium salts. These were also co-crystallised with calix[4]pyrrole, **2.5**, in order to establish if the anion induced electron rich cup could accommodate the pyridinium cation. X-ray quality crystals were obtained by the slow evaporation of dichloromethane solution of **2.5** in the presence of *n*-ethylpyridinium chloride (EtPyCl), *n*-ethylpyridinium bromide (EtPyBr), *n*-propylpyridinium chloride (PrPyCl) and *n*-propylpyridinium bromide (PrPyBr).

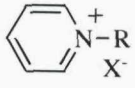

EtPyCl - R = Et, X = Cl
EtPyBr - R = Et, X = Br
PrPyCl - R = Pr, X = Cl
PrPyBr - R = Pr, X = Br

All the structures obtained resulted in the formation of discrete complexes within the crystal. In accordance with all of the previous examples the anion was bound by the four pyrrole NH groups in all four crystal structures (For **2.5**·EtPyCl N···Cl distances between 3.256(2) Å – 3.335(2) Å, for **2.5**·EtPyBr N···Br distances between 3.393(5) Å –

3.505(5) Å, for **2.5**·PrPyCl N···Cl distances between 3.319(3) Å – 3.411(3) Å and for **2.5**·PrPyBr N···Br distances between 3.402(3) Å – 3.513(3) Å). In all cases the pyridinium cations were found to be included in the anion-induced cavity with the 2- and 3-position aromatic protons orientated into the cavity (**Figures 2.18-2.21**).

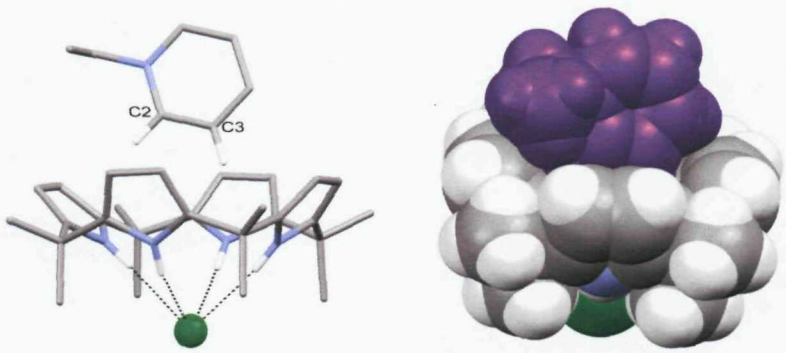

Figure 2.18: X-ray crystal structure and space filling view of **2.5**·EtPyCl respectively.

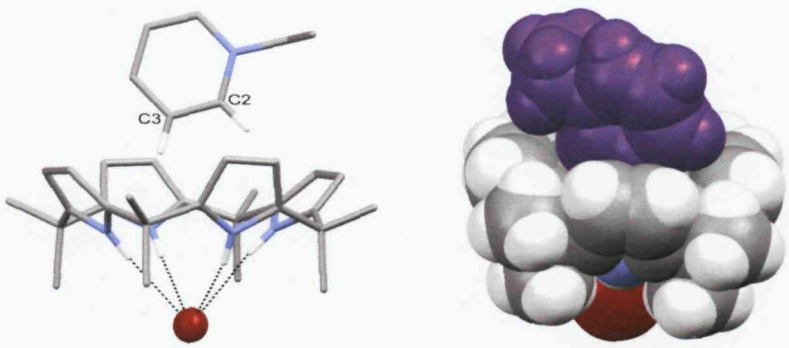

Figure 2.19: X-ray crystal structure and space filling view of **2.5**·EtPyBr respectively.

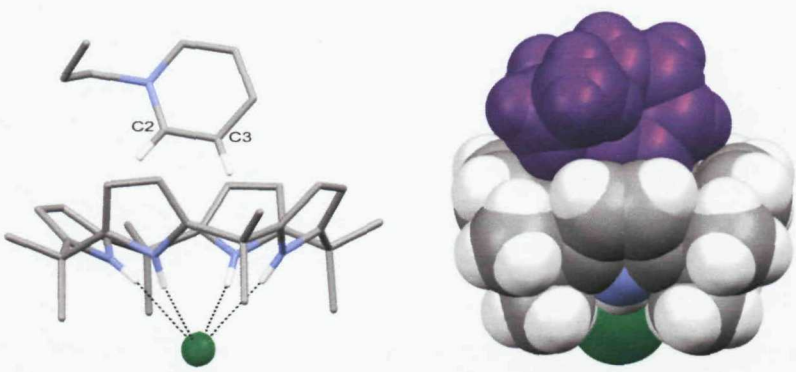

Figure 2.20: X-ray crystal structure and space filling view of **2.5**·PrPyCl respectively.

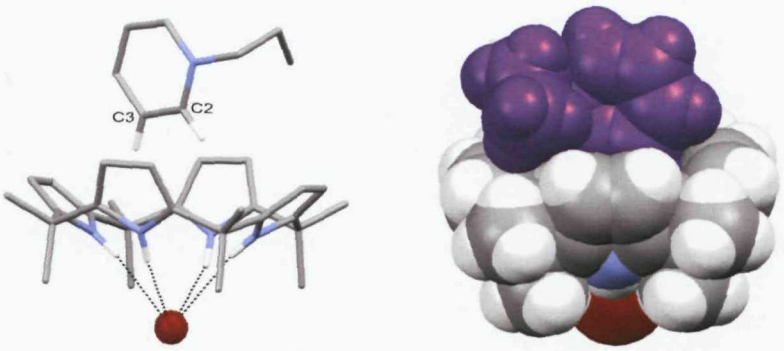

Figure 2.21: X-ray crystal structure and space filling view of **2.5**·PrPyBr respectively.

2.2.4 SOLUTION STUDIES WITH IONIC LIQUID HALIDE SALTS

Initially ^{1}H NMR experiments were carried out on solutions of 0.01M *meso*-octamethylcalix[4]pyrrole, **2.5**, in deuterated dichloromethane in the absence and presence of 1.0 equivalents of each of tetrabutylammonium chloride, 1-*n*-butyl-3-methylimidazolium chloride (**2.5**) and 1-butyl-3-methylimidazolium tetrafluoroborate ($BMIMBF_4$). The addition of the tetrafluoroborate salt to **2.5** caused insignificant changes to the ^{1}H NMR spectrum. Upon addition of tetrabutylammonium chloride, the NH resonance of **2.5** shifted downfield consistent with the binding of the chloride anion. Similarly upon addition of 1-butyl-3-methylimidazolium chloride to **2.5**, the calix[4]pyrrole NH resonances shifted downfield to 10.61 ppm.

Significant changes were observed for the shifts of the imidazolium protons upon the addition of the chloride salt compared to that observed with the tetrafluoroborate salt. The presence of **2.5** led to upfield shifts of the imidazolium protons in the 2-, 4- and 5- positions (to 7.26, 6.42 and 6.11ppm respectively). These shifts may be caused by shielding due to inclusion of the imidazolium cation in the electron rich 'cup' of the calix[4]pyrrole. In the case of $BMIMBF_4$ no significant shifts were observed for the imidazolium proton as the 'innocent' tetrafluoroborate anion does not interact with the macrocycle and hence does not pre-organize the cavity to allow for cation inclusion. Upon addition of 1.0 equivalents of tetrabutylammonium chloride to a solution of the macrocycle in the presence of 1.0 equiv. $BMIMBF_4$, upfield shifts of the imidazolium

cation were observed, consistent with the added chloride pre-organizing the cavity of the macrocycle thus triggering inclusion of the cation. Alternatively the shifts of the imidazolium protons upon the addition of BMIMCl to the calix[4]pyrrole solution might be due to the calix[4]pyrrole competing with the imidazolium cation for the chloride in solution, hence the macrocycle is diminishing the interaction between the ion-pair leading to changes in the imidazolium NMR resonances. However, the fact that innocent tetrafluoroborate salt of the same cation has imidazolium CH resonances at 8.83 and 7.22 ppm suggests that the observed upfield shifts were not caused by perturbations of the interaction between the imidazolium chloride ion pair but rather by inclusion of the cation in the calix[4]pyrrole cavity in solution (**Figure 2.22b**). The proton of interested are illustrated in Figure **2.22a**.

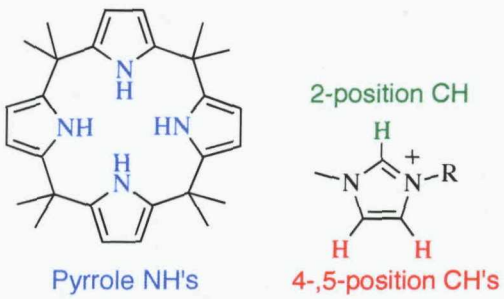

Figure 2.22a: Strucutre of calix[4]pyrrole and the imidazolium cation to illustrate the protons of interest.

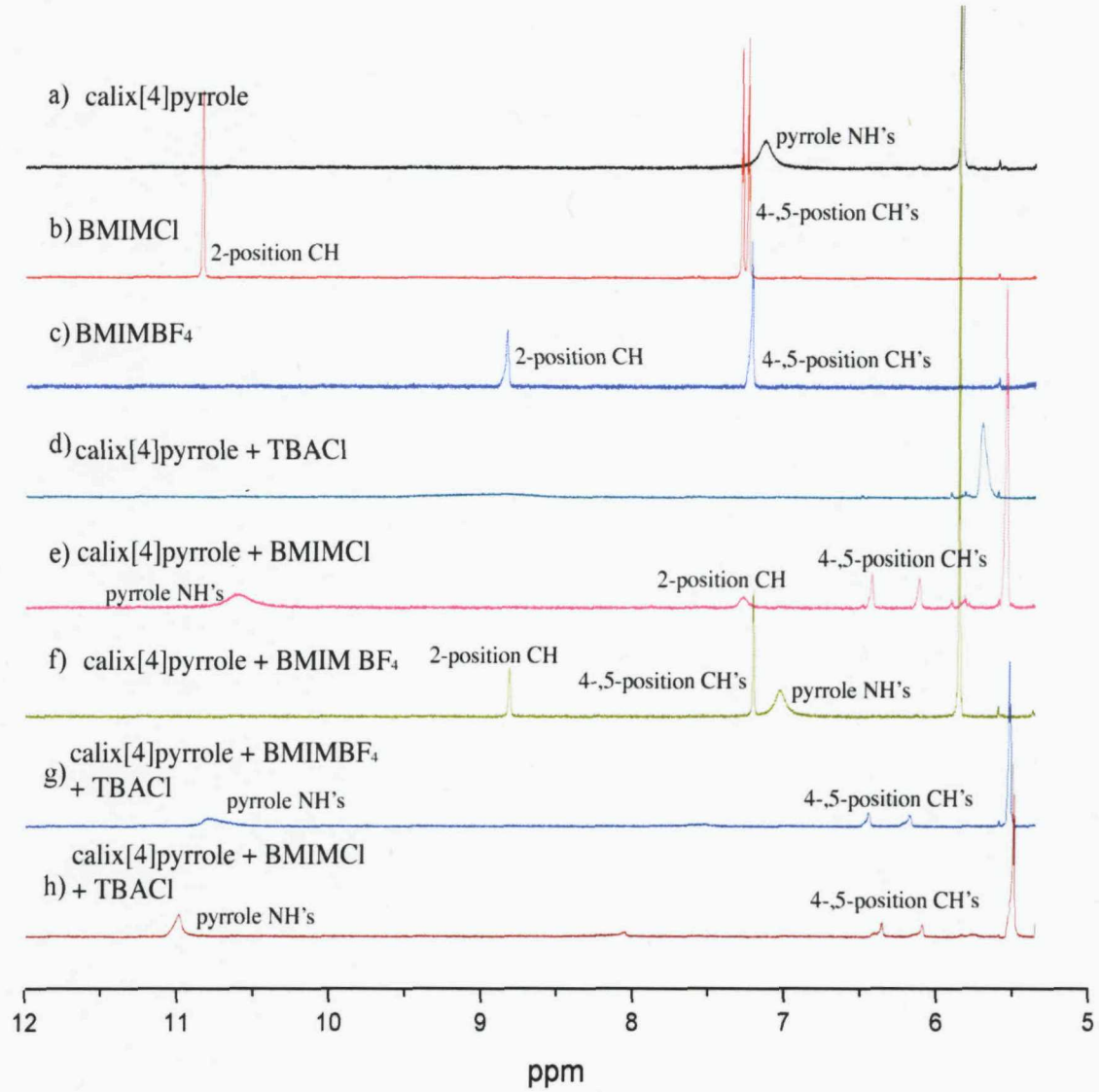

Figure 2.22b: NMR stack plot showing proton shifts with interactions of **2.5** with organic salts
NMR spectra of a) *meso*-octamethylcalix[4]pyrrole (**2.5**); b) 1-*n*-butyl-3-methylimidazolium chloride; c) 1-*n*-butyl-3-methylimidazolium tetrafluoroborate; d) *meso*-octamethylcalix[4]pyrrole + 1.0 equiv. tetrabutylammonium chloride; e) *meso*-octamethylcalix[4]pyrrole + 1.0 equiv. 1-*n*-butyl-3-methylimidazolium chloride; f) *meso*-octamethylcalix[4]pyrrole + 1.0 equiv. 1-*n*-butyl-3-methylimidazolium tetrafluoroborate; (g) *meso*-octamethylcalix[4]pyrrole + 1.0 equiv. 1-*n*-butyl-3-methylimidazolium tetrafluoroborate + 1.0 equiv. tetrabutylammonium chloride; h) *meso*-octamethylcalix[4]pyrrole + 1.0 equiv. 1-*n*-butyl-3-methylimidazolium chloride + 1.0 equiv. tetrabutylammonium chloride.

These results prompted further study into the ion-pair recognition properties of **2.5** in solution. Proton NMR titration experiments were conducted with *meso*-octamethylcalix[4]pyrrole, **2.5**, and various organic chloride salts in both dichloromethane-d_2 and dimethylsulfoxide-d_6 solutions (**Table 2.2**). The data obtained was fitted to a simple 1:1 binding model with EQNMR[87], hence the stability constants account for the binding of the chloride anion to **2.5** and does not measure the association of the various cations. The results obtained from dichloromethane-d_2 revealed that in the presence of different cations significant differences were observed in the chloride stability constants. The titration with tetrabutylammonium chloride resulted in the lowest stability constant (227 M^{-1}) whereas the titrations with the ionic liquids resulted in dramatically increased constants, compared to the tetrabutylammonium salt. A 10-fold increase in the stability constant was observed with 1-ethyl-3-methylimidazolium chloride and a 25-fold increase with 1-butyl-3-methylimidazolium chloride (2240 M^{-1} and 5960 M^{-1} respectively) compared to TBACl. The largest increase in stability constant was observed in the titration with 1-ethylpyridinium chloride (18000 M^{-1}), which is almost an 80-fold increase over the stability constant obtained with TBACl. Clearly the presence of the different cations greatly influences the chloride binding affinity of **2.5** presumably due to the inclusion of the cation in the anion-induced cavity of the calix[4]pyrrole, in non-polar dichloromethane solution, resulting in the stabilisation of the complex.

When the same titration experiments were conducted in the more competitive solvent, dimethylsulfoxide-d_6, the changes in the association constants were much less significant compared to the dichloromethane results. Similar stability constants were obtained from the titration data for **2.5** with the different chloride salts indicating that the cation has much less of an effect on the stabilisation of the complex in the more competitive dimethylsulfoxide-d_6 media (**Table 2.2**). The largest constant was gained with 1-ethyl-3-methylimidazolium chloride (1250 M^{-1}) and lowest was with the imidazolium salt 1-butyl-3-methylimidazolium chloride (825 M^{-1}).

Table 2.2: Stability constants (M^{-1}) of *meso*-octamethylcalix[4]pyrrole, **2.5**, with a number of organic chloride salts in both dichloromethane-d_2 and dimethylsulfoxide-d_6/0.5% water solutions at 298 K. All data fitted to a 1:1 binding profile, using EQNMR.[87] Errors (deviation from fit plot line) were estimated to be no more than ± 15%.

Organic Salt	DCM	DMSO
TBACl	230	980
EMIMCl	2240	1250
BMIMCl	5960	825
EtPyCl	18000	1100

The differences in the chloride stability constants obtained from dichloromethane could be a consequence of the complexation of the ion-pair whereas in the more competitive dimethylsulfoxide the similar constants could be a results of anion binding only and not the complexation of the ion-pair. Evidence for this was shown in stack plots of the ^{1}H NMR spectra of a) 1-ethyl-3-methylimidazolium chloride, b) 1-ethyl-3-methylimidazolium tetrafluoroborate, c) 1-ethyl-3-methylimidazolium chloride and 1eq. of *meso*-octamethylcalix[4]pyrrole, **2.5**, and d) *meso*-octamethylcalix[4]pyrrole, **2.5**, in both dichloromethane-d_2 and dimethylsulfoxide-d_6 (**Figure 2.23** and **Figure 2.24** respectively). The plot in dichloromethane-d_2 revealed significant upfield shifts in the 4- and 5- position protons of the imidazolium chloride salt (approximately 0.9 and 1.2ppm) in the presence of one equivalent of calix[4]pyrrole, **2.5**, which is consistent with cation inclusion. Interestingly in the presence of **2.5** the resonance of the 2-position proton of the imidazolium chloride salt shifted upfield by approximately 3.2ppm relative to the free salt and by approximately 1.4ppm compared to the tetrafluoroborate salt. This is evidence that the shifts are not due to the loss of the ion-pair alone but of another process such as cation inclusion. The same plot in the more competitive dimethylsulfoxide shows insignificant changes in the shifts of the 4- and 5- position protons of the imidazolium cation in the presence and absence of **2.5**, indicating little or no interactions between the *meso*-octamethylcalix[4]pyrrole and cation. There is a slight upfield shift of approximately 0.3ppm of the 2- position proton when 1-ethyl-3-methyl imidazolium chloride is in the presence of 1 equivalent of *meso*-octamethylcalix

[4]pyrrole relative to the free salt. However when compared to 1-ethyl-3-methylimidazolium tetrafluoroborate all the imidazolium proton resonances are similar, indicating that there is no cation inclusion occurring in this solvent mixture but rather anion binding resulting in the loss of the ion-pair.

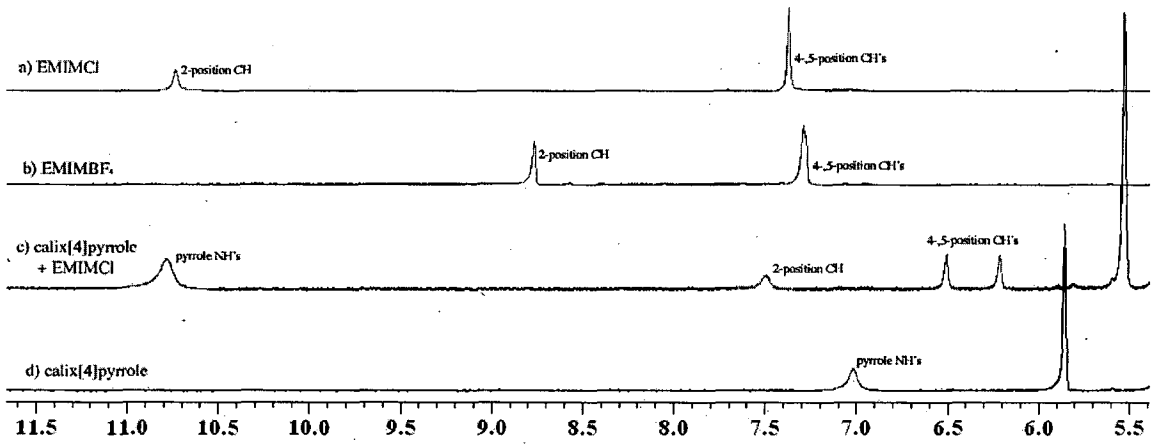

Figure 2.23: ^{1}H NMR stack plot of 1-ethyl-3-methylimidazolium cation and *meso*-octamethylcalix[4]pyrrole in CD_2Cl_2 a) 1-ethyl-3-methylimidazolium chloride, b) 1-ethyl-3-methyl imidazolium tetrafluoroborate, c) 1-ethyl-3-methylimidazolium chloride + 1eq. *meso*-octamethylcalix [4]pyrrole, d) calix[4]pyrrole. Green = 2-position of imidazolium cation. Red = 4- and 5-psotion of imidazolium cation. Blue = NH's of calix[4]pyrrole.

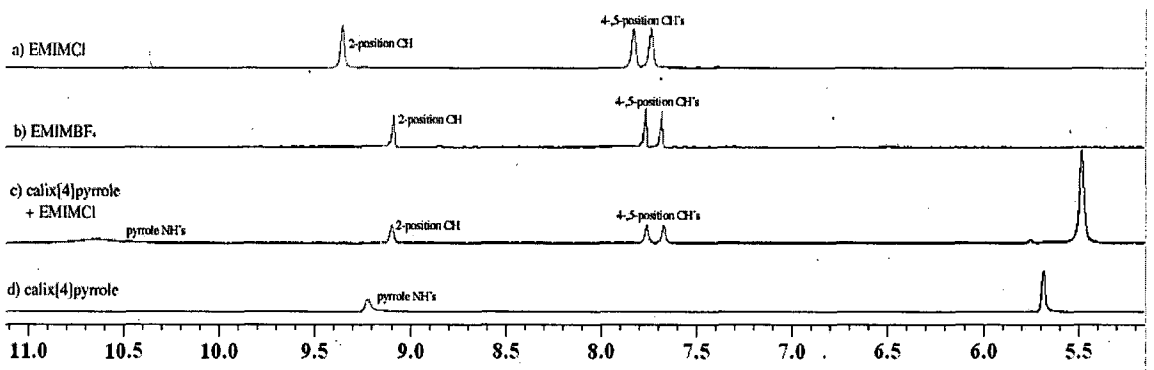

Figure 2.24: ^{1}H NMR stack plot of 1-ethyl-3-methylimidazolium cation and *meso*-octamethylcalix[4]pyrrole in DMSO-d_6 a) 1-ethyl-3-methylimidazolium chloride, b) 1-ethyl-3-methylimidazolium tetrafluoroborate, c) 1-ethyl-3-methylimidazolium chloride + 1eq. *meso*-octamethylcalix[4]pyrrole, d) *meso*-octamethylcalix[4]pyrrole. Green = 2-position of imidazolium cation. Red = 4- and 5-psotion of imidazolium cation. Blue = NH's of calix[4]pyrrole.

Similar studies were carried out using the equivalent bromide salts (**Table 2.3**). In accordance with previous studies of the anion recognition properties of *meso*-octamethylcalix[4]pyrrole, **2.5**, the bromide stability constants were found to be lower than for chloride.[55]

Table 2.3: Stability constants (M^{-1}) of *meso*-octamethylcalix[4]pyrrole with a number of organic bromide salts in both dichloromethane-d_2 and dimethylsulfoxide-d_6/0.5% water solutions at 298 K. All data fitted to a 1:1 binding profile, using EQNMR.[87] Errors (deviation from fit plot line) were estimated to be no more than ± 15%.

Organic Salt	DCM	DMSO
TBABr	<10	18
EMIMBr	200	<10
BMIMBr	280	10
EtPyBr	1180	14

The titrations conducted in dichloromethane-d_2 gave similar results to those observed with the chloride salts in the fact that the bromide stability constants greatly increased in the presence of the imidazolium and pyridinium cation, a result illustrated in the NMR titration curves of the four bromide salts (**Figure 2.25**).

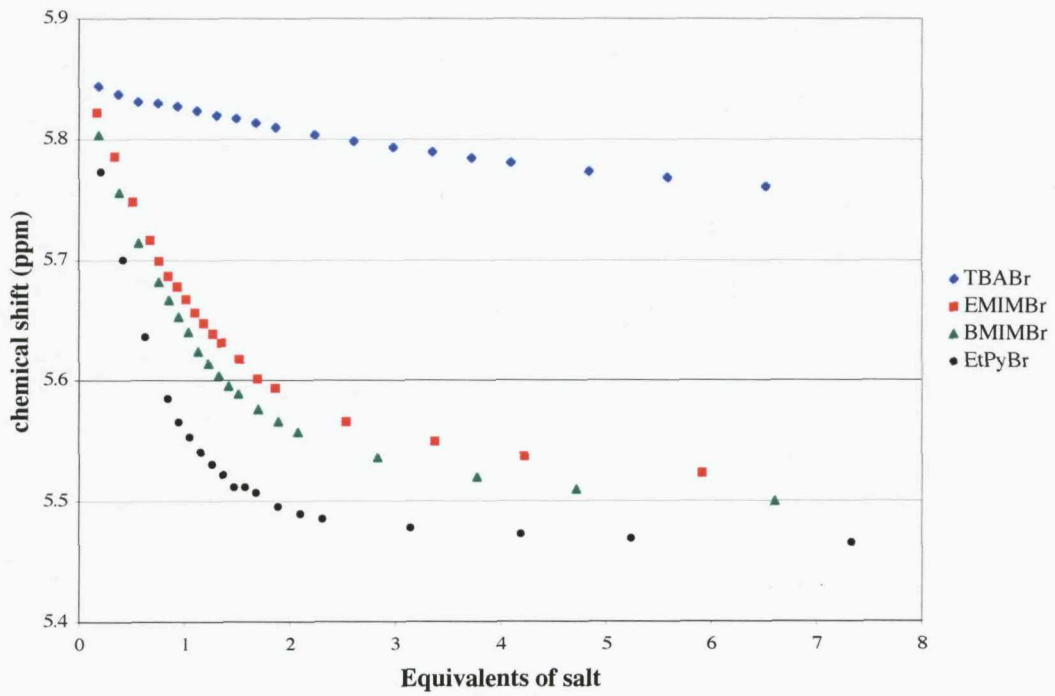

Figure 2.25: ^{1}H NMR titration curves of various bromide salts with *meso*-octamethylcalix[4]pyrrole in dichloromethane-d_2.

When the titrations were conducted in dimethylsuloxide-d_6 with the bromide salts the differences in the stability constants were found to be insignificant with no apparent trend, a result consistent with the results obtained with the chloride salts, again suggesting that in the more competitive solvent anion binding is occurring and not the complexation of the ion-pair.

2.2.5 OXO-ANION IMIDAZOLIUM SALT COMPLEXES

The ion-pair recognition properties of **2.5** were further investigated with the commercially available ionic liquids 1,3-Dimethylimidazolium methylsulfate (DMIM $MeSO_4$) and 1-ethyl-3-methylimidazolium nitrate (EMIMNO_2) in order to ascertain if the presence of the 'non-innocent' imidazolium cation would allow for the complexation and increased binding affinity of different oxoanions that had previously been found to bind weakly to *meso*-octamethylcalix[4]pyrrole, **2.5**. Initially the investigation was conducted in the solid state. X-ray quality crystals of both complexes were obtained *via* slow evaporation of dichloromethane solution of **2.5** in the presence of an excess of the salts.

The crystal structure of the DMIM $MeSO_4$ complex showed that a single oxygen atom (O1) of the methyl sulfate anion was bound by all four pyrrole NH groups with N···O1 distances of 2.952(7)-3.172(7) Å. Interestingly a second oxygen atom (O2) of the oxoanion was bound by the N1 pyrrole NH group with a N1···O2 distance of 3.361(8) Å. The structure also revealed the inclusion of the imidazolium cation in the electron rich cavity with a pendent methyl group (C3) of the imidazolium cation pointing into the cavity toward a nitrogen atom from one pyrrole ring (N3) with a C3···N3 distance of 3.368 Å.

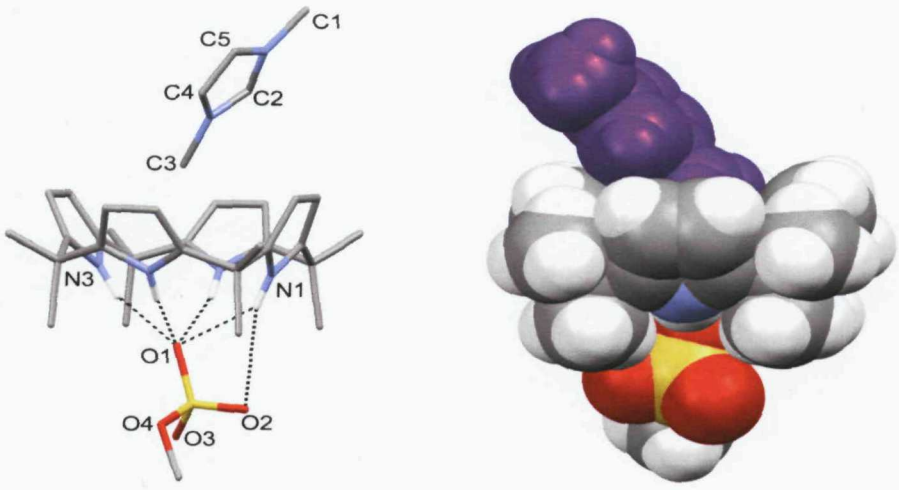

Figure 2.26: X-ray crystal structure and space filling view of the **2.5**·DMIM $MeSO_4$ complex.

Long-range interactions were present in the crystal with a hydrogen-bonded sheet being formed *via* additional interaction between the imidazolium cation and two adjacent oxoanions (**Figure 2.27**). The 2-position proton of the imidazolium cation (C2) was bound to the O3 oxygen of an adjacent oxoanion with a C2···O3 distance of 3.046(8) Å. The O3 oxygen of the same adjacent oxoanion also interacted with a CH proton from the pendent methyl group (C3) that was not included in the cavity of the calix[4]pyrrole (C3···O3 distance of 3.394(7) Å). There was also an interaction between the C5 proton of the imidazolium cation and the O4 oxygen of a second adjacent anion (C5···O4' distance of 3.476(8) Å).

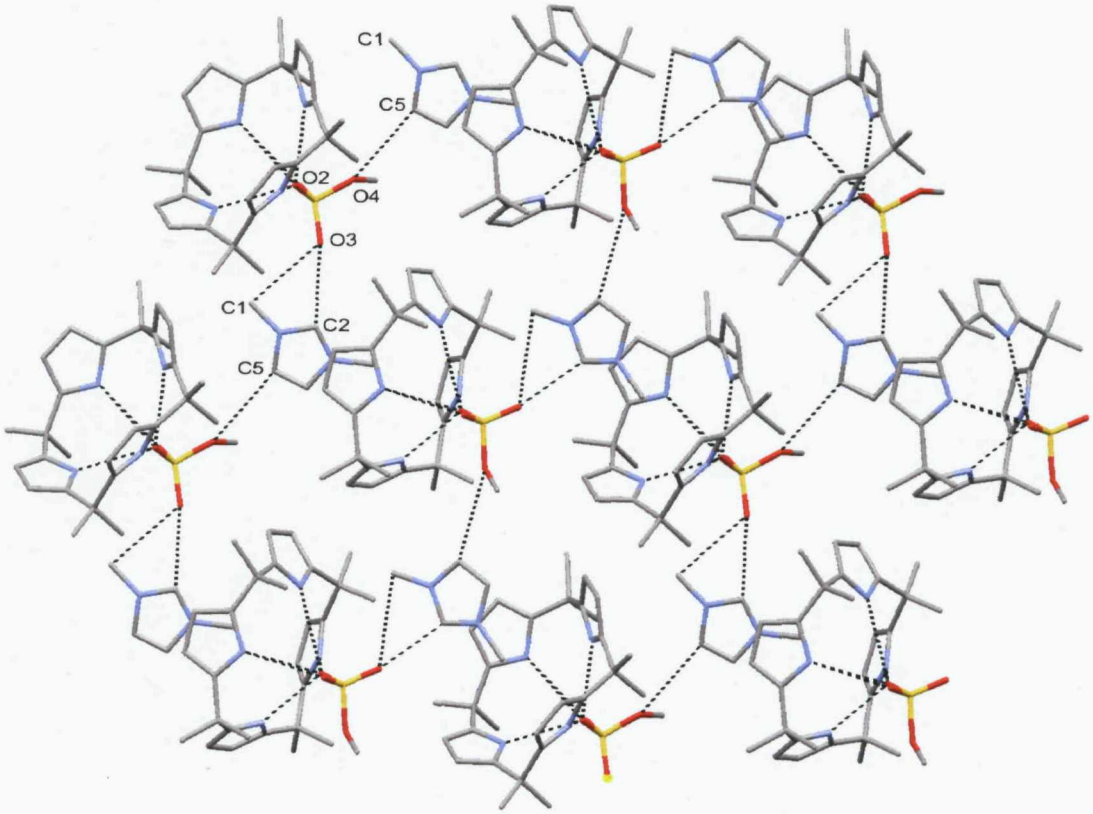

Figure 2.27: Extended crystal structure of **2.5**·DMIM $MeSO_4$ showing hydrogen-bonded sheet.

The crystal structure of the EMIM NO_3 complex revealed that a single oxygen atom (O1) of the nitrate anion was bound to all four pyrrole NH groups with N···O1 distances of 2.990(12)-3.053(12) Å. The imidazolium cation was found to occupy the electron rich 'cup' with the 4- and 5-position CH protons pointing into the cavity shown in the space filling representation in **Figure 2.28**.

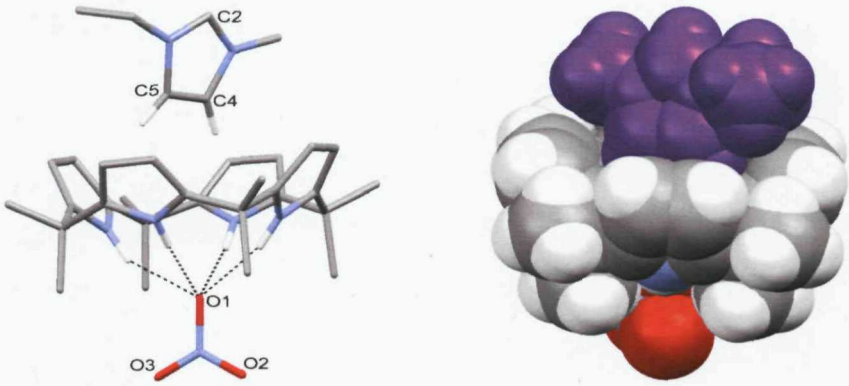

Figure 2.28: Crystal structure of the EMIM NO_3 complex of **2.5** and space filling representation.

In the extended crystal a one-dimensional hydrogen-bonded chain was formed (**Figure 2.29**) by the additional interaction of the 2-postion CH proton (C2) of the imidazolium cation with two oxygens (O2 and O3) of an adjacent nitrate anion (C2···O2 and C2···O3 distances of 3.388(12) Å and 3.398(12) Å respectively).

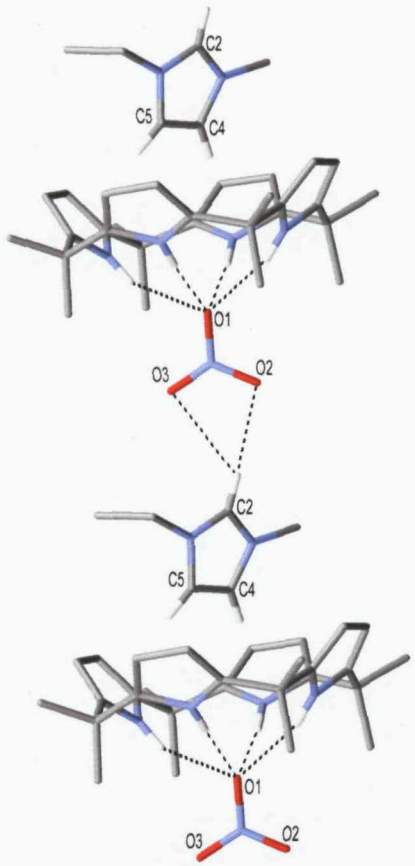

Figure 2.29: Hydrogen bonded chain in EMIM NO_3 complex of *meso*-octamethylcalix[4]pyrrole.

2.2.6 SOLUTION STUIDES WITH 1-ETHYL-3-METHYLIMIDAZOLIUM NITRATE

Proton NMR titration experiments were conducted with tetrabutylammonium nitrate and 1-ethyl-3-methylimidazolium nitrate in dichloromethane-d_2. The data obtained for both titrations could not be fitted to a binding model (possibly due to complex equilibrium occurring in solution). However significant differences were observed in the calix[4]pyrroles NH and β-CH resonances upon the addition of the two salts. Upon the addition of one equivalent of nitrate salt, the NH resonances shift upfield by approximately 0.1ppm in the case of tetrabutylammonium nitrate and by 0.8ppm in the case of 1-ethyl-3-methylimidazolium nitrate. The β-CH resonances shift upfield by <0.01ppm in the case of tetrabutylammonium nitrate and by approximately 0.08ppm for 1-ethyl-3-methylimidazolium nitrate. The resonances of the 4- and 5-position protons of the imidazolium cation are shifted upfield by approximately 0.2 ppm and 0.3ppm in the 1:1 mixture of calix[4]pyrrole and 1-ethyl-3-methylimidazolium nitrate compared to the shifts in the tetrafluoroborate salt (illustrated in **Figure 2.30**).

These results are consistent with the results observed for both the chloride and bromide salts in dichloromethane-d_2 and is evidence for the complexation of the ion-pair occurring in solution.

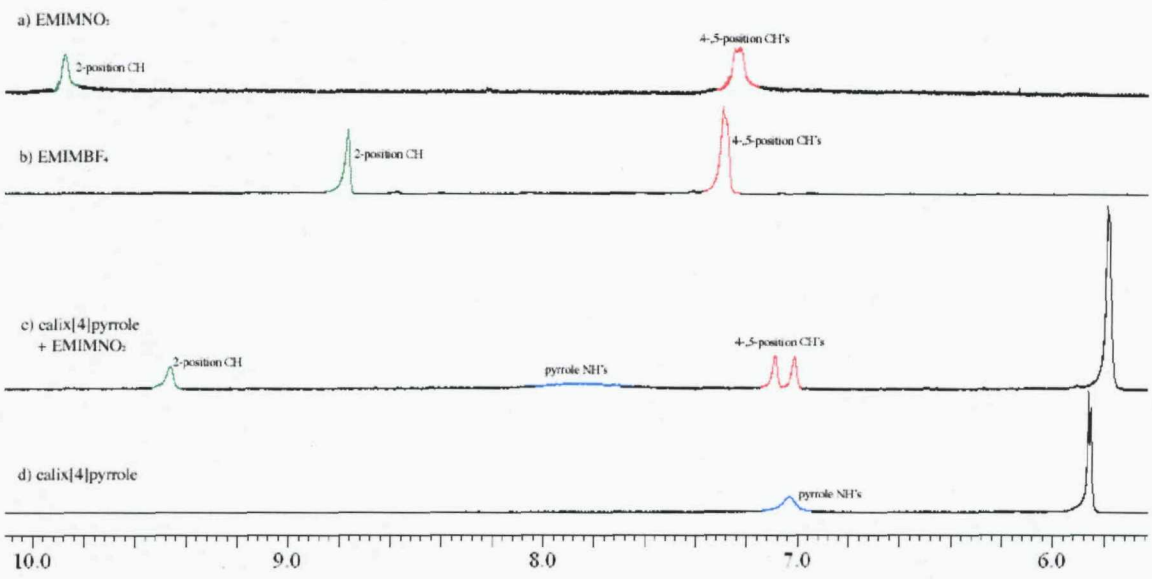

Figure 2.30: ^{1}H NMR stack plot of 1-ethyl-3-methylimidazolium cation and *meso*-octamethylcalix[4]pyrrole in CD_2Cl_2 a) 1-ethyl-3-methylimidazolium nitrate, b) 1-ethyl-3-methyl imidazolium tetrafluoroborate, c) 1-ethyl-3-methylimidazolium nitrate + 1eq. *meso*-octamethylcalix[4]pyrrole, d) *meso*-octamethylcalix[4]pyrrole. Green = 2-position of imidazolium cation. Red = 4- and 5-position of imidazolium cation. Blue = NH's of *meso*-octamethylcalix[4]pyrrole.

2.3 ION-PAIR RECOGNITION PROPERTIES OF *N*-CONFUSED OCTAMETHYLCALIX[4]PYRROLE

2.3.1 *N*-CONFUSED CALIX[4]PYRROLE

In 1999 Dehaen and co-worker discovered that the acid condensation of pyrrole and ketones (such as cyclohexanone) led to the formation of isomers such as *N*-confused calix[4]pyrrole **2.6**.[88]

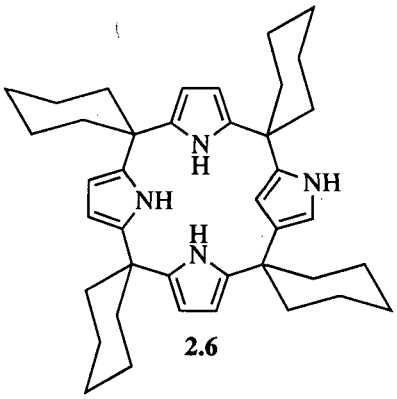

2.6

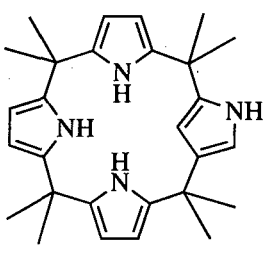

2.7

Dehaen found that the choice of solvent and acid used in the condensation reaction greatly influenced the percentage yields of the isomers. The conditions found to produce the highest yield of **2.6** was reactions in ethanol with trifluoroacetic acid as the catalyst giving a 91% overall yield with 26% of that being **2.6**. The remainder was found to be the expected calix[4]pyrrole. The *N*-confused octamethylcalix[4]pyrrole, **2.7**, was synthesised under the same conditions as **2.6** and recently the anion recognition properties of a number of derivatives of this receptor has been studied.[89,90]

Prompted by the increasing interest in the *N*-confused calix[4]pyrroles and success of the investigation into the ditopic behaviour of calix[4]pyrrole lead to the study of *N*-confused octamethylcalix[4]pyrrole, **2.7**, as a possible ditopic receptor. Solid-state analysis and solution studies of the interactions between **2.7** and various organic chloride salts were therefore carried out.

2.3.2 ORGAINC HALIDE SALT (IONIC LIQUID) COMPLEXES

X-ray quality crystals of the tetraethylammonium chloride and *N,N'*-dialkylimidazolium chloride complexes of **2.7** were prepared by the slow evaporation of dichloromethane solutions of **2.7** in the presence of tetraethylammonium chloride (TEACl) and the ionic liquids 1-butyl-3-methylimiazolium chloride (BMIMCl) and 1-ethyl-3-methylimidazolium chloride (EMIMCl). The *n*-ethyl-pyridinium chloride (EtPyCl) complex was prepared by slow evaporation of acetonitrile solutions of **2.7** in the presence of EtPyCl.

The X-ray crystal structure of the **2.7**·TEACl complex revealed that the *N*-confused calix[4]pyrrole formed a cone-like conformation, similar to that of *meso*-octamethylcalix[4]pyrrole, however the chloride anion was bound by only three pyrrole NH groups with N···Cl distances between 3.252(2) Å and 3.472(3) Å. An additional interaction between the β-position hydrogen of the 'confused' pyrrole ring and the chloride was present with a C···Cl distance of 3.339 Å. The tetraethylammonium cation was also found to be included in the anion-induced cavity of **2.7** with two of the CH_2 groups from the ethyl chains orientated into the cavity (**Figure 2.31**).

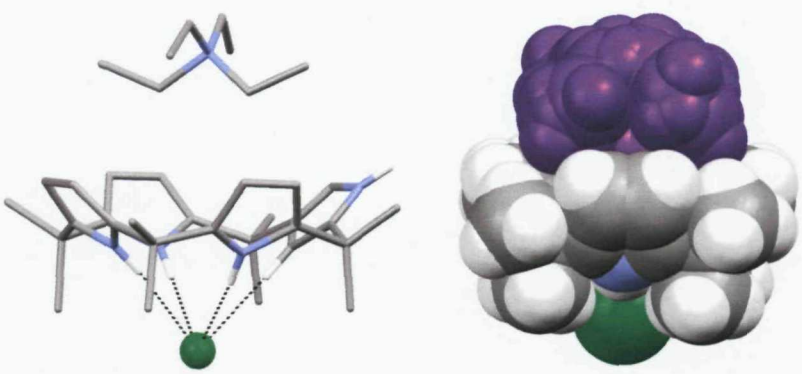

Figure 2.31: X-ray crystal structure and space filling view of the **2.7**·TEACl complex respectively.

The structures of the **2.7**·EMIMCl and the **2.7**·BMIMCl complexes reveal that **2.7** forms a cone conformation (similar to *meso*-octamethylcalix[4]pyrrole) and binds the chloride anion with three pyrrole NH-anion interactions (for **2.7**·EMIMCl N···Cl distances between 3.235(6) Å and 3.566(6) Å and for **2.7**·BMIMCl N···Cl distances

between 3.214(4) Å and 3.473(4) Å) and an additional CH-anion interaction from the β-position hydrogen of the 'confused' pyrrole ring (distances of 3.530 Å and 3.479 Å for **2.7**·EMIMCl and the **2.7**·BMIMCl respectively). In both cases the cation was found to be included in the anion induced cavity with the 4- and 5-postion protons orientated into the cavity.

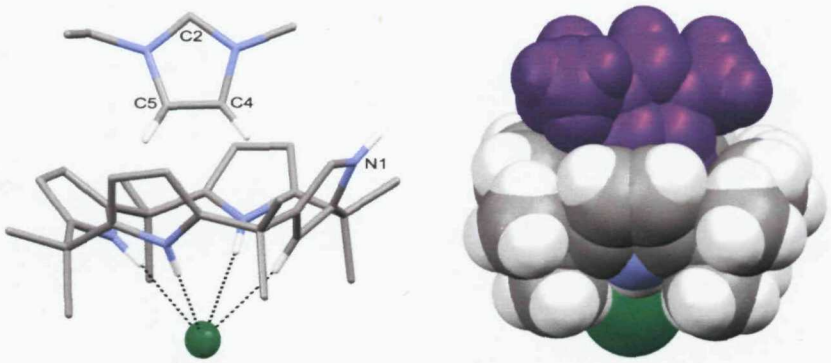

Figure 2.32: X-ray crystal structure and space filling view of the **2.7**·EMIMCl complex respectively.

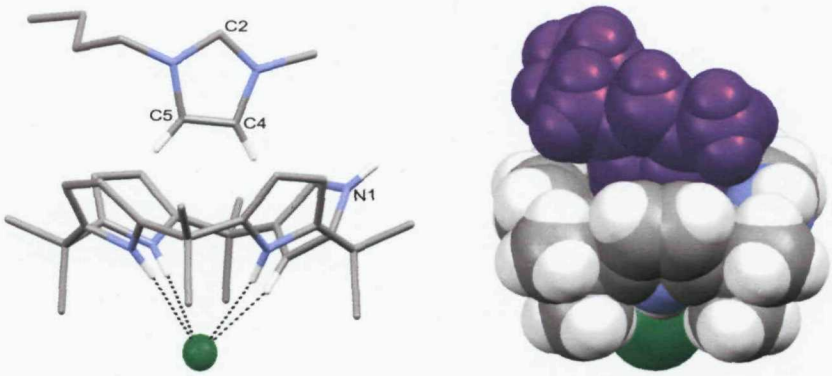

Figure 2.33: X-ray crystal structure and space filling view of the **2.7**·BMIMCl complex respectively.

A one-dimensional chain is formed in the extended crystals of both the **2.7**·EMIMCl and the **2.7**·BMIMCl complexes *via* an additional interaction between the pyrrole NH group of the 'confused' pyrrole (N1) and an adjacent chloride anion with a N1···Cl distance of 3.262(6) Å in the **2.7**·EMIMCl complex and 3.275 Å in the **2.7**·BMIMCl complex (**Figure 2.34**).

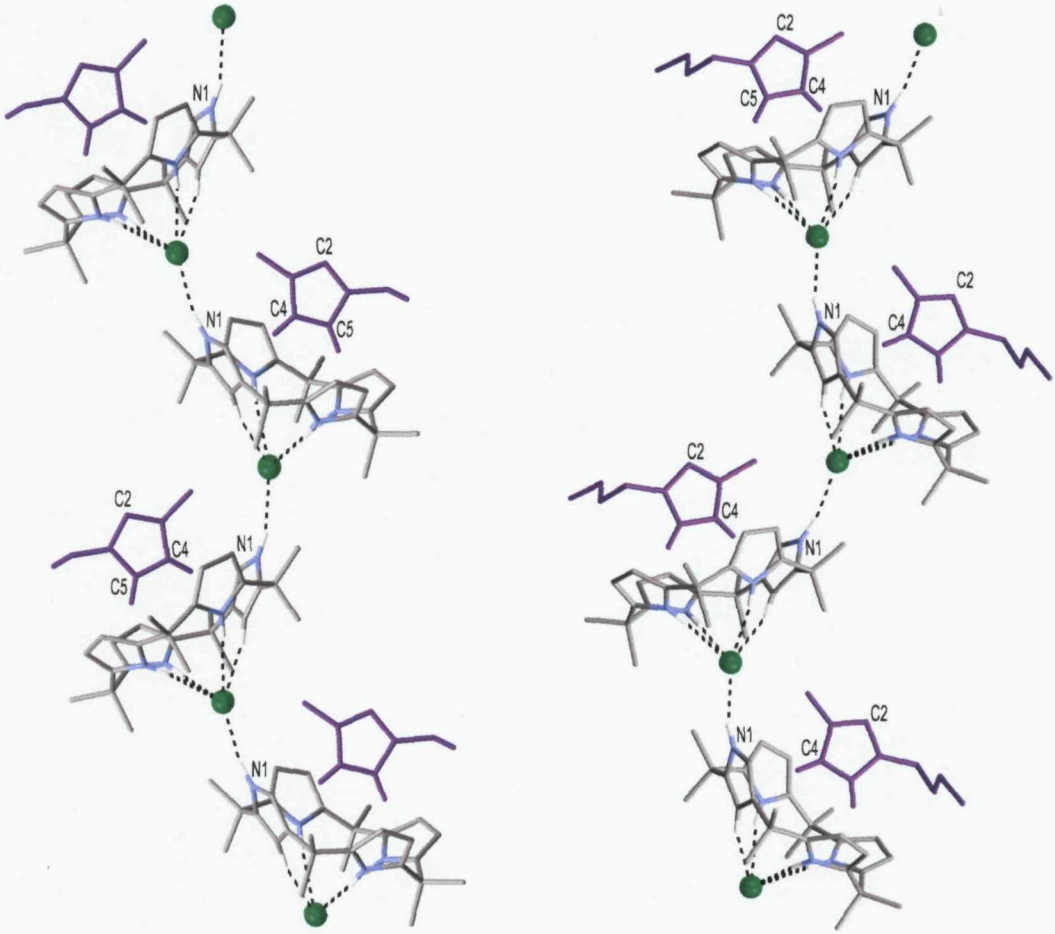

Figure 2.34: Extended crystal structures of **2.7**·EMIMCl and the **2.7**·BMIMCl respectively showing the formation of a one-dimensional chain.

In the structure of **2.7**·EtPyCl the anion was again bound by three NH hydrogen bonds (N···Cl distances between 3.278(3) Å and 3.480(4) Å) and by the β-position hydrogen of the 'confused' pyrrole ring with a C···Cl distance of 3.511 Å. The cation was also found to be included in the anion-induced cavity with the protons in the 2- and 3-position orientated into the cavity. Similar to the **2.7** EMIMCl and **2.7** BMIMCl complexes the **2.7** EtPyCl complex forms a one-dimensional chain in the extended crystal *via* an additional interaction between the 'confused' pyrrole NH group (N1) and an adjacent chloride anion (N1···Cl distance of 3.333(4) Å).

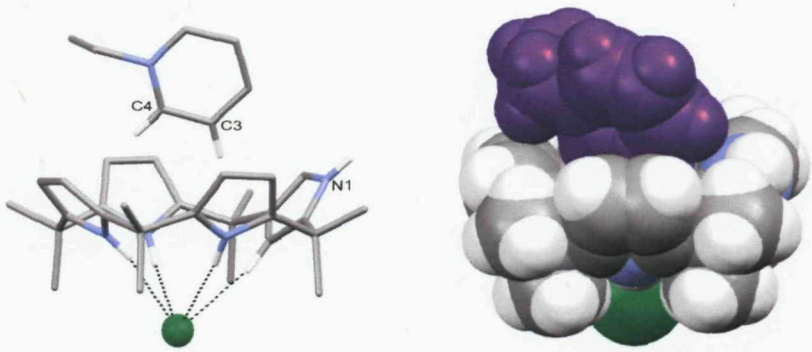

Figure 2.35: X-ray crystal structure and space filling view of the **2.7**·EtPyCl complex respectively.

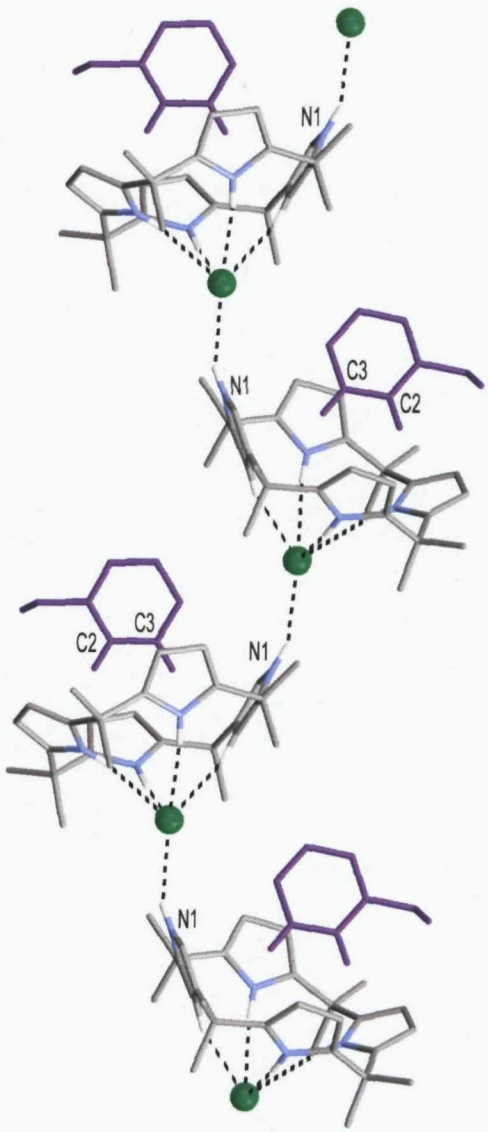

Figure 2.36: One-dimensional chain observed in the extended crystal of **2.7**·EtPyCl.

2.3.3 SOLUTION STUDIES

Proton NMR titration experiments in dichloromethane-d_2 at 298 K were conducted in order to establish if the ditopic behaviour could occur in solution and was not a phenomenon only observed in the solid state. The constants calculated from the titrations showed that chloride was bound more weakly by **2.7** than by *meso*-octamethylcalix[4]pyrrole, **2.5**, presumably due to the absences of the fourth pyrrole NH group involvement in the binding of the anion (**Table 2.4**). Despite the smaller stability constants the cation appeared to have an effect on the binding constants of the chloride anion. Titrations with TEACl resulted in a slight increase in the stability constant compared to the constant obtained with TBACl (36 M^{-1} and 10 M^{-1} respectively). Titrations with EtPyCl resulted in precipitation upon the addition of the salt, a result indicative of strong binding.

Table 2.4: Stability constants (M^{-1}) of **2.7** with a number of organic chloride salts in dichloromethane-d_2 at 298 K. Data fitted to either a 1:1 or a 1:2 binding profiles using EQNMR.[87] Errors (deviation from fit plot line) were estimated to be no more than ± 15% unless stated otherwise.

Organic Salt	
TBACl	10
TEACl	36
EMIMCl	$K_1 = 220^a$ $K_2 = 34$ $\beta = 7425$
EtPyCl	*ppt*[b]

[a] error (deviation from fit plot line) were estimated to be more than ± 30%. [b] precipitation occurred during titration.

Interestingly the titration involving EMIMCl resulted in data that could only be fitted to a 1:2 receptor-anion binding profile with high errors suggesting that a complex equilibrium is present between the EMIMCl salt and **2.7**. Following all the Δδ shifts of the NH resonances throughout the titration shows that they all display similar behaviour and results in sigmoid shaped curves (**Figure 2.37**).

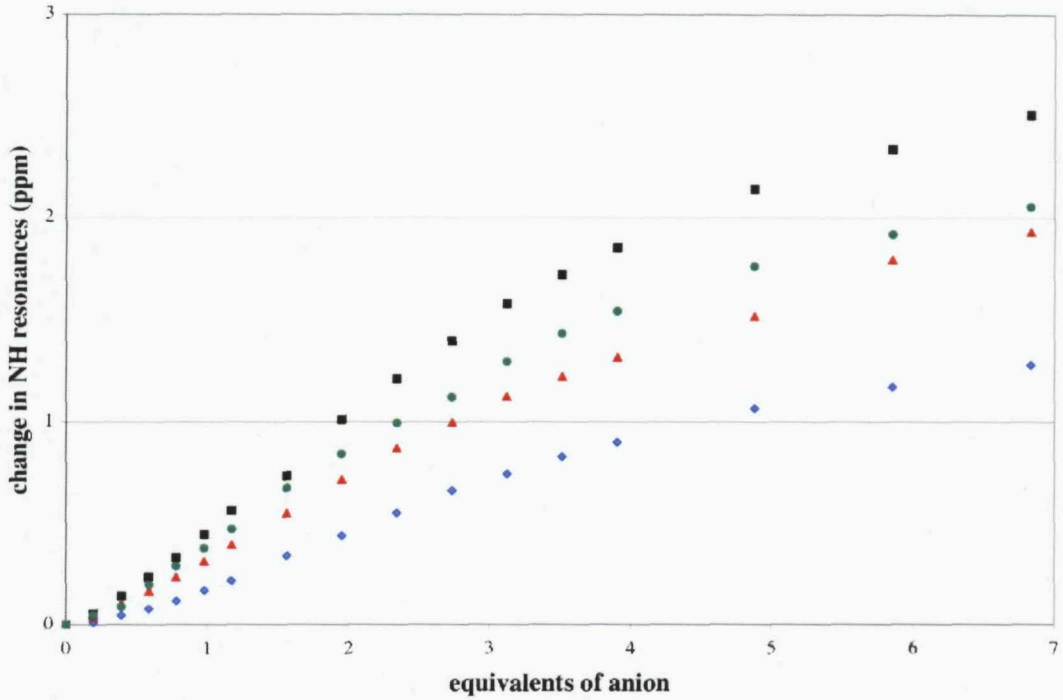

Figure 2.37: Plot of Δδ shifts of the pyrrole NH resonances upon the addition of increasing amounts of EMIMCl.

The complex equilibrium present in the system with EMIMCl could be a consequence of cation-π interaction. Evidence for this was illustrated in a stack plot (**Figure 2.38**) where upon the addition of 1 equivalent of EMIMCl to **2.7** the 4- and 5-postion protons of the imidazolium cation shifted up-field by approximately 0.30 ppm and 0.35 ppm compared to the free EMIMCl salt and by approximately 0.20 ppm and 0.25 ppm when compared to the $EMIMBF_4$ salt. The 2-postion proton shifted upfield by approximately 0.4 ppm compared to the free EMIMCl salt suggesting that complexation of the ion-pair by **2.7** is occurring in dichloromethane-d_2 solution.

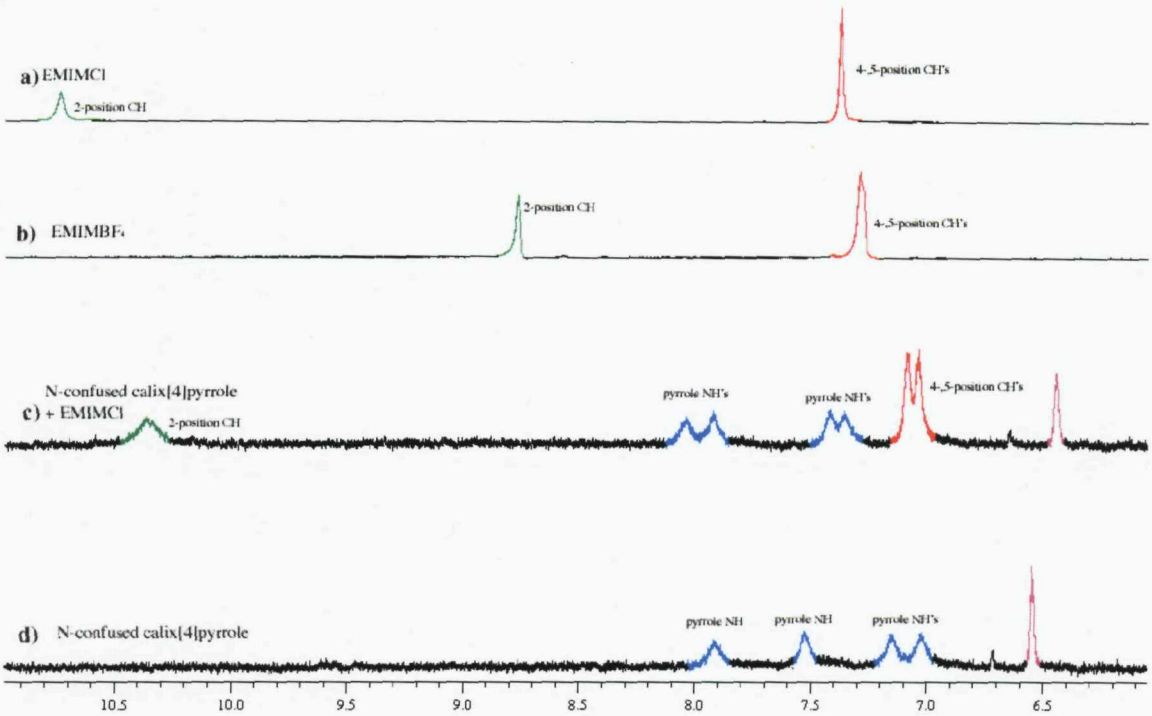

Figure 2.38: ^{1}H NMR stack plot of 1-ethyl-3-methylimidazolium cation and *N*-confused calix[4]pyrrole in DCM-d_2 a) 1-ethyl-3-methylimidazolium chloride, b) 1-ethyl-3-methylimidazolium tetrafluoroborate, c) 1-ethyl-3-methylimidazolium chloride + 1eq. *N*-confused calix[4]pyrrole, d) *N*-confused calix[4]pyrrole. Green = 2-position of imidazolium cation. Red = 4- and 5-psotion of imidazolium cation. Blue = NH's of *N*-confused calix[4]pyrrole, purple = α-CH of 'confused' pyrrole.

2.4 CONCLUSIONS

Meso-octamethylcalix[4]pyrrole and *N*-confused octamethylcalix[4]pyrrole (**2.5** and **2.7** respectively) have been studied with a variety of tetraalkylammonium, *n,n'*-dialkylimidazolium and *n*-alkylpyridinium salts in both the solid state and in solution.

The studies have revealed that *meso*-octamethylcalix[4]pyrrole acts as a ditopic receptor in both the solid state and in non-competitive organic solutions for all organic salts investigated. The solution studies revealed that in non-competitive solvents such as dichloromethane-d_6 the imidazolium and pyridinium cations interact with the anion-induced cavity of the *meso*-octamethylcalix[4]pyrrole, which results in an increase in the stability of the chloride and bromide complexes. However in more competitive solvents only anion binding was observed and therefore insignificant differences were observed between the stability constants for the various salts and **2.5**. The cations' stabilising effect allowed for a nitrate and a methylsulfate complex of *meso*-octamethylcalix[4]pyrrole to be obtained and solution studies showed that in non-competitive solvents the presence of the imidazolium cation effected the stability of the nitrate complex.

Similar studies of *N*-confused octamethylcalix[4]pyrrole have revealed that this receptor too can behave as a ditopic receptor in the solid state. The solution studies are less clear, as a consequence of the poor chloride affinities, however they do suggest that complex equilibria are present in solution possible due to the interaction of the cation with the anion-induced cavity of **2.7**.

CHAPTER 3 - INDOLE BASED ANION RECEPTORS: SOLUTION AND SOLID STATE STUDIES

3.1 INTRODUCTION

The use of the indole subunits has until recently been overlooked as a building block in synthetic receptors for the binding of anions, however in nature the indole functionalised amino acid, tryptophan, has been employed as an important subunit for the binding of anions within a number of protein architectures.[91-95] The crystal structure of the sulfate binding protein found in *Salmonella typhimurium* revealed that the sulfate anion is bound to a site inaccessible to solvent and within the active site one tryptophan residue was found to bind to an oxygen atom of the sulfate anion (**Figure 3.1**).[91-93]

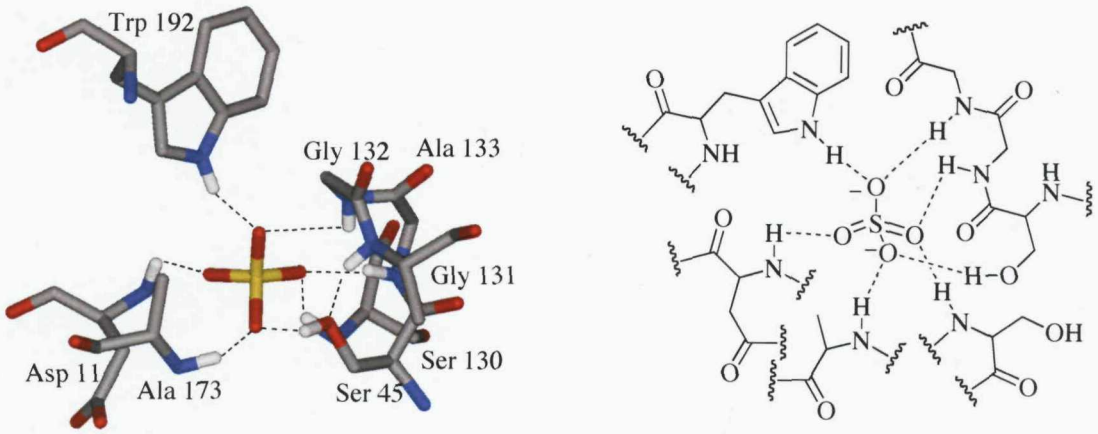

Figure 3.1: Structure of the active site of the sulfate binding protein.

The active site of haloalkane dehalogenase from *Xanthobacter autotrophicus* was found to bind to chloride anions and the X-ray crystal structure reveals that within the active site the chloride anion is bound by Trp 125 and Trp 175 residues with N···Cl distances of 3.6 Å and 3.2 Å respectively.[94,95]

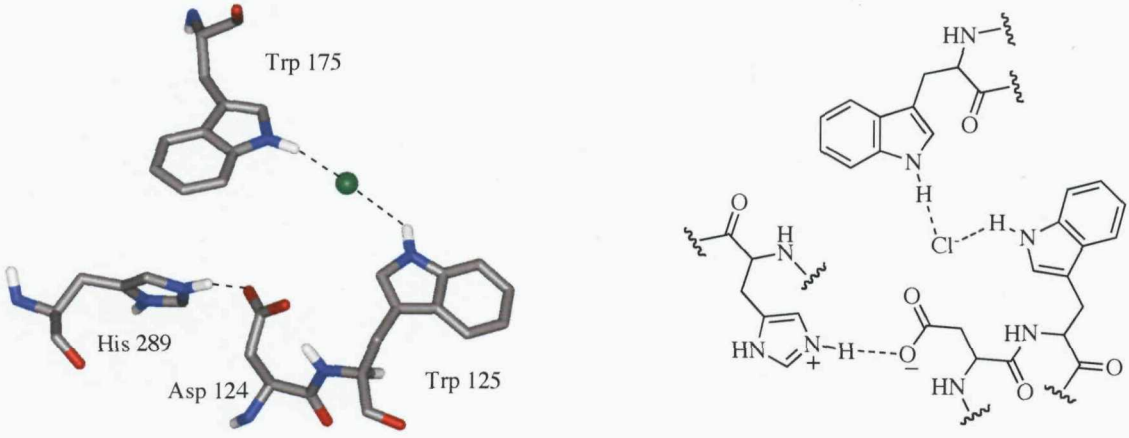

Figure 3.2: Structure of the active site of haloalkane dehalogenase.

In 1996 Black and co-workers reported an early example of a synthetic indole receptor.[96] They found that derivatives of indoles underwent acid-catalysed cyclo-oligomerisation to produce calix[3]indole receptors, such as **3.1**. X-ray crystal structure of **3.1** showed that **3.1** adopted a cone conformation in the solid state and an ethanol molecule was positioned inside the cavity of **3.1**.

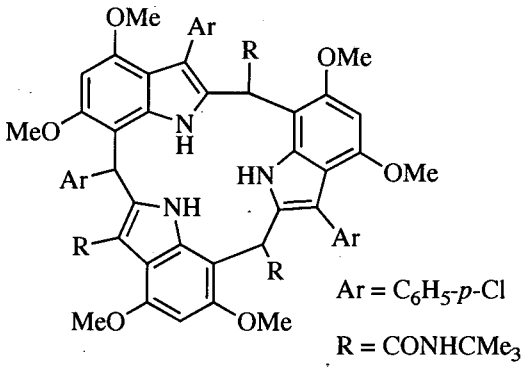

3.1

Recently indole based receptors have attracted increasing attention. Sessler and co-workers have described the use of indole subunits for anion recognition within diindolylquinoxalines receptors (**3.2a** and **3.2b**).[97] Stability constants were determined by UV-vis spectroscopic titrations in dichloromethane at 22 °C and showed that both receptors have appreciable selectivity for dihydrogenphosphate with constants of 6800 M^{-1} and 20000 M^{-1} calculated for compounds **3.2a** and **3.2b** respectively. Receptor **3.2b** was found to be highly coloured and upon the addition of dihydrogenphosphate a visible change in colour was observed.

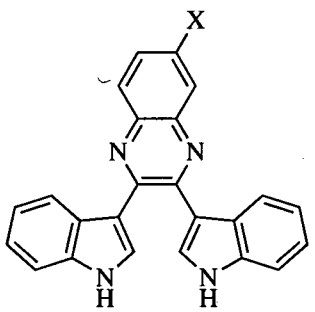

3.2a X= H
3.2b X= NO_2

A number of biindoyl-based systems have been developed by Jeong and co-workers for the binding of anionic species. This group have prepared molecular clefts based on the 2,2'-biindoyl scaffold with amide groups attached *via* alkyne linkers and compared the anion binding ability of **3.3** to the more rigid ethyno-bridged receptor **3.4**.[98]

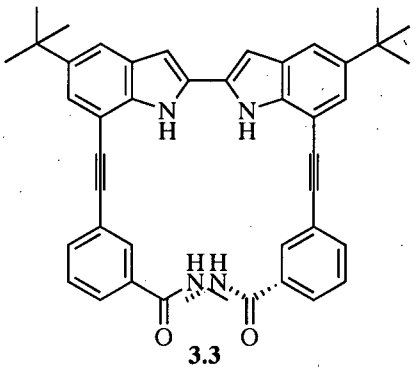

3.3

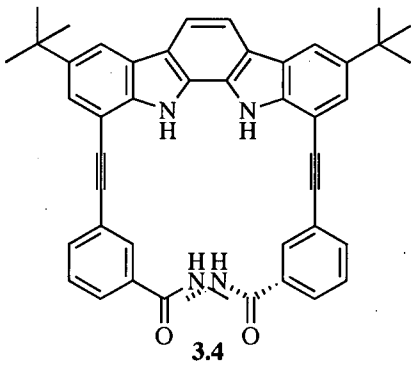

3.4

Stability constants were determined by UV-vis spectroscopy titration experiments in CH_3CN at 22 °C and revealed that receptor **3.4** did indeed bind the anionic species with higher affinities than **3.3**, the less rigid receptor. Chloride was bound 22 times more strongly by receptor **3.4** compared to **3.3** (1.1×10^5 M^{-1} for **3.4** against 5.1×10^3 M^{-1} for **3.3**) whereas bromide was bound 41 times more strongly by **3.4** compared to **3.3** (8.7×10^3 M^{-1} for **3.4** against 2.1×10^2 M^{-1} for **3.3**) illustrating the importance of preorganisation in the binding of small anionic guests.

Jeong and co-workers have extended the research into biindolyl scaffolds as a building block for anion receptors by synthesising new macrocyclic systems **3.5** and **3.6**.[99] Both compounds **3.5** and **3.6** were found to strongly bind various anions (stability constants determined by UV-vis spectroscopy titrations in CH_3CN at 295 K). In the case of the halide anions a size complementarity was observed for both macrocycles where the smaller fluoride and chloride anions were found to bind more strongly to **3.5** and **3.6** than the larger bromide and iodide anions.

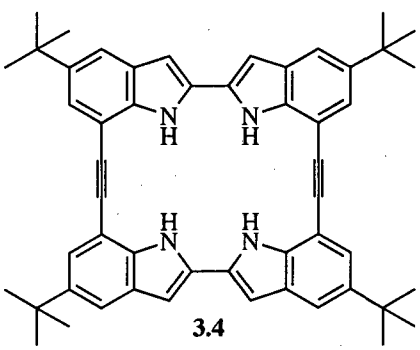

3.4

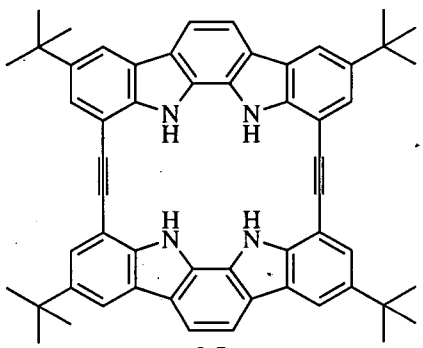

3.5

Pfeffer and co-workers have recently shown that the indole subunit can be used as a scaffold for other hydrogen-bonding groups to be appended to in order to construct new cleft-like receptors for anion recognition.[100]

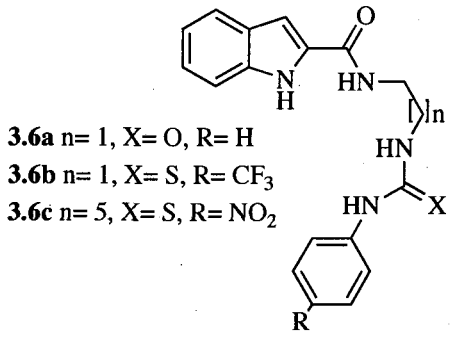

3.6a n= 1, X= O, R= H
3.6b n= 1, X= S, R= CF_3
3.6c n= 5, X= S, R= NO_2

Proton NMR titration experiments in DMSO-d_6 were conducted in order to elucidate binding constants for receptors **3.6a-3.6c** with chloride, acetate and dihydrogen phosphate anions. All the titration data was fitted to a 1:1 binding model and revealed that both receptors **3.6a** and **3.6b** bound dihydrogen phosphate most strongly (logβ = 3.5±0.3 and 3.5 respectively) whereas receptor **3.6c** bound acetate most strongly (logβ = 3.9±0.7).

3.2 ANION RECOGNITION OF ISOPHTHALAMIDE AND PYRIDINE-2,6-DICARBOXAMIDE BIS-INDOLE CLEFTS

We wished to develop anion receptors containing indole subunits in order to investigate their anion recognition properties. The simple bis-indole receptors, **3.7a** and **3.7b**, based on isothphalamides and pyrdine dimaides (previously shown to bind anions[111,112]) were designed with the hope that the amide and indole groups would form a convergent cleft in which to bind anions.

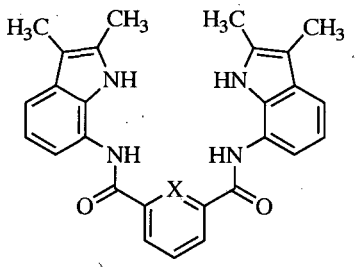

3.7a X = N
3.7b X = CH

3.2.1 SYNTHESIS AND CHARACTERISATION

Compounds **3.7a** and **3.7b** were synthesised by the reduction of commercially available 2,3-dimethyl-7-nitroindole with hydrazine monohydrate and 10% palladium on charcoal and subsequent reaction with pyridine-2,6-dicarbonyl dichloride or isophthaloyl dichloride in dichloromethane in the presence of triethylamine and a catalytic amount of DMAP afforded compounds **3.7a** and **3.7b** in a 63% and 60% overall yield respectively (**Scheme 3.1**).

Scheme 3.1: Reaction scheme for the synthesis of compounds **3.7a** and **3.7b**.

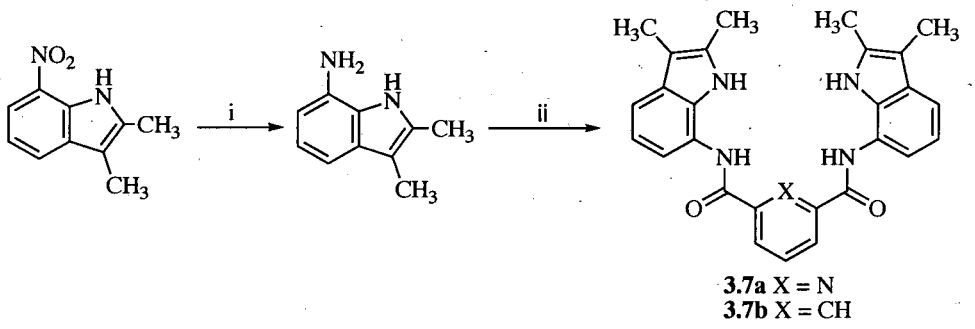

3.7a X = N
3.7b X = CH

i. $NH_2NH_2{\cdot}H_2O$, 10% Pd/C, EtOH, ii) pyridine-2,6-dicarbonyl dichloride (for **3.7a**) or isophthaloyl dichloride (for **3.7b**), Et_3N, DMAP and DCM.

X-ray quality crystals of **3.7a** were obtained *via* slow evaporation of a DMSO solution of the receptor (**Figure 3.3**). The crystal structure reveals that receptor **3.7a** binds to two solvent molecules in the solid sate with one solvent molecule binding to both amide NH groups (N2···O1 distance of 2.895(4) Å and N4···O1 distance of 2.922(4)

Å) and the second binding to the two indole NH groups (N1···O2 distance of 2.839(4) Å and N5···O2 distance of 2.845(4) Å).

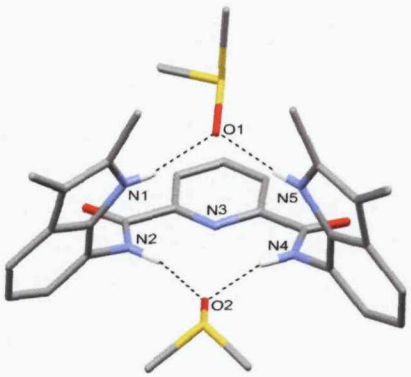

Figure 3.3: X-ray crystal structure of receptor **3.7a** binding two dimethylsulfoxide molecules.

X-ray quality crystals of the free receptor **3.7a** were also grown from acetonitrile in the presence of tetrabutylammonium dihydrogenphosphate and shows that receptor **3.7a** forms a dimer in the solid state. Both indole groups are rotated around it's 7-position carbon-amide bond and bind to an adjacent receptor resulting in the formation of four indole NH-O interactions with N···O distances of 2.804(6) – 3.019(6) Å. The crystal structure also reveals that each receptor binds to a single acetonitrile solvent molecule *via* two amide NH-N interactions with N···N distances of 3.082(7) – 3.248(7) Å (**Figure 3.4**).

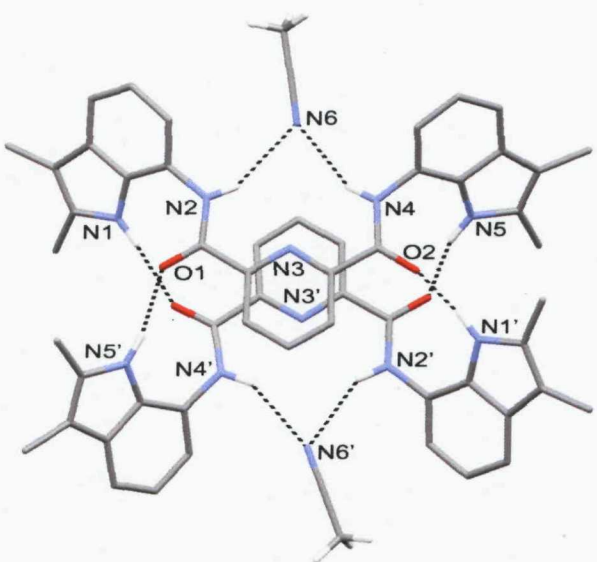

Figure 3.4: X-ray crystal structure of **3.7a** dimer complex obtained from acetonitrile.

3.2.2 SOLUTION STUDIES

Association constants for **3.7a** and **3.7b** with a variety of anionic guests, added as their tetrabutylammonium salts, were elucidated by proton NMR titration experiments in DMSO-d_6/0.5% water solutions at 298 K. Changes in the chemical shift of the proton resonances upon the additions of increasing amounts of anion solution were recorded and the data plotted and fitted to a 1:1 binding model with EQNMR[87] (**Table 3.1**).

Table 3.1: Stability constants (M^{-1}) of compounds **3.7a** and **3.7b** with a variety of putative anionic guests (added as their tetrabutylammonium salts) at 298K DMSO-d_6/0.5% water solutions. All data fitted to a 1:1 binding model using EQNMR[87] unless stated otherwise. Errors (deviation from the fit plot line) were estimated to be no more than ±10%.

Anion	3.7a	3.7b
Fluoride	$>10^4$	[a]
Acetate	250	880
Dihydrogenphosphate	70	1140
Benzoate	17	120
Chloride	<10	17
Bromide	no interaction	no interaction

[a] NMR titration data is consistent with strong binding but could not be successfully fitted to either a 1:1 or 1:2 binding model.

Receptor **3.7a** showed a high affinity for fluoride over other halide anions such as chloride ($>10^4$ M^{-1} for fluoride against <10 M^{-1} for chloride). In the case of **3.7b** an association constant could not be obtained for titration with fluoride because the data could not be fitted to a binding model however significant downfield shifts were observed in both the amide and indole NH resonances upon the addition of the fluoride anion (approx. 1.1 ppm and 3 ppm upon the addition of 2 eq of fluoride), which is indicative of strong anion complexation.

In order to obtain comparative binding constants for receptors **3.7a** and **3.7b** ^{1}H NMR titration experiments were carried out in DMSO-d_6/5% water at 298 K the results of which are shown in **Table 3.2**.

Table 3.2: Stability constants (M^{-1}) of compounds **3.7a** and **3.7b** with a variety of putative anionic guests (added as their tetrabutylammonium salts) at 298K in DMSO-d_6/5% water solutions. All data fitted to a 1:1 binding model using EQNMR[87] unless stated otherwise. Errors (deviation from the fit plot line) were estimated to be no more than ±10%.

Anion	3.7a	3.7b
Fluoride	1360	[a]$K_1 = 940$ $K_2 = 21$ $\beta = 19{,}600$
Acetate	14	110
Dihydrogen Phosphate	26	260
Benzoate	<10	35
Chloride	<10	15

[a]fitted to a 1:2 receptor/anion binding model.

The binding constants again show that receptors **3.7a** and **3.7b** have strong affinity and selectivity for fluoride. Interestingly, **3.7a** was found to bind fluoride in a 1:1 receptor/anion stoichiometry whereas the data for **3.7b** with fluoride could only be fitted to a 1:2 receptor/anion binding model. Job plot analysis failed to confirm that a 1:2 binding stoichiometry was present in solution with **3.7b** and fluoride (**Figure 3.5**), which could be a consequence of the small K_2 value obtained from analysis of the titration data ($K_2 = 21\ M^{-1}$).

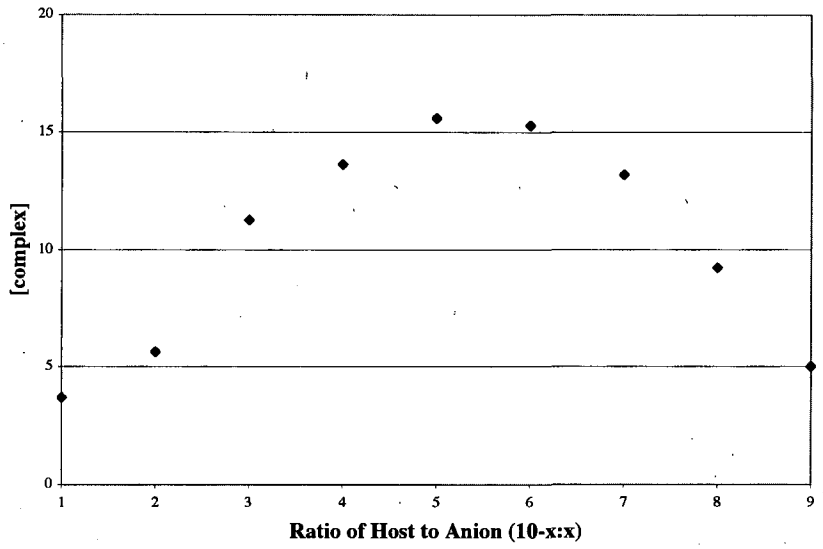

Figure 3.5: Job plot of compound **3.7b** with fluoride showing a 1:1 stoichiometry in DMSO-d_6/5% water solutions.

In both solvent media receptor **3.7a** demonstrates high selectivity for fluoride. The association constant obtained in DMSO-d_6/5% water solvent mixture for **3.7a** with fluoride was found to be approximately 50 times greater than the constant calculated for dihydrogenphosphate (1360 M^{-1} and 26 M^{-1} respectively) and approximately two orders of magnitude greater than the constant obtained with acetate (1360 M^{-1} for F^- against 14 M^{-1} for AcO^-).

Previous studies involving fluoride has revealed that the fluoride anion is able to deprotonate receptors rather than form complexes.[29] As a consequence of the large fluoride selectivity observed for receptors **3.7a** and **3.7b** the titration data was analysed further in order to ascertain if binding or deprotonation is occurring. Stack plots of the titrations of **3.7a** and **3.7b** with fluoride were generated (**Figure 3.6** and **Figure 3.7**) because if deprotonation was occurring then the NH proton resonances would disappear during the titration and a shift attributed to HF_2^- would appear.[25]

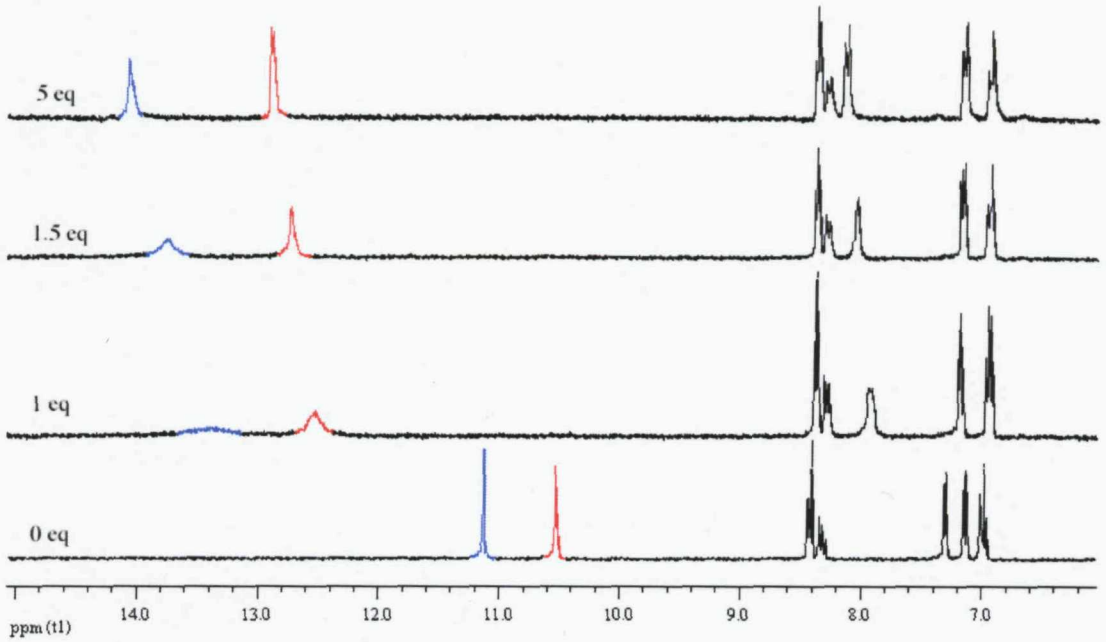

Figure 3.6: ^{1}H NMR stack plot of **3.7a** with increasing amounts of fluoride.

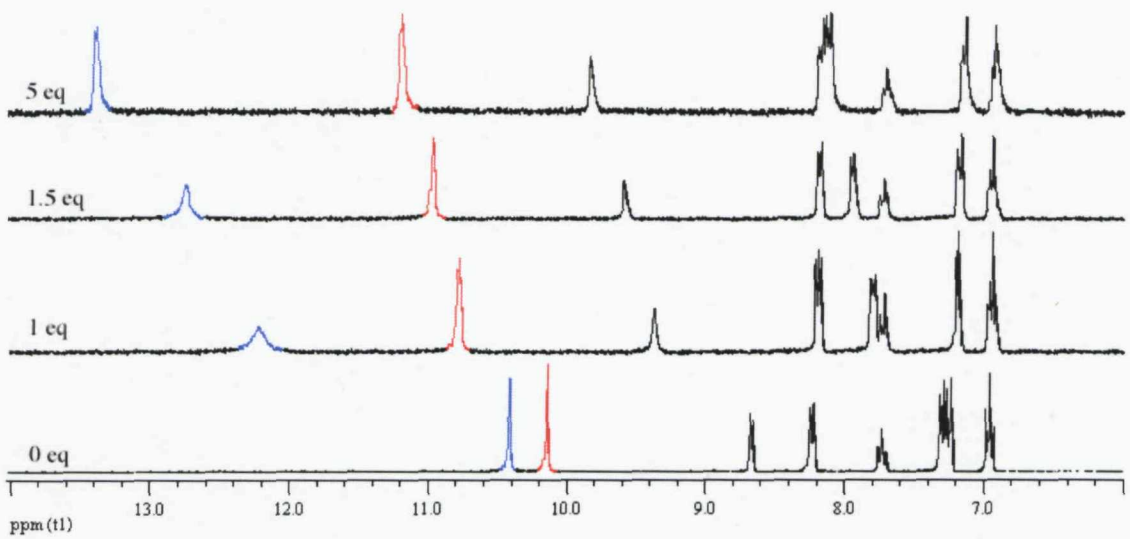

Figure 3.7: ^{1}H NMR stack plot of **3.7b** with increasing amounts of fluoride.

Both stack plots (**Figure 3.6** and **Figure 3.7**) revealed that the amide and indole groups (in blue and red) can be followed throughout the titration and suggests that receptors **3.7a** and **3.7b** bind the fluoride anion and deprotonation is not occurring. The high selectivity for fluoride observed with receptors **3.7a** and **3.7b** can be explained by

the size complementarity between the fluoride anion and the cleft, which was illustrated in the crystal structures.

3.2.3 SOLID PHASE ANALYSIS

X-ray quality crystals of the tetrabutylammonium fluoride complexes of compounds **3.7a** and **3.7b** were obtained by slow evaporation of acetonitrile solution of **37a** and **3.7b** in the presence of an excess of the fluoride salt. The crystal structures of both complexes were found to be similar and revealed a 1:1 receptor/fluoride complex and that the receptors adopted 'twisted' conformations with one indole group orientated above the plane of the central ring and the other indole below the plane of the ring. In the case of the fluoride complex of **3.7a** the anion was bound by four hydrogen bonds interactions from the amide and indole groups (N···F distances between 2.563(5) Å and 2.795(5) Å). However, in the fluoride complex of **3.7b** the hydrogen bond lengths were found to be longer (N···F distances between 2.6102(5) Å and 3.0066(4) Å) and there was an additional short interaction between the isophthalamide 2-position CH group and the anion (C2···F distances of 2.9423(5) Å).

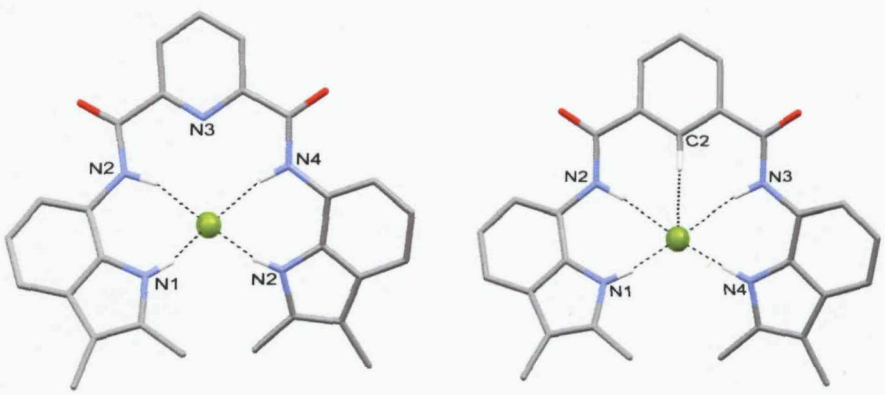

Figure 3.8: X-ray crystal structures of the fluoride complex of **3.7a** and **3.7b** respectively.

The space-filling view of the complexes clearly illustrates the formation of the 'twisted' conformation upon the encapsulation of the anion by the hydrogen bonding groups and the good size complementarity between the fluoride anion and the receptors cavity (**Figure 3.9** and **3.10**).

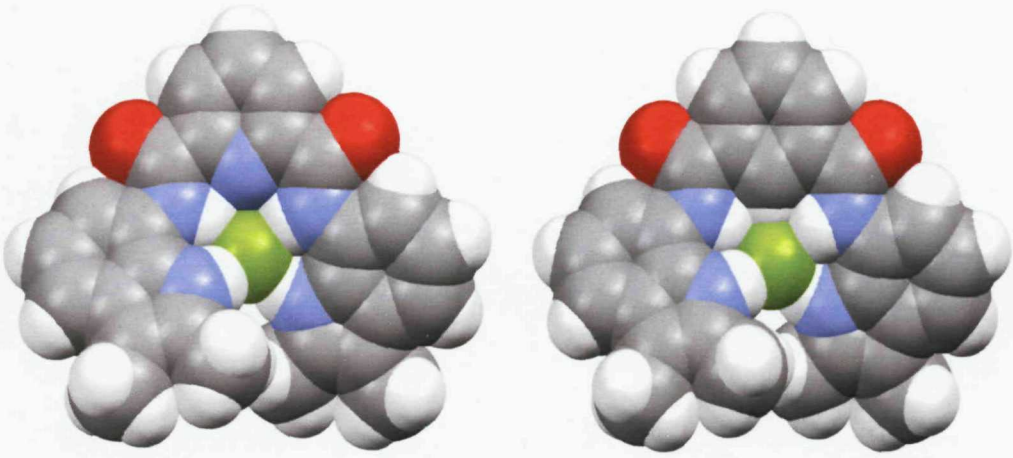

Figure 3.9: Space filling top-view of the fluoride complexes of **3.7a** and **3.7b** respectively.

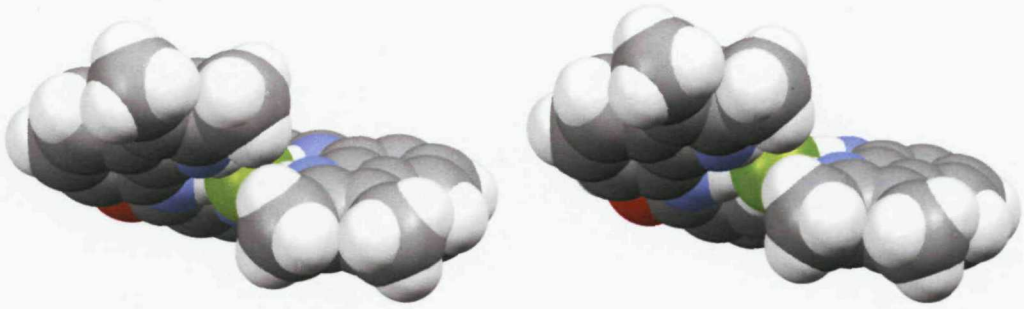

Figure 3.10: Space filling front-view of the fluoride complexes of **3.7a** and **3.7b** respectively.

In addition X-ray quality crystals of the tetrabutylammonium chloride complexes of compounds **3.7a** and **3.7b** were also obtained again by the slow evaporation of acetonitrile solutions of **3.7a** and **3.7b** in the presence of an excess of the chloride salt. The structures revealed that in both cases, the anion was bound by all four NH groups with N···Cl distances between 3.1137(17) Å and 3.4108(16) Å for **3.7a** and N···Cl distances between 3.1474(19) Å and 3.3690(19) Å for **3.7b** (**Figure 3.11**).

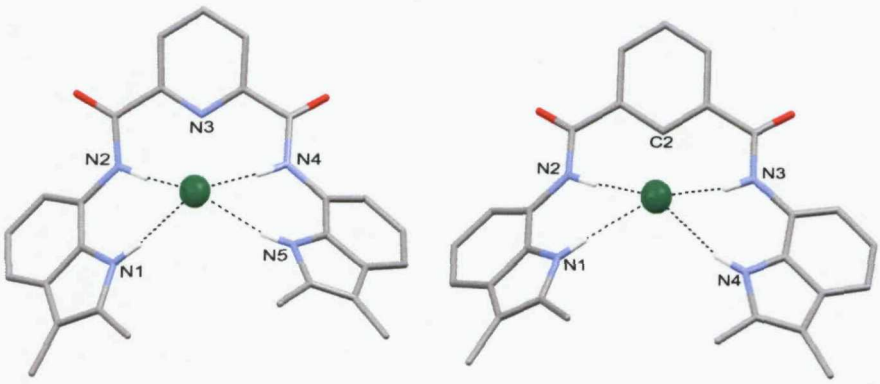

Figure 3.11: X-ray crystal structures of the chloride complex of **3.7a** and **3.7b** respectively.

Space-filling representations of the chloride complexes of **3.7a** and **3.7b** show that the larger chloride anion is not accommodated within the receptors cavity but is perched over the cavity with the hydrogen bond donor NH groups binding to a single face of the anion (**Figure 3.12**).

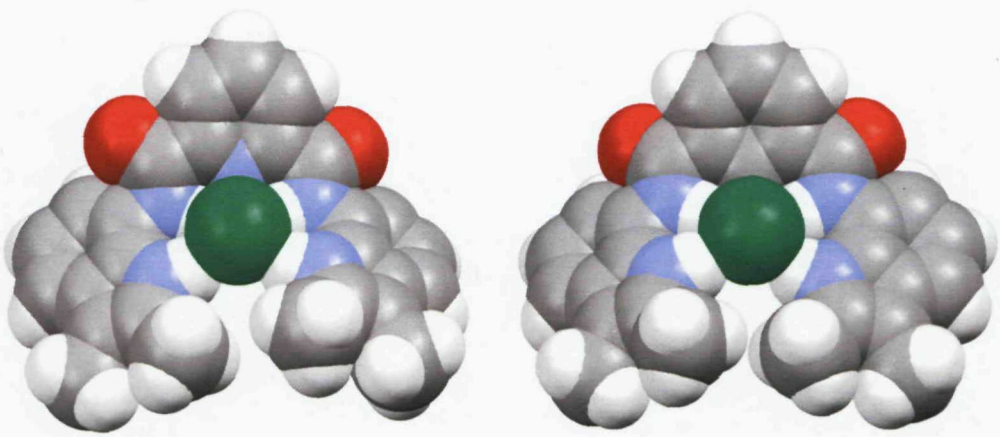

Figure 3.12: Space filling view of the chloride complexes of **3.7a** and **3.7b** respectively

3.3 ANION RECOGNITION OF 2,7-FUNCTIONALISED INDOLE CLEFTS

The success of the simple isophthalamide and pyridine 2,6-diamide bis-indole receptors as anion receptors prompted us, in collaboration with Markus Albrecht of the Institut für Organische Chemie RWTH Aachen, to design new receptors, **3.8** - **3.13**, utilising the indole unit as a scaffold on which to append hydrogen-bonding groups.

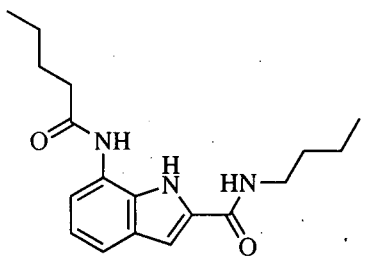

3.8

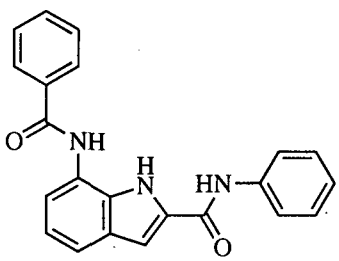

3.9

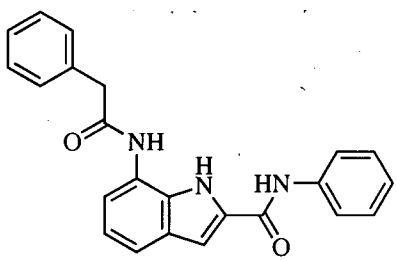

3.10

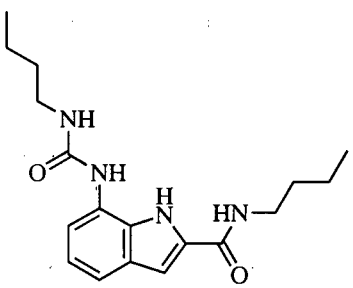

3.11

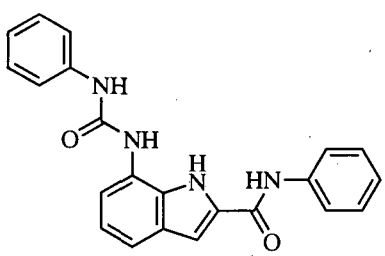

3.12

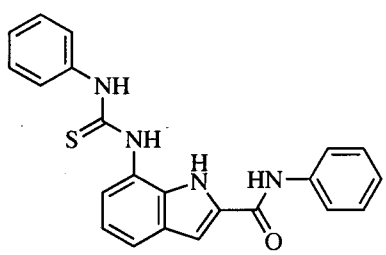

3.13

3.3.1 SYNTHESIS AND CHARACTERISTATION

Compounds **3.8** - **3.11** were synthesized by a simple three-step synthesis. Commercially available 7-nitroindole-2-carboxylic acid (**3.14**) was converted to the acid chloride by reaction with excess thionyl chloride at reflux. The acid chloride was immediately reacted with either butylamine or aniline to afford compounds **3.15a** and **3.15b** in a 78% and 89% yields respectively. Compounds **3.15a** and **3.15b** were then reduced with hydrazine monohydrate/10% Pd/C. The resulting amine **3.16a** was immediately used in subsequent reactions with valeroyl chloride and butylisocyanate to afford compounds **3.8** and **3.11** in 43% and 45% respective yields. Compound **3.16b** was

immediately used in subsequent reactions with benzoyl chloride, phenylacetyl chloride, phenylisocyanate and phenyl isothiocyanate to afford compounds **3.9**, **3.10**, **3.12** and **3.13** in 83%, 83%, 45% and 48% respective yields.

Scheme 2: Reaction scheme for the synthesis of compounds **3.8 – 3.13**.

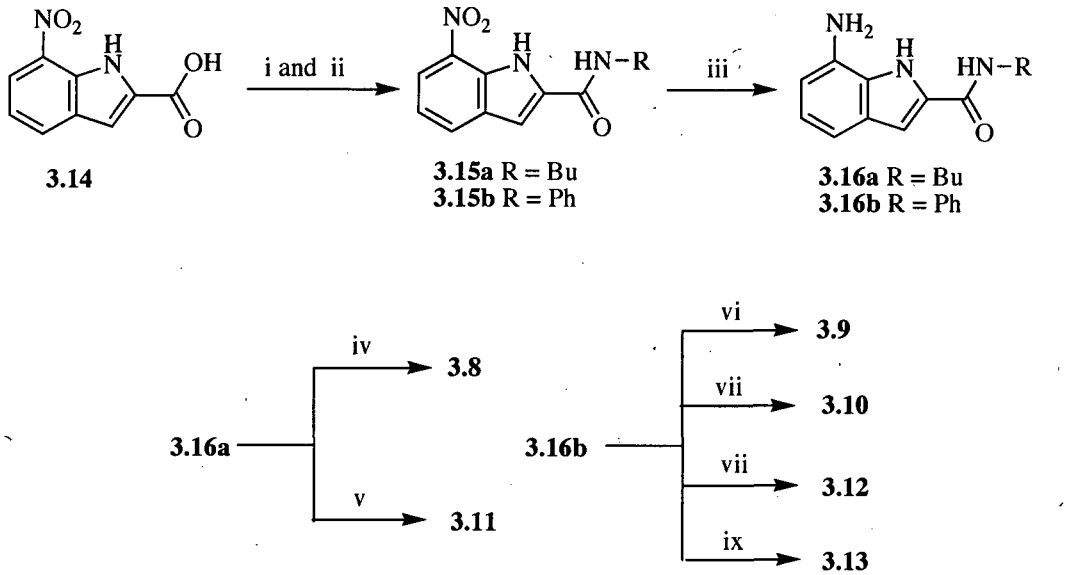

i. $SOCl_2$, ii. R-NH_2, Et_3N, DMAP and DCM, iii. $NH_2NH_2{\cdot}H_2O$, 10% Pd/C, EtOH, iv. *N*-BuCOCl, Et_3N, DMAP and DCM, v. *n*-BuNCO, DCM, vi. C_6H_5COCl, Et_3N, DMAP and DCM, vii, $C_6H_5CH_2COCl$, Et_3N, DMAP and DCM, viii. C_6H_5NCO, DCM, ix. C_6H_5NSO, DCM.

X-ray quality crystals of **3.9** were obtained by slow evaporation of dimethylsulfoxide solutions of **3.9**. The structure of compound **3.9** was elucidated and shows that a solvent molecule is bound to the receptor by two hydrogen bonds from the indole NH and the 7-position amide NH groups with a N1···O2 distance of 2.875(2) Å and a N2···O2 distance of 2.928(2) Å respectively (**Figure 3.13**). Interestingly the amide group in the 2-position (N3) is orientated away from the 'cleft' and is bound to an adjacent 7-position amide (O1') to form a dimer in the solid phase (N3···O1' distances of 2.907(2) Å).

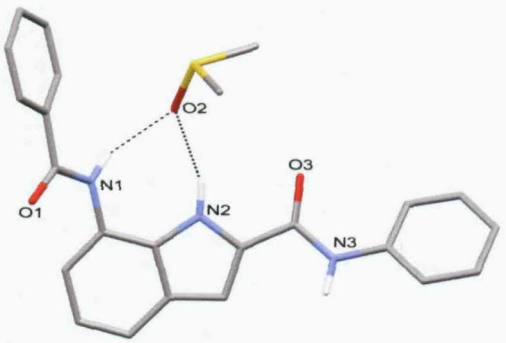

Figure 3.13: X-ray crystal structure of compound **3.9**

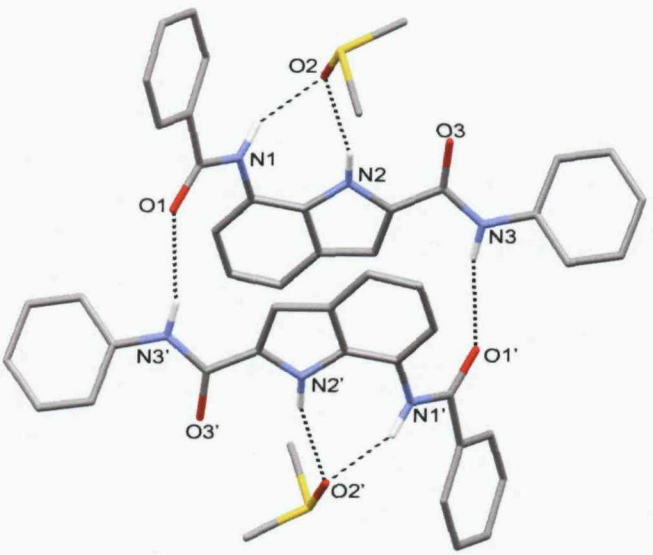

Figure 3.14: Structure of hydrogen bonded dimer of **3.9**

X-ray quality crystals of compound **3.10** were obtained by slow evaporation of separate solutions of the receptor in acetonitrile and DMSO (**Figure 3.15**). The structure resulting from crystals obtained from dimethylsulfoxide was found to have a similar structure to that of **3.9**, in that a dimethylsulfoxide molecule was bound to the indole NH and the 7-position amide NH groups with a N2···O2 distance of 2.856(2) Å and a N1···O2 distance of 2.907(2) Å respectively. The extended structure shows the formation of a dimer *via* the interaction of the 2-position amide NH and the 7-position carbonyl group (N3···O1 distance of 2.859(2) Å). The crystal structure of **3** obtained from acetonitrile solution reveals that the receptor forms a dimer in the solid state with the indole and 7-position amide NH groups bound to an adjacent CO group from the 2-

position amide with a N2···O2' distance of 2.8812(18) Å and a N1···O2' distance of 2.9607(18) Å respectively.

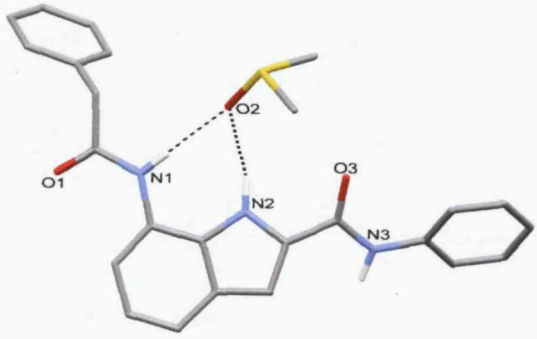

Figure 3.15: X-ray crystal structure of compound **3.10**.

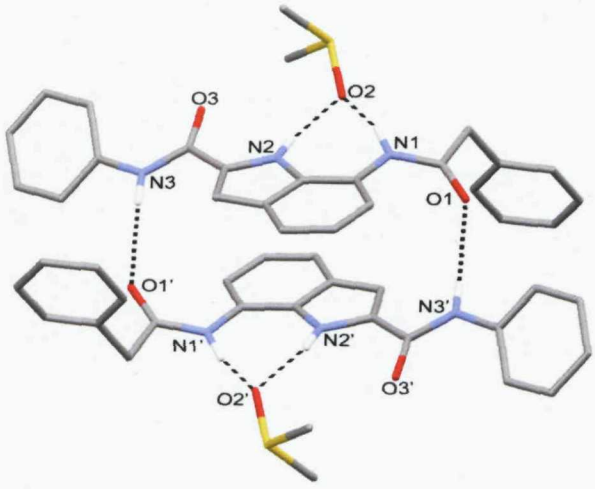

Figure 3.16: Structure of hydrogen bonded dimer of **3.10** from dimethylsulfoxide solutions.

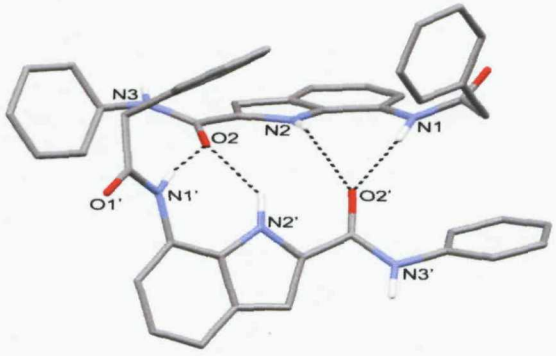

Figure 3.17: Structure of hydrogen bonded dimer of **3.10** from acetonitrile solutions.

A similar dimethylsulfoxide complex of compound **3.12** was obtained by slow evaporation of dimethylsulfoxide solutions of the receptor (**Figure 3.18**). The structure again shows the formation of a dimer (similar to the structures of compounds 2 and 3) by interaction of the amide NH groups in the 2-position with the adjacent carbonyl oxygen atom of the urea group (N4···O1' 2.877(2) Å). The two urea NH groups were found to bind the solvent molecule (N1···O2 distance of 3.012(2) Å and N2···O2 distance of 2.830(2) Å) and the indole NH group (N3···O2 distance of 2.949(2) Å).

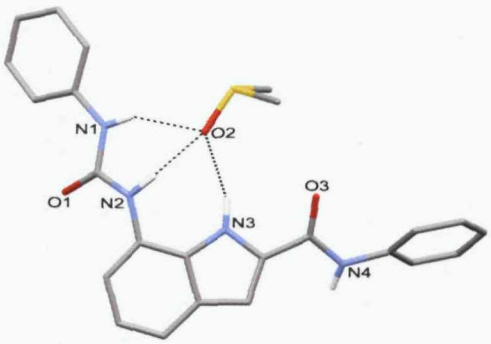

Figure 3.18: X-ray crystal structure of compound **3.12**.

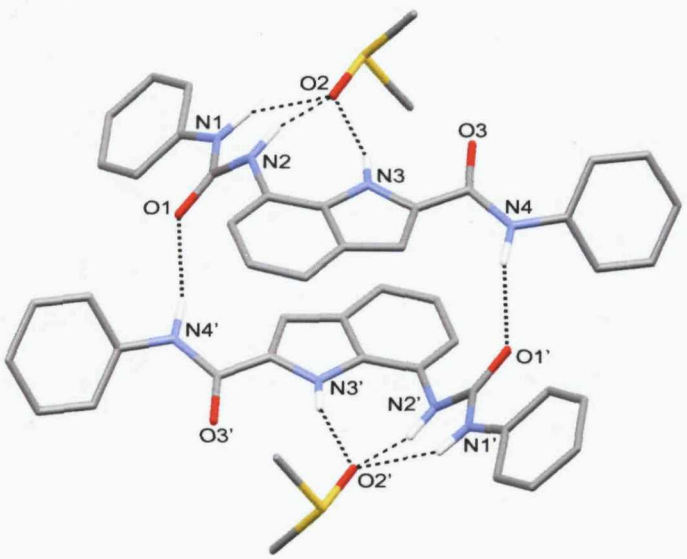

Figure 3.19: Structure of hydrogen bonded dimer of **3.12** from dimethylsulfoxide solutions.

3.3.2 SOLUTION STUDIES

Proton NMR titration experiments were carried out in DMSO-d_6/0.5% water solutions at 298 K in order to elucidate the stability constants for receptors **3.8-3.10** with acetate, benzoate, dihydrogenphosphate and chloride (added as their tetrabutylammonium salts). All the titration curves fitted a 1:1 receptor:anion binding model with EQNMR.[87]

Table 3.3: Stability constants of **3.8-3.10** (M^{-1}) with various anionic guests (added as their TBA salts) in DMSO-d_6/0.5% water at 298 K. Errors (deviation from the fit plot line) were estimated to be no more than ±10%.

Anion	3.8	3.9	3.10
Acetate	425	650	900
Dihydrogenphosphate	390	310	350
Benzoate	115	100	140
Chloride	<10	<10	11

Compounds **3.8-3.10** were found to bind the anions according to their basicity in the order $CH_3CO_2^- > H_2PO_4^- > C_6H_5CO_2^- > Cl^-$. Appreciable differences in the affinity of the receptors were only observed with the titrations involving acetate where compound **1** was found to have the lowest affinity for acetate (425 M^{-1}) and **3** the highest (900 M^{-1}).

The ^1H NMR titration curve of **3.8** shows that all three NH groups shift downfield by over 1 ppm upon the addition of increasing amounts of acetate, a result indicative of anion binding (**Figure 3.20**). In the case of **3.10** the amide resonances shifted significantly further downfield than in **3.8** (**Figure 3.21**), presumably due to stronger interactions between the acetate anion and **3.10**, leading to the higher stability constant obtained for **3.10** for acetate.

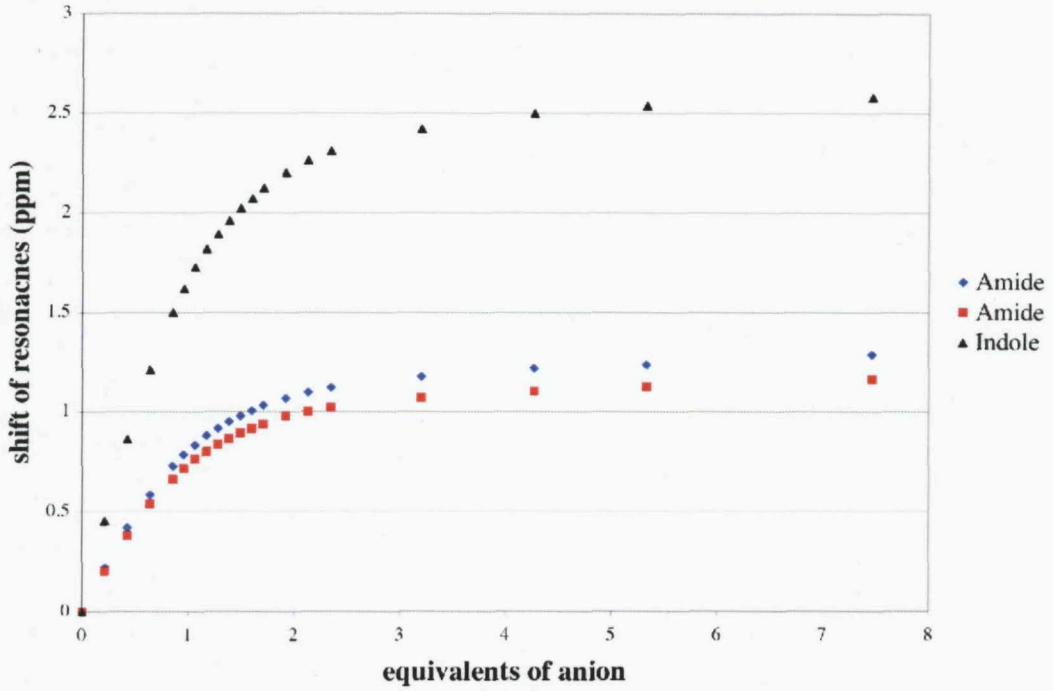

Figure 3.20: ^{1}H NMR titration curve of **3.8** with increasing amounts of TBA acetate.

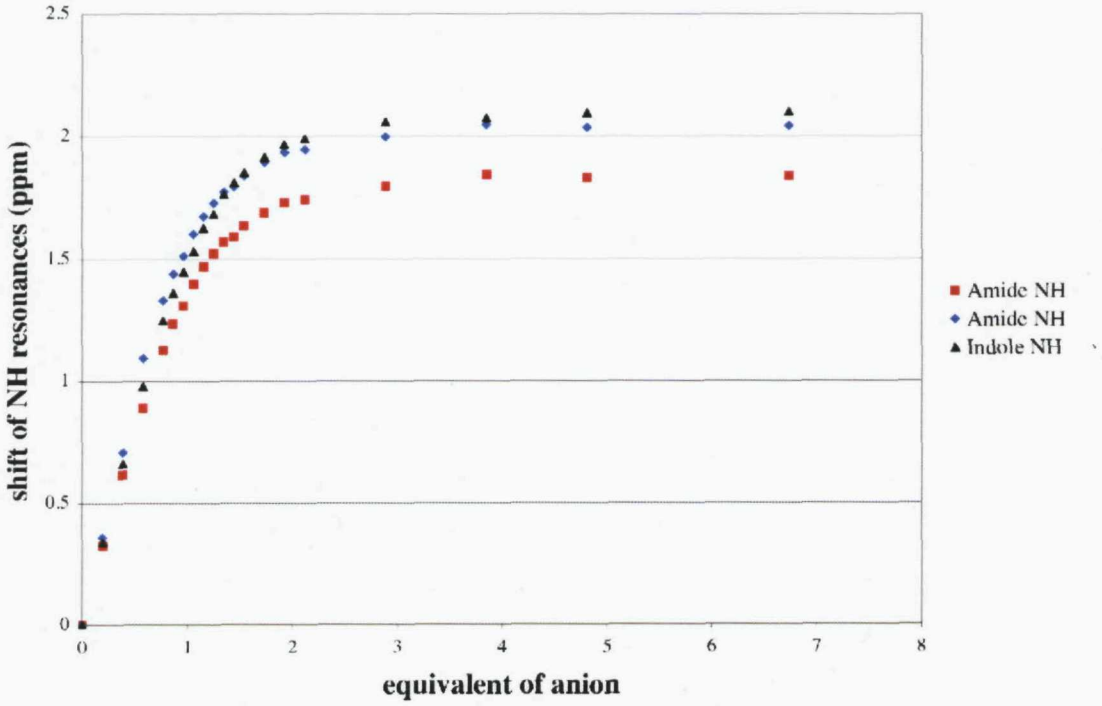

Figure 3.21: ^{1}H NMR titration curve of **3.10** with increasing amounts of TBA acetate.

The appreciable shifts downfield of all the NH resonances suggests that the anion is stabilised by all three NH groups in solution and is bound to the receptor *via* the proposed binding mode illustrated in **Figure 3.23**.

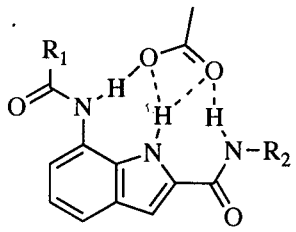

Figure 3.23: Proposed binding mode of the acetate anion to receptors **3.8-3.10**

Stability constants were calculated for receptors **3.11-3.13** by ^{1}H NMR titration experiments under identical condition used to determine the stability constants for compounds **3.8-3.10** (**Table 3.4**).

Table 3.4: Stability constants of **3.11-3.13** (M^{-1}) with various anionic guests (added as their TBA salts) in DMSO-d_6/0.5% water at 298 K. Errors estimated to be no more than ±10%.

Anion	3.11	3.12	3.13
Acetate	2060	10000	[b]
Dihydrogenphosphate	940	4950[a]	1600
Benzoate	680	4460	780
Chloride	20	38	16

[a] Errors estimated to be no more than ±12%. [b] not determined due to peak coalescence and broadening upon the addition on TBA acetate.

Receptors **3.11-3.13** were found to bind the anions in the same trend as for **3.8-3.10** ($CH_3CO_2^- > H_2PO_4^- > C_6H_5CO_2^- > Cl^-$), however much higher affinities for the anions were observed with receptors **3.11-3.13**. The urea functionalized receptor **3.11** was found to bind acetate approximately 5 times more strongly that its amide analogue **3.8** (2060 M^{-1} and 425 M^{-1} respectively). In the case of **3.12**, acetate was found to bind by over two orders of magnitude greater than with the amide analogue **3.10** (10000 M^{-1} and 900 M^{-1} respectively). Interestingly when the urea group in **3.12** was replaced with a more acidic thiourea group (**3.13**) a significant decrease in the association constants

was observed, presumably due to steric interaction between CH groups and the large sulphur atom resulting in the loss of the convergent hydrogen bonding array.

Examination of the ^{1}H NMR titration curves of **3.11** showed that appreciable downfield shifts (> 1.5 ppm) are observed in the NH resonances of the urea and indole groups, however a smaller shift (< 0.5 ppm) is observed in the amide NH resonance indicating that the amide interacts weakly with the acetate anion in solution (**Figure 3.25**). The titration curves of **3.12** with acetate revealed that the urea groups shift further downfield (approximately 2.4 and 2.7 ppm) compared to the urea groups in **3.11** (approximately 1.8 and 1.9 ppm), suggesting much stronger interaction between the urea NH groups and the acetate anion in **3.12** compared to **3.11** which presumably results in the high stability constant obtained for **3.12** with acetate (**Figure 3.26**). Comparisons of the amide NH titration curves to the indole and urea curves in **3.12** show that for the urea and indole curves a plateau is reached after the addition of 1 equivalent of acetate however the amide curve appears to continue to shift downfield throughout the titration suggesting that the amide interacts weakly with the acetate anion (similar to **3.11** titration) and consequently due to it's relative conformational freedom could orientate itself away from the cleft (**Figure 3.24**).

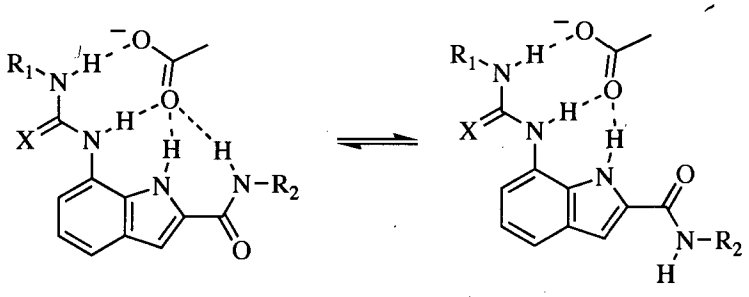

Figure 3.24: Proposed binding mode of the acetate anion to receptors **3.11** and **3.12**.

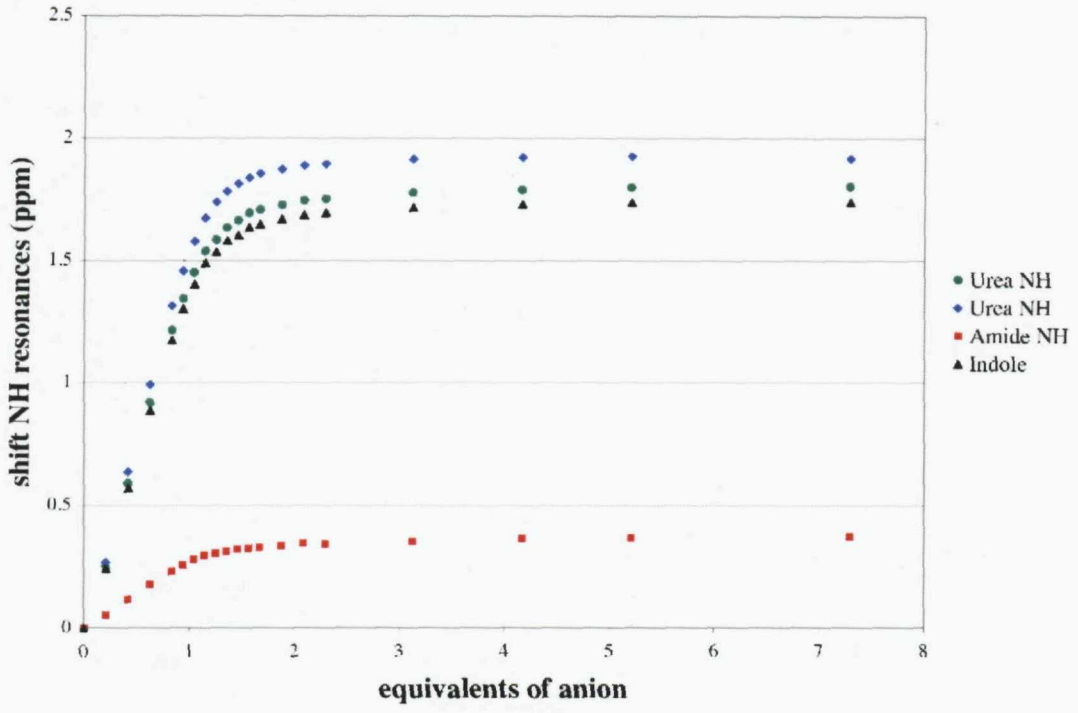

Figure 3.24: ^{1}H NMR titration curve of **3.11** with increasing additions of TBA acetate

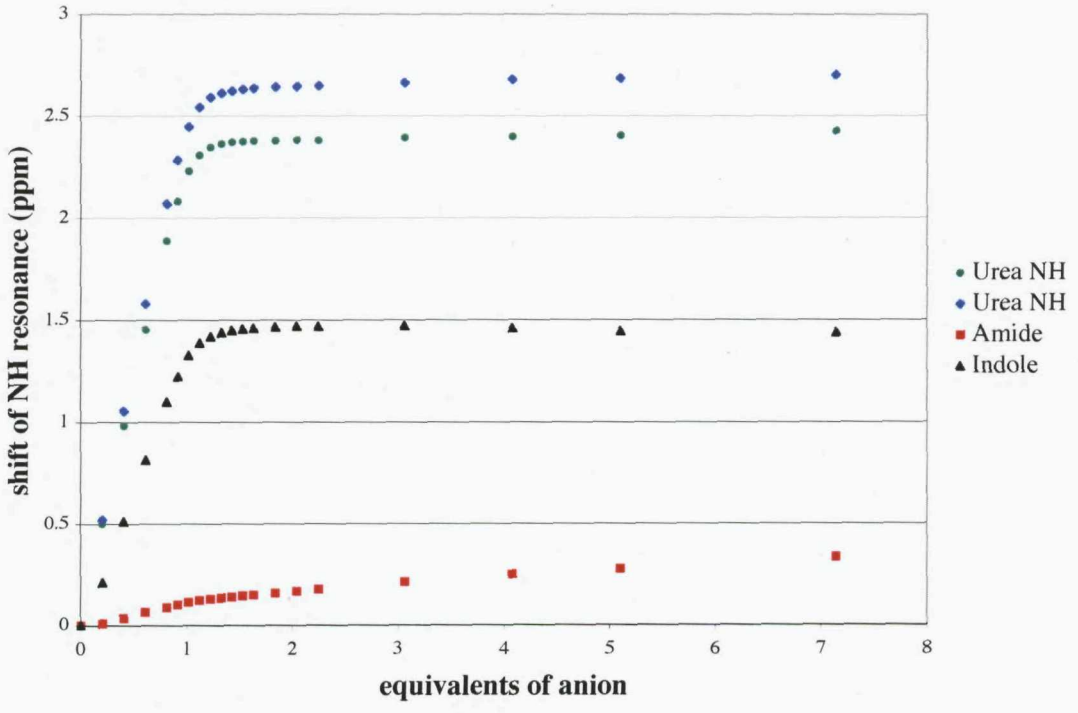

Figure 3.26: ^{1}H NMR titration curve of **3.12** with increasing additions of TBA acetate

3.3.3 SOLID STATE ANAYLSIS

X-ray quality crystals were obtained of the chloride complex of **3.12** by slow evaporation of a dimethylsulfoxide solution of compound **3.12** in the presence of excess tetrabutylammonium chloride. The structure revealed that there are two crystallographically distinct chloride complexes of **3.12** within in the unit cell bridged by a chloride anion bound by two hydrogen bond interactions from the 2-postion amide NH groups of each receptor (N4···Cl2 distance of 3.350(4) Å and a N4'···Cl2 distance of 3.272(4) Å (**Figure 2.20**)). One complex showed that the chloride anion was bound by three hydrogen bond interactions from the urea (N1···Cl1 distances of 3.256(4) Å and a N2···Cl1 distances of 3.144(4) Å) and indole NH groups (N3···Cl1 distances of 3.326(4) Å). The second complex revealed that the chloride again was bound by three hydrogen bond interactions from the urea (N1'···Cl1' distances of 3.330(4) Å and a N2'···Cl1' distances of 3.152(4) Å) and indole NH groups (N3'···Cl1' distances of 3.357(4) Å) however there are additional interactions between a bridging water molecule and the chloride anion (O3···Cl1' distance of 3.172(5) Å). Within the crystal the water molecule was also bound to the carbonyl group of the 2-position amide group (O3···O2' distance of 2.923(6) Å).

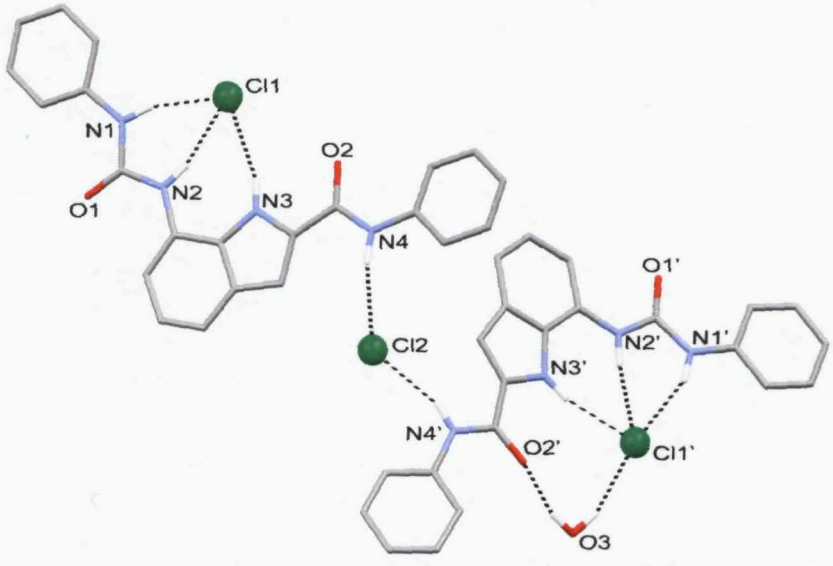

Figure 3.20: Crystal structure of the dimer in the **3.12** chloride complex.

X-ray quality crystals of the benzoate complex of **3.13** were obtained by slow evaporation of a dimethylsulfoxide solution of compound **3.13** in the presence of excess tetrabutylammonium benzoate. The structure showed the formation of a 2:1 anion/receptor complex in the solid state (**Figure 3.24**). One benzoate anion was bound by a single hydrogen bond provided by the 2-position amide NH group with a N4···O4 distance of 2.869(3) Å. The second benzoate anion was bound by three hydrogen bonds with a single benzoate oxygen atom bound to the outer thiourea NH (N1···O1 distances of 2.865(3) Å) and the second bound to both the inner thiourea NH groups and the indole NH (N2···O2 distance of 2.719(3) Å and a N3···O2 distance of 2.2.767(3) Å respectively).

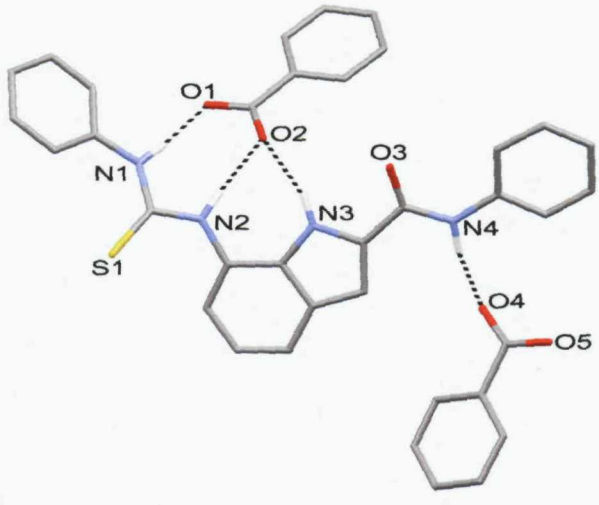

Figure 3.24: Crystal structure of the benzoate complex of **3.13**.

3.4 CONCLUSIONS

A number of indole-based receptors have been synthesised and their anion recognition properties have been studied by ^{1}H NMR titration experiments that have shown that the indole subunit can be used in the complexation of anionic guests.

Receptors **3.7a** and **3.7b** have been shown to be selective for fluoride in competitive solvent media (DMSO/5% water) as a consequence of a good size complementarity between the receptor and fluoride anion, which was also illustrated in the x-ray crystal structures. The solution studies of receptor **3.7b** reveals that fluoride binds to the receptor with a 1:2 receptor/anion stiochiometry presumably due to the relative conformational freedom of the isophthalamide moiety in solution.[19,20] This would allow for a second fluoride anion to bind to the receptor at higher fluoride concentrations.

The 2,7-functionalised indole clefts were shown to bind anions in DMSO-d_6/0.5%water solutions according to the basicity of the anion (acetate > dihydrogenphosphate > benzoate > chloride), however differences between the acetate stability constants were observed with a change in the functionality at the 7-positions of the indole skeleton. Increasing the acidity of the amide groups in receptors **3.8**-**3.10** by replacing the alkyl chains of **3.8** to aromatic groups in **3.9** and **3.10** increased the acetate stability constants. When the 7-position amide was replaced with a urea subunit the acetate stability constants were significantly increased. Closer examination of the titration curves revealed that in the urea substituted receptors the 2-position amide bound weakly to the acetate anion, presumably due to the relative rotational freedom of the amide group.

What is clear from these investigations is that the relatively overlooked indole unit is a useful and functionalisable subunit that should be considered in the design of receptors for the purpose of anion recognition.

CHAPTER 4 – HYDROMETALLURGICAL EXTRACTION OF NICKEL(II) SULFATE BY A DUAL HOST STRATEGY

4.1 INTRODUCTION

Base metals are important commodities in the modern world and recently their demand, consumption and price have increased significantly. In particular nickel, which is used mainly in the production of nickel steels and nickel cast irons, has seen its price almost treble in the past four years due to the rising demand for steel, particularly in China.[112] As a consequence of this demand, major new projects and sources of nickel ores are required. A recent example of such a project is the Bulong operation in Western Australia, which produces nickel and cobolt from a lateritic ore.[113,114]

Metallurgy is the extraction, purification and modification of metals from their ores for a more useful purpose. Metallurgy is known to have existed for over 6000 years where originally metals were combined to form alloys such as bronze.[115]

Currently industry predominantly uses pyrometallurgical smelting techniques in order to obtain metals, however these processes require large amounts of energy and produce large volumes of pollutant and toxic gas emissions.[115,116] Additionally the disposal of the solid residues and by-products of the process is a major issue associated with pyrometallurgy. The reduction of the environmental impact of these operations is becoming an increasingly important issue for the mining and refining industry to address.

4.1.1 HYDROMETALLURGY

Hydrometallurgy involves the extraction of metals from an aqueous solution of their ores. There are a number of hydrometallurical extraction/separation techniques including selective crystallisation, selective reduction and adsorption of ions onto solid matrices. An area of increasing interest is extractive hydrometallurgy where typically the metal of value is leached into an aqueous solution and subsequently transferred to a hydrophobic organic solvent thus separating and concentrating the metal of value (a typical flowsheet for this process is illustrated in **Figure 4.1**).[116-118] This technique offers a number of solutions to the environmental problems associated with pyrometallurgy and also allows for the metal of interest to be recovered from more complex and/or low-grade ore stocks. Other advantages of hydrometallurgical techniques are that the process usually requires less energy in comparison to pyrometallurgical techniques and the ore processing can be done close to mine sites thus removing high ore transport costs.[119]

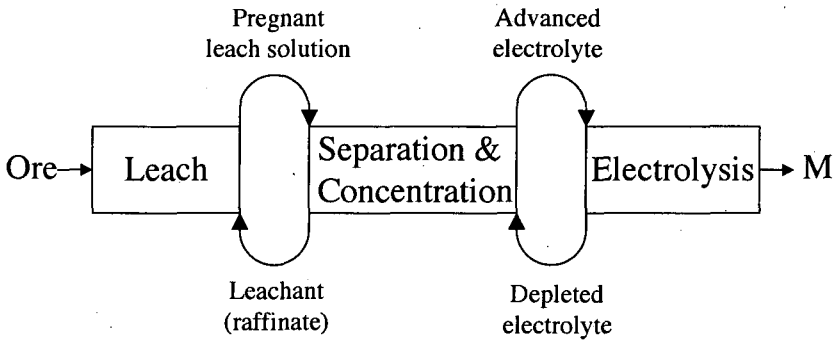

Figure 4.1: The Basic flowsheet for extractive hydrometallurgy.

Liquid-liquid solvent extraction is becoming increasingly used in extractive hydrometallurgy and involves the use of chemical processes, such as the formation of the metal complexes, to selectively extract the metal of value from an aqueous media into an immiscible organic phase (in practice high boiling point hydrocarbons, such as kerosene, are used in large scale solvent extraction processes). This process effects the separation and concentration operations (**Figure 4.2**) as part of a four-step flowsheet involving leaching, extraction, stripping and electrowinning.[120] Leaching involves the dissolution of the metal from the ore to generate an aqueous pregnant leach using a

range of reactants, depending on the chemical composition of the ore.[120] Selective extraction of the metal of value involves the transport of metal cation, metal salts or metallate anions into a non-polar organic phase *via* complexation by a hydrophobic ligand.[120] The organic solubility of the complex is crucial for the success and overall efficiency of the extraction process, therefore the complex ideally is charge neutral and the ligand contains hydrophobic groups, such as large and usually branched alkyl chains. The stripping stage involves the removal of the metal of value from the organic phase and the hydrophobic ligand, transferring it back to an aqueous solution from which the metal is recovered by reduction of the pure metal salt usually by electrolysis. The organic phase containing the regenerated hydrophobic ligand is recycled.

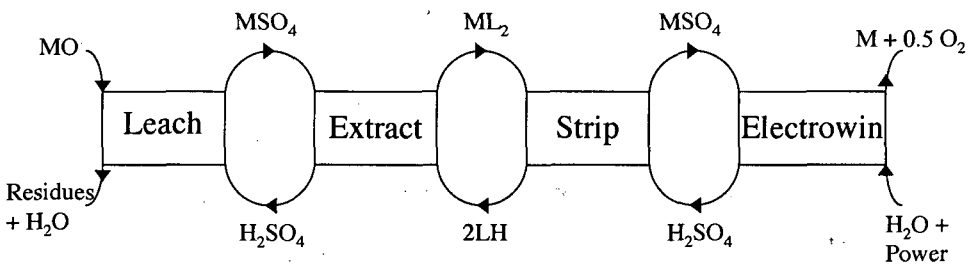

Figure 4.2: A Flowsheet for the liquid-liquid solvent extraction of metals from their oxidic ores.[120]

One of the most successful processes of this type involves the extraction of copper from oxidic ores using phenolic oxime ligands (**Figure 4.3**) to transport the copper from the pregnant leach solution.[120]

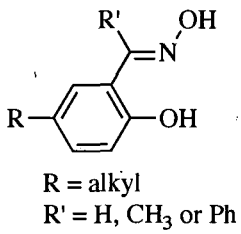

R = alkyl
R' = H, CH_3 or Ph

Figure 4.3: Commercial phenolic oxime copper extractants.[120]

The copper is leached (**Figure 4.5**) from oxidic ores using sulfuric acid, resulting in the formation of a pregnant leach solution containing ca. 3 gl^{-1} Cu(II) and other metal sulfates, principally Fe(III) which is usually present in excess.[118,120] The copper is

selectively extracted from the pregnant leach solution by two hydrophobic ligands and transported into the hydrocarbon solvent. The copper ion displaces a proton from each of the phenol groups to form the charge-neutral complex illustrated in **Figure 4.4** and these protons are released into the aqueous phase, regenerating the sulfuric acid used to leach the metal ore. The copper is stripped from the hydrophobic ligands by contacting the organic phase with an aqueous sulfuric acid solution, at a lower pH than the pregnant leach solution, resulting in the formation of a pure aqueous copper sulfate solution and the regeneration of the protonated ligand in the organic phase, which is recycled. The copper(II) sulfate solution undergoes reductive electrolysis to produce the desired copper metal and sulfuric acid that is fed back into the stripping stage.

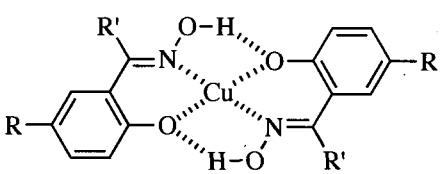

R = alkyl
R' = H, CH_3 or Ph

Figure 4.4: Formation of the charge neutral copper complex with phenolic oxime ligand.

The commercial success of the process is based on the excellent overall material balance (**Figure 4.5**) and the high quality of copper produced by the process. The leachant, extractant and electrolyte are recycled.

$$CuO + H_2SO_{4\,(aq)} \rightleftharpoons CuSO_{4\,(aq)} + H_2O \qquad \text{Leaching}$$

$$CuSO_{4\,(aq)} + 2LH_{(org)} \rightleftharpoons CuL_{2\,(org)} + H_2SO_{4\,(aq)} \qquad \text{Extraction}$$

$$CuL_{2\,(org)} + H_2SO_{4\,(aq)} \rightleftharpoons CuSO_{4\,(aq)} + 2LH_{(org)} \qquad \text{Stripping}$$

$$CuSO_{4\,(aq)} + H_2O \rightleftharpoons Cu + {}^1/_2\,O_2 + H_2SO_{4\,(aq)} \qquad \text{Eletrowinning}$$

$$\mathbf{CuO \rightleftharpoons Cu + {}^1/_2\,O_2} \qquad \mathbf{Net}$$

Figure 4.5: Materials balance for the solvent extraction of copper oxide using phenolic oxime ligands.

4.1.2 SULFIDIC ORES

An area of increasing interest is the extraction of metals of value from sulfidic ores. In hydrometallurgical processes these ores have low solubility and therefore cannot be effectively leached with dilute sulfuric acid under ambient conditions. The ores can be converted into their metal oxides allowing them to be processed according to the flowsheet described in Figures 4.2 and 4.5 by the roasting of the ore in the presence of air (**Figure 4.6**). The roasting process produces SO_2, which is a major pollutant gas that has to be recovered (**Figure 4.6**). This is capital intensive and the generation of sulfuric acid on mining sites is generally not economically viable.[119]

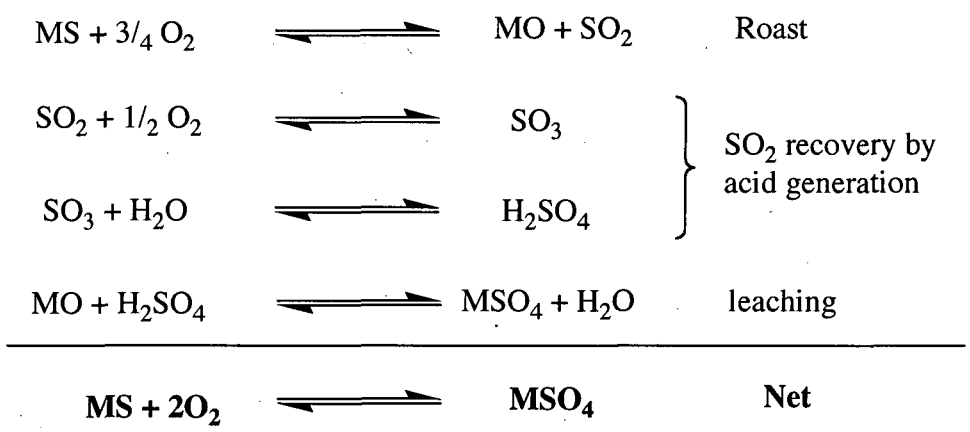

Figure 4.6: The materials balance for the recovery of SO_2 by acid generation.

New microbial leaching and high pressure leaching involve the conversion of the sulfidic ore to the sulfate producing a pregnant leach solution that can be used for the liquid-liquid solvent extraction of the metal of value.[118,121] These leaching techniques are economically more viable compared to the roasting technique described in **Figure 4.6** as they avoid the generation of SO_2. However, if the sulfate pregnant leach solution is extracted with the commercial phenolic oxime ligand system, used for metal oxides (**Figure 4.4**), then during the extraction step sulfuric acid builds up in the system. This doesn't occur in the process for oxidic ores as the sulfuric acid is recycled for the leaching step. The build up of sulfuric acid significantly reduces the extraction

efficiency of the process as the decreasing pH hinders the complexation of the metal ion to the ligand in the aqueous phase (**Figure 4.7**).

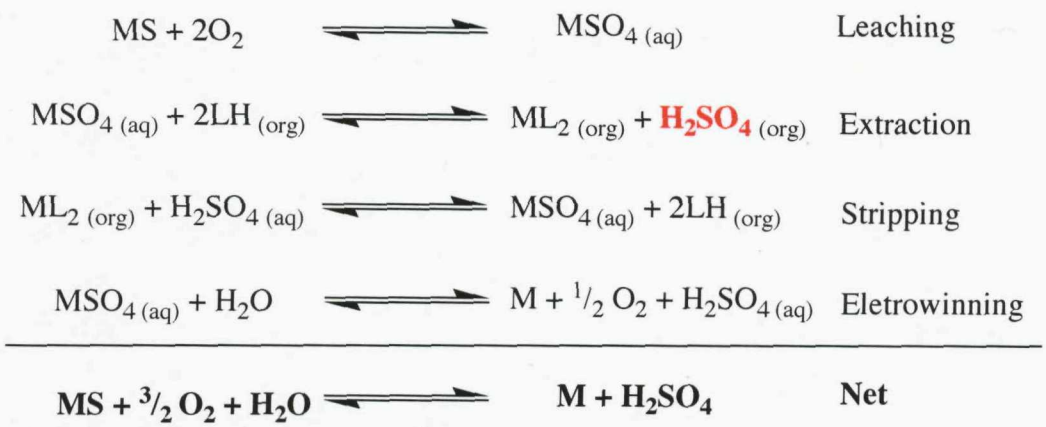

Figure 4.7: Material balance of phenolic oxime extraction of metals from sulfidic ores showing the generation of sulfuric acid during the extraction step.

A way to overcome this problem is to use a ligand system that can extract both the metal cation and the sulfuric acid into the organic phase. Tasker and co-workers have approached this problem by synthesising a number of zwitterionic ditopic receptors where the acid-binding site is covalently attached to a salen-based metal binding site.[122-124]

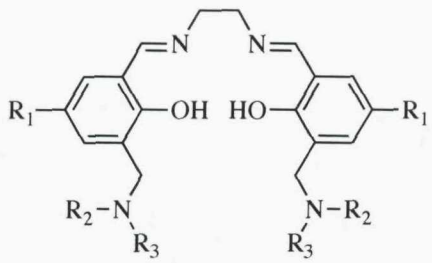

R_1, R_2,R_3 = Alkyl

Figure 4.8: Generic form of salen-based zwitterionic ditopic receptors.[122-124]

The system was designed so that upon the coordination of the metal ion the two phenolic protons would be displaced and protonate the tertiary amine groups attached to the salen scaffold, which would then bind the sulfate anion thus removing the excess sulfuric acid generated in the extraction of the metal (**Figure 4.9**).

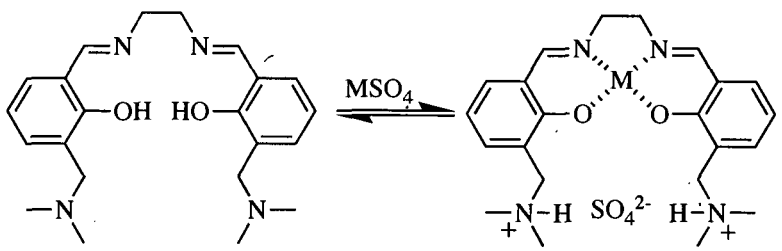

Figure 4.9: expected binding of metal sulfates with salen-based zwitterionic receptors.

Compound **4.1** was found to co-extract copper(II) sulfate from an aqueous feedstock and the copper(II) sulfate could be stripped back from the organic phase, which regenerated **4.1**.

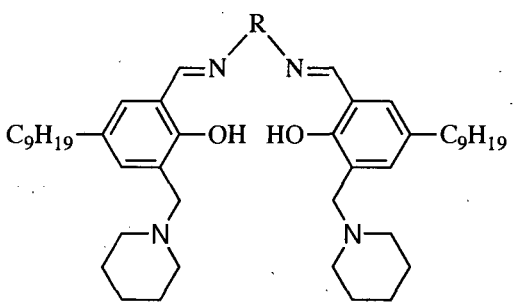

4.1 R = biphenyl

At pH values <1.5 it was found that the percentage of theoretical sulfate extracted exceed 100%, a result consistent with the receptor extracting two hydrogen sulfate anions, which are more abundant at low pH, rather than one sulfate anion (1:1 mixture of SO_4^{2-} and HSO_4^- at pH = 1.92, **Figure 4.10**).

$$HSO_4^- + H_2O \rightleftharpoons SO_4^{2-} + H_3O^+ \qquad pH = 1.92$$

Figure 4.10: Equilibrium between sulfate and hydrogen sulfate in water.

Tasker and co-workers also investigated the possibility of improving the selectivity of the receptors towards sulfate over hydrogen sulfate. One approach was to synthesise the macrocyclic receptor **4.2**.[124,125]

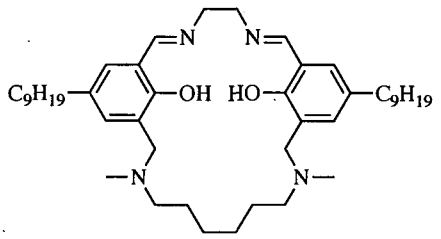

4.2

It was hoped that the macrocycle would have an increased sulfate affinity as a consequence of the macrocyclic effect and the encapsulation of the sulfate anion. Extraction experiments showed that **4.2** could be used for the co-extraction of nickel and sulfate or copper and sulfate. Similarly to **4.1**, at pH < 2.0 hydrogen sulfate anions were extracted preferentially.

Recently Tasker, Schröder and co-workers have synthesised receptors with extra hydrogen bond donor groups present in the pendent amine group, such as **4.3**, and have investigated if these increase affinity for sulfate anions.[126,127] The studies of **4.3** showed that the pH profile was almost ideal for the extraction of copper(II) sulfate and in a single phase system (95% methanol/ water mixture) **4.3** was found to be selective for sulfate over chloride.

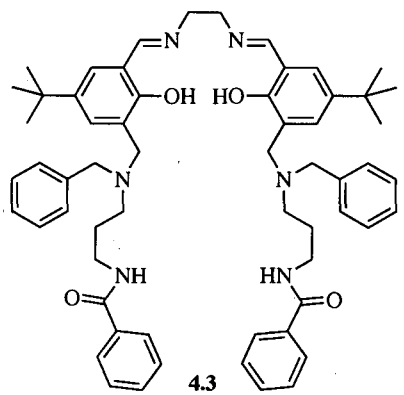

4.3

4.2 DUAL HOST APPROACH TO THE EXTRACTION OF NICKEL(II) SULFATE

The zwitterionic ditopic receptors (**Figure 4.8**) have proven useful for the extraction of copper(II) sulfate and the introduction of hydrogen bonding groups to the pendent arms of the receptor has been shown to improve the sulfate selectivity of the ditopic systems. However, the increasing functionalisation of the ditopic receptors to improve the affinity and selectivity of the receptors for sulfate inevitably requires more complex synthesis and larger ligands, which in turn increases the cost of manufacture and the mass of extractant required per unit mass of metal recovered.

One approach to reduce manufacturing cost is to use simple small molecules to extract the sulfuric acid from the pregnant leach solution independently from the extraction of the metal ion, a strategy that has been successful for the co-extraction of $CsNO_3$.[128] A major advantage of this 'dual host' approach compared to the ditopic ligand approach is that it is much easier to achieve selectivity for the metal cation and the sulfate anion with individual components whereas in the case of the ditopic receptor selectivity for both the metal cation and the sulfate anion needs to be included in a single extractive ligand. A number of groups have previously synthesised receptors that exhibit selectivity towards sulfate and hydrogen sulfate anions.[21,24,52-54]

Recently Sessler, Moyer and co-workers have described the use of **4.4**, a cylcyclo[8]pyrrole, in the extraction of sulfate anions in the presence of nitrate. Toluene solution of **4.4** were contacted with aqueous solutions of sodium sulfate and sodium nitrate and in the presence of the phase transfer catalyst Aliquat 336-nitrate the system preferentially extracted sulfate over nitrate.[129]

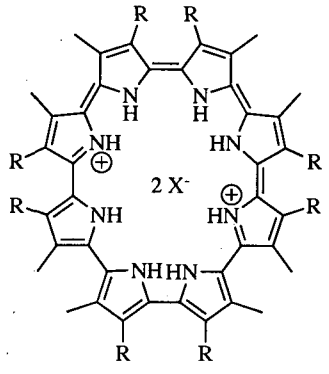

$R = C_{11}H_{23}$

X = anion

4.4

Gale and co-workers have shown that simple acyclic clefts appended with protonatable groups can be used to transport acid, mainly HCl, across membranes. Initially receptor **4.5a**, a prodigiosin mimic, was investigated as a transport agent for HCl across vesicle membranes.[130,131] At pH 7.2 both inside and outside the vesicle a moderated rate of Cl^- efflux was observed upon the addition of **4.5a**. In the presence of a pH gradient (pH 4.0 inside the vesicle and pH 7.2 outside) a much greater rate of efflux was observed upon the introduction of **4.5a**. Compound **4.5b** was also shown to co-transport HCl across vesicle membranes. At pH 7.0 both inside and outside the vesicle compound **4.5b** was found to be an effective chloride transporter.

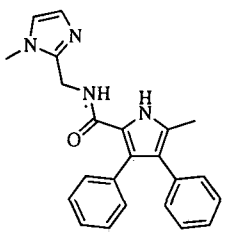

4.5a

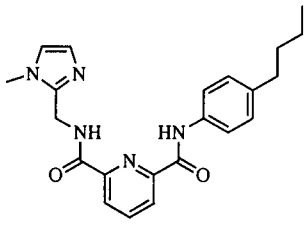

4.5b

Inspired by these results it was decided that receptors **4.6-4.9** (diamidopyrrole receptors appended with protonatable groups) would be synthesised and studied as potential extraction agents for sulfuric acid for potential use in the liquid-liquid solvent extraction of nickel(II) or other metal sulfates.

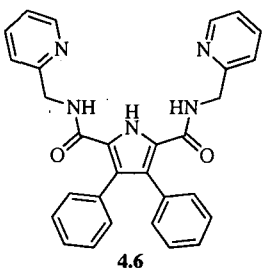

4.6

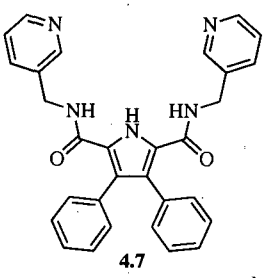

4.7

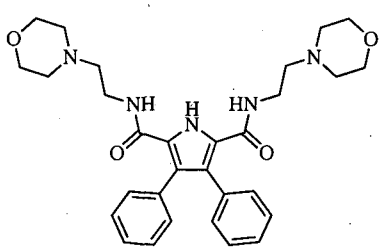

4.8

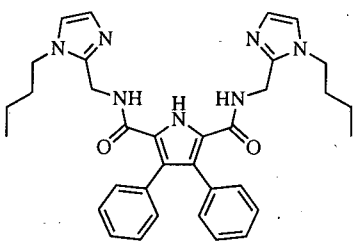

4.9

4.2.1 SYNTHESIS AND CHARACTERISATION

3,4-Diphenyl-1*H*-pyrrole-2,5-dicarboxylic acid was prepared according to literature procedure[131] and converted to the acid chloride *via* reaction with thionyl chloride at reflux. The acid chloride was then dried *in vacuo* and immediately added to a dichloromethane solution of the appropriate amine in the presence of triethylamine and a catalytic amount of DMAP to afford the desired diamidopyrroles **4.6**-**4.9** in 63%, 62%, 48% and 67% yield respectively.

Scheme 4.1: Synthesis of compounds **4.6**-**4.9**.

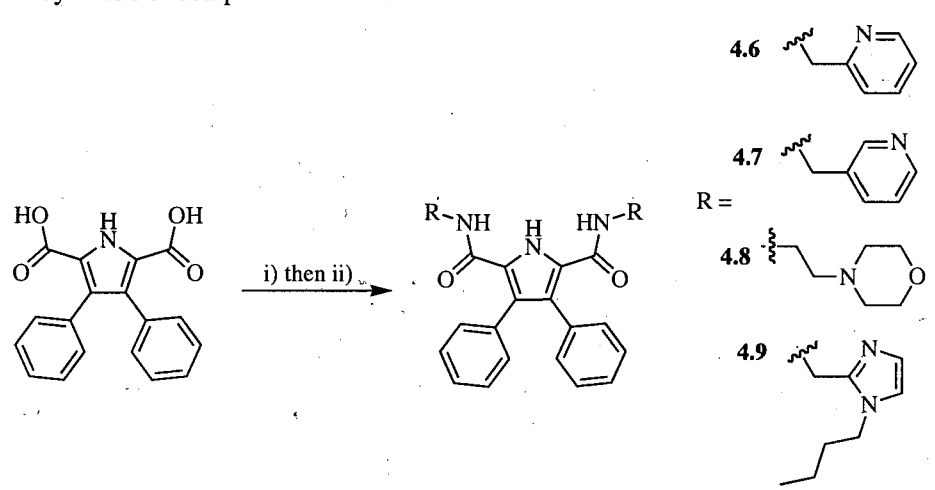

i) $SOCl_2$, ii) 2 RNH_2, DCM, Et_3N, DMAP and amine.

X-ray quality crystals of compounds **4.6** and **4.8** were obtained by the slow evaporation of methanol solutions of **4.6** and **4.8**. Both crystal structures showed that in the solid state **4.6** and **4.8** form hydrogen bonded dimers *via* two hydrogen bond interactions between the pyrrole NH group and an adjacent amide carbonyl group with a N2···O1' distance of 2.9872(16) Å and 3.0166(17) Å for **4.6** and **4.8** respectively.

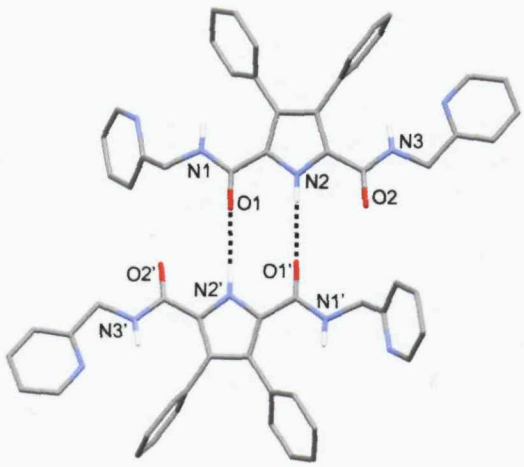

Figure 4.11. X-ray crystal structure of hydrogen bonded dimer in **4.6**.

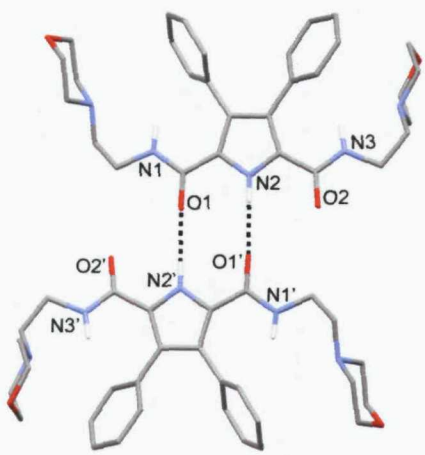

Figure 4.12. X-ray crystal structure of hydrogen bonded dimer in **4.8**.

4.2.2 EXTRACTION STUDIES

0.01 M chloroform solutions of receptors **4.6**-**4.9** were prepared and 5 mL aliquots were added to an equal volume of 0.8 M aqueous sulfate solutions across a pH range. The two phases were stirred vigorously for 24 hours in order for phase transfer processes to reach equilibrium. The two phases were separated and the pH of the aqueous phase recorded. 2 mL of the organic phase was transferred to a 10 mL volumetric flask and the chloroform evaporated *in vacuo*. The residue was dissolved in 10 mL of butanol and analysed by Inductively Coupled Plasma – Optical Emission Spectrometry (ICP-OES), to determine the amount of sulphur present. The percentage loading of sulfate by the ligands, assuming formation of a $[LH_2][SO_4]$ salt, was plotted as a function of the equilibrium pH of the aqueous phase.

The extractions involving receptors **4.6** and **4.7** resulted in the transport of no detectable amounts of sulfate into the organic phase. A small amount of sulfate was extracted into the organic phase with receptor **4.8** with the maximum sulfate loading being approximately 4% at pH 2.8 (**Figure 4.13**).

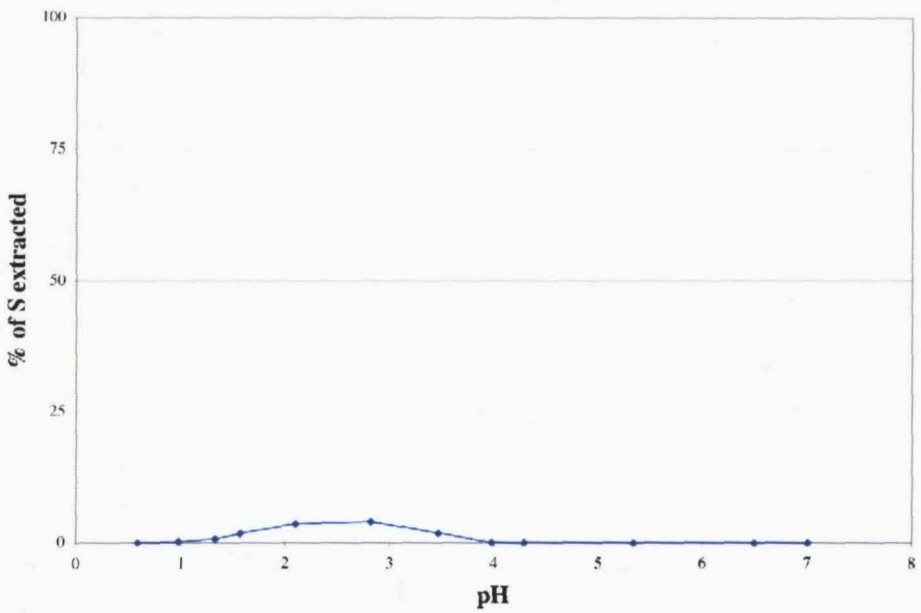

Figure 4.13: The pH dependence of extraction of sulfate by a chloroform solution of compound **4.8**.

During the extraction experiments involving receptor **4.9** a precipitate formed in the organic layer and X-ray quality crystals were grown from methanol solutions of the precipitate. The crystal structure revealed that the precipitate was the sulfate salt. In the solid state a hydrogen-bonded dimer was formed which consists of two doubly protonated receptor molecules and two sulfate anions (**Figure 4.14**). Each receptor is predominantly bound to a single sulfate anion *via* four hydrogen bond interactions (N1···O1 distance of 2.686(3) Å, N2···O2 distance of 2.773(3) Å, N3···O3 distance of 2.740(3) Å and N4···O3 distance of 2.911(4) Å) and the dimer is formed by a bridging interaction between the sulfate and the unused protonated imidazole group of an adjacent ligand with a N5···O4' distance of 2.638(4) Å.

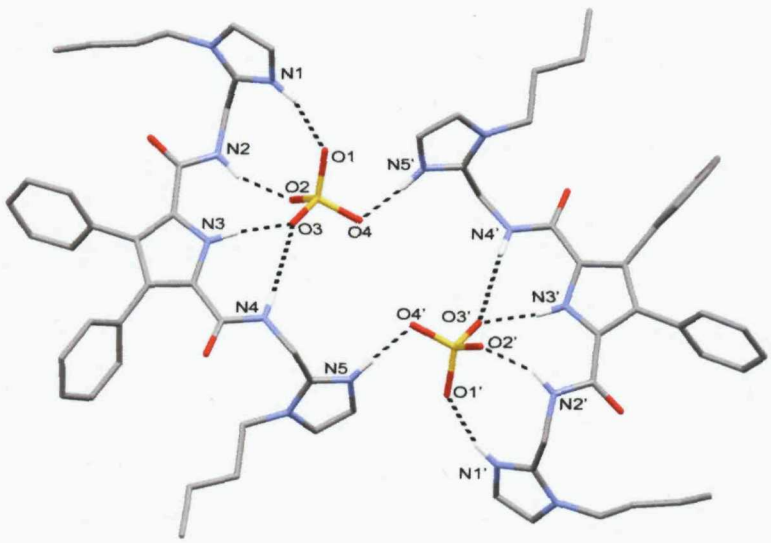

Figure 4.14: X-ray crystal structure of the sulfuric acid dimeric complex of **4.9**.

The poor sulfate extraction exhibited by receptors **4.6**-**4.9** could be a consequence of the solubility properties of the protonated ligands resulting in the stabilisation of the sulfate salt in the aqueous phase rather than the extraction of the sulfuric acid into the organic phase. The precipitation of the acid complex of **4.9** during the extraction is evidence for the low organic solubility of the acid complex. In order to overcome this problem the more hydrophobic N,N-di-n-butylethylenediamine group was appended to

the diamidopyrrole scaffold to afford **4.10**. Compound **4.10** was synthesised according to the same synthetic procedure employed for **4.6**-**4.9** and was obtained in a 67% yield.

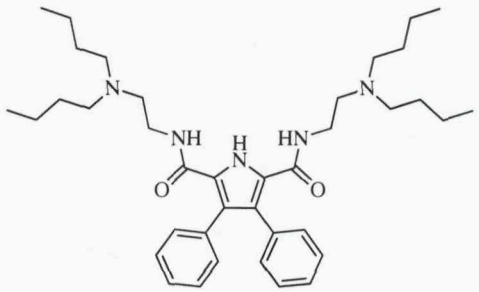

4.10

X-ray quality crystals of **4.10** were obtained *via* slow evaporation of a methanol solution. The crystal structure revealed that, in a similar manner to **4.6** and **4.8**, a hydrogen-bonded dimer was formed in the solid sate by interactions between the pyrrole NH group and a carbonyl group with a N2···O1' distance of 2.9872(16) Å (**Figure 4.15**).

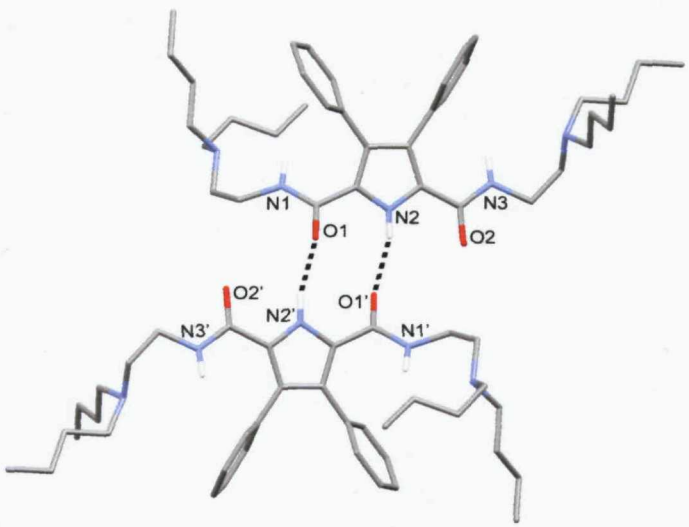

Figure 4.15: X-ray crystal structure of **4.10** showing the formation of the hydrogen bonded dimer.

4.2.3 EXTRACTION STUDIES WITH 4.10

The ability of compound **4.10** to extract sulfuric acid was studied according to the same procedure described in section 4.2.2. In contrast to its less hydrophobic analogues **4.6**-**4.9** the diamidopyrrole **4.10** proved to be an effective extractant for H_2SO_4 (**Figure 4.16**) and prompted the investigation of **4.10** as part of a dual host system to recover nickel(II) sulfate from aqueous feed solutions.

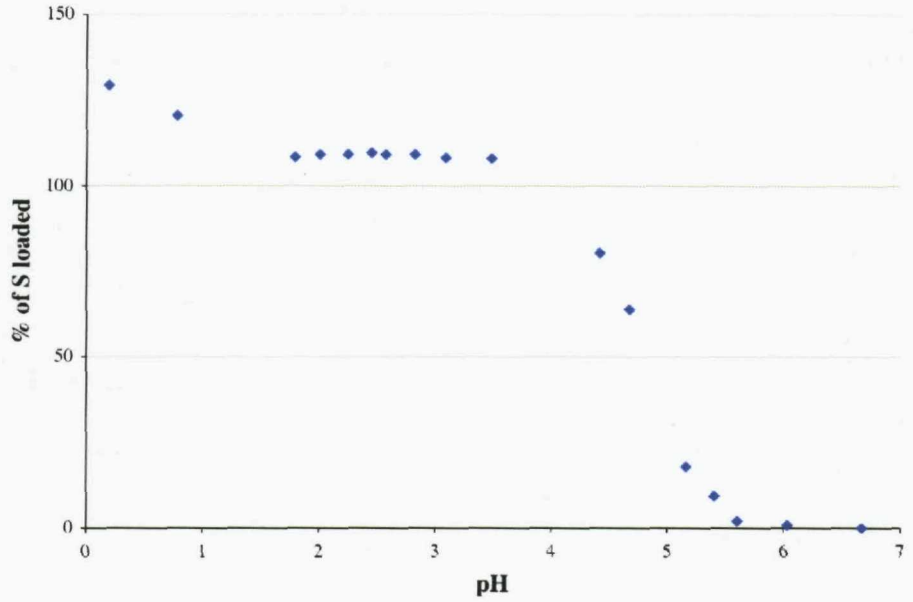

Figure 4.16: The pH dependence extraction profile for sulfate with compound **4.10**.

In these experiments the Ni^{2+}-extractant chosen was the commercial reagent 5-nonylsalicylaldoxime (**4.11**) commonly known as P50, which forms a neutral nickel(II) complex (**4.12** shown in **Figure 4.17**).

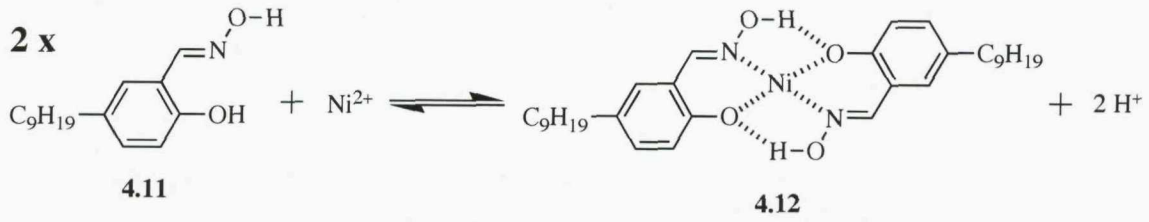

Figure 4.17: Formation of the P50 nickel complex.

A practicable dual host system will show 100% loading of both cation and anion in a pH range corresponding to that of a feed solution (**Figure 4.18**). The common plateau region of the 'S' curve would occur at pH >3 for the flowsheet such as the proposed Bulong circuit where the pH has been raised in order to precipitate Fe(III) prior to the recovery of the base metal. The $pH_{½}$ values (the pH at which 50 % of the ion of interest is loaded in the orgainic phase) for the Ni^{2+} and SO_4^{2-} loading define the operating condition for stripping and in the dual host system sequential stripping of the anion and cation can then be achieved by contacting the loaded organic phase strip solution of appropriate pH allowing for the dual host extraction components to be recycled as their neutral forms. Additionally the $pH_{½}$ value is used by industry to compare the relative strengths of extraction of target components by ligands. For the extraction of metal cations from solution the lower the $pH_{½}$ the more effective the ligand is at extracting the metal and the reverse is the case for anions where the higher the $pH_{½}$, the higher the extraction strength.

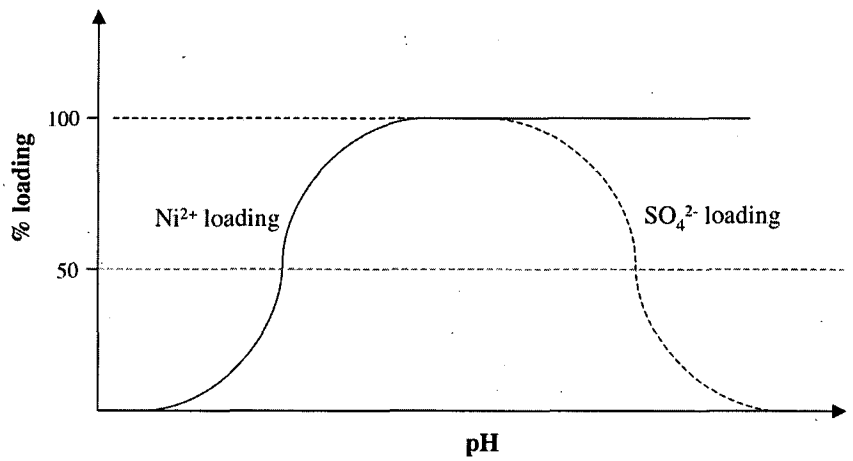

Figure 4.18: The ideal pH profiles for the loading of nickel and sulfate by a dual host system.

In the preliminary experiments using the dual host system the pH profiles were determined by taking chloroform solutions containing 0.01 M of **4.10** and 0.01 M of a nickel-P50 complex (**4.12**) and contacting it with a 0.8 M aqueous sulfate solutions at different pH's. In the case of the of the nickel complex **4.12** the pH profile obtained from this procedure would represent the stripping of the nickel from the ligand however

the nickel stripping and nickel loading profiles would be identical as long as the compositions of the aqueous phase and organic phase remain constant.

The loading profiles of the dual host system showed that as the pH decreased the amount of sulfate extracted increased while the amount nickel extracted decreased (**Figure 4.19**). At approximately pH 4.4 a good overlap between the sulfate extraction and nickel strip was observed with approximately 90% of sulfate extracted and 90% of nickel retained by the P50 ligand **4.11**.

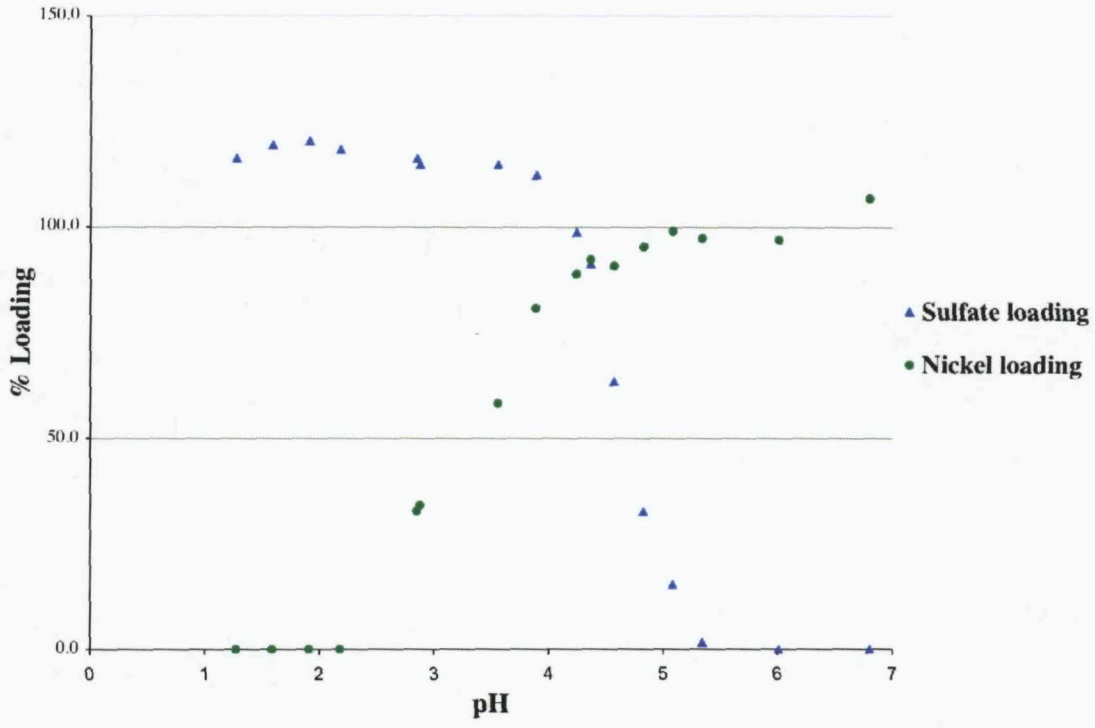

Figure 4.19: pH dependence profile for the loading of nickel (green plot) and sulfate (blue plot) by **4.11** and **4.10** respectively.

The pH dependent loading profile for the extraction of Ni^{2+} in the dual host system (**4.11** and **4.10**) was compared with the nickel loading profile of P50 ligand alone (**4.11**), which was obtained according to the same procedure described in section 4.2.2. The $pH_{½}$ was estimated for both profiles by initially plotting Log D (D = distribution coefficient = [species in organic phase]/[species in aqueous phase]) against pH, then by

inserting a line of best fit the $pH_{½}$ was estimated as the $pH_{½}$ is where log D = 0 (**Figure 4.20**)).

The loading of nickel appeared to be influenced by the presence of **4.10** in solution (**Figure 4.20**) as the $pH_{½}$ of the nickel loading from the dual host system (**4.10** & **4.11**) was approximately 0.43 pH units lower than the $pH_{½}$ of the **4.11** alone (~pH 3.23 versus ~pH 3.66 respectively) indicating that the presence of **4.10** improves the relative extraction 'strength' of **4.11** for nickel. Although the difference in the estimated $pH_{½}$'s appears to be significant but both plots have high errors (approximately ±10%) therefore it is unclear if there is an improvement to the nickel extraction strength in the presence of **4.10** or if the differences are insignificant due to experimental error.

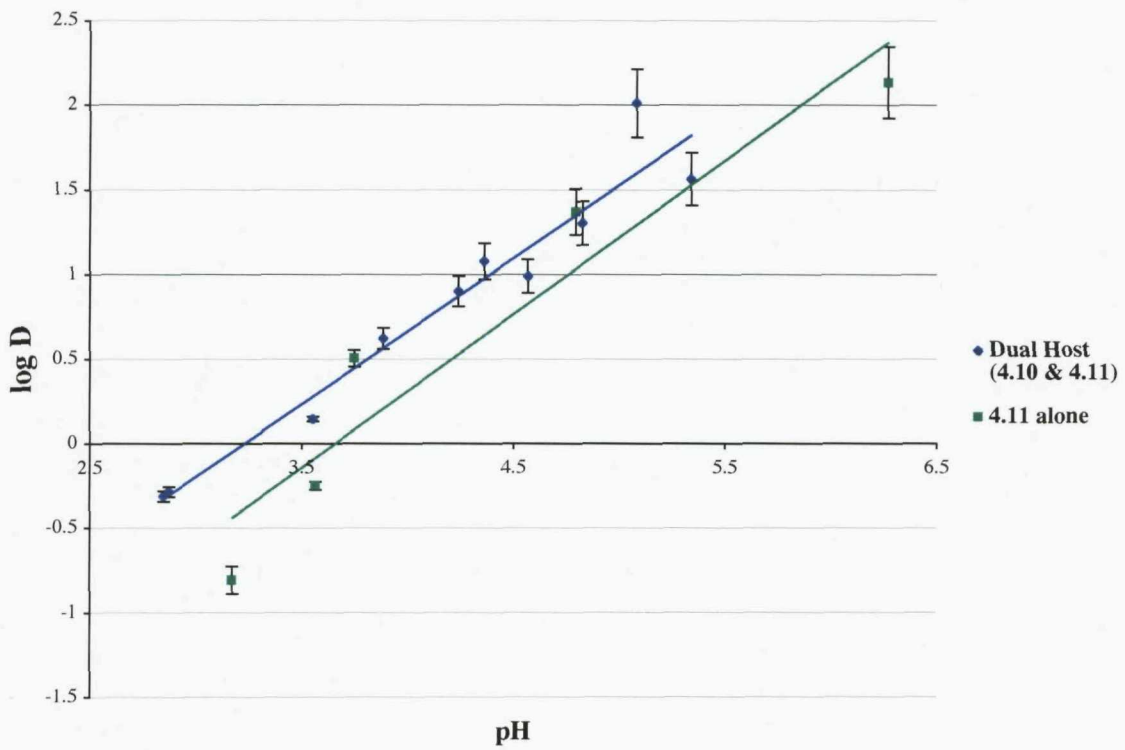

Figure 4.20: Log D vs. pH plots for the extraction of nickel with the dual host system (**4.10** & **4.11,** blue plot) and with **4.11** alone (green plot). Error estimated to be ± 10%.

If the differences observed in the $pH_{½}$'s for the nickel extraction (**Figure 4.20**) were found to be significant then the increase in the nickel extraction strength of **4.11** could be due to a synergistic effect between **4.11** and **4.10** where the independent units

associate in the water-immisicble solvent generating an adduct that has a lower free energy than the sum of its solvated components. If this was the case then in a similar fashion the sulfate extraction strength of **4.10** would also be improved therefore log D vs. pH plots were generated and compared for **4.10** in the dual-host system (**4.10** & **4.11**) and for **4.10** alone (**Figure 4.21**).

Both plots reveal that the estimated $pH_{½}$'s for the extraction of sulfate with the dual host system (**4.10** & **4.11**) and for **4.10** alone are essentially identical showing that there is no synergistic effect occurring in the dual host system for the co-extraction of nickel(II) sulfate. This result indicates that the two components act independently from one another however, the difference in the $pH_{½}$ for the nickel extraction in the dual host system (**4.10** & **4.11**) and for **4.11** alone could be a consequence of **4.10** acting as a modifier.[133,134] It is thought that the presence of a modifier changes the systems equilibrium to favour the complexation of the nickel (in this case) in the organic phase resulting in the increase in extraction strength. Again it is unclear if this modification process is occurring in this dual host system (**4.10** & **4.11**) due to the uncertainty in the estimated $pH_{½}$'s (**Figure 4.20**).

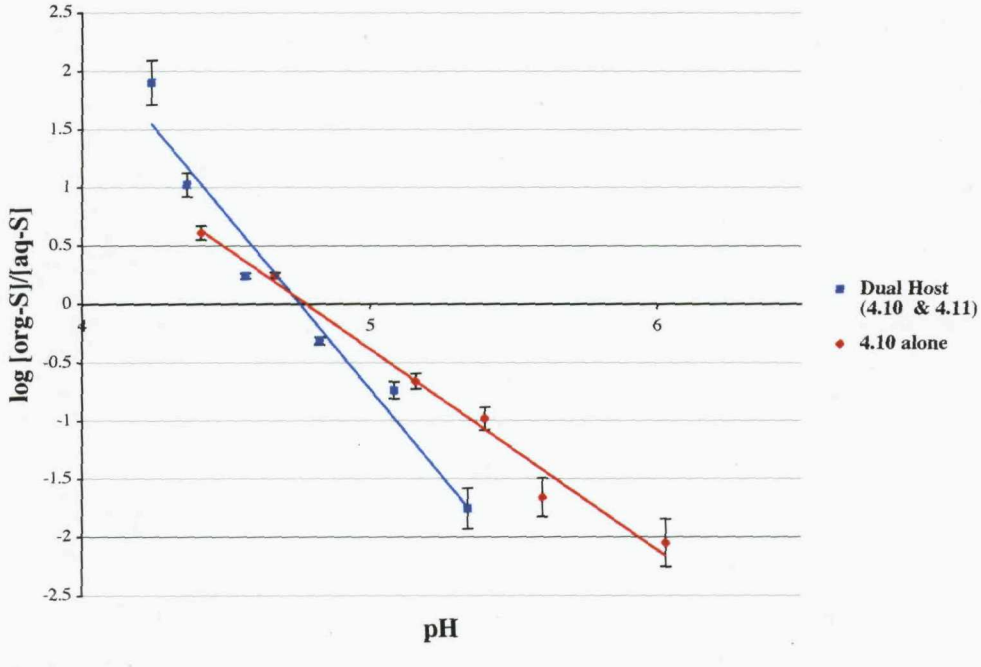

Figure 4.21: log D vs. pH plots for the extraction of sulfate with the dual-host system (**4.10** & **4.11,** blue plot) and with **4.10** alone (red plot). Errors estimated to be ± 10%.

4.3 ISOPHTHALAMIDE AND 2,6-PYRIDINE DIAMIDE BASED LIGANDS

An issue for the commercialisation of ligands in hydrometallurgy is the cost of manufacture and the mass of ligand required per unit mass of ion recovered. For these reasons simpler ligands (relative to the diamidopyrroles) based on 2,6-pyridine diamides (**4.13**) and isophthalamides (**4.14**) were investigated as sulfate extractants in dual host systems because they could be obtained in a single step from commercially available starting materials and have molecular masses approximately 23% less than **4.10**.

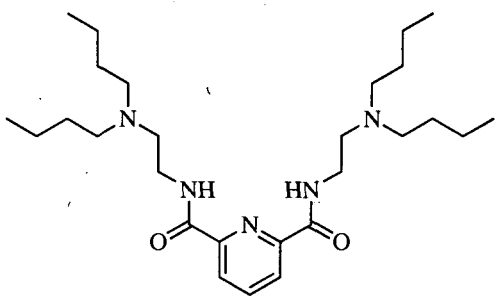

4.13

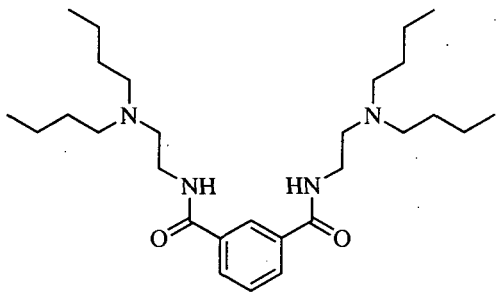

4.14

4.3.1 SYNTHESIS AND CHARACTERISATION

Isophthaloyl dichloride and pyridine 2,6-diacetlydichloride were added to dichloromethane solutions of *N,N*-di-n-butylethylenediamine in the presence of triethylamine and a catalytic amount of DMAP and stirred for 24 hrs to afford **4.13** and **4.14** in 80% and 82% yield respectively (**Scheme 4.2**).

Scheme 4.2: Synthesis of compounds **4.12** and **4.13**.

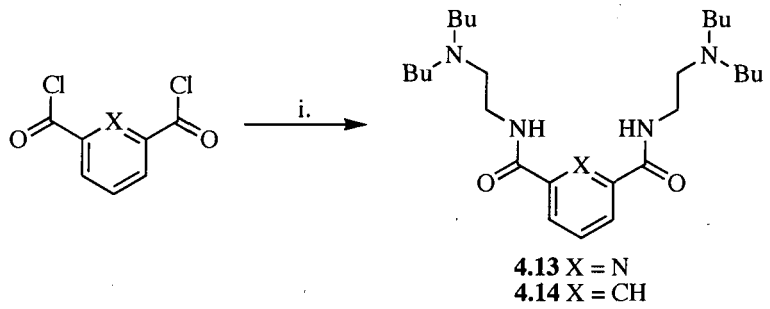

4.13 X = N
4.14 X = CH

i. *N,N*-di-n-butylethylenediamine, Et_3N, DMAP and DCM

4.3.2 DUAL HOST EXTRACTION EXPERIMENTS

Compounds **4.13** and **4.14** were investigated as sulfuric acid extraction ligands in a dual host system. The extraction experiments were carried out under identical conditions to those with **4.10** (section 4.2.3) in order to obtain pH dependence profiles for the loading of nickel(II) sulfate.

Similar trends were obtained for the dual host system containing **4.13** and **4.14** compared to the dual host system containing the diamidopyrrole **4.10**. In the case of the dual host system containing **4.13** (**Figure 4.22**) the loading profiles correspondence was less favourably to the ideal compared to the system containing **4.10**. At pH 4.9 approximately 80% of nickel and 84% of sulfate was loaded in the organic phase by **4.11** and **4.13** respectively, which is below the desired >90% loading required for an ideal system.

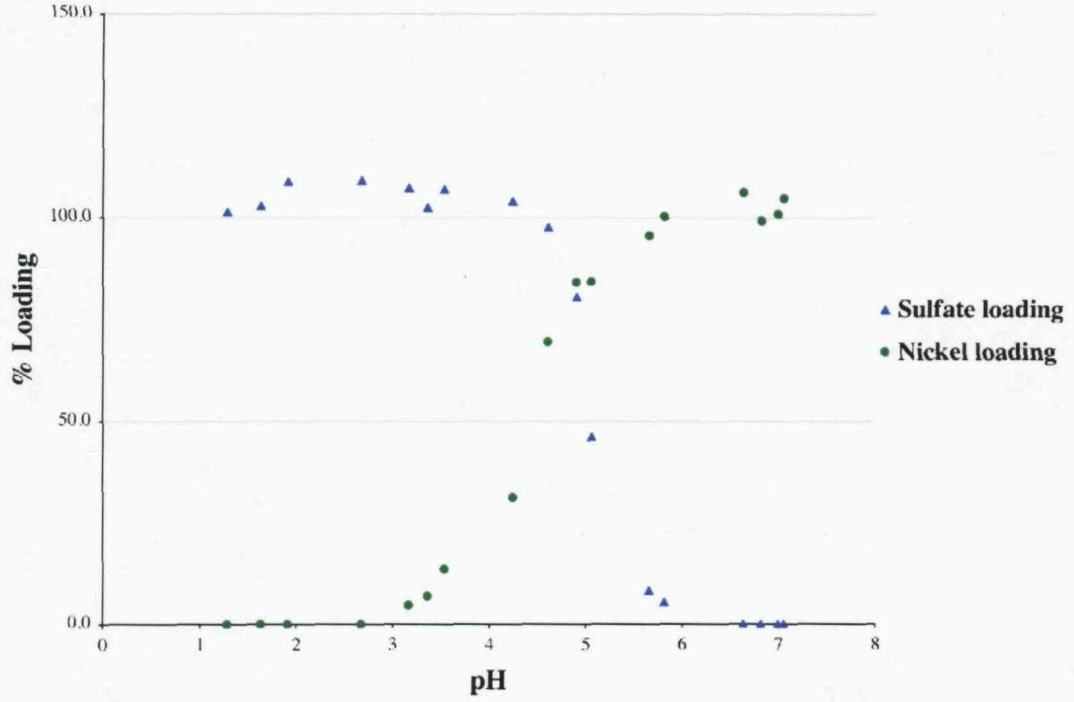

Figure 4.22: pH dependence profile for the loading of nickel (green plot) and sulfate (blue plot) by **4.11** and **4.13** respectively.

The best overlap between the two components was obtained with the system containing **4.14** (**Figure 4.23**). The difference between the $pH_{½}$ value for the sulfate and the nickel loading was approximately 1.8 for the dual host system containing **4.14** compared to 1.4 and 0.6 for the system containing **4.10** and **4.13** respectively. Additionally the dual host system was found to load approximately 94% of sulfate and 88% of nickel into the organic phase at pH 4.8 (**Figure 4.23**) providing loading profiles approaching the ideal shown in **Figure 4.18**.

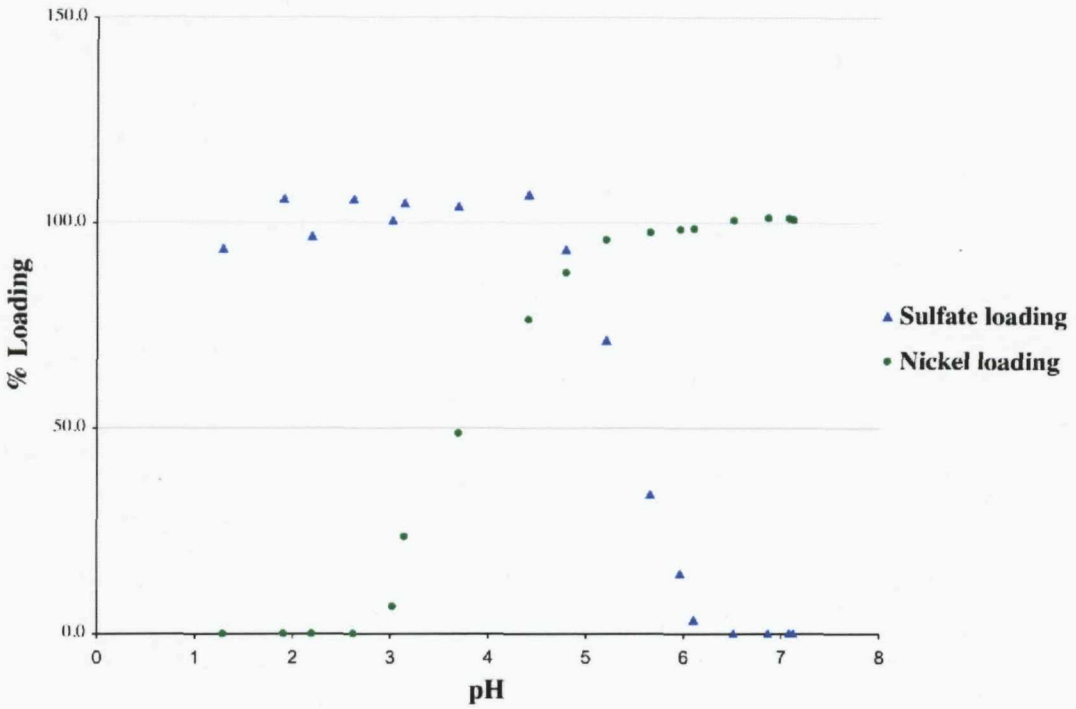

Figure 4.23: pH dependence profile for the loading of nickel (green plot) and sulfate (blue plot) by **4.11** and **4.14** respectively.

Comparison of the nickel loading profile (log D vs. pH) of the dual host systems (**4.14** & **4.11**) compared with the loading profile of **4.11** alone revealed that the $pH_{½}$ values are essentially the same indicating that no synergistic or modification processes are occurring in this system (**Figure 4.24**). In the case of the dual host system (**4.13** & **4.11**) however, a significant reduction of nickel extraction strength was observed compared to the nickel extraction with **4.11** alone (**Figure 4.24**). The estimated $pH_{½}$ for the dual host system (**4.13** & **4.11**) was found to be 0.7 pH units higher (and significantly different with respect to experimental error) than that for **4.11** alone (pH 4.36 and pH 3.66 respectively), indicating that in the presence of **4.13** the nickel extraction strength of **4.11** is reduced.

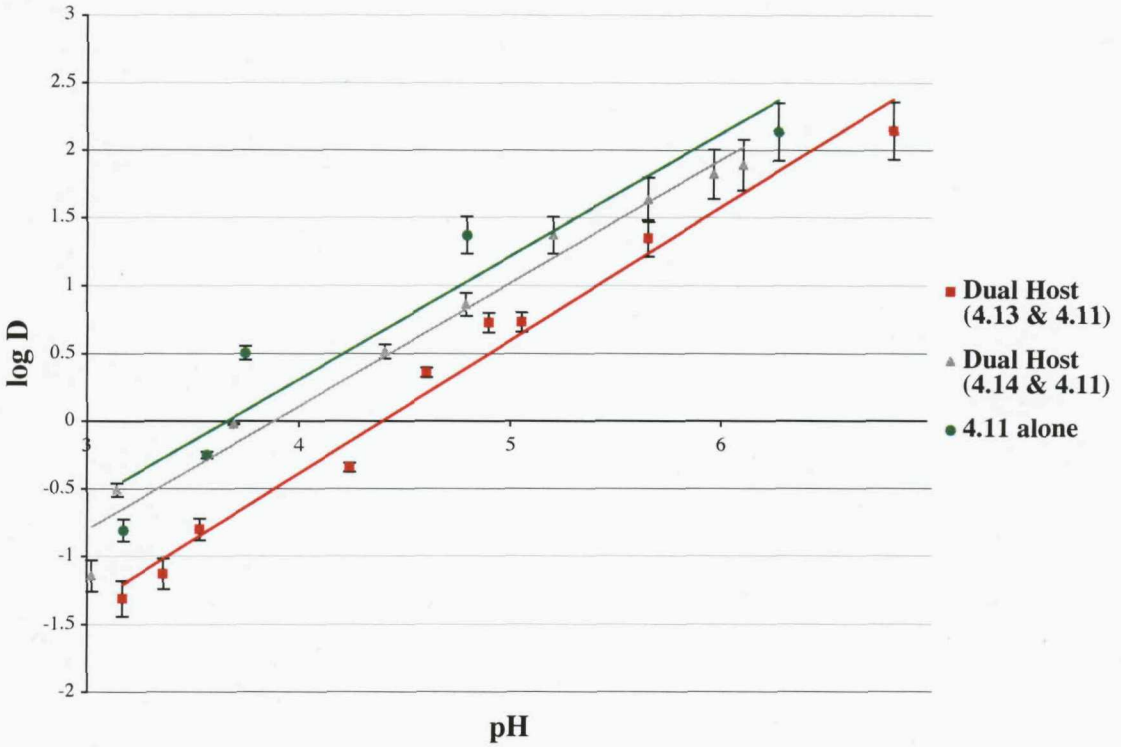

Figure 4.24: Log D vs. pH plots for the extraction of nickel with the dual host system **4.13** & **4.11** (blue plot), **4.14** & **4.11** (grey plot) and with **4.11** alone (green plot). Errors estimated to be ± 10%.

The sulfate loading profiles (log D vs. pH) of **4.13** and **4.14** alone were compared to their equivalent loading profiles in a dual host system (**4.13** & **4.11** and **4.14** & **4.11** respectively). In the case of **4.13** insignificant differences (< 0.1 pH units) were observed between the estimated $pH_{½}$ for both the dual host system (**4.13** & **4.11**) and for **4.13** alone (**Figure 4.25**). Interestingly, in the case of **4.14** the dual host system (**4.14** & **4.11**) a reduction in the sulfate extraction strength was observed compared to **4.14** alone (pH 5.48 and pH 5.65 respectively) indicating that the presence of **4.11** decreases the sulfate affinity of **4.14** (**Figure 4.26**).

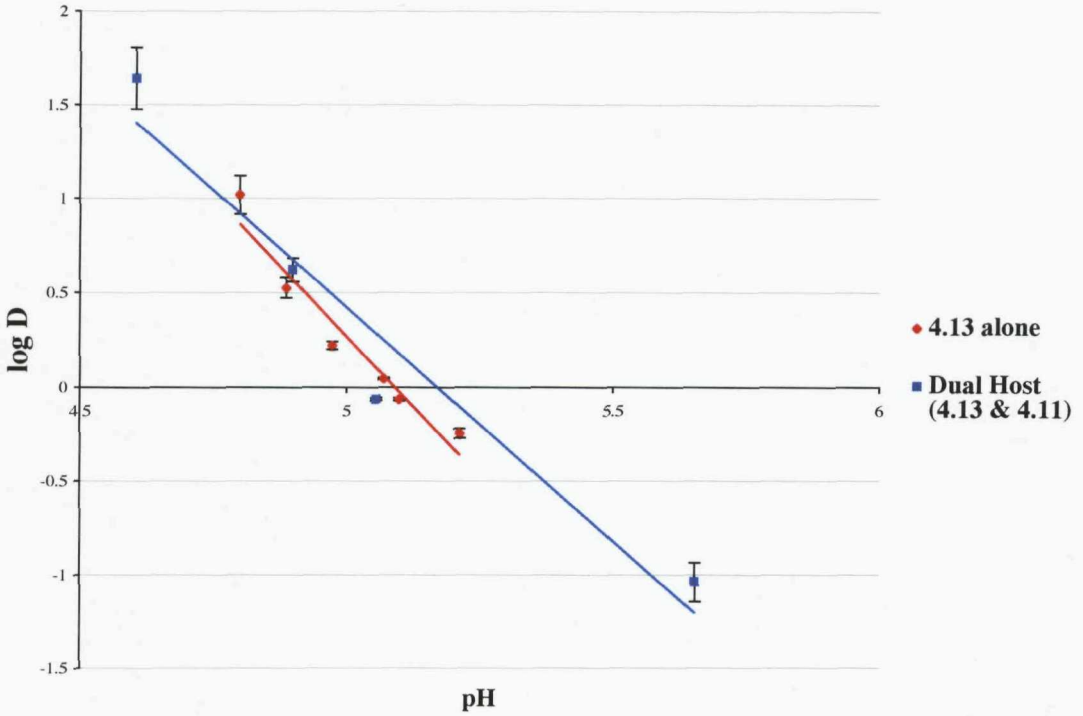

Figure 4.25: log D vs. pH plots for the extraction of sulfate with the dual-host system (**4.13** & **4.11,** blue plot) and with **4.13** alone (red plot). Errors estimated to be ± 10%.

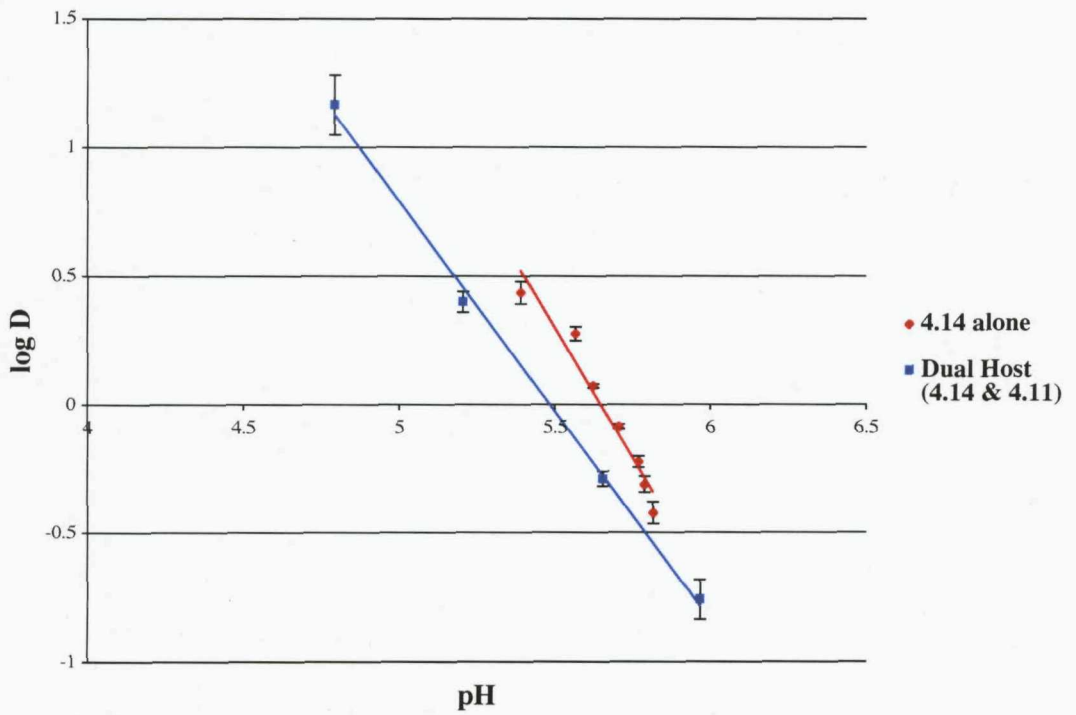

Figure 4.26: log D vs. pH plots for the extraction of sulfate with the dual-host system (**4.14** & **4.11,** blue plot) and with **4.14** alone (red plot). Errors estimated to be ± 10%.

In order to determine which compound shows the highest affinity for sulfuric acid the estimated $pH_{½}$'s from the log D vs. pH plots (**Figure 4.27**) for the dual host systems containing **4.10**, **4.13** and **4.14** were compared. The estimated $pH_{½}$'s revealed that the system containing the relatively simple isophthalamide-based ligand, **4.14**, had the highest $pH_{½}$ and therefore the highest affinity for sulfate ($pH_{½}$ = 5.48) followed by **4.13** ($pH_{½}$ = 5.17) and finally **4.10** ($pH_{½}$ = 4.78).

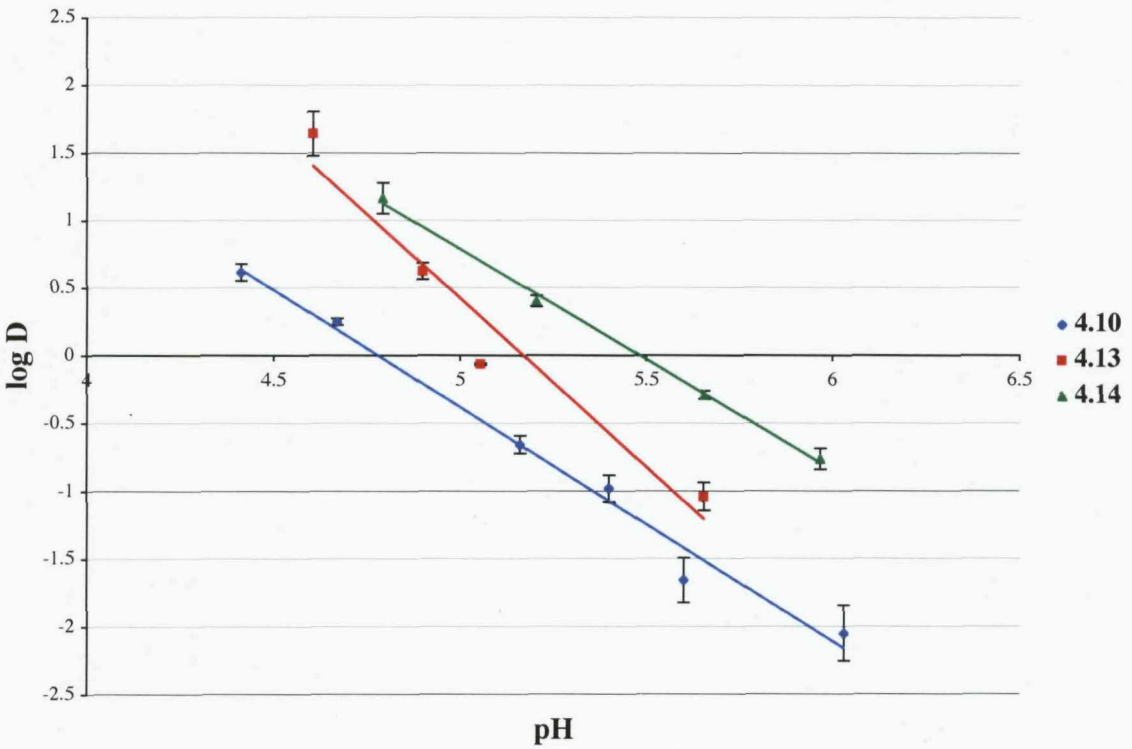

Figure 4.27: log D vs. pH plots for the extraction of sulfate by **4.10** & **4.11** (blue plot), **4.13** & **4.11** (red plot) and **4.14** & **4.11** (green plot). Errors estimated to be ± 10%.

4.4 CONCLUSIONS

A dual host system composed of the commercially available P50 extractant (**4.11**) and a new isophthalamide base hydrophobic sulfate receptor (**4.14**) is capable of loading >90% nickel(II) sulfate at a pH value of approximately 4.9. Such a pH value corresponds to those likely in new nickel-extraction circuits and loading.

Two other hydrophobic sulfate receptors based on 2,6-pyridine diamides (**4.13**) and diamidopyrroles (**4.10**) were also found to extract sulfuric acid in a dual host system however the loading profiles achieved in these systems were further removed from the ideal system (illustrated in **figure 4.18**) compared to the system containing **4.14**.

The dual host system containing **4.14** shows potential as a commercial system however the system needs to be tested in solvents such as kerosene that would be used in a commercial operation. Additionally improvements to the pH range at which the system can operate to allow >90% extraction of the nickel cation and sulfate anion is required. Interestingly due to the apparent success of **4.14** as a sulfate extractant to improve the overall dual host system only an improvement to the nickel extraction strength would be required by using another commercially available nickel extractant with a lower $pH_{½}$ than **4.11**.

CHAPTER 5 – EXPERIMENTAL

5.1 REAGENTS

Where necessary solvents were purified prior to use. Triethylamine was distilled fro KOH and stored under nitrogen in the presence of KOH pellets. Thionyl chloride was distilled from 10% (w/w) triphenyl phosphate and stored under nitrogen. Commercial grade reagents have been used without further purification. Reagents prepared according to literature procedure have been so referenced. *Meso*-octamethylcalix[4]pyrrole was synthesized according to literature procedure.[56] *N*-confused octamethylcalix[4]pyrrole was prepared by Maarten Kostermans of the University of Leuven. 1-Butyl-imidazol-2-yl-methylamine was prepared by Joachim Garric of the University of Southampton. The nickel(II) complex of P-50 ligand was prepared by Ross Forgan of the University of Edinburgh. Ionic liquids and tetralkylammonium salt used for ^{1}H NMR titration experiments had been thoroughly dried under high vacuum.

5.2 INTRUMENTAL METHODS

NMR data was recorded on Bruker AV300 and DPX400 spectrometers. All data was referenced internally using the residual protio-solvent (^{1}H) or the signal of the solvent (^{13}C) with the chemical shifts reported in ppm. Low-resolution mass spectra were recorded on a Micromass Platform single quadrupole spectrometer. High-resolution mass spectra were recorded on a Bruker Daltonics DataAnalysis 3.4, FT-ICR-MS, 4.7T magnet. Medac Ltd performed elemental analysis. Infrared spectra were recorded on a Mattson Satellite (ATR) FTIR and reported in wavenumbers (cm^{-1}). Melting points were recorded in open capillaries on a Gallenkamp melting point apparatus and are uncorrected.

5.3 SYNTHETIC PROCEDURES

5.3.1 SYNTHESIS FOR CHAPTER 3

Pyridine-2,6-dicarboxylic acid bis-[(2,3-dimethyl-1*H*-indol-7-yl)-amide], 3.7a

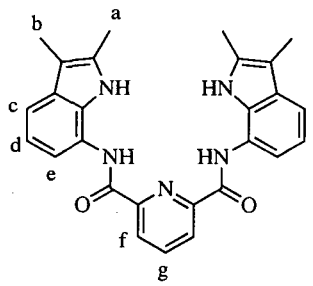

2,3-dimethyl-7-nitroindole (0.70 g, 3.7 mmol) was dissolved in ethanol (100 mL) with 10% Pd/C (100 mg) and hydrazine monohydrate (2 mL). The reaction was refluxed for 2 hours then filtered through celite and washed with further ethanol. The filtrate was concentrated *in vacuo* and the solid residue was used immediately. The solid was dissolved in acetonitrile (50 mL) with triethylamine (5 mL) and a catalytic amount of DMAP. To this was added a solution of pyridine 2,6-diacetlydichloride (0.37 g, 1.8 mmol) in acetonitrile (50 mL) and the reaction was stirred overnight in which time a solid precipitate had formed. This was collected by filtration and washed with further acetonitrile followed by ether. The product was isolated as a yellow solid. Yield 0.52 g (63 %, 1.2 mmol). Mp: decomposed ~220°C; LRMS ES$^+$: 450.2 $(M+H)^+$; IR ν cm^{-1} 3381, 3256, 2915, 1644s, 1544s, 1456s, 1343s; ^{1}H NMR (400 MHz, DMSO-d_6) δ: 2.19 (s, 3H, CH_3-a), 2.36 (s, 3H, CH_3-b), 6.99 (t, ^3J = 7.5 Hz, 2H, Ar-d), 7.15 (d, ^3J= 7.3 Hz, 2H, Ar-c), 7.30 (d, ^3J = 7.5 Hz, 2H, Ar-e), 8.32 (dd, J = 7.3, 8.5 Hz, 1H, Ar-g), 8.43 (d, ^3J = 7.5 Hz, 2H,Ar-f), 10.55 (s, 2H, indole-NH), 11.13 (s, 2H, amide-NH); ^{13}C NMR (100 MHz, DMSO-d_6) δ: 8.2, 11.0, 105.3, 115.2, 116.8, 117.6, 120.5, 124.7, 130.0, 130.1, 131.4, 139.4, 148.8, 161.6; Microanalysis for $C_{27}H_{25}N_5O_2 + 0.15CH_2Cl_2$. Calc. (%) C = 70.20, H = 5.49, N = 15.07. Found (%) C = 70.19, H = 5.60, N = 15.02.

_N,N'_-Bis-(2,3-dimethyl-1_H_-indol-7-yl)-isophthalamide, 3.7b

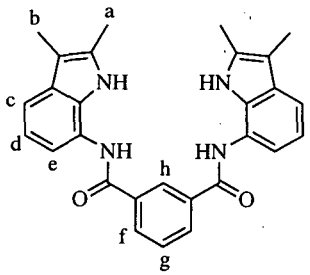

2,3-dimethyl-7-nitroindole (0.70 g, 3.7 mmol) was dissolved in ethanol (100 mL) with 10% Pd/C (100 mg) and hydrazine monohydrate (2 mL). The reaction was refluxed for 2 hours then filtered through celite and washed with further ethanol. The filtrate was concentrated *in vacuo* and the solid residue was used immediately. The solid was dissolved in acetonitrile (50 mL) with triethylamine (5 mL) and a catalytic amount of DMAP. To this was added a solution of isophthaloyl dichloride (0.37 g, 1.8 mmol) in acetonitrile (50 mL) and the reaction was stirred overnight in which time a solid precipitate had formed. This was collected by filtration and washed with further acetonitrile followed by ether. The product was isolated as a white solid. Yield 0.49 g (60 %, 1.1 mmol). Mp: decomposed ~215°C; LRMS ES$^+$: 473.3 $(M+Na)^+$, LRMS ES$^-$: 485.2, 487.2 $(M+Cl)^-$; IR ν cm^{-1} 3415, 3271, 2916, 1631, 1544s, 1456; ^{1}H NMR (400 MHz, DMSO-d_6) δ: 2.18 (s, 3H, CH_3-a), 2.34 (s, 3H, CH_3-b), 6.96 (t, ^3J = 7.8 Hz, 2H, Ar-d), 7.24 (d, ^3J = 7.5 Hz, 2H, Ar-c), 7.33 (d, ^3J = 7.5 Hz, 2H, Ar-e), 7.73 (t, J= 7.8 Hz, 1H, Ar-g), 8.24 (d, ^3J = 7.6 Hz, 2H, Ar-f), 8.70 (s, 1H, Ar-h), 10.14 (s, 2H, indole NH), 10.47 (s, 2H, amide NH); ^{13}C NMR (100 MHz, DMSO-d_6) δ: 8.4, 11.2, 105.6, 114.7, 115.0, 117.9, 121.9, 127.4, 128.4, 128.7, 130.4, 130.7, 131.3, 135.1, 161.9; Microanalysis for $C_{28}H_{26}N_4O_2$+0.12CH_2Cl_2. Calc. (%) C = 73.33, H = 5.74, N = 12.17. Found (%) C = 73.30, H = 5.88, N = 12.17.

7-Nitro-1*H*-indole-2-carboxylic acid butylamide, 3.16a

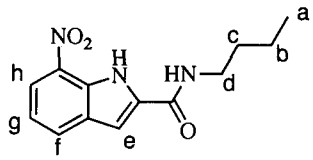

7-nitro-indole-2-carboxylic acid, **3.14**, (2.00 g, 10 mmol) was heated at reflux in thionyl chloride (30 mL) for 2 hrs. The thionyl chloride was then evaporated and the resultant solid was dissolved in DCM (50 mL) and added dropwise to a stirring solution of butylamine (0.75 g, 11 mmol), triethylamine (5 mL) and a catalytic amount of DMAP in DCM (50 mL). After addition the reaction was stirred for 24hrs. The reaction was concentrated and purified *via* column chromatography (SiO_2, DCM/3%methanol). The pure product was isolated as a yellow solid. Yield 2.03 g (78 %, 7.7 mmol). Mp: 124-126°C; IR ν cm^{-1} 3257, 3094, 2958, 2927, 1595, 1329, 1303; ^1H NMR (300 MHz, $CDCl_3$) δ: 0.98 (t, ^3J = 7.3 Hz, 3H, CH_3-a), 1.38–1.50 (m, 2H, CH_2-b), 1.59–1.69 (m, coincident with H_2O, 2H, CH_2-c), 3.51 (m, 2H, CH_2-d), 6.19 (s, 1H, amide NH), 6.94 (d, ^4J = 1.9 Hz, 1H, Ar-e), 7.26 (m, coincident with $CDCl_3$, 1H, Ar-g), 7.99 (d, ^3J = 7.9 Hz, 1H, Ar-f), 8.25 (d, ^3J = 7.9 Hz, 1H, Ar-h), 10.51 (s, 1H, indole NH); ^{13}C NMR (100 MHz, $CDCl_3$) δ: 14.1, 20.5, 32.2, 40.0, 102.9, 120.4, 121.8, 129.6, 130.3, 131.7, 134.0, 160.7; Microanalysis for $C_{13}H_{15}N_3O_3$. Calc. (%) C = 59.76, H = 5.79, N = 16.07. Found (%) C = 59.68, H = 5.74, N = 16.01; HRMS (positive ESI) *m/e* calcd for $C_{13}H_{16}N_3O_3^+$ (M + H^+), 261.1186; found, 262.1186.

7-Nitro-1*H*-indole-2-carboxylic acid phenylamide, 3.16b

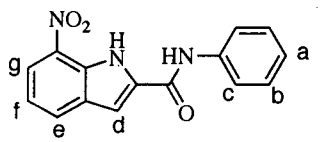

7-nitro-indole-2-carboxylic acid, **3.14**, (2.00 g, 10 mmol) was heated at reflux in thionyl chloride (30 mL) for 2 hrs. The thionyl chloride was then evaporated and the resultant solid was dissolved in DCM (50 mL) and added dropwise to a stirring solution of aniline (1.00 g, 10.7 mmol), triethylamine (5 mL) and a catalytic amount of DMAP in

DCM (50 mL). After addition the reaction was stirred for 24hrs. Water (250 mL) was then added and the organic layer was separated and washed with water. The organic layer was dried with sodium sulfate, filtered and concentrated *in-vacuo*. The pure product was obtained by recrystallization from acetonitrile. The product was isolated as a brown solid. Yield 2.51 g (89 %, 8.9 mmol). Mp: 209-211°C; IR ν cm^{-1} 3849, 3743, 3673, 3455, 2361, 1651, 1544, 1316; ^{1}H NMR (400 MHz, DMSO-d_6) δ: 7.15 (t, ^3J = 7.4 Hz, 1H, Ar-f), 7.35-7.43 (m, 3H, Ar –a,e,g), 7.62 (s, 1H, Ar-d), 7.80 (d, ^3J = 7.5 Hz, 2H, Ar-c), 8.25-8.29 (m, 2H, Ar-b), 10.66 (s, 1H, amide NH), 11.44 (s, 1H, indole NH); ^{13}C NMR (100 MHz, $CDCl_3$) δ: 107.5, 120.0, 121.1, 121.7, 124.7, 129.1, 129.9, 130.6, 131.7, 133.7, 134.9, 138.6, 158.9; Microanalysis for $C_{15}H_{11}N_3O_3$ + 0.2 CH_3OH Calc. (%) C = 63.68, H = 4.06, N = 14.73. Found (%) C = 63.66, H = 3.84, N = 14.73; HRMS (EI) calcd for $C_{15}H_{11}N_3O_3$ $[M]^+$, 281.0800; found, 281.0800.

7-Pentanoylamino-1*H*-indole-2-carboxylic acid butylamide, 3.8

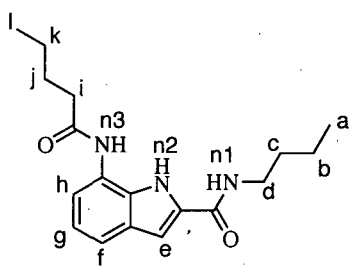

7-Nitro-1*H*-indole-2-carboxylic acid butylamide, **3.16a**, (1.00 g, 3.8 mmol), Pd/C (0.20 g, 10% wt) and hydrazine monohydrate (2 mL) were dissolved in ethanol (100 mL) and heated at reflux for 1 hour. The reaction mixture was then filtered hot through celite and washed with ethanol (50 mL). The filtrate was concentrated *in vacuo* and the resulting white solid was used directly in the next reaction where it was dissolved in DCM (50 mL) with triethylamine (5 mL) and DMAP (catalytic amount). To this solution was added dropwise a solution of valeroyl chloride (0.39 g, 3.8 mmol) and the reaction was stirred overnight. Water (250 mL) was then added and the organic layer was separated and washed with water. The organic layer was dried with sodium sulfate, filtered and concentrated *in vacuo*. The pure product was then obtained by recrystallization from acetonitrile. The product was isolated as a white solid. Yield 0.52

g (43 %, 1.6 mmol). Mp: 126-129°C; IR ν cm^{-1} 3278, 2957, 2929, 2871, 1615, 1569, 1540, 1275; ^{1}H NMR (400 MHz, DMSO-d_6) δ: 0.90-0.95 (m, 6H, CH_3-a,l), 1.30-1.42 (m, 4H, CH_2-b,k), 1.50-1.57 (m, 2H, CH_2-c) 1.60-1.67 (m, 2H, CH_2-j), 2.43 (t, ^3J = 7.4 Hz, 2H, CH_2-i), 3.33 (m, 2H, coincident with H_2O, CH_2-d), 6.98 (t, J = 7.8 Hz, 1H, Ar-g), 7.13 (d, ^4J = 2.0 Hz, 1H, Ar-e), 7.32 (d, ^3J = 7.8 Hz, 1H, Ar-f), 7.92 (d, ^3J = 7.8 Hz, 1H, Ar-h), 8.50 (bt, 1H, amide NH-n1), 9.76 (s, 1H, amide NH-n3) 11.42 (s, 1H, indole NH-n2); ^{13}C NMR (100 MHz, DMSO-d_6) δ: 12.87, 12.93, 18.8, 21.0, 26.5, 30.5, 35.3, 37.6, 101.8, 112.4, 115.9, 119.2, 123.8, 126.2, 127.7, 130.7, 160.0, 170.6; Microanalysis for $C_{18}H_{25}N_3O_2$. Calc. (%) C = 68.54, H = 7.99, N = 13.32. Found (%) C = 68.58, H = 8.03, N = 13.27; HRMS (positive ESI) *m/e* calcd for $C_{18}H_{26}N_3O_2^+$ (M + H^+), 316.2020; found, 316.2019.

7-Benzoylamino-1*H*-indole-2-carboxylic acid phenylamide, 3.9

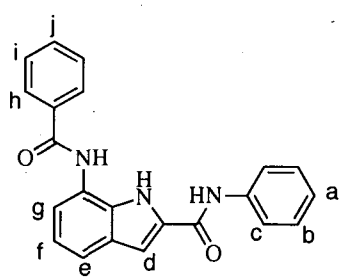

7-nitro-1*H*-indole-2-carboxylic acid phenylamide, **3.16b**, (0.50 g, 1.8 mmol), Pd/C (0.20 g, 10% wt) and hydrazine monohydrate (2 mL) were dissolved in ethanol (100 mL) and heated at reflux for 1 hour. The reaction was then filtered hot through celite and washed with ethanol (50 mL). The filtrate was concentrated *in vacuo* and the resulting white solid was used directly in the next reaction where it was dissolved in DCM (100 mL) with triethylamine (5 mL) and DMAP (catalytic amount). To this solution was added dropwise a solution of benzoyl chloride (0.25 g, 1.8 mmol) and the reaction was stirred overnight. Water (250 mL) was then added and the organic layer was separated and washed with water. The organic layer was dried with sodium sulfate, filtered and concentrated *in vacuo*. The pure product was obtained *via* recrystallization from acetonitrile. The product was isolated as a pale yellow solid. Yield 0.53 g (83 %, 1.5 mmol). Mp: 257-260 °C; IR ν cm^{-1} 3227, 1631, 1598, 1548, 1250; ^{1}H NMR (300 MHz,

DMSO-d_6) δ: 7.11 (m, 2H), 7.38 (t, ^3J = 7.7 Hz, 2H), 7.50-7.66 (br, 5H), 7.80 (d, ^3J = 7.7 Hz, 2H), 7.93 (d, ^3J = 7.7 Hz, 1H), 8.00-8.02 (m, 2H), 10.20 (s, 1H, amide NH), 10.27 (s, 1H, amide NH), 11.83 (s, 1H, indole NH); ^{13}C NMR (100 Mhz, DMSO-d_6) δ: 104.9, 116.6, 118.5, 120.7, 124.1, 124.8, 128.4, 128.8, 129.1, 129.2, 129.4, 131.9, 132.0, 135.7, 139.3, 160.1, 166.6; Microanalysis for $C_{22}H_{17}N_3O_2$. Calc. (%) C = 74.35, H = 4.82, N = 11.82. Found (%) C = 74.41, H = 4.78, N = 11.84; HRMS (positive ESI) *m/e* calcd for $C_{22}H_{18}N_3O_2^+$ (M + H$^+$), 356.1394; found, 356.1390.

7-Phenylacetylamino-1*H*-indole-2-carboxylic acid phenylamide, 3.10

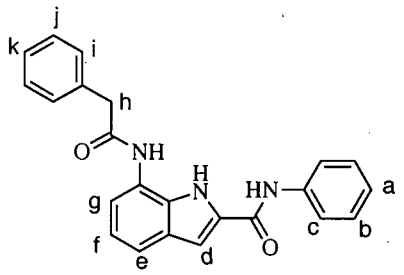

7-Nitro-1*H*-indole-2-carboxylic acid phenylamide, **3.16b**, (0.50 g, 1.8 mmol), Pd/C (0.20 g, 10% wt) and hydrazine monohydrate (2 mL) were dissolved in ethanol (100 mL) and heated at reflux for 1 hour. The reaction mixture was filtered hot through celite and washed with ethanol (50 mL). The filtrate was then concentrated *in vacuo* and the resulting white solid was used directly in the next reaction where it was dissolved in DCM (100 mL) with triethylamine (5 mL) and DMAP (catalytic amount). To this solution was added dropwise a solution of phenylacetyl chloride (0.28 g, 1.8 mmol) and the reaction was stirred overnight. Water (250 mL) was then added and the organic layer was separated and washed with water. The organic layer was dried with sodium sulfate, filtered and concentrated *in vacuo*. The pure product was obtained by recrystallization from acetonitrile. The product was isolated as a white solid. Yield 0.55 g (83 %, 1.5 mmol). Mp: 213-215°C; IR ν cm^{-1} 3378, 3246, 3033, 2360, 2160, 1668, 1539; ^{1}H NMR (300 MHz, DMSO-d_6) δ: 3.78 (s, 2H, CH_2-h), 7.03 (t, ^3J = 7.7 Hz, 1H), 7.13 (t, ^3J = 7.3 Hz, 1H), 7.24-7.44 (br, 8H), 7.49 (d, ^4J = 1.9 Hz, 1H, Ar-d), 7.82 (d, ^3J = 7.7 Hz, 2H), 7.95 (d, ^3J = 7.7 Hz, 1H), 10.08 (s, 1H, amide NH), 10.29 (s, 1H, amide NH), 11.66 (s, 1H, indole NH); ^{13}C NMR (100 Mhz, DMSO-d_6) δ: 42.6, 103.7, 113.3, 116.7, 117.3,

119.6, 123.0, 123.9, 125.9, 127.7, 127.8, 128.1, 128.5, 130.5, 135.3, 138.2, 159.0, 168.62; Microanalysis for $C_{23}H_{19}N_3O_2$+ 0.25 CH_3CN. Calc. (%) C = 74.34, H = 5.24, N = 11.99. Found (%) C = 74.33, H = 5.17, N = 11.72; HRMS (positive ESI) *m/e* calcd for $C_{23}H_{20}N_3O_2^+$ ($M + H^+$), 370.1550; found, 370.1550.

7-(3-Butyl-ureido)-1*H*-indole-2-carboxylic acid butylamide, 3.11

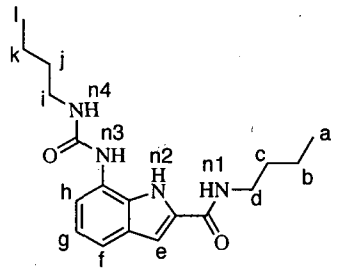

7-Nitro-1*H*-indole-2-carboxylic acid butylamide, **3.16a**, (1.00 g, 3.8 mmol), Pd/C (0.20 g, 10% wt) and hydrazine monohydrate (2 mL) were dissolved in ethanol (100 mL) and heated at reflux for 1 hour. The reaction was then filtered hot through celite and washed with ethanol (50 mL). The filtrate was then concentrated *in vacuo* and the resulting white solid was used directly in the next reaction where it was dissolved in DCM (100 mL). To this solution butylisocyanate (0.38 g, 3.8 mmol) was added dropwise and the reaction was stirred overnight. Water (250 mL) was then added and the organic layer was separated and washed with water. The organic layer was dried with sodium sulfate, filtered and concentrated *in vacuo*. The pure product was obtained by recrystallization from acetonitrile. The product was isolated as a white. Yield 0.57 g (45 %, 1.7 mmol). Mp: 116-118°C; IR ν cm^{-1} 3288, 2957, 2359, 2160, 1615s, 1558s; ^1H NMR (300 MHz, DMSO-d_6) δ: 0.91 (t, 6H, ^3J = 7.2 Hz, CH_3-a,l), 1.28-1.57 (m, 8H, CH_2-b, c, j, k), 3.14 (m, 2H, CH_2-d), 3.33 (m, 2H, coincident with H_2O, CH_2-i), 6.03 (bt, 1H, amide NH-n1), 6.93 (t, ^3J = 7.9 Hz, 1H, Ar-g), 7.10 (d, ^4J = 1.9 Hz, 1H, Ar-e), 7.21 (d, J = 7.9 Hz, 1H, Ar-f), 7.43 (d, J = 7.9 Hz, 1H, Ar-h), 8.47 (bt, 1H, urea NH-n4), 8.61 (s, 1H, urea NH-n3), 11.06 (s, 1H, indole NH-n2); ^{13}C NMR (100 MHz, DMSO-d_6) δ: 14.2, 20.0, 20.1, 31.8, 32.3, 38.9, 103.1, 112.2, 115.3, 120.7, 126.4, 127.5, 129.0, 131.7, 155.8, 161.3; Microanalysis for $C_{18}H_{26}N_4O_3$ + 0.1 CH_2Cl_2. Calc. (%) C = 64.14, H =

7.79, N = 16.53. Found (%) C = 64.17, H = 7.93, N = 16.56; HRMS (positive ESI) *m/e* calcd for $C_{18}H_{26}N_4O_2^+$ ($M + H^+$), 331.2129; found, 331.2128.

7-(3-Phenyl-ureido)-1*H*-indole-2-carboxylic acid phenylamide, 3.12

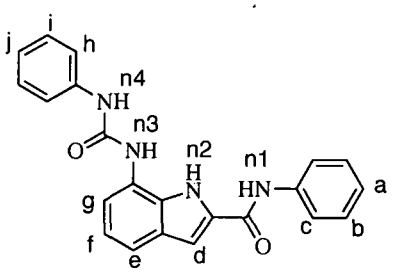

7-Nitro-1*H*-indole-2-carboxylic acid phenylamide, **3.16b**, (1.00 g, 3.6 mmol), Pd/C (0.20 g, 10% wt) and hydrazine monohydrate (2 mL) were dissolved in ethanol (100 mL) and heated at reflux for 1 hour. The reaction was then filtered hot through celite and washed with ethanol (50 mL). The filtrate was then concentrated *in vacuo* and the resulting white solid was used directly in the next reaction where it was dissolved in DCM (100 mL). To this solution phenylisocyanate (0.43 g, 3.6 mmol) was added dropwise and the reaction was stirred overnight. Water (250 mL) was then added and the organic layer was separated and washed with water. The organic layer was dried with sodium sulfate, filtered and concentrated *in vacuo*. The pure product was obtained *via* recrystallization from acetonitrile. The product was isolated as a pale yellow solid. Yield 0.64 g (48 %, 1.7 mmol). Mp: 210-213 °C; IR ν cm^{-1} 3320, 3242, 3033, 1599, 1560, 1497, 1439; ^1H NMR (300 MHz, DMSO-d_6) δ: 6.97-7.14 (m, 3H), 7.28-7.41 (m, 5H), 7.48-7.56 (m, 4H), 7.82 (d, ^3J = 8.0 Hz, 2H), 8.63 (s, 1H, urea NH), 8.91 (s, 1H, urea NH), 10.28 (s, 1H, amide NH-n1), 11.36 (s, 1H, indole NH-n2); ^{13}C NMR (100 MHz, DMSO-d_6) δ: 104.9, 114.2, 116.6, 118.9, 120.7, 121.0, 122.4, 124.1, 125.4, 128.8, 129.0, 129.2, 129.2, 131.6, 139.3, 140.2, 153.3, 160.0; Microanalysis for $C_{22}H_{18}N_4O_2$. Calc. (%) C = 71.34, H = 4.90, N = 15.12. Found (%) C = 71.31, H = 4.87, N = 15.09; HRMS (EI) calcd for $C_{22}H_{18}N_4O_2$ $[M]^+$, 370.1430; found, 370.1430.

7-(3-Phenyl-thioureido)-1*H*-indole-2-carboxylic acid phenyl amide, 3.13

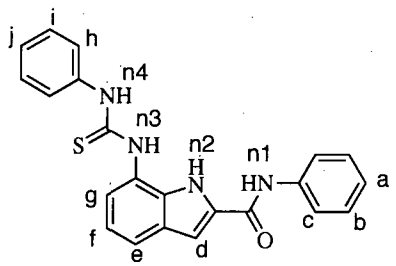

7-Nitro-1*H*-indole-2-carboxylic acid phenylamide, **3.16b**, (1.00 g, 3.6 mmol), Pd/C (0.20 g, 10% wt) and hydrazine monohydrate (2 mL) were dissolved in ethanol (100 mL) and heated at reflux for 1 hour. The reaction was then filtered hot through celite and washed with ethanol (50 mL). The filtrate was then concentrated *in vacuo* and the resulting white solid used directly in the next reaction where it was dissolved in DCM (100 mL). To this solution phenylisothiocyanate (0.49 g, 3.6 mmol) was added dropwise and the reaction was stirred overnight. Water (250 mL) was then added and the organic layer was separated and washed with water. The organic layer was dried with sodium sulfate, filtered and concentrated *in vacuo*. The pure product was obtained *via* recrystallization from acetonitrile. The product was isolated as a pale yellow solid. Yield 0.72 g (52 %, 1.8 mmol). Mp: 185-187°C; IR ν cm^{-1} 3415, 3244, 3058, 2916, 1647, 1632, 1539, 1344, 1316; ^{1}H NMR (300 MHz, DMSO-d_6) δ: 7.06-7.15 (br, 3H), 7.32-7.41 (m, 4H), 7.46-7.59 (m, 5H), 7.81 (d, ^3J = 7.7 Hz, 2H), 9.63 (s, 1H, urea NH), 9.93 (s, 1H, urea NH), 10.28 (s, 1H, amide NH-n1), 11.52 (s, 1H, indole NH-n2); ^{13}C NMR (100 Mhz, DMSO-d_6) δ: 103.9, 117.9, 119.1, 119.2, 122.4, 122.7, 123.3, 123.6, 127.4, 127.8, 130.4, 130.7, 137.9, 138.7, 158.5, 179.1; Microanalysis for $C_{22}H_{18}N_4OS$ + 0.06 CH_2Cl_2. Calc. (%) C = 67.64, H = 4.66, N = 14.30. Found (%) C = 68.35, H = 4.68, N = 14.46; HRMS (positive ESI) *m/e* calcd for $C_{22}H_{19}N_4OS^+$ ($M + H^+$), 387.1274; found, 387.1274.

5.3.2 SYNTHESIS FOR CHAPTER 4

N,N- bis(pyridin-2-ylmethyl)-3.4-diphenyl-1*H*-pyrrole-2,5-carboxamide, 4.6

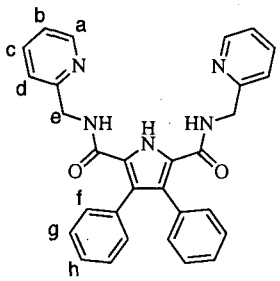

3,4-diphenyl-1*H*-pyrrole-2-carboxylic acid[124] (1.80 g; 5.9 mmol) was refluxed in thionyl chloride (40 mL) for 3 hours. The thionyl chloride was evaporated off and the resultant solid was dissolved in dichloromethane (50 mL). This was then added dropwise to a stirring solution of 2-(aminomethyl)pyridine (1.30 g; 12 mmol), triethylamine (2 mL) in dichloromethane (50 mL) with a catalytic amount of DMAP. The reaction mixture was stirred for 48 hours. Water (100 mL) was added to the reaction mixture and the organic layer was separated, dried with $MgSO_4$, filtered and concentrated *in vacuo*. The product was the recrystallised from acetonitrile to give the product as a pale yellow crystalline powder. Yield 1.82 g (63%, 3.7 mmol). Mp: 181-183° C; IR ν cm^{-1} 3388, 3237, 3053, 3029, 1644, 1556; LRMS ES^+: 488.5 $(M+H)^+$, 975.9 $(2M+H)^+$; ^1H NMR (400 MHz, DMSO-d_6) δ (ppm): 4.45 (d, ^3J = 7.0 Hz, 4H, CH_2-e), 7.10-7.20 (m, 4H, Ar-f), 7.21-7.25 (m, 10H, Ar-g,h and pyridine CH), 7.71 (m, 2H, pyridine CH), 7.89, (bt, 2H, amide NH), 8.38-8.41 (m, 2H, pyridine CH), 12.05 (s, 1H, pyrrole NH); ^{13}C NMR (100 MHz DMSO-d_6) δ: 44.1, 121.2, 122.1, 124.0, 126.6, 127.1, 127.7, 130.7, 133.8, 136.7, 148.6, 157.3, 160.1; Microanalysis for $C_{30}H_{25}N_5O_2$. Calc. (%) C = 73.90, H = 5.17, N = 14.36. Found (%) C = 74.11, H = 5.22, N = 14.34.

N,N- bis(pyridin-3-ylmethyl)-3.4-diphenyl-1*H*-pyrrole-2,5-carboxamide, 4.7

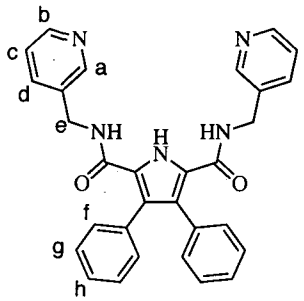

3,4-diphenyl-1*H*-pyrrole-2-carboxylic acid[124] (1.80 g; 5.9 mmol) was refluxed in thionyl chloride (40 mL) for 3 hours. The thionyl chloride was evaporated off and the resultant solid was dissolved in dichloromethane (50 mL). This was then added dropwise to a stirring solution of 3-(aminomethyl)pyridine (1.30 g, 12 mmol), triethylamine (2 mL) in dichloromethane (50 mL) with a catalytic amount of DMAP. The reaction mixture was stirred for 48 hours. Water (100 mL) was added to the reaction mixture and the organic layer was separated, dried with $MgSO_4$, filtered and concentrated *in vacuo*. The product was the recrystallised from acetonitrile to give the product as a white powder. Yield 1.78 g (62%, 3.7 mmol). Mp: 195-198°C; IR ν cm^{-1} 3397, 3338, 3248, 3041, 1645, 1628, 1544; LRMS ES^+: 488.5 $(M+H)^+$, 975.9 $(2M+H)^+$; ^1H NMR (400 MHz, DMSO-d_6) δ: 4.35 (d, ^3J = 5.5 Hz, 4H, CH_2-e), 7.03-7.09 (m, 4H, Ar-f), 7.14-7.18 (m, 8H, Ar-g,h ans pyridne CH), 7.30-7.33 (m, 2H, pyridne CH), 7.54-7.57 (m, 2H, pyridne CH), 7.76 (bt, 2H, amide NH), 8.43-8.45 (m, 2H, pyridine CH), 12.04 (s, 1H, pyrrole NH); ^{13}C NMR (100 MHz, DMSO-d_6) δ: 40.6, 122.1, 122.9, 125.4, 125.5, 126.4, 129.4, 132.6, 133.2, 133.9, 146.9, 147.6, 159.2; Microanalysis for $C_{30}H_{25}N_5O_2$. Calc. (%) C = 73.90, H = 5.17, N = 14.36. Found (%) C = 73.94, H = 5.22, N = 14.26.

N,N- bis(2-morpholinoethyl)-3.4-diphenyl-1*H*-pyrrole-2,5-carboxamide, 4.8

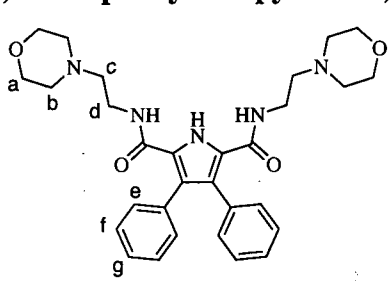

3,4-diphenyl-1*H*-pyrrole-2-carboxylic acid[124] (1.80 g; 5.9 mmol) was refluxed in thionyl chloride (40 mL) for 3 hours. The thionyl chloride was evaporated off and the resultant solid was dissolved in dichloromethane (50 mL). This was then added dropwise to a stirring solution of 4-(2-aminoethyl) morpholine (1.56 g; 12 mmol) and triethylamine (2 mL) in dichloromethane (50 mL) with a catalytic amount of DMAP. The reaction mixture was stirred for 48 hours. Water (100 mL) was added to the reaction mixture and the organic layer was separated, dried with $MgSO_4$, filtered and concentrated *in vacuo*. The product was the recrystallised from methanol to give the product as clear plate-like crystals. Yield 1.50 g (48%, 2.8 mmol). Mp: 155-157° C; IR ν cm^{-1} 3374, 3272, 2937, 2878, 2847, 2815, 1654, 1631; LRMS ES^+: 532.5 $(M+H)^+$, 1063.5 $(2M+H)^+$; ^1H NMR (300 MHz, $CDCl_3$) δ (ppm): 2.26 (br, 12H, CH_2), 3.23 (br, 4H, CH_2), 3.46 (br, 8H, CH_2-c,d), 6.97 (s, 2H, amide NH), 7.07 (m, 4H, Ar-e), 7.19 (m, 6H, Ar-f,g), 11.78 (s, 1H, pyrrole NH); ^{13}C NMR (100 MHz, $CDCl_3$) δ: 35.6, 52.8, 56.8, 123.9, 126.4, 126.8, 127.8, 130.5, 133.8, 159.8; Microanalysis for $C_{30}H_{37}N_5O_4$. Calc. (%) C = 67.78, H = 7.01, N = 13.17. Found (%) C = 68.04, H = 7.05, N = 13.04.

3,4-Diphenyl-1*H*-pyrrole-2,5-dicarboxylic acid bis-[(1-butyl-1*H*-imidazol-2-yl methyl)-amide], 4.9

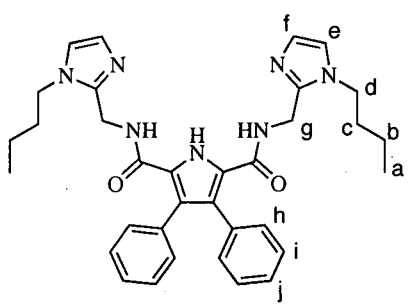

3,4-diphenyl-1*H*-pyrrole-2-carboxylic acid[124] (1.80 g; 5.9 mmol) was refluxed in thionyl chloride (40 mL) for 3 hours. The thionyl chloride was evaporated off and the resultant solid was dissolved in dichloromethane (50 mL). This was then added dropwise to a stirring solution of 1-Butyl-imidazol-2-yl-methylamine (1.30 g, 12 mmol) and triethylamine (2 mL) in dichloromethane (50 mL) with a catalytic amount of DMAP. The reaction mixture was stirred for 48 hours. Water (100 mL) was added to the reaction mixture and the organic layer was separated, dried with $MgSO_4$, filtered and

concentrated *in vacuo*. The product was the recrystallised from acetonitrile to give the product as a white powder in a yield = 67%; 2.28 g; 4 mmol. Mp: 162-164 °C; IR ν cm^{-1} 3428, 3169, 2953, 2930, 2869, 1630, 1550; LRMS ES^+: 578.5 $(M+H)^+$; ^1H NMR (300 MHz, DMSO-d_6) δ: 0.83 (t, ^3J = 7.2 Hz, 6H, CH_3-a), 1.14-1.26 (m, 4H, CH_2-b), 1.52-1.62 (m, 4H, CH_2-c), 3.83 (t, ^3J = 7.15 Hz, 4H, CH_2-d), 4.40 (d, ^3J = 5.3 Hz, 4H), 6.76 (s, 2H, CH-e or f), 7.02-7.14 (m, 12H, Ar-h,i,j and CH-e or f), 7.66 (bt, 2H, amide NH), 12.29 (s, 1H, pyrrole NH); ^{13}C NMR (100 MHz $CDCl_3$) δ: 14.0, 20.2, 30.0, 33.5, 36.0, 46.1, 120.3, 124.0, 127.1, 127.9, 128.4, 129.2, 130.9, 133.0, 143.7, 160.5; Microanalysis for $C_{34}H_{39}N_7O_2$. Calc. (%) C = 70.69, H = 6.80, N = 16.96. Found (%) C = 70.70, H = 6.81, N = 16.96.

3,4-Diphenyl-1*H*-pyrrole-2,5-dicarboxylic acid bis-[(2-dibutylamino-ethyl)-amide], 4.10

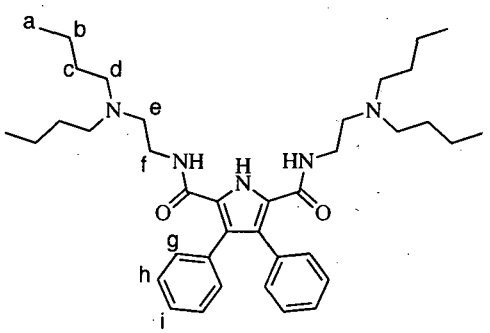

3,4-diphenyl-1*H*-pyrrole-2-carboxylic acid[124] (1.75 g; 5.7 mmol) was refluxed in thionyl chloride (40 mL) for 3 hours. The thionyl chloride was evaporated off and the resultant solid was dissolved in dichloromethane (50 mL). This was then added dropwise to a stirring solution of *N,N*-dibutlyethylenediamine (2 g, 12 mmol) and triethylamine (5 mL) in dichloromethane (50 mL) with a catalytic amount of DMAP. The reaction mixture was stirred for 48 hours. Water (100 mL) was added to the reaction mixture and the organic layer was separated, dried with $MgSO_4$, filtered and concentrated *in vacuo*. The product was the recrystallised from acetonitrile to give the product as a white powder. Yield 2.21 g (67%, 3.8 mmol). Mp: 70-73 °C; IR ν cm^{-1} 3372, 3190, 2949, 2924, 2856, 2805, 1649, 1600, 1550; LRMS ES^+: 616.7 $(M+H)^+$; ^1H NMR (400 MHz $CDCl_3$) δ: 0.84 (bt, 12H, CH_3-a), 1.13 (m, 16H, CH_2-b,c), 2.17 (m, 8H,

CH_2-d), 2.33 (bt, 4H, CH_2-e), 3.28 (br, 4H, CH_2-f), 6.09 (bt, 2H, amide NH), 7.11-7.14 (m, 4H, Ar-g), 7.20-7.24 (m, 6H, Ar-h,i), 10.23 (s, 1H, pyrrole NH); ^{13}C NMR (100 MHz $CDCl_3$) δ: 14.4, 20.1, 29.2, 37.6, 52.9, 53.8, 124.1, 126.2, 128.0, 128.9, 131.1, 133.8, 160.8; Microanalysis for $C_{38}H_{57}N_5O_2$. Calc. (%) C = 74.11, H = 9.33, N = 11.37. Found (%) C = 74.04, H = 9.43, N = 11.36.

Pyridine-2,6-dicarboxylic acid bis-[(2-dibutylamino-ethyl)-amide], 4.13

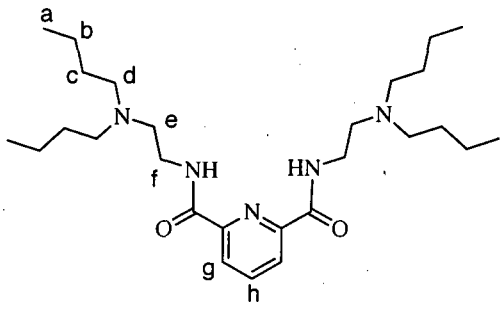

Pyridine 2,6-diacetlydichloride (2.00 g, 9.8 mmol) was dissolved in dichloromethane (50 mL) and added dropwise to a stirring solution of *N,N*-dibutlyethylenediamine (3.45 g, 20 mmol) and triethylamine (5 mL) in dichloromethane (50 mL) with a catalytic amount of DMAP. The reaction mixture was stirred for 24 hours. Water (100 mL) was added to the reaction mixture and the organic layer was separated, dried with $MgSO_4$, filtered and concentrated *in vacuo*. The resulting oil was purified *via* a flash column chromatography (SiO_2, DCM/1% MeOH) to give the product as viscous orange oil. Yield 3.73 g (80%, 8.1 mmol). ^1H NMR (400 MHz, $CDCl_3$) δ: 0.88 (t, ^3J = 7.3 Hz, 12H, CH_3-a), 1.26-1.35 (m, 8H, CH_2-b), 1.41-1.49 (m, 8H, CH_2-c), 2.49 (t, ^3J = 7.5 Hz, 8H, CH_2-d), 2.67 (t, ^3J = 6.3 Hz, 4H, CH_2-e), 3.56 (q, ^3J = 6.3 Hz, 4H, CH_2-f), 8.00 (t, ^3J = 7.8 Hz, 1H, Ar-h), 8.33 (d, ^3J = 7.8 Hz, 2H, Ar-g), 8.43 (s, 2H, amide NH); ^{13}C NMR (100 MHz, $CDCl_3$) δ: 14.4, 20.1, 29.6, 37.8, 53.8, 54.5, 125.1, 139.2, 149.4, 164.0; LRMS ES$^+$: 476.5 $(M+H)^+$; LRMS ES$^-$: 474.5 $(M-H)^-$; Microanalysis for $C_{27}H_{49}N_5O_2$. Calc. (%) C = 68.17, H = 10.38, N = 14.71. Found (%) C = 68.15, H = 10.32, N = 14.70.

N,N'-Bis-(2-dibutylamino-ethyl)-isophthalamide, 4.14

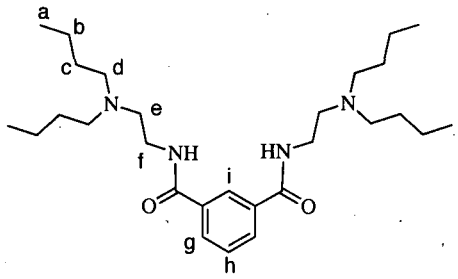

Isophthaloyl dichloride (2.00 g, 9.9 mmol) was dissolved in dichloromethane (50 mL) and added dropwise to a stirring solution of *N,N*-dibutlyethylenediamine (3.45 g, 20 mmol) and triethylamine (5 mL) in dichloromethane (50 mL) with a catalytic amount of DMAP. The reaction mixture was stirred for 24 hours. Water (100 mL) was added to the reaction mixture and the organic layer was separated, dried with $MgSO_4$, filtered and concentrated *in vacuo*. The resulting oil was purified *via* a flash column chromatography (SiO_2, DCM/1% MeOH) to give the product as viscous yellow oil. Yield 3.85 g (82%, 8.1mmol). ^{1}H NMR (400 MHz, $CDCl_3$) δ: 0.88 (t, ^3J = 7.3 Hz, 12H, CH_3-a), 125-1.35 (m, 8H, CH_2-b), 1.38-1.46 (m, 8H, CH_2-c), 2.45 (t, ^3J = 7.3 Hz, 8H, CH_2-d), 2.63 (t, ^3J = 5.9 Hz, 4H, CH_2-e), 3.48 (q, ^3J = 5.9 Hz, 4H, CH_2-f), 6.97 (s, 2H, amide NH); 7.49 (t, ^3J = 7.8 Hz, 1H, Ar-h), 8.33 (d, ^3J = 1.8 Hz (w coupling), 7.8 Hz, 2H, Ar-g), 8.23 (t, J = 1.8 Hz (w coupling), 1H, Ar-i); ^{13}C NMR (100 MHz, $CDCl_3$) δ: 14.4, 21.1, 29.6, 37.9, 52.9, 54.0, 125.8, 129.2, 129.9, 135.6, 166.8; LRMS ES$^+$: 475.5 $(M+H)^+$; LRMS ES$^-$: 473.5 $(M-H)^-$; Microanalysis for $C_{28}H_{50}N_4O_2$. Calc. (%) C = 70.84, H = 10.62, N = 11.80. Found (%) C = 70.77, H = 10.53, N = 11.79.

REFERENCES

(1) Lehn, J.-M. *Angew. Chem. Int. Ed.* **1988**, *27*, 89.
(2) Lehn, J.-M. *Supramolecular Chemistry: Concepts and Perspective*; VCH, 1995.
(3) Sessler, J. L.; Gale, P. A.; Cho, W.-S. *Anion Receptor Chemistry*; RSC Publishing: Cambridge, 2006.
(4) Beer, P. D.; Gale, P. A. *Angew. Chem. Int. Ed.* **2001**, *40*, 486-516.
(5) Gale, P. A. *Coord. chem. rev.* **2003**, *240*, 191-221.
(6) Gale, P. A.; Quesada, R. *Coord. chem. rev.* **2006**, *250*, 3219-3244.
(7) Pascal, R. A.; Spergel, J.; Engbersen, D. V. *Tetrahedron Lett.* **1986**, *27*, 4099.
(8) Valiyaveettil, S.; Engbersen, J. F. J.; Verboom, W.; Reinhoudt, D. *Angew. Chem. Int. Ed.* **1993**, *32*, 900-901.
(9) Kavallieratos, K.; Gala, S.; Austin, D.; Crabtree, R. *J. Am. Chem. Soc.* **1997**, *119*, 2325-2326.
(10) Hughes, M.; Smith, B. *J. Org. Chem.* **1997**, *62*, 4492-4499.
(11) Santacroce, P. V.; Davis, J. T.; Light, M. E.; Gale, P. A.; Iglesias-Sanchez, J. C.; Prados, P.; Quesada, R. *J. Am. Chem. Soc.* **2007**, *129*, 1886-1887.
(12) Webb, J. E. A.; Crossley, M. J.; Turner, P.; Thordarson, P. *J. Am. Chem. Soc.* **2007**, *129*, 7155-7162.
(13) Prohens, R.; Tomas, S.; Morey, J.; Deya, P. M.; Ballester, P.; Costa, A. *Tetrahedron Lett.* **1998**, *39*, 1063-1066.
(14) Davis, A. P.; Perry, J. J.; Williams, R. P. *J. Am. Chem. Soc.* **1997**, *119*, 1793-1794.
(15) Choi, K.; Hamilton, A. D. *J. Am. Chem. Soc.* **2001**, *123*, 2456-2457.
(16) Szumna, A.; Jurczak, J. *Eur. J. Org. Chem.* **2001**, 4031-4039.
(17) Chmielewski, M. J.; Jurczak, J. *Chem. Eur. J.* **2005**, *11*, 6080-6094.
(18) Chmielewski, M. J.; Jurczak, J. *Chem. Eur. J.* **2006**, *12*, 7652-7667.
(19) Hamuro, Y.; Geib, S. J.; Hamilton, A. D. *J. Am. Chem. Soc.* **1996**, *118*, 7529-7541.
(20) Hunter, C. A.; Purvis, D. A. *Angew. Chem. Int. Ed. Engl.* **1992**, *31*, 792.
(21) Kang, S. O.; Powell, D.; Bowman-James, K. *J. Am. Chem. Soc.* **2005**, *127*, 13478-13479.
(22) Kang, S. O.; Powell, D.; Day, V. W.; Bowman-James, K. *Angew. Chem. Int. Ed.* **2006**, *45*, 1921-1925.
(23) Kubik, S.; Goddard, R.; Kirchner, R.; Nolting, D.; Seidel, J. *Angew. Chem. Int. Ed.* **2001**, *40*, 2648-2649.
(24) Kubik, S.; Kirchner, R.; Nolting, D.; Seidel, J. *J. Am. Chem. Soc.* **2002**, *124*, 12752-12760.
(25) Gunnlaugsson, T.; Kruger, P. E.; Jensen, P.; Pfeffer, F. M.; Hussey, G. M. *tetrahedron lett.* **2003**, *44*, 8909-8913.
(26) Camiolo, S.; Gale, P. A.; Hursthouse, M. B.; Light, M. E.; Shi, A. J. *Chem. Commun.* **2002**, 758-759.
(27) Gale, P. A.; Navakhun, K.; Camiolo, S.; Light, M. E.; Hursthouse, M. B. *J. Am. Chem. Soc.* **2002**, *124*, 11228-11229.
(28) Camiolo, S.; Gale, P. A.; Hursthouse, M. B.; Light, M. E. *Org. Biomol. Chem.* **2003**, *1*, 741-744.

(29) Amendola, V.; Esteban-Gomez, D.; Fabbrizzi, L.; Licchelli, M. *Acc. Chem. Res.* **2006**, *39*, 343-353.
(30) Boiocchi, M.; Boca, L. D.; Gomez, D. E.; Fabbrizzi, L.; Licchelli, M.; Monzani, E. *J. Am. Chem. Soc.* **2004**, *126*, 16507-16514.
(31) Gunnlaugsson, T.; Davis, A. P.; Hussey, G. M.; Tierney, J.; Glynn, M. *Org. Biomol. Chem.* **2004**, *2*, 1856-1863.
(32) Kwon, J. Y.; Jang, Y. J.; Kim, S. K.; Lee, K.; Kim, J. S.; Yoon, J. *J. Org. Chem.* **2004**, *69*, 5155-5157.
(33) Brooks, S. J.; Gale, P. A.; Light, M. E. *Chem. Commun.* **2005**, 4696-4698.
(34) Brooks, S. J.; Gale, P. A.; Light, M. E. *Chem. Commun.* **2006**, 4344-4346.
(35) Brooks, S. J.; Edwards, P. R.; Gale, P. A.; Light, M. E. *New J. Chem.* **2006**, *30*, 65-70.
(36) Kondo, S.; Nagamine, M.; Yano, Y. *tetrahedron lett.* **2003**, *44*, 8801-8804.
(37) Pfeffer, F. M.; Gunnlaugsson, T.; Jensen, P.; Kruger, P. E. *Org. Lett.* **2005**, *7*, 5357-5360.
(38) Ayling, A. J.; Perez-Payan, N.; Davis, A. P. *J. Am. Chem. Soc.* **2001**, *123*, 12716-12717.
(39) Clare, J. P.; Ayling, A. J.; Joos, J.; Sisson, A. L.; Magro, G.; Perez-Payan, N.; Lambert, T. N.; Shukla, R.; Smith, B. D.; Davis, A. P. *J. Am. Chem. Soc.* **2005**, *127*, 10739-10746.
(40) Koulov, A. V.; Lambert, T. N.; Shukla, R.; Jain, M.; Boon, J. M.; Smith, B. D.; Li, H.; Sheppard, D. N.; Joos, J.-B.; Clare, J. P.; Davis, A. P. *Angew. Chem. Int. Ed.* **2003**, *42*, 4931-4933.
(41) Snellink-Ruel, B. H. M.; Antonisse, M. M. G.; Engbersen, J. F. J.; Timmerman, P.; Reinhoudt, D. N. *Eur. J. Org. Chem.* **2000**, 165-170.
(42) Lee, K. H.; Hong, J. *tetrahedron lett.* **2000**, *41*, 6083-6087.
(43) Hisaki, I.; Sasaki, S.; Hirose, K.; Tobe, Y. *Eur. J. Org. Chem.* **2007**, 607-615.
(44) Sessler, J. L.; Camiolo, S.; Gale, P. A. *Coord. Chem. Rev.* **2003**, *240*, 17-55.
(45) Shionoya, M.; Furuta, H.; Lynch, V.; Harriman, A.; Sessler, J. L. *J. Am. Chem. Soc.* **1992**, *114*, 5714-5722.
(46) Kral, V.; Furuta, H.; Shreder, K.; Lynch, V.; Sessler, J. L. *J. Am. Chem. Soc.* **1996**, *118*, 1595-1607.
(47) Gale, P. A.; Camiolo, S.; Tizzard, G. J.; Chapman, C. P.; Light, M. E.; Coles, S. J.; Hursthouse, M. B. *J. Org. Chem.* **2001**, *66*, 7849-7853.
(48) Sessler, J. L.; Pantos, G. D.; Gale, P. A.; Light, M. E. *Org. Lett.* **2006**, *8*, 1593-1596.
(49) Sessler, J. L.; Barkey, N. M.; Pantos, G. D.; Lynch, V. *New J. Chem.* **2007**, *31*, 646-654.
(50) Vega, I. E. D.; Camiolo, S.; Gale, P. A.; Hursthouse, M. B.; Light, M. E. *Chem. Commun.* **2003**, 1686.
(51) Vega, I. E. D.; Gale, P. A.; Hursthouse, M. B.; Light, M. E. *Org. Biomol. Chem.* **2004**, *2*, 2935-2941.
(52) Sessler, J. L.; Katayev, E.; Pantos, G. D.; Ustynyuk, Y. A. *Chem. Commun.* **2004**, 1276-1277.

(53) Sessler, J. L.; Katayev, E.; Pantos, G. D.; Scherbakov, P.; Reshetova, M. D.; Khurstalev, V. N.; Lynch, V.; Ustynyuk, Y. A. *J. Am. Chem. Soc.* **2005**, *127*, 11442-11446.
(54) Katayev, E.; Boev, N.; Khurstalev, V. N.; Ustynyuk, Y. A.; Tananaev, I. G.; Sessler, J. L. *J. Org. Chem.* **2007**, *72*, 2886-2896.
(55) Gale, P. A.; Sessler, J. L.; Kral, V.; Lynch, V. *J. Am. Chem. Soc.* **1996**, *118*, 5140-5141.
(56) Baeyer, A. *Ber. Dtsch. Chem. Ges.* **1886**, *19*, 2184-2185.
(57) Lee, C.-H.; Lee, J.-S.; Na, H.-K.; Yoon, D.-W.; Miyaji, H.; Cho, W.-S.; Sessler, J. L. *J. Org. Chem.* **2005**, *70*, 2067-2074.
(58) Miyaji, H.; Hong, S.-J.; Jeong, S.-D.; Yoon, D.-W.; Na, H.-K.; Hong, J.; Ham, S.; Sessler, J. L.; Lee, C.-H. *Angew. Chem. Int. Ed.* **2007**, *46*, 2508-2511.
(59) Cafeo, G.; Kohnke, F. H.; La Torre, G. L.; White, A. J. P.; Williams, D. J. *Angew. Chem. Int. Ed.* **2000**, *39*, 1496-1498.
(60) Cafeo, G.; Kohnke, F. H.; La Torre, G. L.; Parisi, M. F.; Nascone, R. P.; White, A. J. P.; Williams, D. J. *Chem. Eur. J.* **2002**, *8*, 3148-3156.
(61) Cafeo, G.; Kohnke, F. H.; White, A. J. P.; Garozzo, D.; Messina, A. *Chem. Eur. J.* **2007**, *13*, 649-656.
(62) Chmielewski, M. J.; Charon, M.; Jurczak, J. *Org. Lett.* **2004**, *6*, 3501-3504.
(63) Piatek, P.; Lynch, V.; Sessler, J. L. *J. Am. Chem. Soc.* **2004**, *126*, 16073-16076.
(64) Curiel, D.; Cowley, A.; Beer, P. D. *Chem. Commun.* **2005**, 236-238.
(65) Smith, D. K. *Org. Biomol. Chem.* **2003**, *1*, 3874-3877.
(66) Winstanley, K. J.; Smith, D. K. *J. Org. Chem.* **2007**, *72*, 2803-2815.
(67) Ghosh, S.; Choudhury, A. R.; Row, T. N.; Maitra, U. *Org. Lett.* **2005**, *7*, 1441-1444.
(68) Kim, H.; Kang, J. *Tetrahedron Lett.* **2005**, *46*, 5443-5445.
(69) Yoon, J.; Kim, S. K.; Singh, J.; Lee, J. W.; Yang, Y. J.; Chellappan, K.; Kim, K. S. *J. Org. Chem.* **2004**, *69*, 581-583.
(70) Wong, W. W. H.; Vickers, M. S.; Cowley, A. R.; Paul, R. L.; Beer, P. D. *Org. Biomol. Chem.* **2005**, *3*, 4201-4208.
(71) Alcalde, E.; Mesquida, N.; Perez-Garcia, L. *Eur. J. Org. Chem.* **2006**, 3988-3996.
(72) Abouderbala, L. O.; Belcher, W. J.; Boutelle, M. G.; Cragg, P. J.; Dhaliwal, J.; Fabre, M.; Steed, J. W.; Turner, D. R.; Wallace, K. J. *Chem. Commun.* **2002**, 358-359.
(73) Wallace, K. J.; Belcher, W. J.; Turner, D. R.; Syed, K. F.; Steed, J. W. *J. Am. Chem. Soc.* **2003**, *125*, 9699-9715.
(74) Shinoda, S.; Tadokoro, M.; Tsukube, H.; Arakawa, R. *Chem. Commun.* **1998**, 181-182.
(75) Haj-Zaroubi, M.; Mitzel, N. W.; Schmidtchen, F. P. *Angew. Chem. Int. Ed.* **2002**, *41*, 104-107.
(76) Schmuck, C. *Chem. Commun.* **1999**, 843-844.
(77) Schmuck, C. *Chem. Eur. J.* **2000**, *6*, 709-718.
(78) Schmuck, C.; Schwegmann, M. *J. Am. Chem. Soc.* **2005**, *127*, 3373-3379.
(79) Blondeau, P.; Benet-Buchholz, J.; de Mendoza, J. *New J. Chem.* **2007**, *31*, 736-740.

(80) Arduini, A.; Giorgi, G.; Pochini, A.; Secchi, A.; Ugozzoli, F. *J. Org. Chem.*, **2001**, *66*, 8302-8308.
(81) Atwood, J. L.; Szumna, A. *J. Am. Chem. Soc.* **2002**, *124*, 10646-10647.
(82) Atwood, J. L.; Szumna, A. *Chem. Commun.*, **2003**, 940-941.
(83) Mahoney, J. M.; Davis, J. P.; Beatty, A. M.; Smith, B. D. *J. Org. Chem.*, **2003**, *68*, 9819-9820.
(84) Cametti, M.; Nissinen, M.; Cort, A. D.; Mandolini, L.; Rissanen, K. *Chem. Commun.*, **2003**.
(85) Cametti, M.; Nissinen, M.; Cort, A. D.; Mandolini, L.; Rissanen, K. *J. Am. Chem. Soc.* **2007**, *129*, 3641-3648.
(86) Sessler, J. L.; Gross, D. E.; Cho, W.-S.; Lynch, V. M.; Schmidtchen, F. P.; Bates, G. W.; Light, M. E.; Gale, P. A. *J. Am. Chem. Soc.* **2006**, *128*, 12281-12288.
(87) Hynes, M. J. *J. Chem. Soc. Dalton Trans.* **1993**, 311-312.
(88) Depraetere, S.; Smet, M.; Dehaen, W. *Angew. Chem. Int. Ed.* **1999**, *38*, 3359-3361.
(89) Nishiyabu, R.; Palacios, M. A.; Dehaen, W.; Anzenbacher, P. *J. Am. Chem. Soc.* **2006**, *128*, 11496-11504.
(90) Dehaen, W.; Gale, P. A.; Garcia-Garrido, S. E.; Kostermans, M.; Light, M. E. *New J. Chem.*, **2007**, *31*, 691-696.
(91) Pflugrath, J. W.; Quiocho, F. A. *Nature* **1985**, *314*, 257.
(92) Pflugrath, J. W.; Quiocho, F. A. *J. Mol. Biol.* **1988**, *200*, 163.
(93) He, J. J.; Quiocho, F. A. *Science* **1991**, *251*, 1479.
(94) Verschueren, K. H. G.; Seljee, F.; Rozeboom, H. J.; Kalk, K. H.; Dijkstra, B. W. *Nature* **1993**, *363*, 693.
(95) Verschueren, K. H. G.; Franken, S. M.; Rozeboom, H. J.; Kalk, K. H.; Dijkstra, B. W. *J. Mol. Biol.* **1993**, *232*, 856.
(96) Black, D. C.; Craig, D. C.; Kumar, N.; McConnell, D. B. *Tetrahedron Lett.* **1996**, *37*, 241-244.
(97) Sessler, J. L.; Cho, D.-G.; Lynch, V. *J. Am. Chem. Soc.* **2006**, *128*, 16518-16519.
(98) Chang, K.-J.; Chae, M. K.; Lee, C.-H.; Lee, J.-Y.; Jeong, K.-S. *Tetrahedron Lett.* **2006**, *47*, 6385-6388.
(99) Chang, K.-J.; Moon, D.; Lah, M. S.; Jeong, K.-S. *Angew. Chem. Int. Ed.* **2005**, *44*, 7926-7929.
(100) Pfeffer, F. M.; Lim, K. F.; Sedgwick, K. J. *Org. Biomol. Chem.* **2007**, *5*, 1795-1799.
(111) Kavallieratos, K.; Bertao, C. M.; Crabtree, R. H. *J. Org. Chem.* **1999**, *64*, 1675-1683.
(112) Bream, R. *'Xstrata to proceed with $4bn nickel site'; www.FT.com,* October 17 **2007**
(113) Donegan, S. *Miner. Eng.* **2006**, *19*, 1234-1245
(114) Whittington, B.I.; Johnson, J.A.; Quan, L.P.; McDonald, R.G.; Muir, D.M. *Hydrometallurgy*, **2003**, *70*, 47-62
(115) Shriver, D. F.; Atkins, P. W. *Inorganic chemistry*; 2nd Edition ed.; W.H. Freeman and Co., 1994.
(116) Habashi, F. *Miner. Eng.* **1994**, *7*, Chpt. 2.
(117) Tasker, P. A.; Tong, C. C.; Westra, A. N. *Coord. chem. rev.* **2007**, *251*, 1868-1877.

(118) Szymanowski, J. *Hydroxyoximes and Copper Hydrometallurgy*; CRC Press Inc.: London, 1993.
(119) Swaddle, T. W. *Inorganic Chemistry: An Industrial and Environmental Perspective*; Academic Press, 1997.
(120) Tasker, P. A.; Plieger, P. G.; West, L. C. in: McCleverty J.A.; Meyer T.J. (Eds.), *Comprehensive Coordination Chemistry II,* vol. 9, Elsevier, London, 2004.
(121) Dreisinger, D. *Hydrometallurgy*, 83, **2006**, 10.
(122) White, D. J.; Laing, N.; Miller, H.; Parsons, S.; Coles, S.; Tasker, P. A. *Chem. Commun.* **1999**, 2077-2078.
(123) Coxall, R. A.; Lindoy, L. F.; Miller, H. A.; Parkin, A.; Parsons, S.; Tasker, P. A.; White, D. J. *Dalton Trans.* **2003**, 55-64.
(124) Galbraith, S. G., University of Edinburgh, 2004.
(125) Plieger; P. G.; Tasker, P. A.; Galbraith, S. G. *Dalton Trans.* **2004**, 313-318.
(126) Galbraith, S. G.; Lindoy, L. F.; Tasker, P. A.; P.G., P. *Dalton trans.* **2006**, 1134-1136.
(127) Galbraith, S. G.; Wang, Q.; Li, L.; Blake, A. J.; Wilson, C.; Collinson, S. R.; Lindoy, L. F.; Plieger, P. G.; Schroder, M.; Tasker, P. A. *Chem. Eur. J.* **2007**, *13*, 6091-6107.
(128) Kavallieratos, K.; Sachleben, R.A.; Berkel, G.J.V.; Moyer, B.A. *Chem Commun.*, **2000**, 187-188
(129) Eller, L.R.; Stepien, M.; Fowler, C.J.; Lee, J.T.; Sessler, J.L.; Moyer, B.A., *J. Am. Chem. Soc.*, **2007**, *129*, 11020-11021.
(130) Gale, P. A.; Light, M. E.; McNally, B.; Navakhun, K.; Sliwinski, K. E.; Smith, B. D. *Chem. Commun.* **2005**, 3773-3775.
(131) Gale, P. A.; Garric, J.; Light, M. E.; McNally, B. A.; Smith, B. D. *Chem. Commun.* **2007**, 1736-1738.
(132) Friedman, M. *J. Org. Chem.* **1965**, *30*, 859.
(133) Bogacki, M. A. *Solvent Extr. Ion Exch.* **1997**, *15*, 731-755.
(134) Sastre, A. M.; Szymanowski, J. *Solvent Extr. Ion Exch.* **2004**, *22*, 737-759.

APPENDIX 1 – X-RAY CRYSTAL STRUCUTRE DATA

The crystal structures presented in chapters 2, 3 and 4 were solved by the EPSRC National Crystallography Service (Dr M. E. Light). The refinement of the structure and the fractional coordinates are reported for the sake of completeness and so that the structures may be regenerated from the text if necessary.

STRUCUTRES FROM CHAPTER 2

2.5·TMAF complex

Table 1. Crystal data and structure refinement details.

Empirical formula	$C_{32}H_{48}FN_5$
Formula weight	521.75
Temperature	120(2) K
Wavelength	0.71073 Å
Crystal system	Tetragonal
Space group	*P4/n*
Unit cell dimensions	a = 12.5651(15) Å
	c = 9.275(3) Å
Volume	1464.3(5) Å^3
Z	2
Density (calculated)	1.183 Mg / m^3
Absorption coefficient	0.075 mm^{-1}
F(000)	568
Crystal	Prism; Colourless
Crystal size	0.2 × 0.1 × 0.05 mm^3
θ range for data collection	3.92 – 26.42°
Index ranges	$-15 \le h \le 9$, $-15 \le k \le 15$, $-11 \le l \le 11$
Reflections collected	8440
Independent reflections	1507 [R_{int} = 0.0756]
Completeness to θ = 26.42°	99.5 %
Absorption correction	Semi–empirical from equivalents
Max. and min. transmission	0.9963 and 0.9752
Refinement method	Full-matrix least-squares on F^2
Data / restraints / parameters	1507 / 0 / 100
Goodness-of-fit on F^2	1.053
Final R indices [$F^2 > 2\sigma(F^2)$]	$R1$ = 0.0565, $wR2$ = 0.1248
R indices (all data)	$R1$ = 0.1067, $wR2$ = 0.1461
Extinction coefficient	0.0162(5)
Largest diff. peak and hole	0.345 and –0.279 e Å^{-3}

Diffractometer: *Nonius KappaCCD* area detector (ϕ scans and ω scans to fill *asymmetric unit*). **Cell determination:** DirAx (Duisenberg, A.J.M.(1992). J. Appl. Cryst. 25, 92-96.) **Data collection:** Collect (Collect: Data collection software, R. Hooft, Nonius B.V., 1998). **Data reduction and cell refinement**: *Denzo* (Z. Otwinowski & W. Minor, *Methods in Enzymology* (1997) Vol. **276**: *Macromolecular Crystallography*, part A, pp. 307–326; C. W. Carter, Jr. & R. M. Sweet, Eds., Academic Press). **Absorption correction**: Sheldrick, G. M. SADABS - Bruker Nonius area detector scaling and absorption correction - V2.10 **Structure solution**: *SHELXS97* (G. M. Sheldrick, Acta Cryst. (1990) **A46** 467–473). **Structure refinement**: *SHELXL97* (G. M. Sheldrick (1997), University of Göttingen, Germany). **Graphics:** Cameron - A Molecular Graphics Package. (D. M. Watkin, L. Pearce and C. K. Prout, Chemical Crystallography Laboratory, University of Oxford, 1993).

Special details: All hydrogen atoms were placed in idealised positions and refined using a riding model.

Table 2. Atomic coordinates [$\times 10^4$], equivalent isotropic displacement parameters [$Å^2 \times 10^3$] and site occupancy factors. U_{eq} is defined as one third of the trace of the orthogonalized U^{ij} tensor.

Atom	*x*	*y*	*z*	U_{eq}	*S.o.f.*
N1	823(1)	1680(1)	1656(1)	25(1)	1
C1	32(1)	2293(1)	2258(1)	25(1)	1
C2	−480(1)	1669(1)	3241(1)	29(1)	1
C3	11(1)	655(1)	3238(1)	29(1)	1
C4	820(1)	678(1)	2249(1)	24(1)	1
C5	1579(1)	−189(1)	1770(1)	26(1)	1
C6	1216(1)	−1246(1)	2427(1)	34(1)	1
C7	1557(1)	−296(1)	119(1)	31(1)	1
C9A	−2390(1)	−3590(1)	3449(2)	82(1)	0.38
C9B	−3135(1)	−3411(1)	3516(2)	82(1)	0.38
C8	−2500	−2500	5624(1)	69(1)	1
N2	−2500	−2500	4033(1)	27(1)	1
F1	2500	2500	−9(1)	27(1)	1

2.5·TMACl COMPLEX

Table 1. Crystal data and structure refinement details for $C_{28}H_{36}N_4 \cdot C_4H_{12}N \cdot Cl$

Empirical formula	$C_{32}H_{48}ClN_5$
Formula weight	538.20
Temperature	120(2) K
Wavelength	0.71073 Å
Crystal system	Tetragonal
Space group	*P4/n*
Unit cell dimensions	a = 12.2382(17) Å
	c = 10.0176(15) Å
Volume	1500.4(4) $Å^3$
Z	2
Density (calculated)	1.191 Mg / m^3
Absorption coefficient	0.156 mm^{-1}
F(000)	584
Crystal	Block; Colourless
Crystal size	0.2 × 0.11 × 0.05 mm^3
θ range for data collection	3.90 – 27.48°
Index ranges	$-15 \le h \le 15$, $-15 \le k \le 15$, $-12 \le l \le 10$
Reflections collected	11263
Independent reflections	1723 [R_{int} = 0.0815]
Completeness to θ = 27.48°	99.6 %
Absorption correction	Semi-empirical from equivalents
Max. and min. transmission	0.9922 and 0.9694

Refinement method	Full-matrix least-squares on F^2
Data / restraints / parameters	1723 / 0 / 100
Goodness-of-fit on F^2	1.031
Final R indices $[F^2 > 2\sigma(F^2)]$	$R1 = 0.0611$, $wR2 = 0.1470$
R indices (all data)	$R1 = 0.1033$, $wR2 = 0.1743$
Largest diff. peak and hole	0.668 and −0.569 e Å^{-3}

Diffractometer: *Nonius KappaCCD* area detector (ϕ scans and ω scans to fill *asymmetric unit*). **Cell determination:** DirAx (Duisenberg, A.J.M.(1992). J. Appl. Cryst. 25, 92-96.) **Data collection:** Collect (Collect: Data collection software, R. Hooft, Nonius B.V., 1998). **Data reduction and cell refinement**: *Denzo* (Z. Otwinowski & W. Minor, *Methods in Enzymology* (1997) Vol. **276**: *Macromolecular Crystallography*, part A, pp. 307–326; C. W. Carter, Jr. & R. M. Sweet, Eds., Academic Press). **Absorption correction**: Sheldrick, G. M. SADABS - Bruker Nonius area detector scaling and absorption correction - V2.10 **Structure solution**: *SHELXS97* (G. M. Sheldrick, Acta Cryst. (1990) A**46** 467–473). **Structure refinement**: *SHELXL97* (G. M. Sheldrick (1997), University of Göttingen, Germany). **Graphics:** Cameron - A Molecular Graphics Package. (D. M. Watkin, L. Pearce and C. K. Prout, Chemical Crystallography Laboratory, University of Oxford, 1993).

Special details: All hydrogen atoms were placed in idealised positions and refined using a riding model. The tetramethyl ammonium is disordered over the 4-fold axis

Table 2. Atomic coordinates [× 10^4], equivalent isotropic displacement parameters [Å^2 × 10^3] and site occupancy factors. U_{eq} is defined as one third of the trace of the orthogonalized U^{ij} tensor.

Atom	*x*	*y*	*z*	U_{eq}	*S.o.f.*
N2	2500	2500	5554(1)	25(1)	1
C8	2500	2500	4053(1)	33(1)	1
C9A	2989(1)	1426(1)	6000(1)	64(1)	0.38
C9B	2242(1)	1410(1)	6059(1)	64(1)	0.38
Cl1	2500	2500	9405(1)	27(1)	1
N1	4261(1)	1647(1)	1655(1)	22(1)	1
C1	4991(1)	641(1)	3237(1)	28(1)	1
C4	4228(1)	632(1)	2252(1)	24(1)	1
C5	3455(1)	−268(1)	1804(1)	24(1)	1
C7	3475(1)	−398(1)	275(1)	26(1)	1
C3	5035(1)	2296(1)	2262(1)	23(1)	1
C2	5496(1)	1686(1)	3250(1)	28(1)	1
C6	3834(1)	−1351(1)	2427(1)	31(1)	1

2.5·TMABr COMPLEX

Table 1. Crystal data and structure refinement details $C_{28}H_{36}N_4$. $C_4H_{12}N$. Br.

Empirical formula	$C_{32}H_{48}BrN_5$
Formula weight	582.66
Temperature	120(2) K
Wavelength	0.71073 Å
Crystal system	Tetragonal
Space group	*P*4/*n*

Unit cell dimensions	a = 12.1249(5) Å b = 12.1249(5) Å c = 10.3262(6) Å
Volume	1518.09(12) Å^3
Z	2
Density (calculated)	1.275 Mg / m^3
Absorption coefficient	1.383 mm^{-1}
F(000)	620
Crystal	Fragment; Colourless
Crystal size	0.2 × 0.2 × 0.03 mm^3
θ range for data collection	3.90 – 27.48°
Index ranges	$-15 \le h \le 15$, $-15 \le k \le 13$, $-11 \le l \le 13$
Reflections collected	12374
Independent reflections	1746 [R_{int} = 0.0493]
Completeness to θ = 27.48°	99.7 %
Absorption correction	Semi–empirical from equivalents
Max. and min. transmission	0.9597 and 0.7695
Refinement method	Full-matrix least-squares on F^2
Data / restraints / parameters	1746 / 0 / 99
Goodness-of-fit on F^2	1.043
Final R indices [$F^2 > 2\sigma(F^2)$]	$R1$ = 0.0384, $wR2$ = 0.0897
R indices (all data)	$R1$ = 0.0496, $wR2$ = 0.0945
Largest diff. peak and hole	0.735 and –0.734 e Å^{-3}

Diffractometer: *Nonius KappaCCD* area detector (ϕ scans and ω scans to fill *asymmetric unit*). **Cell determination:** DirAx (Duisenberg, A.J.M.(1992). J. Appl. Cryst. 25, 92-96.) **Data collection:** Collect (Collect: Data collection software, R. Hooft, Nonius B.V., 1998). **Data reduction and cell refinement**: *Denzo* (Z. Otwinowski & W. Minor, *Methods in Enzymology* (1997) Vol. **276**: *Macromolecular Crystallography*, part A, pp. 307–326; C. W. Carter, Jr. & R. M. Sweet, Eds., Academic Press). **Absorption correction**: Sheldrick, G. M. SADABS - Bruker Nonius area detector scaling and absorption correction - V2.10 **Structure solution**: *SHELXS97* (G. M. Sheldrick, Acta Cryst. (1990) **A46** 467–473). **Structure refinement**: *SHELXL97* (G. M. Sheldrick (1997), University of Göttingen, Germany). **Graphics:** Cameron - A Molecular Graphics Package. (D. M. Watkin, L. Pearce and C. K. Prout, Chemical Crystallography Laboratory, University of Oxford, 1993).

Special details: All hydrogen atoms were placed in idealised positions and refined using a riding model. The tetramethyl ammonium is disordered over the 4-fold axis.

Table 2. Atomic coordinates [× 10^4], equivalent isotropic displacement parameters [Å^2 × 10^3] and site occupancy factors. U_{eq} is defined as one third of the trace of the orthogonalized U^{ij} tensor.

Atom	*x*	*y*	*z*	U_{eq}	*S.o.f.*
N2	2500	2500	5428(1)	19(1)	1
C8	2500	2500	3978(1)	26(1)	1
C9A	2858(1)	1355(1)	5856(1)	59(1)	0.38
C9B	2027(1)	1500(1)	5937(1)	59(1)	0.38
Br1	2500	2500	9283(1)	21(1)	1
N1	4290(1)	1641(1)	1674(1)	16(1)	1
C1	5006(1)	642(1)	3240(1)	21(1)	1
C4	4251(1)	620(1)	2259(1)	17(1)	1

C5	3474(1)	−291(1)	1825(1)	18(1)	1
C7	3499(1)	−431(1)	344(1)	21(1)	1
C3	5059(1)	2305(1)	2271(1)	17(1)	1
C2	5510(1)	1699(1)	3254(1)	21(1)	1
C6	3866(1)	−1381(1)	2436(1)	25(1)	1

2.5·TEAF COMPLEX

Table 1. Crystal data and structure refinement details.

Empirical formula	$C_{36}H_{56}FN_5$
Formula weight	577.86
Temperature	120(2) K
Wavelength	0.71073 Å
Crystal system	Tetragonal
Space group	*P4/n*
Unit cell dimensions	a = 13.164(3) Å
	b = 13.164(3) Å
	c = 9.484(2) Å
Volume	1643.5(6) Å^3
Z	2
Density (calculated)	1.168 Mg / m^3
Absorption coefficient	0.073 mm^{-1}
F(000)	632
Crystal	Fragment; Colourless
Crystal size	0.2 × 0.2 × 0.04 mm^3
θ range for data collection	3.07 – 27.48°
Index ranges	$-14 \le h \le 16$, $-16 \le k \le 17$, $-12 \le l \le 12$
Reflections collected	10126
Independent reflections	1889 [R_{int} = 0.0943]
Completeness to θ = 27.48°	99.8 %
Absorption correction	Semi-empirical from equivalents
Max. and min. transmission	0.9971 and 0.9856
Refinement method	Full-matrix least-squares on F^2
Data / restraints / parameters	1889 / 0 / 102
Goodness-of-fit on F^2	0.992
Final R indices [$F^2 > 2\sigma(F^2)$]	$R1$ = 0.0639, $wR2$ = 0.1465
R indices (all data)	$R1$ = 0.1446, $wR2$ = 0.1849
Largest diff. peak and hole	0.260 and −0.262 e Å^{-3}

Diffractometer: *Nonius KappaCCD* area detector (ϕ scans and ω scans to fill *asymmetric unit*). **Cell determination:** DirAx (Duisenberg, A.J.M.(1992). J. Appl. Cryst. 25, 92-96.) **Data collection:** Collect (Collect: Data collection software, R. Hooft, Nonius B.V., 1998). **Data reduction and cell refinement**: *Denzo* (Z. Otwinowski & W. Minor, *Methods in Enzymology* (1997) Vol. **276**: *Macromolecular Crystallography*, part A, pp. 307–326; C. W. Carter, Jr. & R. M. Sweet, Eds., Academic Press). **Absorption**

correction: Sheldrick, G. M. SADABS - Bruker Nonius area detector scaling and absorption correction - V2.10 **Structure solution**: *SHELXS97* (G. M. Sheldrick, Acta Cryst. (1990) A**46** 467–473). **Structure refinement**: *SHELXL97* (G. M. Sheldrick (1997), University of Göttingen, Germany). **Graphics:** Cameron - A Molecular Graphics Package. (D. M. Watkin, L. Pearce and C. K. Prout, Chemical Crystallography Laboratory, University of Oxford, 1993).

Special details: All hydrogen atoms were placed in idealised positions and refined using a riding model. The TEA is disordered over 2 confomations.

Table 2. Atomic coordinates [$\times 10^4$], equivalent isotropic displacement parameters [$Å^2 \times 10^3$] and site occupancy factors. U_{eq} is defined as one third of the trace of the orthogonalized U^{ij} tensor.

Atom	*x*	*y*	*z*	U_{eq}	*S.o.f.*
F1	2500	2500	56(3)	28(1)	1
N2A	2500	2500	6041(4)	24(1)	0.50
C8A	4410(2)	2210(2)	6055(3)	44(1)	0.50
C9A	3396(3)	2334(4)	6991(5)	27(1)	0.50
N2B	2500	2500	6041(4)	24(1)	0.50
C8B	4410(2)	2210(2)	6055(3)	44(1)	0.50
C9B	2333(3)	1590(3)	5079(5)	27(1)	0.50
N1	3378(1)	970(1)	1606(2)	26(1)	1
C4	4339(2)	1017(2)	2165(2)	26(1)	1
C3	4434(2)	221(2)	3077(2)	29(1)	1
C1	2861(2)	150(2)	2149(2)	28(1)	1
C2	3509(2)	-323(2)	3062(3)	31(1)	1
C5	5111(2)	1796(2)	1686(3)	31(1)	1
C6	5194(2)	1757(2)	64(3)	42(1)	1
C7	6144(2)	1511(2)	2310(3)	47(1)	1

2.5·TEACl COMPLEX

Table 1. Crystal data and structure refinement details.

Empirical formula	$C_{37}H_{58}Cl_3N_5$	
Formula weight	679.23	
Temperature	120(2) K	
Wavelength	0.71073 Å	
Crystal system	Triclinic	
Space group	*P*–1	
Unit cell dimensions	a = 10.3552(8) Å	α = 95.319(6)°
	b = 10.3566(9) Å	β = 91.844(5)°
	c = 17.4107(10) Å	γ = 97.234(6)°
Volume	1842.5(2) $Å^3$	
Z	2	
Density (calculated)	1.224 Mg / m^3	
Absorption coefficient	0.282 mm^{-1}	
F(000)	732	
Crystal	Slab; Colourless	

Crystal size	$0.3 \times 0.25 \times 0.06$ mm^3
θ range for data collection	3.14 – 27.48°
Index ranges	$-13 \le h \le 13$, $-13 \le k \le 13$, $-22 \le l \le 22$
Reflections collected	25472
Independent reflections	8397 [$R_{int} = 0.0564$]
Completeness to $\theta = 27.48°$	99.2 %
Absorption correction	Semi–empirical from equivalents
Max. and min. transmission	0.9833 and 0.9203
Refinement method	Full-matrix least-squares on F^2
Data / restraints / parameters	8397 / 0 / 419
Goodness-of-fit on F^2	1.009
Final R indices [$F^2 > 2\sigma(F^2)$]	$R1 = 0.0506$, $wR2 = 0.1082$
R indices (all data)	$R1 = 0.1048$, $wR2 = 0.1291$
Extinction coefficient	0.0051(11)
Largest diff. peak and hole	0.431 and –0.459 e Å^{-3}

Diffractometer: *Nonius KappaCCD* area detector (ϕ scans and ω scans to fill *asymmetric unit*). **Cell determination:** DirAx (Duisenberg, A.J.M.(1992). J. Appl. Cryst. 25, 92-96.) **Data collection:** Collect (Collect: Data collection software, R. Hooft, Nonius B.V., 1998). **Data reduction and cell refinement**: *Denzo* (Z. Otwinowski & W. Minor, *Methods in Enzymology* (1997) Vol. **276**: *Macromolecular Crystallography*, part A, pp. 307–326; C. W. Carter, Jr. & R. M. Sweet, Eds., Academic Press). **Absorption correction**: Sheldrick, G. M. SADABS - Bruker Nonius area detector scaling and absorption correction - V2.10 **Structure solution**: *SHELXS97* (G. M. Sheldrick, Acta Cryst. (1990) A**46** 467–473). **Structure refinement**: *SHELXL97* (G. M. Sheldrick (1997), University of Göttingen, Germany). **Graphics:** Cameron - A Molecular Graphics Package. (D. M. Watkin, L. Pearce and C. K. Prout, Chemical Crystallography Laboratory, University of Oxford, 1993).

Special details: All hydrogen atoms were placed in idealised positions and refined using a riding model.

Table 2. Atomic coordinates [$\times 10^4$], equivalent isotropic displacement parameters [Å$^2 \times 10^3$] and site occupancy factors. U_{eq} is defined as one third of the trace of the orthogonalized U^{ij} tensor.

Atom	*x*	*y*	*z*	U_{eq}	*S.o.f.*
C1	12871(2)	7111(2)	860(1)	16(1)	1
C2	13674(2)	6515(2)	372(1)	20(1)	1
C3	13283(2)	5146(2)	318(1)	20(1)	1
C4	12232(2)	4922(2)	771(1)	17(1)	1
C5	11392(2)	3660(2)	898(1)	19(1)	1
C6	11776(2)	2560(2)	334(1)	26(1)	1
C7	9938(2)	3772(2)	732(1)	23(1)	1
C8	11566(2)	3288(2)	1715(1)	17(1)	1
C9	12136(2)	2297(2)	1997(1)	17(1)	1
C10	11931(2)	2340(2)	2801(1)	17(1)	1
C11	11257(2)	3361(2)	3000(1)	16(1)	1
C12	10784(2)	3896(2)	3767(1)	19(1)	1
C13	10876(2)	2890(2)	4354(1)	25(1)	1
C14	9347(2)	4102(2)	3673(1)	24(1)	1
C15	11600(2)	5163(2)	4068(1)	17(1)	1
C16	12557(2)	5442(2)	4648(1)	21(1)	1
C17	12979(2)	6803(2)	4708(1)	21(1)	1
C18	12287(2)	7342(2)	4169(1)	18(1)	1
C19	12295(2)	8749(2)	3987(1)	20(1)	1
C20	13043(2)	9644(2)	4651(1)	30(1)	1

C21	10891(2)	9074(2)	3935(1)	24(1)	1
C22	12969(2)	8992(2)	3242(1)	18(1)	1
C23	14144(2)	9681(2)	3113(1)	20(1)	1
C24	14287(2)	9629(2)	2301(1)	20(1)	1
C25	13194(2)	8904(2)	1949(1)	17(1)	1
C26	12808(2)	8545(2)	1103(1)	17(1)	1
C27	13753(2)	9366(2)	621(1)	23(1)	1
C28	11416(2)	8863(2)	930(1)	20(1)	1
C29	4874(2)	3755(2)	3641(1)	29(1)	1
C30	4559(2)	4749(2)	3096(1)	22(1)	1
C31	5213(2)	6339(2)	2188(1)	21(1)	1
C32	6247(2)	7123(2)	1769(1)	27(1)	1
C33	6453(2)	4415(2)	2272(1)	23(1)	1
C34	5643(2)	3505(2)	1665(1)	33(1)	1
C35	6712(2)	6161(2)	3321(1)	22(1)	1
C36	6215(2)	7215(2)	3839(1)	30(1)	1
N1	11997(2)	6122(2)	1099(1)	16(1)	1
N2	11043(2)	3938(2)	2330(1)	17(1)	1
N3	11454(2)	6330(2)	3780(1)	19(1)	1
N4	12400(2)	8522(2)	2530(1)	18(1)	1
N5	5732(2)	5412(2)	2719(1)	19(1)	1
Cl1	9623(1)	6647(1)	2242(1)	20(1)	1
C37	8933(2)	204(3)	2216(1)	36(1)	1
Cl2	7931(1)	403(1)	3006(1)	48(1)	1
Cl3	8104(1)	345(1)	1336(1)	52(1)	1

2.5·TEABr COMPLEX

Table 1. Crystal data and structure refinement details for $C_{28}H_{36}N_4 . C_8H_{20}N . Br . 3CH_2Cl_2$.

Empirical formula	$C_{39}H_{62}BrCl_6N_5$	
Formula weight	893.55	
Temperature	120(2) K	
Wavelength	0.71073 Å	
Crystal system	Monoclinic	
Space group	*Cc*	
Unit cell dimensions	a = 23.867(5) Å	
	b = 13.603(3) Å	β = 119.68(3)°
	c = 15.661(3) Å	
Volume	4417.5(16) Å^3	
Z	4	
Density (calculated)	1.344 Mg / m^3	
Absorption coefficient	1.327 mm^{-1}	
F(000)	1872	
Crystal	Slab; Colourless	
Crystal size	0.2 × 0.2 × 0.05 mm^3	
θ range for data collection	2.99 – 27.48°	

Index ranges	$-30 \le h \le 28, -17 \le k \le 17, -18 \le l \le 20$
Reflections collected	25899
Independent reflections	8196 [$R_{int} = 0.0502$]
Completeness to $\theta = 27.48°$	99.7 %
Absorption correction	Semi–empirical from equivalents
Max. and min. transmission	0.9366 and 0.7772
Refinement method	Full-matrix least-squares on F^2
Data / restraints / parameters	8196 / 2 / 473
Goodness-of-fit on F^2	1.028
Final R indices [$F^2 > 2\sigma(F^2)$]	$R1 = 0.0444$, $wR2 = 0.1062$
R indices (all data)	$R1 = 0.0631$, $wR2 = 0.1157$
Absolute structure parameter	0.870(7)
Largest diff. peak and hole	0.849 and –0.502 e Å^{-3}

Diffractometer: *Nonius KappaCCD* area detector (ϕ scans and ω scans to fill *asymmetric unit*). **Cell determination:** DirAx (Duisenberg, A.J.M.(1992). J. Appl. Cryst. 25, 92-96.) **Data collection:** Collect (Collect: Data collection software, R. Hooft, Nonius B.V., 1998). **Data reduction and cell refinement**: *Denzo* (Z. Otwinowski & W. Minor, *Methods in Enzymology* (1997) Vol. **276**: *Macromolecular Crystallography*, part A, pp. 307–326; C. W. Carter, Jr. & R. M. Sweet, Eds., Academic Press). **Absorption correction**: Sheldrick, G. M. SADABS - Bruker Nonius area detector scaling and absorption correction - V2.10 **Structure solution**: *SHELXS97* (G. M. Sheldrick, Acta Cryst. (1990) A**46** 467–473). **Structure refinement**: *SHELXL97* (G. M. Sheldrick (1997), University of Göttingen, Germany). **Graphics:** Cameron - A Molecular Graphics Package. (D. M. Watkin, L. Pearce and C. K. Prout, Chemical Crystallography Laboratory, University of Oxford, 1993).

Special details: All hydrogen atoms were placed in idealised positions and refined using a riding model.

Table 2. Atomic coordinates [× 10^4], equivalent isotropic displacement parameters [Å^2 × 10^3] and site occupancy factors. U_{eq} is defined as one third of the trace of the orthogonalized U^{ij} tensor.

Atom	*x*	*y*	*z*	U_{eq}	*S.o.f.*
C1	2147(2)	3406(3)	3509(3)	12(1)	1
C2	2512(2)	4095(3)	4219(3)	14(1)	1
C3	2717(2)	4819(3)	3791(3)	16(1)	1
C4	2477(2)	4576(3)	2817(3)	14(1)	1
C5	2511(2)	5112(3)	1993(3)	17(1)	1
C6	2973(2)	4605(2)	1727(3)	15(1)	1
C7	3565(2)	4875(3)	1872(3)	18(1)	1
C8	3774(2)	4160(3)	1428(3)	17(1)	1
C9	3300(2)	3448(3)	1021(3)	13(1)	1
C10	3256(2)	2519(2)	454(3)	14(1)	1
C11	3342(2)	1611(3)	1066(3)	13(1)	1
C12	3841(2)	938(3)	1470(3)	17(1)	1
C13	3672(2)	211(3)	1957(3)	19(1)	1
C14	3077(2)	437(3)	1833(3)	14(1)	1
C15	2647(2)	–104(3)	2135(3)	17(1)	1
C16	2586(2)	437(3)	2934(3)	15(1)	1
C17	2817(2)	225(3)	3907(3)	16(1)	1
C18	2577(2)	935(3)	4304(3)	15(1)	1
C19	2193(2)	1582(3)	3566(3)	14(1)	1
C20	1823(2)	2481(2)	3562(3)	12(1)	1
C21	2759(2)	6160(3)	2336(3)	27(1)	1
C22	1828(2)	5177(3)	1086(3)	21(1)	1

C23	2597(2)	2477(3)	−496(3)	17(1)	1
C24	3790(2)	2545(3)	182(3)	18(1)	1
C25	1971(2)	−262(3)	1239(3)	24(1)	1
C26	2951(2)	−1115(3)	2535(3)	26(1)	1
C27	1131(2)	2436(3)	2687(3)	17(1)	1
C28	1786(2)	2492(3)	4513(3)	18(1)	1
C29	4841(2)	1724(3)	5158(3)	22(1)	1
C30	4555(2)	712(3)	4788(4)	34(1)	1
C31	4223(2)	2555(3)	3516(3)	18(1)	1
C32	4783(2)	2567(3)	3328(3)	24(1)	1
C33	4797(2)	3512(3)	5097(3)	24(1)	1
C34	4451(2)	4466(3)	4673(4)	30(1)	1
C35	3780(2)	2557(3)	4635(3)	21(1)	1
C36	3864(2)	2577(3)	5661(4)	31(1)	1
C43	1148(2)	5711(3)	3406(4)	35(1)	1
C44	1085(2)	512(3)	8448(4)	33(1)	1
C67	111(4)	2988(6)	4436(7)	87(3)	1
Br1	1427(1)	2434(1)	469(1)	23(1)	1
Cl1	727(1)	618(1)	7171(1)	69(1)	1
Cl2	585(1)	−163(1)	8758(1)	41(1)	1
Cl3	475(1)	2107(1)	5301(1)	57(1)	1
Cl4	−471(1)	2545(2)	3286(1)	100(1)	1
Cl5	516(1)	4950(1)	3243(1)	49(1)	1
Cl6	920(1)	6537(1)	2420(1)	56(1)	1
N1	2132(2)	3720(2)	2653(2)	14(1)	1
N2	2206(1)	1265(2)	2728(2)	15(1)	1
N3	2882(1)	1295(2)	1286(2)	13(1)	1
N4	2814(1)	3730(2)	1202(2)	13(1)	1
N5	4409(2)	2588(2)	4602(2)	17(1)	1

2.5·BMIMCl COMPLEX

Table 1. Crystal data and structure refinement details.

	$C_{28}H_{36}N_4 \cdot C_8H_{15}N_2^+ \cdot Cl^- \cdot CH_2Cl_2 \cdot CH_3OH$	
Empirical formula	$C_{38}H_{57}Cl_3N_6O$	
Formula weight	720.25	
Temperature	120(2) K	
Wavelength	0.71073 Å	
Crystal system	Triclinic	
Space group	*P*−1	
Unit cell dimensions	$a = 10.4222(14)$ Å	$\alpha = 74.664(11)°$
	$b = 10.7682(11)$ Å	$\beta = 81.603(13)°$
	$c = 17.993(2)$ Å	$\gamma = 84.951(10)°$
Volume	1923.9(4) $Å^3$	
Z	2	
Density (calculated)	1.243 Mg / m^3	

Absorption coefficient	0.276 mm^{-1}
F(000)	772
Crystal	Prism; Pale Red
Crystal size	0.2 × 0.2 × 0.2 mm^3
θ range for data collection	3.00 – 27.67°
Index ranges	$-13 \le h \le 13$, $-14 \le k \le 12$, $-23 \le l \le 23$
Reflections collected	41654
Independent reflections	8681 [R_{int} = 0.0566]
Completeness to θ = 25.00°	99.1 %
Absorption correction	Semi–empirical from equivalents
Max. and min. transmission	0.9468 and 0.9468
Refinement method	Full-matrix least-squares on F^2
Data / restraints / parameters	8681 / 2 / 470
Goodness-of-fit on F^2	1.026
Final *R* indices [$F^2 > 2\sigma(F^2)$]	*R1* = 0.0554, *wR2* = 0.1387
R indices (all data)	*R1* = 0.0729, *wR2* = 0.1495
Largest diff. peak and hole	1.223 and –0.661 e $Å^{-3}$

Diffractometer: *Nonius KappaCCD* area detector (ϕ scans and ω scans to fill *asymmetric unit*). **Cell determination:** DirAx (Duisenberg, A.J.M.(1992). J. Appl. Cryst. 25, 92-96.) **Data collection:** Collect (Collect: Data collection software, R. Hooft, Nonius B.V., 1998). **Data reduction and cell refinement**: *Denzo* (Z. Otwinowski & W. Minor, *Methods in Enzymology* (1997) Vol. **276**: *Macromolecular Crystallography*, part A, pp. 307–326; C. W. Carter, Jr. & R. M. Sweet, Eds., Academic Press). **Absorption correction**: Sheldrick, G. M. SADABS - Bruker Nonius area detector scaling and absorption correction - V2.10 **Structure solution**: *SHELXS97* (G. M. Sheldrick, Acta Cryst. (1990) A**46** 467–473). **Structure refinement**: *SHELXL97* (G. M. Sheldrick (1997), University of Göttingen, Germany). **Graphics:** Cameron - A Molecular Graphics Package. (D. M. Watkin, L. Pearce and C. K. Prout, Chemical Crystallography Laboratory, University of Oxford, 1993).

Special details: All hydrogen atoms were placed in idealised positions and refined using a riding model, except thos on N which were fully refined. The solvent methanol is disordered over 2 sites (80:20)

Table 2. Atomic coordinates [× 10^4], equivalent isotropic displacement parameters [$Å^2$ × 10^3] and site occupancy factors. U_{eq} is defined as one third of the trace of the orthogonalized U^{ij} tensor.

Atom	*x*	*y*	*z*	U_{eq}	*S.o.f.*
N1	1223(2)	–576(2)	3563(1)	19(1)	1
N2	2540(2)	–2220(2)	2239(1)	17(1)	1
N3	2775(2)	593(2)	840(1)	18(1)	1
N4	1425(2)	2235(2)	2157(1)	18(1)	1
C1	227(2)	303(2)	3694(1)	20(1)	1
C2	–879(2)	–370(2)	3945(1)	23(1)	1
C3	–538(2)	–1686(2)	3971(1)	22(1)	1
C4	767(2)	–1797(2)	3732(1)	19(1)	1
C5	1649(2)	–2971(2)	3662(1)	19(1)	1
C6	2971(2)	–2893(2)	3934(1)	24(1)	1
C7	1019(2)	–4181(2)	4191(1)	24(1)	1
C8	1854(2)	–3094(2)	2833(1)	18(1)	1
C9	1424(2)	–3976(2)	2510(1)	20(1)	1
C10	1857(2)	–3621(2)	1698(1)	20(1)	1
C11	2551(2)	–2533(2)	1543(1)	17(1)	1
C12	3249(2)	–1748(2)	787(1)	18(1)	1

C13	3211(2)	-2454(2)	154(1)	24(1)	1
C14	4676(2)	-1639(2)	882(1)	21(1)	1
C15	2579(2)	-420(2)	537(1)	18(1)	1
C16	1733(2)	41(2)	-1(1)	22(1)	1
C17	1409(2)	1359(2)	-26(1)	23(1)	1
C18	2063(2)	1688(2)	498(1)	18(1)	1
C19	2082(2)	2963(2)	703(1)	19(1)	1
C20	3467(2)	3235(2)	796(1)	24(1)	1
C21	1619(2)	4038(2)	33(1)	24(1)	1
C22	1172(2)	2983(2)	1439(1)	18(1)	1
C23	22(2)	3668(2)	1554(1)	21(1)	1
C24	-428(2)	3326(2)	2362(1)	21(1)	1
C25	447(2)	2434(2)	2726(1)	19(1)	1
C26	443(2)	1724(2)	3574(1)	20(1)	1
C27	1728(2)	1896(2)	3851(1)	25(1)	1
C28	-677(2)	2303(2)	4058(1)	27(1)	1
N5	7883(2)	433(2)	1987(1)	22(1)	1
N6	8182(2)	-1590(2)	2020(1)	21(1)	1
C29	9206(2)	169(2)	1893(1)	23(1)	1
C30	9391(2)	-1099(2)	1914(1)	24(1)	1
C31	7287(2)	-645(2)	2063(1)	22(1)	1
C32	7215(2)	1677(2)	2016(2)	32(1)	1
C33	7908(2)	-2945(2)	2112(1)	26(1)	1
C34	7748(2)	-3709(2)	2962(1)	28(1)	1
C35	6614(2)	-3239(3)	3468(1)	32(1)	1
C36	6477(3)	-4077(3)	4298(2)	43(1)	1
Cl1	4033(1)	265(1)	2462(1)	21(1)	1
Cl2	5695(1)	4682(1)	1763(1)	44(1)	1
Cl3	4914(1)	3675(1)	3421(1)	64(1)	1
C37	4419(3)	4103(4)	2506(2)	59(1)	1
O1A	4150(2)	-1008(2)	5015(2)	39(1)	0.80
C38A	5478(3)	-1157(4)	4706(2)	37(1)	0.80
O1B	5333(9)	-422(10)	4351(7)	39(1)	0.20
C38B	4457(12)	228(13)	4703(8)	37(1)	0.20

2.5·BMIMBr COMPLEX

Table 1. Crystal data and structure refinement details.

$C_{28}H_{36}N_4 \cdot C_8H_{15}N_2^+ \cdot Br^- \cdot CH_2Cl_2 \cdot CH_3OH$		
Empirical formula	$C_{38}H_{57}BrCl_2N_6O$	
Formula weight	764.71	
Temperature	120(2) K	
Wavelength	0.71069 Å	
Crystal system	Triclinic	
Space group	*P*-1	
Unit cell dimensions	a = 10.5710(14) Å	α = 74.528(11)°
	b = 10.7800(11) Å	β = 81.155(13)°

	c = 18.082(2) Å γ = 84.715(10)°
Volume	1959.4(4) Å^3
Z	2
Density (calculated)	1.296 Mg / m^3
Absorption coefficient	1.223 mm^{-1}
F(000)	808
Crystal	Rod; Colourless
Crystal size	0.18 × 0.05 × 0.05 mm^3
θ range for data collection	3.17 – 25.30°
Index ranges	$-12 \le h \le 12$, $-12 \le k \le 12$, $-21 \le l \le 21$
Reflections collected	21008
Independent reflections	6576 [R_{int} = 0.1857]
Completeness to θ = 25.00°	94.8 %
Absorption correction	Semi–empirical from equivalents
Max. and min. transmission	0.9414 and 0.8099
Refinement method	Full-matrix least-squares on F^2
Data / restraints / parameters	6576 / 2 / 454
Goodness-of-fit on F^2	1.010
Final R indices [$F^2 > 2\sigma(F^2)$]	$R1$ = 0.1103, $wR2$ = 0.2893
R indices (all data)	$R1$ = 0.2712, $wR2$ = 0.3713
Largest diff. peak and hole	0.729 and –1.044 e Å^{-3}

Diffractometer: *Nonius KappaCCD* area detector (ϕ scans and ω scans to fill *asymmetric unit*). **Cell determination:** DirAx (Duisenberg, A.J.M.(1992). J. Appl. Cryst. 25, 92-96.) **Data collection:** Collect (Collect: Data collection software, R. Hooft, Nonius B.V., 1998). **Data reduction and cell refinement**: *Denzo* (Z. Otwinowski & W. Minor, *Methods in Enzymology* (1997) Vol. **276**: *Macromolecular Crystallography*, part A, pp. 307–326; C. W. Carter, Jr. & R. M. Sweet, Eds., Academic Press). **Absorption correction**: Sheldrick, G. M. SADABS - Bruker Nonius area detector scaling and absorption correction - V2.10 **Structure solution**: *SHELXS97* (G. M. Sheldrick, Acta Cryst. (1990) A**46** 467–473). **Structure refinement**: *SHELXL97* (G. M. Sheldrick (1997), University of Göttingen, Germany). **Graphics:** Cameron - A Molecular Graphics Package. (D. M. Watkin, L. Pearce and C. K. Prout, Chemical Crystallography Laboratory, University of Oxford, 1993).

Special details: All hydrogen atoms were placed in idealised positions and refined using a riding model.
Isostructural with 04SOT0964

Table 2. Atomic coordinates [× 10^4], equivalent isotropic displacement parameters [Å^2 × 10^3] and site occupancy factors. U_{eq} is defined as one third of the trace of the orthogonalized U^{ij} tensor.

Atom	*x*	*y*	*z*	U_{eq}	*S.o.f.*
N1	1235(8)	–571(7)	3566(5)	24(2)	1
N2	2535(7)	–2207(7)	2236(4)	18(2)	1
N3	2772(8)	609(7)	843(4)	19(2)	1
N4	1411(8)	2221(7)	2157(5)	24(2)	1
C1	234(10)	296(10)	3688(6)	25(3)	1
C2	–848(11)	–352(10)	3930(7)	35(3)	1
C3	–505(10)	–1673(10)	3955(6)	28(3)	1
C4	754(10)	–1789(9)	3731(6)	25(3)	1
C5	1669(10)	–2983(9)	3662(6)	25(3)	1
C6	2954(10)	–2894(10)	3932(6)	29(3)	1
C7	1017(11)	–4172(9)	4200(6)	28(3)	1

C8	1855(9)	−3099(9)	2845(6)	21(2)	1
C9	1441(10)	−3960(9)	2522(6)	30(3)	1
C10	1883(9)	−3621(9)	1709(6)	25(3)	1
C11	2594(10)	−2515(9)	1553(6)	26(3)	1
C12	3264(10)	−1730(9)	797(6)	25(3)	1
C13	3247(11)	−2437(10)	154(6)	33(3)	1
C14	4680(9)	−1628(9)	888(6)	27(3)	1
C15	2571(10)	−400(9)	541(6)	23(3)	1
C16	1731(11)	64(10)	22(6)	31(3)	1
C17	1386(10)	1353(10)	3(6)	26(3)	1
C18	2049(10)	1681(9)	493(6)	26(3)	1
C19	2084(10)	2958(9)	704(6)	27(3)	1
C20	3446(10)	3241(9)	777(6)	28(3)	1
C21	1598(11)	4035(9)	40(6)	32(3)	1
C22	1162(10)	2995(9)	1446(6)	26(3)	1
C23	47(10)	3678(9)	1580(6)	24(3)	1
C24	−370(10)	3358(9)	2362(6)	26(3)	1
C25	437(10)	2450(9)	2720(6)	24(3)	1
C26	447(10)	1729(10)	3568(6)	28(3)	1
C27	1682(11)	1889(10)	3842(6)	34(3)	1
C28	−671(11)	2326(10)	4037(6)	38(3)	1
N5	7953(8)	392(8)	1955(5)	30(2)	1
N6	8196(9)	−1574(8)	2008(5)	28(2)	1
C29	9251(11)	131(11)	1874(6)	34(3)	1
C30	9404(11)	−1124(12)	1915(6)	37(3)	1
C31	7361(10)	−629(11)	2049(6)	31(3)	1
C32	7321(11)	1680(11)	1972(8)	50(4)	1
C33	7908(11)	−2944(10)	2118(6)	36(3)	1
C34	7737(11)	−3687(10)	2950(7)	37(3)	1
C35	6596(12)	−3212(11)	3463(7)	48(3)	1
C36	6456(13)	−4039(13)	4295(8)	59(4)	1
Br1	4118(2)	305(1)	2482(1)	68(1)	1
Cl2	5694(4)	4664(3)	1744(2)	67(1)	1
Cl3	4903(5)	3709(5)	3401(3)	100(2)	1
C37	4430(15)	4097(15)	2481(9)	79(5)	1
O1A	4127(13)	−1018(11)	5033(9)	56(4)	0.80
C38A	5389(16)	−1080(20)	4675(12)	88(8)	0.80
O1B	5290(50)	−160(50)	4380(30)	56(4)	0.20
C38B	4180(80)	−470(80)	4900(60)	88(8)	0.20

2.5·EMIMCl COMPLEX

Table 1. Crystal data and structure refinement details.

Empirical formula	$C_{34}H_{47}ClN_6$
Moiety formula	$C_{28}H_{36}N_4 \,.\, C_6H_{11}N_2^+ \,.\, Cl^-$
Formula weight	575.23
Temperature	120(2) K
Wavelength	0.71073 Å

Crystal system	Monoclinic
Space group	$P2_1/c$
Unit cell dimensions	a = 10.587(7) Å
	b = 16.49(4) Å β = 105.87(9)°
	c = 18.55(2) Å
Volume	3116(8) Å^3
Z	4
Density (calculated)	1.226 Mg / m^3
Absorption coefficient	0.156 mm^{-1}
F(000)	1240
Crystal	Needle; Colourless
Crystal size	0.2 × 0.03 × 0.02 mm^3
θ range for data collection	3.18 – 25.03°
Index ranges	$-11 \le h \le 12$, $-19 \le k \le 19$, $-22 \le l \le 22$
Reflections collected	25395
Independent reflections	5482 [R_{int} = 0.1335]
Completeness to θ = 25.03°	99.4 %
Absorption correction	Semi–empirical from equivalents
Max. and min. transmission	0.9969 and 0.9694
Refinement method	Full-matrix least-squares on F^2
Data / restraints / parameters	5482 / 0 / 381
Goodness-of-fit on F^2	1.012
Final R indices [$F^2 > 2\sigma(F^2)$]	$R1$ = 0.0747, $wR2$ = 0.1320
R indices (all data)	$R1$ = 0.1494, $wR2$ = 0.1561
Extinction coefficient	0.0053(7)
Largest diff. peak and hole	0.244 and –0.245 e Å^{-3}

Diffractometer: *Nonius KappaCCD* area detector (ϕ scans and ω scans to fill *asymmetric unit*). **Cell determination:** DirAx (Duisenberg, A.J.M.(1992). J. Appl. Cryst. 25, 92-96.) **Data collection:** Collect (Collect: Data collection software, R. Hooft, Nonius B.V., 1998). **Data reduction and cell refinement**: *Denzo* (Z. Otwinowski & W. Minor, *Methods in Enzymology* (1997) Vol. **276**: *Macromolecular Crystallography*, part A, pp. 307–326; C. W. Carter, Jr. & R. M. Sweet, Eds., Academic Press). **Absorption correction**: Sheldrick, G. M. SADABS - Bruker Nonius area detector scaling and absorption correction - V2.10 **Structure solution**: *SHELXS97* (G. M. Sheldrick, Acta Cryst. (1990) A**46** 467–473). **Structure refinement**: *SHELXL97* (G. M. Sheldrick (1997), University of Göttingen, Germany). **Graphics:** Cameron - A Molecular Graphics Package. (D. M. Watkin, L. Pearce and C. K. Prout, Chemical Crystallography Laboratory, University of Oxford, 1993).

Special details: All hydrogen atoms were placed in idealised positions and refined using a riding model.

Table 2. Atomic coordinates [× 10^4], equivalent isotropic displacement parameters [Å^2 × 10^3] and site occupancy factors. U_{eq} is defined as one third of the trace of the orthogonalized U^{ij} tensor.

Atom	*x*	*y*	*z*	U_{eq}	*S.o.f.*
Cl1	6487(1)	7631(1)	2126(1)	27(1)	1
C1	4673(3)	5361(2)	2249(2)	24(1)	1
C2	4311(4)	4809(2)	2702(2)	28(1)	1
C3	4689(4)	5105(2)	3443(2)	29(1)	1
C4	5283(3)	5851(2)	3441(2)	25(1)	1
C5	5898(4)	6422(2)	4078(2)	28(1)	1

C6	5592(4)	6125(3)	4797(2)	37(1)	1
C7	5305(4)	7280(2)	3896(2)	32(1)	1
C8	7373(4)	6452(2)	4222(2)	24(1)	1
C9	8370(4)	6044(2)	4721(2)	30(1)	1
C10	9569(4)	6322(2)	4623(2)	29(1)	1
C11	9304(4)	6895(2)	4072(2)	26(1)	1
C12	10186(3)	7395(2)	3726(2)	25(1)	1
C13	9591(4)	8248(2)	3520(2)	28(1)	1
C14	11526(4)	7495(2)	4301(2)	30(1)	1
C15	10399(4)	6976(2)	3037(2)	24(1)	1
C16	11479(4)	6608(2)	2920(2)	26(1)	1
C17	11127(4)	6277(2)	2191(2)	26(1)	1
C18	9827(4)	6433(2)	1862(2)	22(1)	1
C19	8945(3)	6217(2)	1095(2)	24(1)	1
C20	9782(4)	5807(2)	644(2)	30(1)	1
C21	8325(4)	6991(2)	673(2)	30(1)	1
C22	7871(3)	5628(2)	1146(2)	23(1)	1
C23	7721(4)	4813(2)	990(2)	26(1)	1
C24	6486(4)	4573(2)	1077(2)	26(1)	1
C25	5893(4)	5238(2)	1275(2)	24(1)	1
C26	4565(4)	5344(2)	1415(2)	25(1)	1
C27	3691(4)	4623(2)	1065(2)	31(1)	1
C28	3916(4)	6127(2)	1029(2)	31(1)	1
N1	5267(3)	5999(2)	2708(2)	23(1)	1
N2	7962(3)	6962(2)	3828(2)	26(1)	1
N3	9389(3)	6870(2)	2386(2)	23(1)	1
N4	6750(3)	5877(2)	1324(2)	24(1)	1
C29	−1425(4)	9315(3)	1798(3)	36(1)	1
C30	722(4)	8649(2)	1897(2)	31(1)	1
C31	1972(4)	9717(2)	1961(2)	31(1)	1
C32	752(4)	9976(2)	1899(2)	30(1)	1
C33	3056(4)	8354(2)	1953(3)	35(1)	1
C34	3213(4)	8320(3)	1171(3)	40(1)	1
N5	−24(3)	9303(2)	1858(2)	28(1)	1
N6	1947(3)	8885(2)	1965(2)	28(1)	1

2.5·EMIMBr COMPLEX

Table 1. Crystal data and structure refinement details.

	$C_{28}H_{36}N_4 \cdot C_7H_{11}N_2^+ \cdot Br^-$	
Empirical formula	$C_{34}H_{47}BrN_6$	
Formula weight	619.69	
Temperature	120(2) K	
Wavelength	0.71073 Å	
Crystal system	Monoclinic	
Space group	$P2_1/c$	
Unit cell dimensions	a = 21.238(3) Å	
	b = 17.043(4) Å	β = 108.477(14)°

	c = 18.287(4) Å
Volume	6278(2) Å^3
Z	8 (2 Molecules in asymmetric unit)
Density (calculated)	1.311 Mg / m^3
Absorption coefficient	1.343 mm^{-1}
F(000)	2624
Crystal	Block; Colourless
Crystal size	0.2 × 0.05 × 0.04 mm^3
θ range for data collection	3.03 – 25.03°
Index ranges	$-25 \le h \le 23$, $-20 \le k \le 20$, $-21 \le l \le 21$
Reflections collected	54773
Independent reflections	11067 [R_{int} = 0.1162]
Completeness to θ = 25.03°	99.7 %
Absorption correction	Semi–empirical from equivalents
Max. and min. transmission	0.9482 and 0.7750
Refinement method	Full-matrix least-squares on F^2
Data / restraints / parameters	11067 / 60 / 749
Goodness-of-fit on F^2	1.052
Final R indices [$F^2 > 2\sigma(F^2)$]	$R1$ = 0.0885, $wR2$ = 0.2409
R indices (all data)	$R1$ = 0.1574, $wR2$ = 0.2853
Largest diff. peak and hole	1.382 and −1.252 e Å–3

Diffractometer: *Nonius KappaCCD* area detector (ϕ scans and ω scans to fill *asymmetric unit*). **Cell determination:** DirAx (Duisenberg, A.J.M.(1992). J. Appl. Cryst. 25, 92-96.) **Data collection:** Collect (Collect: Data collection software, R. Hooft, Nonius B.V., 1998). **Data reduction and cell refinement**: *Denzo* (Z. Otwinowski & W. Minor, *Methods in Enzymology* (1997) Vol. **276**: *Macromolecular Crystallography*, part A, pp. 307–326; C. W. Carter, Jr. & R. M. Sweet, Eds., Academic Press). **Absorption correction**: Sheldrick, G. M. SADABS - Bruker Nonius area detector scaling and absorption correction - V2.10 **Structure solution**: *SHELXS97* (G. M. Sheldrick, Acta Cryst. (1990) A**46** 467–473). **Structure refinement**: *SHELXL97* (G. M. Sheldrick (1997), University of Göttingen, Germany). **Graphics:** Cameron - A Molecular Graphics Package. (D. M. Watkin, L. Pearce and C. K. Prout, Chemical Crystallography Laboratory, University of Oxford, 1993).

Special details: All hydrogen atoms were placed in idealised positions and refined using a riding model. One of ethylmethylimidazolium ions is disordered over 2 positions 63/37.

Table 2. Atomic coordinates [× 10^4], equivalent isotropic displacement parameters [Å^2 × 10^3] and site occupancy factors. U_{eq} is defined as one third of the trace of the orthogonalized U^{ij} tensor.

Atom	*x*	*y*	*z*	U_{eq}	*S.o.f.*
N1	3471(2)	6910(3)	1154(2)	12(1)	1
N2	2768(2)	6884(2)	2594(2)	10(1)	1
N3	4075(2)	5856(2)	3730(2)	11(1)	1
N4	4786(2)	5883(2)	2321(2)	13(1)	1
C1	3733(2)	6382(3)	762(3)	13(1)	1
C2	3207(2)	6009(3)	252(3)	17(1)	1
C3	2613(2)	6322(3)	331(3)	14(1)	1
C4	2788(2)	6880(3)	883(3)	13(1)	1
C5	2364(2)	7412(3)	1228(3)	12(1)	1
C6	2703(2)	8213(3)	1440(3)	14(1)	1
C7	1687(2)	7537(3)	606(3)	18(1)	1
C8	2254(2)	7026(3)	1907(3)	12(1)	1

C9	1688(2)	6743(3)	2030(3)	17(1)	1
C10	1862(2)	6423(3)	2775(3)	17(1)	1
C11	2526(2)	6510(3)	3120(3)	11(1)	1
C12	2981(2)	6265(3)	3905(3)	9(1)	1
C13	3341(2)	6983(3)	4374(3)	15(1)	1
C14	2549(2)	5894(3)	4349(3)	17(1)	1
C15	3481(2)	5658(3)	3844(3)	11(1)	1
C16	3487(2)	4860(3)	3931(3)	16(1)	1
C17	4097(2)	4565(3)	3864(3)	15(1)	1
C18	4454(2)	5199(3)	3743(3)	13(1)	1
C19	5135(2)	5231(3)	3640(3)	16(1)	1
C20	5513(2)	5967(3)	4054(3)	16(1)	1
C21	5528(3)	4501(3)	4015(3)	23(1)	1
C22	5071(2)	5252(3)	2797(3)	15(1)	1
C23	5243(2)	4704(3)	2339(3)	17(1)	1
C24	5052(2)	5010(3)	1573(3)	21(1)	1
C25	4773(2)	5728(3)	1572(3)	16(1)	1
C26	4484(2)	6311(3)	929(3)	16(1)	1
C27	4614(3)	6008(4)	199(3)	24(2)	1
C28	4819(2)	7112(3)	1130(3)	19(1)	1
N5	2480(2)	9151(2)	3199(2)	17(1)	1
N6	1455(2)	8861(2)	3043(2)	15(1)	1
C29	3182(2)	9086(3)	3262(3)	22(1)	1
C30	2166(2)	9843(3)	3263(3)	20(1)	1
C31	1522(2)	9667(3)	3166(3)	19(1)	1
C32	2042(2)	8571(3)	3072(3)	18(1)	1
C33	840(2)	8420(3)	2980(3)	22(1)	1
C34	723(3)	8364(4)	3712(3)	30(2)	1
N7	980(2)	4110(3)	6432(2)	14(1)	1
N8	222(2)	3904(2)	7786(2)	11(1)	1
N9	1658(2)	3131(3)	9031(2)	17(1)	1
N10	2403(2)	3331(3)	7636(2)	15(1)	1
C35	1526(2)	4399(3)	6262(3)	18(1)	1
C36	1399(3)	5176(3)	6069(3)	22(1)	1
C37	758(3)	5359(3)	6122(3)	21(1)	1
C38	510(2)	4687(3)	6345(3)	14(1)	1
C39	−153(2)	4537(3)	6454(3)	15(1)	1
C40	−635(3)	5208(4)	6080(3)	27(2)	1
C41	−447(2)	3753(3)	6051(3)	19(1)	1
C42	−101(2)	4496(3)	7287(3)	17(1)	1
C43	−319(2)	5018(3)	7739(3)	19(1)	1
C44	−123(2)	4724(3)	8505(3)	20(1)	1
C45	213(2)	4034(3)	8519(3)	15(1)	1
C46	546(2)	3488(3)	9189(3)	17(1)	1
C47	331(3)	3738(4)	9882(3)	33(2)	1
C48	320(2)	2642(3)	8985(3)	22(1)	1
C49	1296(2)	3560(3)	9406(3)	20(1)	1
C50	1735(3)	4002(3)	9942(3)	21(1)	1
C51	2383(2)	3842(4)	9903(3)	22(1)	1
C52	2326(2)	3315(3)	9343(3)	16(1)	1
C53	2855(2)	2921(3)	9042(3)	24(1)	1
C54	2678(3)	2053(3)	8873(4)	33(2)	1
C55	3522(3)	2988(4)	9688(4)	36(2)	1
C56	2897(2)	3337(3)	8340(3)	19(1)	1
C57	3395(2)	3790(3)	8236(3)	20(1)	1

C58	3197(2)	4062(3)	7459(3)	21(1)	1
C59	2575(2)	3772(3)	7096(3)	18(1)	1
C60	2118(2)	3879(3)	6277(3)	17(1)	1
C61	1876(3)	3087(4)	5898(3)	25(2)	1
C62	2508(3)	4300(4)	5812(3)	29(2)	1
N11A	2399(3)	540(4)	6887(7)	14(1)	0.37
N12A	3292(3)	1227(4)	7177(6)	14(1)	0.37
C63A	1728(4)	298(8)	6845(9)	24(1)	0.37
C64A	2898(4)	42(5)	6846(10)	24(1)	0.37
C65A	3450(4)	488(5)	6951(9)	24(1)	0.37
C66A	2662(3)	1237(5)	7131(8)	24(1)	0.37
C67A	3784(5)	1858(5)	7419(7)	24(1)	0.37
C68A	3722(7)	2544(6)	7013(8)	24(1)	0.37
N11B	2501(2)	593(3)	6998(4)	14(1)	0.63
N12B	3429(2)	1071(3)	6958(4)	14(1)	0.63
C63B	1832(3)	533(5)	7059(5)	24(1)	0.63
C64B	2861(3)	−24(4)	6854(6)	24(1)	0.63
C65B	3461(3)	263(4)	6869(6)	24(1)	0.63
C66B	2856(3)	1245(4)	7051(5)	24(1)	0.63
C67B	3992(3)	1583(4)	6972(5)	24(1)	0.63
C68B	3889(4)	2367(4)	6861(6)	24(1)	0.63
Br1	4330(1)	7606(1)	2972(1)	37(1)	1
Br2	982(1)	2287(1)	7276(1)	46(1)	1

2.5·BMIMF COMPLEX

Table 1. Crystal data and structure refinement details.

Empirical formula	$C_{37}H_{53}Cl_2FN_6$
Formula weight	671.75
Temperature	120(2) K
Wavelength	0.71073 Å
Crystal system	Monoclinic
Space group	$P2_1/n$
Unit cell dimensions	a = 11.7074(5) Å
	b = 20.4168(9) Å β = 101.144(2)°
	c = 15.4801(5) Å
Volume	3630.4(3) Å^3
Z	4
Density (calculated)	1.229 Mg / m^3
Absorption coefficient	0.219 mm^{-1}
F(000)	1440
Crystal	Rod; Colourless
Crystal size	0.2 × 0.06 × 0.04 mm^3
θ range for data collection	3.08 – 25.03°
Index ranges	$-13 \le h \le 13$, $-24 \le k \le 22$, $-18 \le l \le 18$
Reflections collected	31232

Independent reflections	6381 [R_{int} = 0.1402]
Completeness to θ = 25.03°	99.6 %
Absorption correction	Semi–empirical from equivalents
Max. and min. transmission	0.9913 and 0.9476
Refinement method	Full-matrix least-squares on F^2
Data / restraints / parameters	6381 / 0 / 425
Goodness-of-fit on F^2	1.162
Final R indices [$F^2 > 2\sigma(F^2)$]	$R1$ = 0.1065, $wR2$ = 0.1688
R indices (all data)	$R1$ = 0.1767, $wR2$ = 0.1949
Largest diff. peak and hole	0.330 and –0.315 e Å^{-3}

Diffractometer: *Nonius KappaCCD* area detector (ϕ scans and ω scans to fill *asymmetric unit*). **Cell determination:** DirAx (Duisenberg, A.J.M.(1992). J. Appl. Cryst. 25, 92-96.) **Data collection:** Collect (Collect: Data collection software, R. Hooft, Nonius B.V., 1998). **Data reduction and cell refinement**: *Denzo* (Z. Otwinowski & W. Minor, *Methods in Enzymology* (1997) Vol. **276**: *Macromolecular Crystallography*, part A, pp. 307–326; C. W. Carter, Jr. & R. M. Sweet, Eds., Academic Press). **Absorption correction**: Sheldrick, G. M. SADABS - Bruker Nonius area detector scaling and absorption correction - V2.10 **Structure solution**: *SHELXS97* (G. M. Sheldrick, Acta Cryst. (1990) A**46** 467–473). **Structure refinement**: *SHELXL97* (G. M. Sheldrick (1997), University of Göttingen, Germany). **Graphics:** Cameron - A Molecular Graphics Package. (D. M. Watkin, L. Pearce and C. K. Prout, Chemical Crystallography Laboratory, University of Oxford, 1993).

Special details: All hydrogen atoms were placed in idealised positions and refined using a riding model.

Table 2. Atomic coordinates [× 10^4], equivalent isotropic displacement parameters [Å^2 × 10^3] and site occupancy factors. U_{eq} is defined as one third of the trace of the orthogonalized U^{ij} tensor.

Atom	*x*	*y*	*z*	U_{eq}	*S.o.f.*
C37	7774(5)	91(3)	1375(4)	43(2)	1
Cl1	6521(1)	357(1)	638(1)	48(1)	1
Cl2	9052(2)	363(1)	1052(1)	54(1)	1
C1	5427(5)	2550(3)	4450(3)	26(1)	1
C2	4462(5)	2164(3)	4420(3)	30(1)	1
C3	4833(5)	1542(3)	4759(3)	28(1)	1
C4	6025(5)	1560(3)	5002(3)	24(1)	1
C5	6227(4)	435(3)	5620(4)	28(1)	1
C6	6893(4)	1038(3)	5402(3)	25(1)	1
C7	7646(5)	1301(3)	6260(3)	25(1)	1
C8	7668(4)	834(3)	4769(3)	22(1)	1
C9	7628(5)	296(3)	4246(3)	27(1)	1
C10	8612(4)	317(3)	3831(3)	26(1)	1
C11	9218(5)	875(3)	4106(3)	26(1)	1
C12	10959(5)	585(3)	3508(4)	32(1)	1
C13	10355(4)	1133(3)	3925(3)	24(1)	1
C14	11150(4)	1320(3)	4809(3)	30(1)	1
C15	10188(4)	1718(3)	3319(3)	22(1)	1
C16	10466(5)	1812(3)	2513(3)	27(1)	1
C17	10157(4)	2465(3)	2243(3)	30(1)	1
C18	9694(4)	2755(3)	2898(3)	25(1)	1
C19	9481(5)	3859(3)	2233(4)	33(1)	1
C20	9249(5)	3441(3)	2999(3)	26(1)	1
C21	9917(5)	3737(3)	3859(4)	33(1)	1
C22	7953(5)	3444(3)	2977(3)	26(1)	1
C23	7032(5)	3605(3)	2321(3)	27(1)	1

C24	6003(5)	3548(3)	2667(3)	29(1)	1
C25	6293(4)	3357(2)	3526(3)	23(1)	1
C26	4347(5)	3559(3)	3878(4)	37(2)	1
C27	5554(5)	3266(3)	4224(3)	29(1)	1
C28	6114(5)	3627(3)	5075(3)	32(1)	1
C29	7562(5)	2115(3)	772(4)	41(2)	1
C30	7266(5)	1728(3)	2260(4)	33(1)	1
C31	6348(5)	1654(3)	2650(4)	38(2)	1
C32	5715(5)	2019(3)	1312(4)	29(1)	1
C33	4168(5)	1854(3)	2158(4)	38(2)	1
C34	3705(5)	1187(3)	2333(4)	43(2)	1
C35	3719(5)	676(3)	1635(4)	40(2)	1
C36	2933(5)	93(3)	1722(4)	46(2)	1
N1	6380(4)	2172(2)	4814(3)	24(1)	1
N2	8630(4)	1186(2)	4673(3)	23(1)	1
N3	9725(3)	2295(2)	3550(3)	23(1)	1
N4	7487(4)	3297(2)	3709(3)	25(1)	1
N5	6863(4)	1960(2)	1429(3)	28(1)	1
N6	5375(4)	1835(2)	2042(3)	26(1)	1
F1	8733(2)	2526(1)	5027(2)	25(1)	1

2.5·EMIMF COMPLEX

Table 1. Crystal data and structure refinement details.

Empirical formula	$C_{34}H_{47}FN_6$
Formula weight	558.78
Temperature	120(2) K
Wavelength	0.71073 Å
Crystal system	Monoclinic
Space group	$P2_1/c$
Unit cell dimensions	a = 12.5489(3) Å
	b = 12.8461(3) Å β = 106.162(2)°
	c = 20.2911(5) Å
Volume	3141.74(13) Å^3
Z	4
Density (calculated)	1.181 Mg / m^3
Absorption coefficient	0.075 mm^{-1}
F(000)	1208
Crystal	Fragment; Colourless
Crystal size	0.2 × 0.15 × 0.05 mm^3
θ range for data collection	3.03 – 27.48°
Index ranges	$-16 \le h \le 16$, $-16 \le k \le 16$, $-24 \le l \le 26$
Reflections collected	35425
Independent reflections	7185 [R_{int} = 0.1574]
Completeness to θ = 27.48°	99.5 %

Absorption correction	Semi–empirical from equivalents
Max. and min. transmission	0.9963 and 0.9751
Refinement method	Full-matrix least-squares on F^2
Data / restraints / parameters	7185 / 0 / 380
Goodness-of-fit on F^2	1.067
Final R indices $[F^2 > 2\sigma(F^2)]$	$R1 = 0.1109$, $wR2 = 0.1871$
R indices (all data)	$R1 = 0.1952$, $wR2 = 0.2248$
Largest diff. peak and hole	0.341 and –0.368 e Å^{-3}

Diffractometer: *Nonius KappaCCD* area detector (ϕ scans and ω scans to fill *asymmetric unit*). **Cell determination:** DirAx (Duisenberg, A.J.M.(1992). J. Appl. Cryst. 25, 92-96.) **Data collection:** Collect (Collect: Data collection software, R. Hooft, Nonius B.V., 1998). **Data reduction and cell refinement**: *Denzo* (Z. Otwinowski & W. Minor, *Methods in Enzymology* (1997) Vol. **276**: *Macromolecular Crystallography*, part A, pp. 307–326; C. W. Carter, Jr. & R. M. Sweet, Eds., Academic Press). **Absorption correction**: Sheldrick, G. M. SADABS - Bruker Nonius area detector scaling and absorption correction - V2.10 **Structure solution**: *SHELXS97* (G. M. Sheldrick, Acta Cryst. (1990) A**46** 467–473). **Structure refinement**: *SHELXL97* (G. M. Sheldrick (1997), University of Göttingen, Germany). **Graphics:** Cameron - A Molecular Graphics Package. (D. M. Watkin, L. Pearce and C. K. Prout, Chemical Crystallography Laboratory, University of Oxford, 1993).

Special details: All hydrogen atoms were placed in idealised positions and refined using a riding model.

Table 2. Atomic coordinates [× 10^4], equivalent isotropic displacement parameters [Å^2 × 10^3] and site occupancy factors. U_{eq} is defined as one third of the trace of the orthogonalized U^{ij} tensor.

Atom	*x*	*y*	*z*	U_{eq}	*S.o.f.*
F1	7521(2)	2555(2)	92(1)	22(1)	1
C1	6316(3)	4393(3)	1115(2)	20(1)	1
C2	5559(3)	4498(3)	1484(2)	22(1)	1
C3	5037(3)	3512(3)	1486(2)	21(1)	1
C4	5492(3)	2833(3)	1123(2)	20(1)	1
C5	5196(3)	1702(3)	917(2)	22(1)	1
C6	4288(4)	1352(4)	1241(2)	29(1)	1
C7	4740(4)	1643(3)	129(2)	27(1)	1
C8	6185(3)	972(3)	1159(2)	21(1)	1
C9	6411(4)	222(3)	1657(2)	24(1)	1
C10	7389(4)	–314(3)	1622(2)	25(1)	1
C11	7743(3)	123(3)	1107(2)	20(1)	1
C12	8726(4)	–132(3)	832(2)	23(1)	1
C13	8349(4)	–182(4)	45(2)	31(1)	1
C14	9170(4)	–1209(3)	1110(3)	31(1)	1
C15	9660(3)	655(3)	1070(2)	20(1)	1
C16	10705(4)	556(4)	1507(2)	25(1)	1
C17	11246(3)	1530(3)	1535(2)	24(1)	1
C18	10523(3)	2202(3)	1116(2)	19(1)	1
C19	10656(3)	3339(3)	938(2)	20(1)	1
C20	10432(4)	3445(3)	153(2)	24(1)	1
C21	11861(3)	3672(4)	1273(2)	28(1)	1
C22	9889(3)	4051(3)	1194(2)	20(1)	1
C23	10093(3)	4693(3)	1750(2)	23(1)	1
C24	9085(3)	5208(3)	1740(2)	24(1)	1
C25	8282(3)	4864(3)	1179(2)	18(1)	1
C26	7069(3)	5174(3)	908(2)	21(1)	1
C27	6908(4)	6238(3)	1213(2)	28(1)	1
C28	6733(4)	5270(4)	118(2)	27(1)	1

N1	6270(3)	3366(3)	898(2)	20(1)	1
N2	7006(3)	908(3)	825(2)	20(1)	1
N3	9561(3)	1663(3)	830(2)	19(1)	1
N4	8780(3)	4154(3)	850(2)	19(1)	1
C29	1084(4)	7286(4)	2795(2)	27(1)	1
C30	1380(4)	7004(3)	1622(2)	24(1)	1
C31	2128(4)	7339(4)	1303(2)	28(1)	1
C32	2529(3)	8050(3)	2328(2)	20(1)	1
C33	3807(4)	8520(4)	1621(2)	28(1)	1
C34	4702(4)	7739(4)	1613(3)	36(1)	1
N5	1647(3)	7457(3)	2264(2)	20(1)	1
N6	2838(3)	8004(3)	1753(2)	22(1)	1

2.5·EtPyCl COMPLEX

Table 1. Crystal data and structure refinement details.

Empirical formula	$C_{36}H_{48}Cl_3N_5$
Formula weight	657.14
Temperature	120(2) K
Wavelength	0.71073 Å
Crystal system	Monoclinic
Space group	$P2_1$
Unit cell dimensions	a = 10.3713(4) Å
	b = 16.0168(6) Å β = 99.974(2)°
	c = 10.5997(2) Å
Volume	1734.16(10) Å^3
Z	2
Density (calculated)	1.258 Mg / m^3
Absorption coefficient	0.297 mm^{-1}
F(000)	700
Crystal	Block; Yellow
Crystal size	0.4 × 0.16 × 0.05 mm^3
θ range for data collection	3.21 – 27.48°
Index ranges	$-13 \le h \le 13$, $-20 \le k \le 20$, $-13 \le l \le 13$
Reflections collected	24575
Independent reflections	7755 [R_{int} = 0.0545]
Completeness to θ = 27.48°	99.8 %
Absorption correction	Semi–empirical from equivalents
Max. and min. transmission	0.9853 and 0.8804
Refinement method	Full-matrix least-squares on F^2
Data / restraints / parameters	7755 / 1 / 406
Goodness-of-fit on F^2	0.968
Final R indices [$F^2 > 2\sigma(F^2)$]	$R1$ = 0.0432, $wR2$ = 0.0825
R indices (all data)	$R1$ = 0.0708, $wR2$ = 0.0917

Absolute structure parameter	–0.03(4)
Largest diff. peak and hole	0.233 and –0.279 e $Å^{-3}$

Diffractometer: *Nonius KappaCCD* area detector (ϕ scans and ω scans to fill *asymmetric unit*). **Cell determination:** DirAx (Duisenberg, A.J.M.(1992). J. Appl. Cryst. 25, 92-96.) **Data collection:** Collect (Collect: Data collection software, R. Hooft, Nonius B.V., 1998). **Data reduction and cell refinement**: *Denzo* (Z. Otwinowski & W. Minor, *Methods in Enzymology* (1997) Vol. **276**: *Macromolecular Crystallography*, part A, pp. 307–326; C. W. Carter, Jr. & R. M. Sweet, Eds., Academic Press). **Absorption correction**: Sheldrick, G. M. SADABS - Bruker Nonius area detector scaling and absorption correction - V2.10 **Structure solution**: *SHELXS97* (G. M. Sheldrick, Acta Cryst. (1990) A**46** 467–473). **Structure refinement**: *SHELXL97* (G. M. Sheldrick (1997), University of Göttingen, Germany). **Graphics:** Cameron - A Molecular Graphics Package. (D. M. Watkin, L. Pearce and C. K. Prout, Chemical Crystallography Laboratory, University of Oxford, 1993).

Special details: All hydrogen atoms were placed in idealised positions and refined using a riding model.

Table 2. Atomic coordinates [$\times 10^4$], equivalent isotropic displacement parameters [$Å^2 \times 10^3$] and site occupancy factors. U_{eq} is defined as one third of the trace of the orthogonalized U^{ij} tensor.

Atom	*x*	*y*	*z*	U_{eq}	*S.o.f.*
N1	2790(2)	4487(1)	6705(2)	18(1)	1
N2	5289(2)	4292(1)	9165(2)	16(1)	1
N3	7187(2)	3462(1)	7202(2)	17(1)	1
N4	4744(2)	3653(1)	4696(2)	16(1)	1
C1	2077(2)	4006(1)	5751(2)	16(1)	1
C2	1164(2)	3582(2)	6299(2)	18(1)	1
C3	1326(2)	3821(2)	7612(2)	19(1)	1
C4	2339(2)	4380(1)	7845(2)	17(1)	1
C5	2974(2)	4829(1)	9063(2)	17(1)	1
C6	1984(2)	4865(2)	9990(2)	23(1)	1
C7	3331(2)	5730(2)	8768(2)	19(1)	1
C8	4164(2)	4341(1)	9698(2)	17(1)	1
C9	4393(2)	3886(2)	10806(2)	19(1)	1
C10	5676(2)	3552(2)	10948(2)	21(1)	1
C11	6221(2)	3809(2)	9919(2)	17(1)	1
C12	7587(2)	3672(2)	9613(2)	18(1)	1
C13	8414(3)	3222(2)	10751(2)	25(1)	1
C14	8238(2)	4523(2)	9450(2)	23(1)	1
C15	7581(2)	3148(2)	8425(2)	17(1)	1
C16	8008(2)	2349(2)	8289(2)	25(1)	1
C17	7880(3)	2177(2)	6956(2)	26(1)	1
C18	7371(2)	2872(2)	6298(2)	18(1)	1
C19	7027(2)	3041(1)	4866(2)	18(1)	1
C20	7664(3)	2349(2)	4174(2)	23(1)	1
C21	7594(2)	3892(2)	4545(2)	21(1)	1
C22	5559(2)	3028(2)	4411(2)	17(1)	1
C23	4775(2)	2428(2)	3733(2)	21(1)	1
C24	3461(2)	2701(2)	3612(2)	21(1)	1
C25	3456(2)	3459(2)	4211(2)	16(1)	1
C26	2329(2)	4029(2)	4382(2)	18(1)	1
C27	1082(2)	3732(2)	3484(2)	27(1)	1
C28	2621(3)	4932(2)	4017(2)	23(1)	1
C29	4023(2)	2267(2)	8226(2)	23(1)	1
C30	4360(3)	2185(2)	7039(2)	26(1)	1
C31	4520(2)	1400(2)	6548(2)	27(1)	1

C32	4344(2)	710(2)	7277(2)	25(1)	1
C33	3988(2)	812(2)	8456(2)	23(1)	1
N5	3835(2)	1582(1)	8912(2)	20(1)	1
C34	3392(3)	1698(2)	10165(2)	31(1)	1
C35	1984(3)	1940(2)	9982(3)	49(1)	1
C37	9232(3)	5607(2)	6195(2)	35(1)	1
Cl1	9806(1)	6348(1)	7385(1)	34(1)	1
Cl2	9170(1)	6021(1)	4640(1)	46(1)	1
Cl3	5749(1)	5257(1)	6563(1)	19(1)	1

2.5·EtPyBr COMPLEX

Table 1. Crystal data and structure refinement details.

Empirical formula	$C_{36}H_{48}BrCl_2N_5$
Formula weight	701.60
Temperature	120(2) K
Wavelength	0.71073 Å
Crystal system	Monoclinic
Space group	$P2_1$
Unit cell dimensions	a = 10.441(10) Å
	b = 16.283(15) Å β = 100.42(5)°
	c = 10.634(4) Å
Volume	1778(2) Å^3
Z	2
Density (calculated)	1.310 Mg / m^3
Absorption coefficient	1.338 mm^{-1}
F(000)	736
Crystal	Prism; Yellow
Crystal size	0.15 × 0.12 × 0.04 mm^3
θ range for data collection	3.02 – 27.48°
Index ranges	$-13 \le h \le 13$, $-21 \le k \le 20$, $-13 \le l \le 13$
Reflections collected	19818
Independent reflections	7950 [R_{int} = 0.0656]
Completeness to θ = 27.48°	98.7 %
Absorption correction	Semi–empirical from equivalents
Max. and min. transmission	0.9484 and 0.8245
Refinement method	Full-matrix least-squares on F^2
Data / restraints / parameters	7950 / 1 / 406
Goodness-of-fit on F^2	1.030
Final R indices [$F^2 > 2\sigma(F^2)$]	$R1$ = 0.0603, $wR2$ = 0.1247
R indices (all data)	$R1$ = 0.0924, $wR2$ = 0.1368

Absolute structure parameter	0.093(9)
Largest diff. peak and hole	0.686 and −0.649 e Å^{-3}

Diffractometer: *Nonius KappaCCD* area detector (ϕ scans and ω scans to fill *asymmetric unit*). **Cell determination:** DirAx (Duisenberg, A.J.M.(1992). J. Appl. Cryst. 25, 92-96.) **Data collection:** Collect (Collect: Data collection software, R. Hooft, Nonius B.V., 1998). **Data reduction and cell refinement**: *Denzo* (Z. Otwinowski & W. Minor, *Methods in Enzymology* (1997) Vol. **276**: *Macromolecular Crystallography*, part A, pp. 307–326; C. W. Carter, Jr. & R. M. Sweet, Eds., Academic Press). **Absorption correction**: Sheldrick, G. M. SADABS - Bruker Nonius area detector scaling and absorption correction - V2.10 **Structure solution**: *SHELXS97* (G. M. Sheldrick, Acta Cryst. (1990) A**46** 467–473). **Structure refinement**: *SHELXL97* (G. M. Sheldrick (1997), University of Göttingen, Germany). **Graphics:** Cameron - A Molecular Graphics Package. (D. M. Watkin, L. Pearce and C. K. Prout, Chemical Crystallography Laboratory, University of Oxford, 1993).

Special details: All hydrogen atoms were placed in idealised positions and refined using a riding model.

Table 2. Atomic coordinates [× 10^4], equivalent isotropic displacement parameters [Å^2 × 10^3] and site occupancy factors. U_{eq} is defined as one third of the trace of the orthogonalized U^{ij} tensor.

Atom	*x*	*y*	*z*	U_{eq}	*S.o.f.*
N1	7184(4)	5517(2)	3263(3)	16(1)	1
N2	4685(4)	5741(2)	780(3)	16(1)	1
N3	2778(4)	6570(2)	2721(3)	17(1)	1
N4	5222(4)	6351(2)	5244(3)	16(1)	1
C1	7870(5)	5995(3)	4222(4)	16(1)	1
C2	8777(4)	6442(3)	3682(4)	17(1)	1
C3	8612(5)	6204(3)	2370(4)	19(1)	1
C4	7626(5)	5635(3)	2132(4)	18(1)	1
C5	7013(5)	5200(3)	922(4)	18(1)	1
C6	7993(5)	5166(3)	−8(4)	24(1)	1
C7	6624(5)	4307(3)	1178(5)	20(1)	1
C8	5801(4)	5682(3)	253(4)	16(1)	1
C9	5589(5)	6132(3)	−859(4)	20(1)	1
C10	4291(5)	6469(3)	−1014(5)	23(1)	1
C11	3761(5)	6221(3)	4(4)	17(1)	1
C12	2386(5)	6379(3)	303(4)	19(1)	1
C13	1588(5)	6839(3)	−833(4)	23(1)	1
C14	1718(5)	5549(3)	428(5)	24(1)	1
C15	2409(4)	6898(3)	1492(4)	17(1)	1
C16	2022(5)	7684(3)	1641(4)	24(1)	1
C17	2147(5)	7853(3)	2970(4)	24(1)	1
C18	2618(5)	7141(3)	3624(4)	17(1)	1
C19	2944(5)	6977(3)	5052(4)	18(1)	1
C20	2309(5)	7671(3)	5754(5)	24(1)	1
C21	2364(5)	6137(3)	5367(4)	20(1)	1
C22	4420(4)	6979(3)	5536(4)	16(1)	1
C23	5189(5)	7555(3)	6232(4)	19(1)	1
C24	6518(5)	7276(3)	6368(4)	21(1)	1
C25	6520(4)	6542(3)	5762(4)	15(1)	1
C26	7638(5)	5975(3)	5587(4)	20(1)	1
C27	8887(5)	6263(3)	6502(4)	23(1)	1
C28	7343(5)	5071(3)	5956(5)	24(1)	1
C29	5982(5)	7747(3)	1721(5)	22(1)	1
C30	5627(5)	7810(3)	2896(5)	24(1)	1
C31	5518(5)	8580(3)	3417(5)	28(1)	1

C32	5718(5)	9271(3)	2734(5)	23(1)	1
C33	6061(5)	9184(3)	1560(4)	23(1)	1
N5	6200(4)	8436(2)	1075(3)	18(1)	1
C34	6616(6)	8326(4)	−189(5)	35(2)	1
C35	8044(6)	8109(4)	12(6)	48(2)	1
C37	614(6)	4414(3)	3810(5)	36(1)	1
Cl1	142(1)	3642(1)	2655(1)	32(1)	1
Cl2	792(2)	4026(1)	5382(1)	44(1)	1
Br1	4113(1)	4684(1)	3377(1)	28(1)	1

2.5·PrPyCl COMPLEX

Table 1. Crystal data and structure refinement details.

Empirical formula	$C_{37}H_{50}Cl_3N_5$
Formula weight	671.17
Temperature	120(2) K
Wavelength	0.71073 Å
Crystal system	Monoclinic
Space group	$P2_1$
Unit cell dimensions	a = 10.4518(5) Å
	b = 16.2074(8) Å β = 99.626(2)°
	c = 10.5977(3) Å
Volume	1769.94(13) Å^3
Z	2
Density (calculated)	1.259 Mg / m^3
Absorption coefficient	0.293 mm^{-1}
F(000)	716
Crystal	Slab; Yellow
Crystal size	0.35 × 0.2 × 0.06 mm^3
θ range for data collection	3.25 – 27.48°
Index ranges	$-13 \le h \le 13$, $-21 \le k \le 21$, $-13 \le l \le 13$
Reflections collected	24884
Independent reflections	7902 [R_{int} = 0.0507]
Completeness to θ = 27.48°	99.7 %
Absorption correction	Semi–empirical from equivalents
Max. and min. transmission	0.9827 and 0.9145
Refinement method	Full-matrix least-squares on F^2
Data / restraints / parameters	7902 / 1 / 415
Goodness-of-fit on F^2	1.026
Final R indices [$F^2 > 2\sigma(F^2)$]	$R1$ = 0.0575, $wR2$ = 0.1417

R indices (all data)	$R1 = 0.0877$, $wR2 = 0.1582$
Absolute structure parameter	−0.67(6)
Largest diff. peak and hole	0.884 and −0.573 e Å^{-3}

Diffractometer: *Nonius KappaCCD* area detector (ϕ scans and ω scans to fill *asymmetric unit*). **Cell determination:** DirAx (Duisenberg, A.J.M.(1992). J. Appl. Cryst. 25, 92-96.) **Data collection:** Collect (Collect: Data collection software, R. Hooft, Nonius B.V., 1998). **Data reduction and cell refinement**: *Denzo* (Z. Otwinowski & W. Minor, *Methods in Enzymology* (1997) Vol. **276**: *Macromolecular Crystallography*, part A, pp. 307–326; C. W. Carter, Jr. & R. M. Sweet, Eds., Academic Press). **Absorption correction**: Sheldrick, G. M. SADABS - Bruker Nonius area detector scaling and absorption correction - V2.10 **Structure solution**: *SHELXS97* (G. M. Sheldrick, Acta Cryst. (1990) A**46** 467–473). **Structure refinement**: *SHELXL97* (G. M. Sheldrick (1997), University of Göttingen, Germany). **Graphics:** Cameron - A Molecular Graphics Package. (D. M. Watkin, L. Pearce and C. K. Prout, Chemical Crystallography Laboratory, University of Oxford, 1993).

Special details: All hydrogen atoms were located from the difference map and All hydrogen atoms were placed in idealised positions and refined using a riding model.

Table 2. Atomic coordinates [× 10^4], equivalent isotropic displacement parameters [Å^2 × 10^3] and site occupancy factors. U_{eq} is defined as one third of the trace of the orthogonalized U^{ij} tensor.

Atom	*x*	*y*	*z*	U_{eq}	*S.o.f.*
Cl3	9222(1)	8037(1)	8420(1)	11(1)	1
N2	9769(3)	7049(2)	5817(3)	23(1)	1
N5	11106(3)	4377(2)	6049(3)	22(1)	1
C4	12932(3)	6775(2)	9234(3)	23(1)	1
C11	10888(3)	7121(2)	5276(3)	23(1)	1
C1	12378(4)	7684(2)	10985(3)	28(1)	1
N1	12229(3)	7259(2)	8286(3)	23(1)	1
N4	10276(3)	6417(2)	10303(3)	22(1)	1
N3	7861(3)	6203(2)	7766(3)	25(1)	1
C14	8866(4)	6578(2)	5042(3)	23(1)	1
C32	10724(4)	3489(3)	7705(4)	32(1)	1
C18	7586(3)	5883(2)	6558(3)	24(1)	1
C9	12059(4)	7605(2)	5925(3)	26(1)	1
C10	13069(4)	7640(3)	5028(3)	29(1)	1
C24	7399(4)	5106(3)	10794(4)	31(1)	1
C21	7749(4)	5614(2)	8665(3)	24(1)	1
C22	7436(4)	6620(3)	10410(3)	27(1)	1
C31	10589(4)	4160(3)	8472(3)	33(1)	1
C33	10998(3)	3608(2)	6502(3)	27(1)	1
C7	12680(3)	7157(2)	7162(3)	24(1)	1
C34	11498(4)	4503(3)	4761(3)	31(1)	1
C30	10696(4)	4948(3)	7991(4)	34(1)	1
C5	13823(4)	6355(2)	8682(3)	25(1)	1
C26	10271(4)	5203(2)	11261(3)	26(1)	1
C2	12663(4)	6797(2)	10606(3)	24(1)	1
C25	9476(4)	5792(2)	10583(3)	23(1)	1
C19	7306(4)	5057(2)	6695(3)	28(1)	1
C29	10945(4)	5036(3)	6757(3)	29(1)	1
C13	9407(4)	6357(2)	3998(3)	27(1)	1
C12	10672(4)	6700(2)	4154(3)	25(1)	1
C28	11569(3)	6233(2)	10775(3)	23(1)	1
C8	11700(4)	8481(2)	6239(3)	27(1)	1
C6	13668(4)	6591(2)	7375(3)	27(1)	1

C15	6829(4)	7221(3)	5532(4)	31(1)	1
C16	7524(4)	6407(3)	5361(3)	27(1)	1
C17	6737(4)	5934(3)	4232(4)	34(1)	1
C3	13902(4)	6511(3)	11493(4)	32(1)	1
C20	7407(4)	4899(3)	8023(3)	28(1)	1
C27	11549(4)	5469(3)	11371(3)	29(1)	1
C23	8019(4)	5786(2)	10103(3)	25(1)	1
C35	12817(4)	4910(3)	4913(4)	33(1)	1
C36	13894(4)	4460(3)	5797(5)	44(1)	1
Cl1	5235(1)	9120(1)	7576(1)	44(1)	1
Cl2	5785(1)	8760(1)	10314(1)	56(1)	1
C37	5745(5)	8368(3)	8761(4)	45(1)	1

2.5·PrPyBr COMPLEX

Table 1. Crystal data and structure refinement details.

Empirical formula	$C_{36}H_{48}BrN_5$
Formula weight	630.70
Temperature	120(2) K
Wavelength	0.71073 Å
Crystal system	Monoclinic
Space group	$P2_1/c$
Unit cell dimensions	a = 10.6105(4) Å
	b = 16.9689(9) Å β = 105.356(3)°
	c = 18.5412(10) Å
Volume	3219.1(3) Å^3
Z	4
Density (calculated)	1.301 Mg / m^3
Absorption coefficient	1.310 mm^{-1}
F(000)	1336
Crystal	Block; Yellow
Crystal size	0.2 × 0.11 × 0.06 mm^3
θ range for data collection	3.12 – 27.48°
Index ranges	$-12 \le h \le 13$, $-19 \le k \le 21$, $-22 \le l \le 24$
Reflections collected	22995
Independent reflections	7363 [R_{int} = 0.1101]
Completeness to θ = 27.48°	99.7 %
Absorption correction	Semi–empirical from equivalents
Max. and min. transmission	0.9255 and 0.7696
Refinement method	Full-matrix least-squares on F^2
Data / restraints / parameters	7363 / 0 / 388

Goodness-of-fit on F^2	1.004
Final R indices $[F^2 > 2\sigma(F^2)]$	$R1 = 0.0574$, $wR2 = 0.0936$
R indices (all data)	$R1 = 0.1431$, $wR2 = 0.1154$
Largest diff. peak and hole	0.750 and –0.671 e Å^{-3}

Diffractometer: *Nonius KappaCCD* area detector (ϕ scans and ω scans to fill *asymmetric unit*). **Cell determination:** DirAx (Duisenberg, A.J.M.(1992). J. Appl. Cryst. 25, 92-96.) **Data collection:** Collect (Collect: Data collection software, R. Hooft, Nonius B.V., 1998). **Data reduction and cell refinement**: *Denzo* (Z. Otwinowski & W. Minor, *Methods in Enzymology* (1997) Vol. **276**: *Macromolecular Crystallography*, part A, pp. 307–326; C. W. Carter, Jr. & R. M. Sweet, Eds., Academic Press). **Absorption correction**: Sheldrick, G. M. SADABS - Bruker Nonius area detector scaling and absorption correction - V2.10 **Structure solution**: *SHELXS97* (G. M. Sheldrick, Acta Cryst. (1990) A**46** 467–473). **Structure refinement**: *SHELXL97* (G. M. Sheldrick (1997), University of Göttingen, Germany). **Graphics:** Cameron - A Molecular Graphics Package. (D. M. Watkin, L. Pearce and C. K. Prout, Chemical Crystallography Laboratory, University of Oxford, 1993).

Special details: All hydrogen atoms were placed in idealised positions and refined using a riding model.

Table 2. Atomic coordinates [× 10^4], equivalent isotropic displacement parameters [Å^2 × 10^3] and site occupancy factors. U_{eq} is defined as one third of the trace of the orthogonalized U^{ij} tensor.

Atom	*x*	*y*	*z*	U_{eq}	*S.o.f.*
C1	3871(3)	8825(2)	945(2)	23(1)	1
C2	4516(3)	9563(2)	1375(2)	21(1)	1
C3	3686(3)	10285(2)	1062(2)	26(1)	1
C4	4579(3)	9490(2)	2204(2)	19(1)	1
C5	4109(3)	9969(2)	2663(2)	22(1)	1
C6	4443(3)	9629(2)	3387(2)	24(1)	1
C7	5126(3)	8946(2)	3358(2)	18(1)	1
C8	5468(4)	8612(2)	4703(2)	32(1)	1
C9	5751(3)	8360(2)	3969(2)	21(1)	1
C10	5169(3)	7533(2)	3762(2)	27(1)	1
C11	7229(3)	8338(2)	4085(2)	19(1)	1
C12	8202(3)	8749(2)	4568(2)	20(1)	1
C13	9413(3)	8487(2)	4465(2)	20(1)	1
C14	9157(3)	7921(2)	3919(2)	16(1)	1
C15	9481(3)	6605(2)	3371(2)	22(1)	1
C16	10065(3)	7433(2)	3579(2)	18(1)	1
C17	11380(3)	7328(2)	4170(2)	21(1)	1
C18	10296(3)	7862(2)	2906(2)	16(1)	1
C19	11406(3)	8208(2)	2809(2)	21(1)	1
C20	11078(3)	8588(2)	2102(2)	20(1)	1
C21	9773(3)	8464(2)	1770(2)	18(1)	1
C22	8274(3)	8038(2)	545(2)	22(1)	1
C23	8914(3)	8750(2)	1030(2)	18(1)	1
C24	9770(3)	9187(2)	614(2)	24(1)	1
C25	7855(3)	9309(2)	1127(2)	16(1)	1
C26	7752(3)	10114(2)	1051(2)	21(1)	1
C27	6511(3)	10339(2)	1141(2)	20(1)	1
C28	5878(3)	9673(2)	1265(2)	18(1)	1
C29	10563(4)	6418(2)	1670(2)	26(1)	1
C30	9415(4)	6023(2)	1621(2)	32(1)	1
C31	9445(4)	5227(2)	1757(2)	39(1)	1
C32	10618(5)	4833(2)	1942(2)	40(1)	1
C33	11756(4)	5249(2)	1990(2)	34(1)	1

C34	12914(4)	6470(2)	1803(2)	37(1)	1
C35	12872(4)	6599(2)	990(2)	32(1)	1
C36	12757(3)	5836(2)	546(2)	31(1)	1
N1	5200(3)	8862(2)	2635(2)	19(1)	1
N2	7818(2)	7839(2)	3687(2)	18(1)	1
N3	9313(2)	8013(1)	2268(2)	16(1)	1
N4	6709(2)	9050(2)	1269(2)	17(1)	1
N5	11708(3)	6030(2)	1847(2)	24(1)	1
Br1	6304(1)	7165(1)	1905(1)	20(1)	1

2.5·DMIM $MeSO_4$ COMPLEX

Table 1. Crystal data and structure details for $C_{28}H_{36}N_4 \cdot SO_4CH_3 \cdot C_5H_9N_2 \cdot 2(CH_2Cl_2)$

Empirical formula	$C_{36}H_{52}Cl_4N_6O_4S$
Formula weight	806.70
Temperature	120(2) K
Wavelength	0.71073 Å
Crystal system	Monoclinic
Space group	$P2_1$
Unit cell dimensions	a = 10.611(5) Å
	b = 18.193(6) Å β = 106.36(2)°
	c = 10.803(3) Å
Volume	2001.0(12) $Å^3$
Z	2
Density (calculated)	1.339 Mg / m^3
Absorption coefficient	0.394 mm^{-1}
F(000)	852
Crystal	Plate; Colourless
Crystal size	0.4 × 0.3 × 0.05 mm^3
θ range for data collection	4.89 – 27.77°
Index ranges	$-13 \le h \le 12$, $-23 \le k \le 23$, $-14 \le l \le 14$
Reflections collected	17479
Independent reflections	17479 [no merging during twin refinement]
Completeness to θ = 27.50°	96.9 %
Absorption correction	Semi–empirical from equivalents
Max. and min. transmission	0.9883 and 0.8584
Refinement method	Full-matrix least-squares on F^2
Data / restraints / parameters	17479 / 5 / 467
Goodness-of-fit on F^2	1.173
Final R indices [$F^2 > 2\sigma(F^2)$]	$R1$ = 0.1005, $wR2$ = 0.1831
R indices (all data)	$R1$ = 0.1725, $wR2$ = 0.2216
Absolute structure parameter	not reliably determined due to twinning

Largest diff. peak and hole 1.461 and −1.164 e Å^{-3}

Diffractometer: *Nonius KappaCCD* area detector (ϕ scans and ω scans to fill *asymmetric unit*). **Cell determination:** DirAx (Duisenberg, A.J.M.(1992). J. Appl. Cryst. 25, 92-96.) **Data collection:** Collect (Collect: Data collection software, R. Hooft, Nonius B.V., 1998). **Data reduction and cell refinement**: *Denzo* (Z. Otwinowski & W. Minor, *Methods in Enzymology* (1997) Vol. **276**: *Macromolecular Crystallography*, part A, pp. 307–326; C. W. Carter, Jr. & R. M. Sweet, Eds., Academic Press). **Absorption correction**: Sheldrick, G. M. SADABS - Bruker Nonius area detector scaling and absorption correction - V2.10 **Structure solution**: *SHELXS97* (G. M. Sheldrick, Acta Cryst. (1990) A**46** 467–473). **Structure refinement**: *SHELXL97* (G. M. Sheldrick (1997), University of Göttingen, Germany). **Graphics:** Cameron - A Molecular Graphics Package. (D. M. Watkin, L. Pearce and C. K. Prout, Chemical Crystallography Laboratory, University of Oxford, 1993).

Special details: All hydrogen atoms were placed in idealised positions and refined using a riding model. The crystals were twinned via 180° rotation about 1 0 0.

Table 2. Atomic coordinates [× 10^4], equivalent isotropic displacement parameters [Å^2 × 10^3] and site occupancy factors. U_{eq} is defined as one third of the trace of the orthogonalized U^{ij} tensor.

Atom	*x*	*y*	*z*	U_{eq}	*S.o.f.*
N1	9172(5)	5513(3)	−96(5)	19(1)	1
N2	6301(6)	5902(3)	−2366(5)	24(1)	1
N3	4605(5)	4913(3)	−653(5)	21(1)	1
N4	7490(5)	4510(3)	1664(5)	18(1)	1
C1	9994(6)	4991(4)	625(6)	19(2)	1
C2	10826(6)	4792(4)	−74(6)	19(2)	1
C3	10482(7)	5208(4)	−1247(6)	27(2)	1
C4	9429(7)	5646(4)	−1255(7)	26(2)	1
C5	8679(7)	6180(4)	−2249(6)	22(2)	1
C6	9405(7)	6315(4)	−3264(7)	34(2)	1
C7	8531(7)	6920(4)	−1590(6)	26(2)	1
C8	7322(7)	5888(4)	−2915(6)	21(2)	1
C9	6846(7)	5575(4)	−4109(7)	28(2)	1
C10	5472(7)	5407(4)	−4278(6)	25(2)	1
C11	5177(7)	5626(4)	−3182(6)	19(2)	1
C12	3874(7)	5576(4)	−2821(6)	19(2)	1
C13	3664(7)	6311(4)	−2174(7)	28(2)	1
C14	2767(7)	5480(4)	−4066(6)	31(2)	1
C15	3897(6)	4934(4)	−1948(6)	17(2)	1
C16	3258(7)	4282(4)	−2177(6)	29(2)	1
C17	3632(7)	3856(4)	−1027(6)	28(2)	1
C18	4438(6)	4260(4)	−105(5)	16(2)	1
C19	5115(7)	4065(4)	1303(6)	24(2)	1
C20	4529(7)	3346(4)	1629(7)	29(2)	1
C21	4919(7)	4664(4)	2227(6)	29(2)	1
C22	6554(7)	3943(4)	1471(6)	20(2)	1
C23	7253(7)	3308(4)	1445(6)	25(2)	1
C24	8584(8)	3500(4)	1602(6)	26(2)	1
C25	8702(7)	4247(4)	1749(6)	21(2)	1
C26	9898(7)	4727(4)	1938(6)	23(2)	1
C27	11129(7)	4276(4)	2602(6)	27(2)	1
C28	9854(7)	5391(4)	2800(6)	24(2)	1
N5	12231(5)	7191(3)	1346(5)	21(1)	1
N6	12427(6)	8360(3)	1627(5)	22(1)	1

C29	12556(8)	6414(4)	1218(8)	36(2)	1
C30	11039(7)	7459(4)	1425(7)	32(2)	1
C31	11154(8)	8175(5)	1575(7)	35(2)	1
C32	13052(7)	7764(4)	1478(6)	23(2)	1
C33	13014(7)	9108(4)	1757(6)	29(2)	1
S1	6630(2)	6572(1)	1474(2)	26(1)	1
O1	6709(5)	6087(3)	434(4)	32(1)	1
O2	7920(4)	7049(3)	1674(5)	32(1)	1
O3	5528(5)	7058(3)	1118(5)	46(2)	1
O4	6779(6)	6169(3)	2661(5)	53(2)	1
C34	8302(8)	7448(4)	2890(7)	47(2)	1
C35	11649(7)	8606(4)	5250(7)	34(2)	1
Cl1	10403(2)	9140(1)	4241(2)	46(1)	1
Cl2	11152(2)	7684(1)	5323(2)	48(1)	1
C36	5620(7)	7271(4)	4795(10)	67(3)	1
Cl3	3959(3)	7322(1)	4594(3)	75(1)	1
Cl4	6402(3)	8131(2)	5103(2)	75(1)	1

2.5·EMIM NO_3 COMPLEX

Table 1. Crystal data and structure refinement for $C_{28}H_{36}N_4 \cdot C_6H_{11}N_2 \cdot NO_3 \cdot 1.5CH_2Cl_2$

Empirical formula	$C_{35.50}H_{50}Cl_3N_7O_3$
Formula weight	729.17
Temperature	120(2) K
Wavelength	0.71073 Å
Crystal system	Monoclinic
Space group	*C*2/*c*
Unit cell dimensions	$a = 43.504(9)$ Å
	$b = 14.730(3)$ Å $\quad \beta = 101.66(3)°$
	$c = 11.894(2)$ Å
Volume	7465(3) $Å^3$
Z	8
Density (calculated)	1.298 Mg / m^3
Absorption coefficient	0.290 mm^{-1}
F(000)	3096
Crystal	Slab; Colourless
Crystal size	0.12 × 0.08 × 0.02 mm^3
θ range for data collection	2.93 – 25.03°
Index ranges	$-45 \le h \le 51$, $-16 \le k \le 17$, $-13 \le l \le 14$
Reflections collected	21083
Independent reflections	6274 [$R_{int} = 0.1755$]
Completeness to $\theta = 25.03°$	95.0 %
Absorption correction	Semi–empirical from equivalents

Max. and min. transmission	0.9942 and 0.9660
Refinement method	Full-matrix least-squares on F^2
Data / restraints / parameters	6274 / 0 / 449
Goodness-of-fit on F^2	1.082
Final R indices [$F^2 > 2\sigma(F^2)$]	$R1$ = 0.1650, $wR2$ = 0.3889
R indices (all data)	$R1$ = 0.2849, $wR2$ = 0.4468
Extinction coefficient	0.0050(8)
Largest diff. peak and hole	0.858 and –0.725 e Å^{-3}

Diffractometer: *Nonius KappaCCD* area detector (ϕ scans and ω scans to fill *asymmetric unit*). **Cell determination:** DirAx (Duisenberg, A.J.M.(1992). J. Appl. Cryst. 25, 92-96.) **Data collection:** Collect (Collect: Data collection software, R. Hooft, Nonius B.V., 1998). **Data reduction and cell refinement**: *Denzo* (Z. Otwinowski & W. Minor, *Methods in Enzymology* (1997) Vol. **276**: *Macromolecular Crystallography*, part A, pp. 307–326; C. W. Carter, Jr. & R. M. Sweet, Eds., Academic Press). **Absorption correction**: Sheldrick, G. M. SADABS - Bruker Nonius area detector scaling and absorption correction - V2.10 **Structure solution**: *SHELXS97* (G. M. Sheldrick, Acta Cryst. (1990) A**46** 467–473). **Structure refinement**: *SHELXL97* (G. M. Sheldrick (1997), University of Göttingen, Germany). **Graphics:** Cameron - A Molecular Graphics Package. (D. M. Watkin, L. Pearce and C. K. Prout, Chemical Crystallography Laboratory, University of Oxford, 1993).

Special details: All hydrogen atoms were placed in idealised positions and refined using a riding model.

Table 2. Atomic coordinates [× 10^4], equivalent isotropic displacement parameters [Å^2 × 10^3] and site occupancy factors. U_{eq} is defined as one third of the trace of the orthogonalized U^{ij} tensor.

Atom	*x*	*y*	*z*	U_{eq}	*S.o.f.*
N1	1916(2)	3058(6)	3699(8)	34(2)	1
N2	1555(2)	1073(6)	2999(8)	35(2)	1
N3	849(2)	2141(6)	2488(8)	28(2)	1
N4	1197(2)	4121(6)	3048(8)	31(2)	1
C1	1938(3)	3930(7)	3260(10)	33(3)	1
C2	2154(3)	3859(8)	2547(10)	39(3)	1
C3	2256(3)	2953(7)	2589(10)	32(3)	1
C4	2111(3)	2456(8)	3307(10)	35(3)	1
C5	2132(3)	1488(7)	3643(10)	34(3)	1
C6	2137(3)	1361(7)	4891(10)	38(3)	1
C7	2441(3)	1105(7)	3383(10)	35(3)	1
C8	1863(3)	977(7)	2897(10)	35(3)	1
C9	1850(3)	348(7)	2052(10)	36(3)	1
C10	1537(3)	87(7)	1665(10)	33(3)	1
C11	1355(3)	543(7)	2276(9)	30(3)	1
C12	1014(3)	517(7)	2297(10)	37(3)	1
C13	864(3)	–289(7)	1515(12)	43(3)	1
C14	970(3)	315(8)	3533(11)	41(3)	1
C15	839(3)	1337(9)	1847(11)	41(3)	1
C16	634(3)	1501(8)	841(12)	46(3)	1
C17	524(3)	2416(7)	881(11)	39(3)	1
C18	656(3)	2792(7)	1910(10)	33(3)	1
C19	631(3)	3707(7)	2361(10)	36(3)	1
C20	342(3)	4194(7)	1646(11)	41(3)	1
C21	572(3)	3644(8)	3599(10)	39(3)	1
C22	913(3)	4279(7)	2349(10)	28(3)	1
C23	960(3)	4990(8)	1682(11)	37(3)	1
C24	1272(3)	5283(7)	2034(11)	44(3)	1

C25	1429(3)	4714(7)	2896(9)	30(3)	1
C26	1754(3)	4706(8)	3556(10)	38(3)	1
C27	1748(3)	4678(8)	4871(10)	39(3)	1
C28	1917(3)	5606(7)	3324(10)	35(3)	1
N5	1177(2)	3145(6)	-524(9)	38(3)	1
N6	1518(2)	2085(6)	-566(8)	32(2)	1
C29	924(3)	3780(8)	-915(11)	46(3)	1
C30	1326(3)	3002(9)	574(11)	43(3)	1
C31	1538(3)	2347(8)	578(12)	45(3)	1
C32	1298(3)	2555(8)	-1190(12)	44(3)	1
C33	1717(3)	1410(8)	-968(11)	48(4)	1
C34	2048(3)	1716(9)	-796(15)	61(4)	1
C36	332(4)	2194(10)	6368(13)	67(4)	1
Cl1	447(1)	1923(3)	7861(4)	74(1)	1
Cl2	237(1)	3326(3)	6183(4)	70(1)	1
C37	0	1097(13)	2500	52(5)	1
Cl3	-103(1)	485(4)	1253(4)	94(2)	1
O1	1587(2)	2515(6)	6368(7)	48(2)	1
O2	1076(2)	2437(6)	5910(8)	52(2)	1
O3	1341(2)	2487(5)	4553(7)	42(2)	1
N7	1336(3)	2477(6)	5649(10)	41(3)	1

2.7·TEACl COMPLEX

Table 1. Crystal data and structure refinement details.

Empirical formula	$C_{36}H_{56}ClN_5$
Formula weight	594.31
Temperature	120(2) K
Wavelength	0.71073 Å
Crystal system	Orthorhombic
Space group	$Pna2_1$
Unit cell dimensions	a = 18.0598(16) Å
	b = 10.1251(5) Å
	c = 18.8428(15) Å
Volume	3445.5(4) Å^3
Z	4
Density (calculated)	1.146 Mg / m^3
Absorption coefficient	0.142 mm^{-1}
F(000)	1296
Crystal	Block; Pale Orange
Crystal size	0.2 × 0.11 × 0.03 mm^3
θ range for data collection	3.12 – 26.13°
Index ranges	$-18 \le h \le 22$, $-12 \le k \le 9$, $-22 \le l \le 23$
Reflections collected	20888
Independent reflections	6498 [R_{int} = 0.1074]

Completeness to $\theta = 26.13°$	98.4 %
Absorption correction	Semi–empirical from equivalents
Max. and min. transmission	0.9957 and 0.9621
Refinement method	Full-matrix least-squares on F^2
Data / restraints / parameters	6498 / 473 / 379
Goodness-of-fit on F^2	1.117
Final R indices $[F^2 > 2\sigma(F^2)]$	$R1 = 0.1340$, $wR2 = 0.3189$
R indices (all data)	$R1 = 0.2411$, $wR2 = 0.3836$
Absolute structure parameter	0.50(12)
Largest diff. peak and hole	0.928 and –0.574 e Å^{-3}

Diffractometer: *Nonius KappaCCD* area detector (ϕ scans and ω scans to fill *asymmetric unit*). **Cell determination:** DirAx (Duisenberg, A.J.M.(1992). J. Appl. Cryst. 25, 92-96.) **Data collection:** Collect (Collect: Data collection software, R. Hooft, Nonius B.V., 1998). **Data reduction and cell refinement**: *Denzo* (Z. Otwinowski & W. Minor, *Methods in Enzymology* (1997) Vol. **276**: *Macromolecular Crystallography*, part A, pp. 307–326; C. W. Carter, Jr. & R. M. Sweet, Eds., Academic Press). **Absorption correction**: Sheldrick, G. M. SADABS - Bruker Nonius area detector scaling and absorption correction - V2.10 **Structure solution**: *SHELXS97* (G. M. Sheldrick, Acta Cryst. (1990) A**46** 467–473). **Structure refinement**: *SHELXL97* (G. M. Sheldrick (1997), University of Göttingen, Germany). **Graphics:** Cameron - A Molecular Graphics Package. (D. M. Watkin, L. Pearce and C. K. Prout, Chemical Crystallography Laboratory, University of Oxford, 1993).

Special details: All hydrogen atoms were placed in idealised positions and refined using a riding model.

Table 2. Atomic coordinates [× 10^4], equivalent isotropic displacement parameters [Å^2 × 10^3] and site occupancy factors. U_{eq} is defined as one third of the trace of the orthogonalized U^{ij} tensor.

Atom	*x*	*y*	*z*	U_{eq}	*S.o.f.*
N5A	9495(1)	3756(2)	1224(1)	82(1)	0.50
C36B	9043(3)	5356(7)	309(3)	83(1)	0.50
C35B	9653(3)	4904(4)	839(2)	83(1)	0.50
C31B	10118(3)	3651(5)	1721(2)	83(1)	0.50
C32B	10165(4)	2598(5)	2317(3)	83(1)	0.50
C29A	8911(3)	4048(4)	1723(2)	83(1)	0.50
C30A	8930(4)	5244(5)	2239(3)	83(1)	0.50
C33A	9409(2)	2595(4)	815(3)	83(1)	0.50
C34A	10119(3)	2166(7)	417(4)	83(1)	0.50
N5B	9495(1)	3756(2)	1224(1)	82(1)	0.50
C36A	8730(4)	5108(4)	233(3)	83(1)	0.50
C35A	8909(3)	3901(4)	705(2)	83(1)	0.50
C31A	9347(3)	2442(4)	1441(2)	83(1)	0.50
C32A	9876(3)	2013(7)	2040(3)	83(1)	0.50
C29B	9590(2)	4871(4)	1642(2)	83(1)	0.50
C30B	8933(3)	4924(8)	2169(3)	83(1)	0.50
C33B	10132(3)	3606(5)	738(2)	83(1)	0.50
C34B	10203(5)	2531(5)	160(3)	83(1)	0.50
Cl1	12738(1)	7459(1)	1227(1)	76(1)	1
C26	11571(2)	6237(3)	–27(1)	50(1)	1
N2	11579(2)	6189(2)	2474(1)	55(1)	1
N1	12370(1)	4315(2)	1216(2)	64(1)	1
C27	11673(2)	5017(3)	–332(2)	66(1)	1
N3	10860(1)	8183(2)	1273(2)	74(1)	1
C18	10434(2)	8268(3)	1822(2)	62(1)	1

C4	12231(2)	3557(3)	647(2)	60(1)	1
C21	10401(2)	8214(3)	628(2)	57(1)	1
C5	12080(2)	2336(3)	875(2)	65(1)	1
C11	11723(2)	4969(3)	2761(2)	59(1)	1
C9	12328(2)	4070(3)	2571(2)	67(1)	1
C7	12282(2)	3559(3)	1844(2)	58(1)	1
C28	11177(2)	4855(3)	-779(2)	79(1)	1
C13	10704(2)	5956(3)	3258(2)	79(1)	1
C16	10709(2)	8142(3)	2559(2)	67(1)	1
C19	9700(2)	8286(3)	1594(2)	72(1)	1
C12	11153(2)	4757(3)	3286(2)	71(1)	1
C23	10683(2)	8232(3)	-146(2)	66(1)	1
C2	12340(2)	4145(3)	-117(2)	63(1)	1
C20	9704(2)	8339(3)	861(2)	72(1)	1
C25	10970(2)	6769(3)	-306(2)	63(1)	1
C8	12284(2)	2826(3)	3093(2)	84(1)	1
C3	12430(2)	3018(4)	-642(2)	77(1)	1
C24	11341(2)	9138(3)	-199(2)	83(1)	1
C14	10966(2)	6837(3)	2785(2)	65(1)	1
C17	11341(3)	9200(4)	2686(2)	113(2)	1
C1	13033(2)	4825(4)	-261(2)	86(1)	1
C22	9998(3)	8485(3)	-616(2)	86(1)	1
C10	13101(2)	4996(3)	2602(2)	62(1)	1
C6	12076(2)	2314(3)	1610(2)	67(1)	1
C15	10165(3)	8682(4)	3133(2)	98(1)	1
N4	10714(2)	5968(3)	-815(2)	96(1)	1

2.7·EMIMCl COMPLEX

Table 1. Crystal data and structure refinement details.

Empirical formula	$C_{35}H_{49}Cl_3N_6$	
Formula weight	660.15	
Temperature	120(2) K	
Wavelength	0.71073 Å	
Crystal system	Monoclinic	
Space group	$P2_1$	
Unit cell dimensions	a = 10.5513(19) Å	
	b = 15.868(2) Å	β = 100.578(6)°
	c = 10.5844(19) Å	
Volume	1742.0(5) Å^3	
Z	2	
Density (calculated)	1.259 Mg / m^3	
Absorption coefficient	0.297 mm^{-1}	
F(000)	704	
Crystal	Lath; Colourless	

Crystal size	$0.2 \times 0.04 \times 0.02$ mm^3
θ range for data collection	3.23 – 27.26°
Index ranges	$-11 \le h \le 13$, $-16 \le k \le 20$, $-10 \le l \le 13$
Reflections collected	15161
Independent reflections	6950 [$R_{int} = 0.1688$]
Completeness to $\theta = 27.26°$	98.9 %
Absorption correction	Semi–empirical from equivalents
Max. and min. transmission	0.9941 and 0.9330
Refinement method	Full-matrix least-squares on F^2
Data / restraints / parameters	6950 / 1 / 407
Goodness-of-fit on F^2	1.019
Final R indices [$F^2 > 2\sigma(F^2)$]	$R1 = 0.0932$, $wR2 = 0.1866$
R indices (all data)	$R1 = 0.1819$, $wR2 = 0.2228$
Absolute structure parameter	0.05(11)
Largest diff. peak and hole	0.573 and –0.354 e Å^{-3}

Diffractometer: *Nonius KappaCCD* area detector (ϕ scans and ω scans to fill *asymmetric unit*). **Cell determination:** DirAx (Duisenberg, A.J.M.(1992). J. Appl. Cryst. 25, 92-96.) **Data collection:** Collect (Collect: Data collection software, R. Hooft, Nonius B.V., 1998). **Data reduction and cell refinement**: *Denzo* (Z. Otwinowski & W. Minor, *Methods in Enzymology* (1997) Vol. **276**: *Macromolecular Crystallography*, part A, pp. 307–326; C. W. Carter, Jr. & R. M. Sweet, Eds., Academic Press). **Absorption correction**: Sheldrick, G. M. SADABS - Bruker Nonius area detector scaling and absorption correction - V2.10 **Structure solution**: *SHELXS97* (G. M. Sheldrick, Acta Cryst. (1990) A**46** 467–473). **Structure refinement**: *SHELXL97* (G. M. Sheldrick (1997), University of Göttingen, Germany). **Graphics:** Cameron - A Molecular Graphics Package. (D. M. Watkin, L. Pearce and C. K. Prout, Chemical Crystallography Laboratory, University of Oxford, 1993).

Special details: All hydrogen atoms were placed in idealised positions and refined using a riding model.

Table 2. Atomic coordinates [$\times 10^4$], equivalent isotropic displacement parameters [Å$^2 \times 10^3$] and site occupancy factors. U_{eq} is defined as one third of the trace of the orthogonalized U^{ij} tensor.

Atom	*x*	*y*	*z*	U_{eq}	*S.o.f.*
C1	–3104(6)	2194(4)	991(6)	26(2)	1
C2	–4030(6)	1823(4)	1601(7)	29(2)	1
C3	–3782(7)	2124(4)	2888(7)	34(2)	1
C4	–2765(6)	2665(4)	3042(7)	28(2)	1
C5	–2068(7)	3129(4)	4211(7)	31(2)	1
C6	–3009(7)	3227(4)	5180(7)	33(2)	1
C7	–1701(7)	4031(4)	3869(7)	33(2)	1
C8	–888(6)	2649(4)	4868(6)	27(2)	1
C9	–671(7)	2180(5)	5963(7)	32(2)	1
C10	574(7)	1827(5)	6096(7)	33(2)	1
C11	1113(6)	2083(4)	5080(6)	27(2)	1
C12	2452(6)	1908(4)	4786(6)	26(2)	1
C13	3260(8)	1472(5)	5943(7)	41(2)	1
C14	3108(7)	2756(5)	4583(8)	38(2)	1
C15	2421(6)	1353(4)	3619(7)	30(2)	1

C16	2897(6)	549(4)	3513(7)	32(2)	1
C17	2732(7)	331(5)	2206(7)	33(2)	1
C18	2162(6)	1005(4)	1504(7)	30(2)	1
C19	1782(6)	1136(4)	76(6)	26(2)	1
C20	2307(7)	408(4)	−633(7)	32(2)	1
C21	2381(6)	1971(4)	−289(7)	32(2)	1
C22	320(6)	1209(4)	−317(6)	27(2)	1
C23	−466(6)	1862(4)	−108(6)	25(2)	1
C24	−1766(6)	1612(4)	−525(7)	28(2)	1
C25	−1728(6)	807(4)	−965(7)	28(2)	1
C26	−2948(6)	2131(4)	−394(7)	28(2)	1
C27	−4138(7)	1747(5)	−1205(8)	39(2)	1
C28	−2771(8)	3043(4)	−899(7)	38(2)	1
C29	−3200(11)	230(7)	5205(12)	86(4)	1
C30	−1801(10)	4(5)	5404(8)	57(3)	1
C31	−1195(7)	636(5)	3403(7)	37(2)	1
C32	−801(7)	349(4)	2374(7)	33(2)	1
C33	−1046(6)	−736(4)	3600(7)	33(2)	1
C34	−232(8)	−1093(5)	1618(8)	48(2)	1
N1	−2355(5)	2685(3)	1877(5)	28(1)	1
N2	213(5)	2585(3)	4321(5)	24(1)	1
N3	1982(5)	1628(3)	2371(5)	26(1)	1
N4	−466(5)	563(3)	−845(5)	30(1)	1
N5	−1366(6)	−35(3)	4181(6)	32(1)	1
N6	−694(5)	−511(4)	2513(6)	31(1)	1
Cl1	714(2)	3610(1)	1817(2)	33(1)	1
C35	4110(8)	3759(5)	1105(8)	46(2)	1
Cl2	4881(2)	4494(1)	2212(2)	54(1)	1
Cl3	3882(2)	4145(1)	−482(2)	59(1)	1

2.7·BMIMCl COMPLEX

Table 1. Crystal data and structure refinement details.

Empirical formula	$C_{37}H_{53}Cl_3N_6$
Formula weight	688.20
Temperature	120(2) K
Wavelength	0.6709 Å
Crystal system	Monoclinic
Space group	*P*21/*c*
Unit cell dimensions	*a* = 10.5860(11) Å

	$b = 15.8800(17)$ Å $\quad \beta = 94.452(2)°$
	$c = 21.868(2)$ Å
Volume	3665.0(6) Å^3
Z	4
Density (calculated)	1.247 Mg / m^3
Absorption coefficient	0.285 mm^{-1}
F(000)	1472
Crystal	Lath; Colourless
Crystal size	0.15 × 0.05 × 0.01 mm^3
θ range for data collection	2.90 – 23.54°
Index ranges	$-12 \le h \le 12$, $-18 \le k \le 18$, $-26 \le l \le 26$
Reflections collected	27170
Independent reflections	6453 [$R_{int} = 0.0700$]
Completeness to $\theta = 23.54°$	99.6 %
Absorption correction	Semi–empirical from equivalents
Max. and min. transmission	0.9972 and 0.9585
Refinement method	Full-matrix least-squares on F^2
Data / restraints / parameters	6453 / 0 / 425
Goodness-of-fit on F^2	1.050
Final R indices [$F^2 > 2\sigma(F^2)$]	$R1 = 0.0813$, $wR2 = 0.1776$
R indices (all data)	$R1 = 0.1131$, $wR2 = 0.1925$
Largest diff. peak and hole	0.799 and –0.754 e Å^{-3}

Diffractometer: *Nonius KappaCCD* area detector (ϕ scans and ω scans to fill *asymmetric unit*). **Cell determination:** DirAx (Duisenberg, A.J.M.(1992). J. Appl. Cryst. 25, 92-96.) **Data collection:** Collect (Collect: Data collection software, R. Hooft, Nonius B.V., 1998). **Data reduction and cell refinement**: *Denzo* (Z. Otwinowski & W. Minor, *Methods in Enzymology* (1997) Vol. **276**: *Macromolecular Crystallography*, part A, pp. 307–326; C. W. Carter, Jr. & R. M. Sweet, Eds., Academic Press). **Absorption correction**: Sheldrick, G. M. SADABS - Bruker Nonius area detector scaling and absorption correction - V2.10 **Structure solution**: *SHELXS97* (G. M. Sheldrick, Acta Cryst. (1990) **A46** 467–473). **Structure refinement**: *SHELXL97* (G. M. Sheldrick (1997), University of Göttingen, Germany). **Graphics:** Cameron - A Molecular Graphics Package. (D. M. Watkin, L. Pearce and C. K. Prout, Chemical Crystallography Laboratory, University of Oxford, 1993).

Special details: All hydrogen atoms were placed in idealised positions and refined using a riding model.

Table 2. Atomic coordinates [× 10^4], equivalent isotropic displacement parameters [Å^2 × 10^3] and site occupancy factors. U_{eq} is defined as one third of the trace of the orthogonalized U^{ij} tensor.

Atom	*x*	*y*	*z*	U_{eq}	*S.o.f.*
C1	10018(4)	1115(3)	1712(2)	28(1)	1
C2	10437(4)	1933(3)	1731(2)	30(1)	1
N1	10634(3)	2171(2)	2330(2)	34(1)	1
C4	10359(4)	1507(3)	2708(2)	27(1)	1
C5	10327(4)	1570(3)	3399(2)	31(1)	1
C6	10862(4)	754(3)	3697(2)	35(1)	1
C7	11129(5)	2316(3)	3655(2)	41(1)	1
C8	8966(4)	1689(3)	3551(2)	29(1)	1
C9	8344(4)	2376(3)	3762(2)	32(1)	1
C10	7077(4)	2137(3)	3840(2)	31(1)	1
C11	6934(4)	1310(3)	3678(2)	28(1)	1

C12	5793(4)	721(3)	3704(2)	28(1)	1
C13	6222(5)	−101(3)	4033(2)	36(1)	1
C14	4825(5)	1154(3)	4082(2)	36(1)	1
C15	5167(4)	527(3)	3072(2)	25(1)	1
C16	3990(4)	749(3)	2815(2)	28(1)	1
C17	3832(4)	393(3)	2225(2)	28(1)	1
C18	4918(4)	−44(3)	2118(2)	25(1)	1
C19	5282(4)	−510(3)	1554(2)	26(1)	1
C20	4082(4)	−616(3)	1112(2)	32(1)	1
C21	5785(4)	−1399(3)	1725(2)	28(1)	1
C22	6270(4)	−28(3)	1231(2)	27(1)	1
C23	6159(5)	431(3)	698(2)	37(1)	1
C24	7365(5)	745(3)	590(2)	38(1)	1
C25	8204(4)	487(3)	1055(2)	29(1)	1
C26	9636(4)	594(3)	1145(2)	29(1)	1
C27	10103(5)	1019(3)	572(2)	40(1)	1
C28	10239(4)	−288(3)	1214(2)	34(1)	1
C29	8299(5)	3745(3)	2237(2)	40(1)	1
C30	7355(4)	2287(3)	2108(2)	33(1)	1
C31	6180(4)	1989(3)	1958(2)	35(1)	1
C32	6058(4)	3368(3)	1965(2)	28(1)	1
C33	3985(4)	2624(3)	1734(2)	37(1)	1
C34	3629(5)	2124(4)	1153(3)	49(1)	1
C35	4019(7)	2525(4)	597(3)	63(2)	1
C36	3473(6)	2025(4)	3(2)	54(2)	1
C46	8738(6)	1112(5)	5106(3)	66(2)	1
C3	9988(4)	852(3)	2328(2)	26(1)	1
N2	8094(3)	1043(2)	3503(2)	29(1)	1
N3	5723(3)	44(2)	2645(2)	25(1)	1
N4	7528(3)	21(2)	1450(2)	27(1)	1
N5	7250(3)	3156(2)	2104(2)	27(1)	1
N6	5376(3)	2665(2)	1869(2)	26(1)	1
Cl1	8414(1)	−891(1)	2862(1)	32(1)	1
Cl2	10233(2)	1232(1)	5486(1)	66(1)	1
Cl3	7502(2)	1282(2)	5576(1)	119(1)	1

2.7·EtPyCl COMPLEX

Table 1. Crystal data and structure refinement details.

Empirical formula	$C_{37}H_{49}ClN_6$ $C_{28}H_{36}N_4$, $C_7H_{10}N$, C_2H_3N, Cl
Formula weight	613.27
Temperature	120(2) K
Wavelength	0.71073 Å
Crystal system	Monoclinic
Space group	$P2_1/c$
Unit cell dimensions	a = 10.6535(6) Å

	$b = 15.9296(9)$ Å $\quad \beta = 102.516(4)°$
	$c = 20.5194(13)$ Å
Volume	3399.5(3) Å^3
Z	4
Density (calculated)	1.198 Mg / m^3
Absorption coefficient	0.147 mm^{-1}
F(000)	1320
Crystal	Block; Pale Yellow
Crystal size	0.15 × 0.1 × 0.08 mm^3
θ range for data collection	3.22 – 25.03°
Index ranges	$-12 \le h \le 12$, $-18 \le k \le 18$, $-23 \le l \le 24$
Reflections collected	28953
Independent reflections	5989 [$R_{int} = 0.1076$]
Completeness to $\theta = 25.03°$	99.8 %
Absorption correction	Semi–empirical from equivalents
Max. and min. transmission	0.9883 and 0.9682
Refinement method	Full-matrix least-squares on F^2
Data / restraints / parameters	5989 / 20 / 407
Goodness-of-fit on F^2	1.077
Final R indices [$F^2 > 2\sigma(F^2)$]	$R1 = 0.0897$, $wR2 = 0.1998$
R indices (all data)	$R1 = 0.1485$, $wR2 = 0.2255$
Largest diff. peak and hole	1.032 and –0.371 e Å^{-3}

Diffractometer: *Nonius KappaCCD* area detector (ϕ scans and ω scans to fill *asymmetric unit*). **Cell determination:** DirAx (Duisenberg, A.J.M.(1992). J. Appl. Cryst. 25, 92-96.) **Data collection:** Collect (Collect: Data collection software, R. Hooft, Nonius B.V., 1998). **Data reduction and cell refinement**: *Denzo* (Z. Otwinowski & W. Minor, *Methods in Enzymology* (1997) Vol. **276**: *Macromolecular Crystallography*, part A, pp. 307–326; C. W. Carter, Jr. & R. M. Sweet, Eds., Academic Press). **Absorption correction**: Sheldrick, G. M. SADABS - Bruker Nonius area detector scaling and absorption correction - V2.10 **Structure solution**: *SHELXS97* (G. M. Sheldrick, Acta Cryst. (1990) A**46** 467–473). **Structure refinement**: *SHELXL97* (G. M. Sheldrick (1997), University of Göttingen, Germany). **Graphics:** Cameron - A Molecular Graphics Package. (D. M. Watkin, L. Pearce and C. K. Prout, Chemical Crystallography Laboratory, University of Oxford, 1993).

Special details: All hydrogen atoms were placed in idealised positions and refined using a riding model.

Table 2. Atomic coordinates [× 10^4], equivalent isotropic displacement parameters [Å^2 × 10^3] and site occupancy factors. U_{eq} is defined as one third of the trace of the orthogonalized U^{ij} tensor.

Atom	*x*	*y*	*z*	U_{eq}	*S.o.f.*
Cl1	3305(1)	10403(1)	2191(1)	39(1)	1
N1	2796(3)	8422(2)	1510(2)	34(1)	1
N2	893(3)	9265(2)	2448(2)	29(1)	1
N3	3453(3)	9501(2)	3751(2)	36(1)	1
N4	6257(4)	7475(2)	2767(2)	42(1)	1
C1	3693(4)	7826(3)	1438(2)	32(1)	1
C2	3033(4)	7132(3)	1192(3)	42(1)	1
C3	1705(4)	7301(3)	1111(2)	42(1)	1
C4	1571(4)	8104(3)	1312(2)	29(1)	1
C5	365(4)	8629(3)	1281(2)	32(1)	1
C6	498(4)	9469(3)	927(2)	37(1)	1

C7	−780(4)	8157(3)	868(2)	38(1)	1
C8	103(4)	8788(3)	1967(2)	28(1)	1
C9	−910(4)	8536(3)	2238(2)	33(1)	1
C10	−726(4)	8875(3)	2890(2)	32(1)	1
C11	387(4)	9324(3)	3010(2)	31(1)	1
C12	1071(4)	9798(3)	3633(2)	32(1)	1
C13	192(4)	9810(3)	4139(2)	43(1)	1
C14	1317(4)	10713(3)	3457(2)	38(1)	1
C15	2311(4)	9368(3)	3946(2)	31(1)	1
C16	2575(4)	8785(3)	4440(2)	38(1)	1
C17	3883(4)	8571(3)	4547(2)	41(1)	1
C18	4421(4)	9022(3)	4121(2)	30(1)	1
C19	5806(4)	9043(3)	4028(2)	31(1)	1
C20	6696(4)	8708(3)	4667(2)	46(1)	1
C21	6183(4)	9958(3)	3921(3)	41(1)	1
C22	5920(4)	8519(2)	3430(2)	27(1)	1
C23	6448(4)	7744(3)	3420(2)	36(1)	1
C24	5407(4)	8733(2)	2765(2)	23(1)	1
C25	5615(4)	8082(3)	2356(2)	29(1)	1
C26	5134(4)	8000(3)	1608(2)	32(1)	1
C27	5402(4)	8819(3)	1264(2)	41(1)	1
C28	5822(4)	7273(3)	1344(3)	44(1)	1
N5	1142(3)	6536(2)	3098(2)	34(1)	1
C29	1542(4)	5772(3)	2956(2)	37(1)	1
C30	2724(5)	5677(3)	2797(2)	45(1)	1
C31	3481(5)	6369(3)	2786(3)	50(1)	1
C32	3042(5)	7146(3)	2933(2)	45(1)	1
C33	1874(5)	7217(3)	3088(2)	42(1)	1
C34	−123(4)	6629(3)	3287(2)	42(1)	1
C35	39(5)	6817(3)	4020(3)	54(1)	1
N6	2955(5)	5423(4)	4590(3)	81(2)	1
C36	3249(6)	4877(5)	4983(4)	82(2)	1
C37	3786(9)	4163(5)	5491(4)	112(3)	1

STRUCUTRES FROM CHATPER 3

DIMETHYLSULFOXIDE COMPLEX 3.7a

Table 1. Crystal data and structure refinement details.

Empirical formula	$C_{31}H_{37}N_5O_4S_2$
Formula weight	607.78
Temperature	120(2) K
Wavelength	0.71073 Å
Crystal system	Monoclinic
Space group	*C*2/*c*
Unit cell dimensions	a = 26.9646(10) Å
	b = 9.8223(3) Å β = 119.586(3)°
	c = 27.2375(10) Å
Volume	6273.4(4) Å^3
Z	8
Density (calculated)	1.287 Mg / m^3
Absorption coefficient	0.213 mm^{-1}
F(000)	2576
Crystal	Slab; Colourless
Crystal size	0.35 × 0.2 × 0.08 mm^3
θ range for data collection	2.99 – 27.48°
Index ranges	$-34 \le h \le 34$, $-12 \le k \le 11$, $-35 \le l \le 35$
Reflections collected	37226
Independent reflections	7183 [R_{int} = 0.0784]
Completeness to θ = 27.48°	99.8 %
Absorption correction	Semi–empirical from equivalents
Max. and min. transmission	0.9831 and 0.9191
Refinement method	Full-matrix least-squares on F^2
Data / restraints / parameters	7183 / 510 / 392
Goodness-of-fit on F^2	1.050
Final *R* indices [$F^2 > 2\sigma(F^2)$]	*R1* = 0.0925, *wR2* = 0.2375
R indices (all data)	*R1* = 0.1403, *wR2* = 0.2748
Extinction coefficient	0.0039(5)
Largest diff. peak and hole	1.238 and –1.454 e Å^{-3}

Diffractometer: *Nonius KappaCCD* area detector (ϕ scans and ω scans to fill *asymmetric unit*). **Cell determination:** DirAx (Duisenberg, A.J.M.(1992). J. Appl. Cryst. 25, 92-96.) **Data collection:** Collect (Collect: Data collection software, R. Hooft, Nonius B.V., 1998). **Data reduction and cell refinement**: *Denzo* (Z. Otwinowski & W. Minor, *Methods in Enzymology* (1997) Vol. **276**: *Macromolecular Crystallography*, part A, pp. 307–326; C. W. Carter, Jr. & R. M. Sweet, Eds., Academic Press). **Absorption correction**: Sheldrick, G. M. SADABS - Bruker Nonius area detector scaling and absorption correction - V2.10 **Structure solution**: *SHELXS97* (G. M. Sheldrick, Acta Cryst. (1990) A**46** 467–473). **Structure refinement**: *SHELXL97* (G. M. Sheldrick (1997), University of Göttingen, Germany). **Graphics:** Cameron - A Molecular Graphics Package. (D. M. Watkin, L. Pearce and C. K. Prout, Chemical Crystallography Laboratory, University of Oxford, 1993).

Special details: All hydrogen atoms were placed in idealised positions and refined using a riding model.

Table 2. Atomic coordinates [× 10^4], equivalent isotropic displacement parameters [$Å^2$ × 10^3] and site occupancy factors. U_{eq} is defined as one third of the trace of the orthogonalized U^{ij} tensor.

Atom	*x*	*y*	*z*	U_{eq}	*S.o.f.*
O1	214(1)	8197(3)	−338(1)	51(1)	1
O2	2726(1)	8305(3)	2309(1)	52(1)	1
N1	1058(1)	4065(3)	−105(1)	38(1)	1
N2	1039(1)	7070(3)	−124(1)	39(1)	1
N3	1560(1)	8034(3)	916(1)	35(1)	1
N4	2625(1)	7097(3)	1550(1)	37(1)	1
N5	2722(1)	4090(3)	1705(1)	34(1)	1
C1	1110(4)	1633(5)	153(3)	103(3)	1
C2	972(2)	2725(4)	−273(2)	56(1)	1
C3	737(2)	2641(5)	−850(2)	52(1)	1
C4	559(3)	1378(6)	−1209(3)	93(2)	1
C5	666(2)	4003(4)	−1051(2)	39(1)	1
C6	421(2)	4591(5)	−1591(2)	51(1)	1
C7	391(2)	5988(6)	−1634(2)	69(2)	1
C8	596(2)	6834(5)	−1161(2)	65(1)	1
C9	831(2)	6272(4)	−625(1)	38(1)	1
C10	869(1)	4867(4)	−575(1)	30(1)	1
C11	716(2)	7901(4)	−6(2)	39(1)	1
C12	1016(2)	8414(4)	595(2)	37(1)	1
C13	720(2)	9177(4)	798(2)	43(1)	1
C14	1009(2)	9559(4)	1361(2)	44(1)	1
C15	1574(2)	9186(4)	1701(2)	42(1)	1
C16	1834(2)	8413(4)	1459(2)	37(1)	1
C17	2439(2)	7945(4)	1816(2)	37(1)	1
C18	3155(2)	6414(4)	1828(2)	38(1)	1
C19	3677(2)	7072(6)	2058(2)	59(1)	1
C20	4187(2)	6333(8)	2333(2)	77(2)	1
C21	4195(2)	4948(8)	2385(2)	68(2)	1
C22	3681(2)	4247(5)	2158(2)	48(1)	1
C23	3166(1)	5000(4)	1878(1)	33(1)	1
C24	3930(3)	1672(7)	2429(3)	95(2)	1
C25	3524(2)	2860(5)	2154(2)	55(1)	1
C26	2942(2)	2795(4)	1877(2)	47(1)	1
C27	2546(3)	1631(5)	1764(2)	68(2)	1
S1	1185(1)	4883(1)	1356(1)	45(1)	1
O3	1523(1)	4486(3)	1075(1)	38(1)	1
C28	1021(2)	3346(6)	1586(2)	65(1)	1
C29	486(2)	5221(5)	803(2)	58(1)	1
S2	2510(1)	5231(2)	218(1)	113(1)	1
O4A	2221(1)	6237(3)	387(1)	32(1)	0.823(4)
O4B	2577(6)	3712(14)	325(5)	32(1)	0.177(4)
C30	3171(3)	5367(15)	512(4)	190(6)	1
C31	2241(2)	5407(6)	−521(2)	62(1)	1

ACETONITRILE COMPLEX 3.7a

Table 1. Crystal data and structure refinement details.

Empirical formula	$C_{29}H_{28}N_6O_2$
Formula weight	492.57
Temperature	120(2) K
Wavelength	0.71073 Å
Crystal system	Monoclinic
Space group	*C*2/*c*
Unit cell dimensions	$a = 25.8659(7)$ Å
	$b = 15.8073(7)$ Å $\quad \beta = 95.051(3)°$
	$c = 24.7824(9)$ Å
Volume	10093.4(6) Å^3
Z	16
Density (calculated)	1.297 Mg / m^3
Absorption coefficient	0.085 mm^{-1}
F(000)	4160
Crystal	Plate; Pale Yellow
Crystal size	0.09 × 0.07 × 0.02 mm^3
θ range for data collection	2.96 – 27.48°
Index ranges	$-33 \le h \le 33$, $-20 \le k \le 19$, $-32 \le l \le 31$
Reflections collected	79465
Independent reflections	11562 [$R_{int} = 0.2315$]
Completeness to $\theta = 27.48°$	99.8 %
Absorption correction	Semi–empirical from equivalents
Max. and min. transmission	0.9983 and 0.9884
Refinement method	Full-matrix least-squares on F^2
Data / restraints / parameters	11562 / 0 / 677
Goodness-of-fit on F^2	1.147
Final *R* indices [$F^2 > 2\sigma(F^2)$]	*R1* = 0.1433, *wR2* = 0.1811
R indices (all data)	*R1* = 0.2857, *wR2* = 0.2276
Largest diff. peak and hole	0.399 and –0.331 e Å^{-3}

Diffractometer: *Nonius KappaCCD* area detector (ϕ scans and ω scans to fill *asymmetric unit*). **Cell determination:** DirAx (Duisenberg, A.J.M.(1992). J. Appl. Cryst. 25, 92-96.) **Data collection:** Collect (Collect: Data collection software, R. Hooft, Nonius B.V., 1998). **Data reduction and cell refinement**: *Denzo* (Z. Otwinowski & W. Minor, *Methods in Enzymology* (1997) Vol. **276**: *Macromolecular Crystallography*, part A, pp. 307–326; C. W. Carter, Jr. & R. M. Sweet, Eds., Academic Press). **Absorption correction**: Sheldrick, G. M. SADABS - Bruker Nonius area detector scaling and absorption correction - V2.10 **Structure solution**: *SHELXS97* (G. M. Sheldrick, Acta Cryst. (1990) A**46** 467–473). **Structure refinement**: *SHELXL97* (G. M. Sheldrick (1997), University of Göttingen, Germany). **Graphics:** Cameron - A Molecular Graphics Package. (D. M. Watkin, L. Pearce and C. K. Prout, Chemical Crystallography Laboratory, University of Oxford, 1993).

Special details: All hydrogen atoms were placed in idealised positions and refined using a riding model.

Table 2. Atomic coordinates [× 10^4], equivalent isotropic displacement parameters [$Å^2$ × 10^3] and site occupancy factors. U_{eq} is defined as one third of the trace of the orthogonalized U^{ij} tensor.

Atom	*x*	*y*	*z*	U_{eq}	*S.o.f.*
N1	1671(2)	5824(3)	5320(2)	26(1)	1
N2	1177(2)	7584(3)	5040(2)	23(1)	1
N3	879(2)	8463(3)	4111(2)	22(1)	1
N4	1239(2)	10057(3)	3999(2)	25(1)	1
N5	1794(2)	10915(3)	3090(2)	28(1)	1
O1	744(2)	6440(2)	4700(2)	31(1)	1
O2	809(2)	10153(2)	3160(2)	27(1)	1
C1	2046(2)	4372(4)	5337(3)	36(2)	1
C2	1850(2)	5122(4)	5620(3)	29(2)	1
C3	1809(2)	5269(4)	6155(3)	28(2)	1
C4	1959(2)	4700(4)	6630(3)	39(2)	1
C5	1597(2)	6110(4)	6195(2)	25(1)	1
C6	1510(2)	6630(4)	6633(2)	28(1)	1
C7	1327(2)	7434(4)	6540(2)	31(2)	1
C8	1224(2)	7741(4)	6016(2)	30(2)	1
C9	1305(2)	7247(3)	5571(2)	22(1)	1
C10	1506(2)	6433(4)	5666(2)	24(1)	1
C11	882(2)	7181(3)	4657(2)	23(1)	1
C12	705(2)	7669(4)	4153(2)	22(1)	1
C13	374(2)	7279(4)	3756(2)	26(1)	1
C14	206(2)	7723(4)	3298(3)	27(1)	1
C15	384(2)	8538(4)	3241(2)	26(1)	1
C16	718(2)	8882(4)	3650(2)	24(1)	1
C17	926(2)	9762(4)	3580(2)	23(1)	1
C18	1471(2)	10875(4)	4021(2)	25(1)	1
C19	1467(2)	11352(4)	4493(2)	29(2)	1
C20	1691(3)	12157(4)	4532(3)	36(2)	1
C21	1910(2)	12516(4)	4100(3)	32(2)	1
C22	1925(2)	12057(4)	3621(3)	28(2)	1
C23	1712(2)	11234(3)	3588(2)	24(1)	1
C24	2388(2)	13033(4)	2976(3)	37(2)	1
C25	2137(2)	12223(4)	3116(3)	29(2)	1
C26	2054(2)	11520(4)	2809(3)	28(2)	1
C27	2220(2)	11298(4)	2262(3)	36(2)	1
N6	844(2)	4758(3)	4363(2)	26(1)	1
N7	1314(2)	5611(3)	3403(2)	27(1)	1
N8	1623(2)	7232(3)	3260(2)	21(1)	1
N9	1286(2)	7984(3)	2320(2)	25(1)	1
N10	754(2)	9688(3)	1975(2)	24(1)	1
O3	1834(2)	5534(2)	4192(2)	29(1)	1
O4	1689(2)	9210(2)	2591(2)	27(1)	1
C28	520(2)	4373(4)	5243(2)	31(2)	1
C29	599(2)	4165(4)	4670(2)	27(1)	1
C30	487(2)	3465(3)	4369(2)	25(1)	1
C31	224(3)	2672(4)	4526(3)	36(2)	1
C32	679(2)	3608(4)	3847(2)	26(1)	1
C33	673(2)	3124(4)	3376(3)	32(2)	1
C34	878(2)	3468(4)	2928(3)	35(2)	1
C35	1091(2)	4280(4)	2948(2)	31(2)	1

C36	1107(2)	4770(4)	3407(2)	29(2)	1
C37	898(2)	4425(4)	3863(2)	23(1)	1
C38	1652(2)	5935(4)	3791(2)	23(1)	1
C39	1803(2)	6836(4)	3717(2)	24(1)	1
C40	2122(2)	7235(4)	4116(2)	30(2)	1
C41	2249(2)	8080(4)	4057(3)	31(2)	1
C42	2066(2)	8484(4)	3587(2)	28(1)	1
C43	1755(2)	8039(3)	3195(2)	23(1)	1
C44	1567(2)	8467(4)	2670(3)	26(1)	1
C45	1102(2)	8228(4)	1785(2)	26(1)	1
C46	1136(2)	7656(4)	1363(2)	26(1)	1
C47	942(2)	7848(4)	836(3)	31(2)	1
C48	701(2)	8615(4)	712(3)	31(2)	1
C49	670(2)	9202(4)	1125(2)	25(1)	1
C50	865(2)	9019(3)	1659(2)	24(1)	1
C51	171(3)	10488(4)	661(3)	38(2)	1
C52	446(2)	10025(4)	1133(2)	30(2)	1
C53	511(2)	10308(3)	1655(2)	24(1)	1
C54	334(2)	11114(3)	1897(2)	28(2)	1
N11	712(2)	6171(3)	2268(2)	41(2)	1
C55	539(2)	5623(4)	2019(3)	31(2)	1
C56	333(3)	4903(4)	1692(3)	46(2)	1
N12	1633(2)	9377(4)	5202(2)	50(2)	1
C57	1798(3)	9818(4)	5527(3)	38(2)	1
C58	2011(3)	10405(4)	5948(3)	48(2)	1

3.7a FLUORIDE COMPLEX

Table 1. Crystal data and structure refinement details.

Empirical formula	$C_{43}H_{61}FN_6O_2$	
Formula weight	712.98	
Temperature	120(2) K	
Wavelength	0.71073 Å	
Crystal system	Monoclinic	
Space group	$P2_1$	
Unit cell dimensions	a = 9.8813(4) Å	
	b = 18.1336(7) Å	β = 103.333(2)°
	c = 11.4775(5) Å	
Volume	2001.15(14) Å^3	
Z	2	
Density (calculated)	1.183 Mg / m^3	
Absorption coefficient	0.077 mm^{-1}	
F(000)	772	
Crystal	Fragment; Pale Yellow	
Crystal size	0.2 × 0.18 × 0.03 mm^3	
θ range for data collection	3.30 – 27.48°	
Index ranges	$-12 \le h \le 12$, $-23 \le k \le 23$, $-14 \le l \le 14$	

Reflections collected	17825
Independent reflections	4709 [R_{int} = 0.0580]
Completeness to θ = 27.48°	99.5 %
Absorption correction	Semi–empirical from equivalents
Max. and min. transmission	0.9977 and 0.9733
Refinement method	Full-matrix least-squares on F^2
Data / restraints / parameters	4709 / 1 / 493
Goodness-of-fit on F^2	1.155
Final R indices [$F^2 > 2\sigma(F^2)$]	$R1$ = 0.0754, $wR2$ = 0.1329
R indices (all data)	$R1$ = 0.1058, $wR2$ = 0.1484
Largest diff. peak and hole	0.418 and –0.267 e Å^{-3}

Diffractometer: *Nonius KappaCCD* area detector (ϕ scans and ω scans to fill *asymmetric unit*). **Cell determination:** DirAx (Duisenberg, A.J.M.(1992). J. Appl. Cryst. 25, 92-96.) **Data collection:** Collect (Collect: Data collection software, R. Hooft, Nonius B.V., 1998). **Data reduction and cell refinement**: *Denzo* (Z. Otwinowski & W. Minor, *Methods in Enzymology* (1997) Vol. **276**: *Macromolecular Crystallography*, part A, pp. 307–326; C. W. Carter, Jr. & R. M. Sweet, Eds., Academic Press). **Absorption correction**: Sheldrick, G. M. SADABS - Bruker Nonius area detector scaling and absorption correction - V2.10 **Structure solution**: *SHELXS97* (G. M. Sheldrick, Acta Cryst. (1990) A**46** 467–473). **Structure refinement**: *SHELXL97* (G. M. Sheldrick (1997), University of Göttingen, Germany). **Graphics:** Cameron - A Molecular Graphics Package. (D. M. Watkin, L. Pearce and C. K. Prout, Chemical Crystallography Laboratory, University of Oxford, 1993).

Special details: All hydrogen atoms were placed in idealised positions and refined using a riding model, except those of the NH which were freely refined.

Table 2. Atomic coordinates [× 10^4], equivalent isotropic displacement parameters [Å^2 × 10^3] and site occupancy factors. U_{eq} is defined as one third of the trace of the orthogonalized U^{ij} tensor.

Atom	*x*	*y*	*z*	U_{eq}	*S.o.f.*
F1	8748(3)	4403(2)	6007(3)	42(1)	1
O1	4573(3)	4455(2)	2683(3)	35(1)	1
O2	6700(4)	6275(2)	8184(4)	45(1)	1
N1	8688(4)	3056(2)	5319(3)	26(1)	1
N2	6542(4)	4093(2)	4060(4)	29(1)	1
N3	6095(4)	5176(2)	5563(4)	30(1)	1
N4	8129(4)	5429(2)	7616(4)	31(1)	1
N5	10939(4)	4873(2)	7493(4)	30(1)	1
C1	10568(6)	2415(3)	6761(5)	41(1)	1
C2	9588(5)	2470(3)	5572(4)	28(1)	1
C3	9407(5)	2006(3)	4606(4)	29(1)	1
C4	10139(6)	1292(3)	4508(5)	36(1)	1
C5	8331(5)	2325(3)	3687(4)	24(1)	1
C6	7674(5)	2109(3)	2512(4)	29(1)	1
C7	6680(5)	2571(3)	1872(4)	34(1)	1
C8	6285(5)	3231(3)	2328(4)	31(1)	1
C9	6891(4)	3450(3)	3500(4)	25(1)	1
C10	7926(5)	2983(3)	4159(4)	24(1)	1
C11	5399(5)	4521(3)	3656(5)	30(1)	1
C12	5157(5)	5106(3)	4516(5)	31(1)	1
C13	3959(5)	5535(3)	4215(5)	39(1)	1
C14	3710(6)	6042(3)	5017(6)	43(1)	1
C15	4656(6)	6119(3)	6104(6)	41(1)	1
C16	5847(5)	5684(3)	6324(5)	33(1)	1
C17	6934(5)	5815(3)	7469(5)	34(1)	1

C18	9333(5)	5538(3)	8547(4)	30(1)	1
C19	9341(6)	5923(3)	9599(5)	39(1)	1
C20	10577(7)	6034(3)	10455(5)	41(1)	1
C21	11853(6)	5785(3)	10321(5)	40(1)	1
C22	11883(6)	5381(3)	9274(4)	34(1)	1
C23	10628(5)	5258(3)	8419(4)	28(1)	1
C24	14486(6)	5058(4)	9435(5)	46(2)	1
C25	12969(5)	5053(3)	8821(4)	32(1)	1
C26	12348(5)	4748(3)	7734(4)	29(1)	1
C27	12964(5)	4361(3)	6832(5)	35(1)	1
N6	11060(4)	3387(2)	11398(4)	30(1)	1
C28	12157(5)	3473(3)	10673(4)	30(1)	1
C29	12533(5)	2766(3)	10116(4)	32(1)	1
C30	13572(5)	2899(3)	9356(4)	32(1)	1
C31	14042(6)	2178(3)	8889(5)	38(1)	1
C32	11509(5)	2829(3)	12395(5)	33(1)	1
C33	12869(5)	3024(3)	13285(5)	36(1)	1
C34	13020(6)	2568(3)	14423(5)	38(1)	1
C35	14375(6)	2742(4)	15323(5)	48(2)	1
C36	9702(5)	3095(3)	10634(5)	36(1)	1
C37	9073(6)	3516(3)	9509(5)	44(1)	1
C38	7652(6)	3185(4)	8931(7)	65(2)	1
C39	6898(7)	3547(5)	7883(6)	68(2)	1
C40	10832(5)	4144(3)	11890(5)	33(1)	1
C41	10005(6)	4141(3)	12866(5)	43(1)	1
C42	9479(6)	4910(3)	13062(6)	49(2)	1
C43	8204(6)	5130(4)	12125(6)	58(2)	1

3.7b FLUORIDE COMPLEX

Table 1. Crystal data and structure refinement details.

Empirical formula	$C_{44}H_{62}FN_5O_2$	
Formula weight	711.99	
Temperature	120(2) K	
Wavelength	0.71073 Å	
Crystal system	Monoclinic	
Space group	$P2_1$	
Unit cell dimensions	a = 9.7830(4) Å	
	b = 18.6247(5) Å	β = 102.697(2)°
	c = 11.3671(5) Å	
Volume	2020.50(13) Å^3	
Z	2	
Density (calculated)	1.170 Mg / m^3	
Absorption coefficient	0.075 mm^{-1}	
F(000)	772	
Crystal	Fragment; Pale Yellow	
Crystal size	0.34 × 0.3 × 0.2 mm^3	

θ range for data collection	3.11 – 27.48°
Index ranges	$-12 \le h \le 12$, $-24 \le k \le 23$, $-14 \le l \le 14$
Reflections collected	27652
Independent reflections	4764 [R_{int} = 0.0818]
Completeness to θ = 27.48°	99.5 %
Absorption correction	Semi–empirical from equivalents
Max. and min. transmission	0.9851 and 0.9649
Refinement method	Full-matrix least-squares on F^2
Data / restraints / parameters	4764 / 18 / 474
Goodness-of-fit on F^2	1.198
Final R indices [$F^2 > 2\sigma(F^2)$]	$R1$ = 0.0605, $wR2$ = 0.1233
R indices (all data)	$R1$ = 0.0915, $wR2$ = 0.1339
Extinction coefficient	0.1466(8)
Largest diff. peak and hole	0.458 and –0.438 e Å^{-3}

Diffractometer: *Nonius KappaCCD* area detector (ϕ scans and ω scans to fill *asymmetric unit*). **Cell determination:** DirAx (Duisenberg, A.J.M.(1992). J. Appl. Cryst. 25, 92-96.) **Data collection:** Collect (Collect: Data collection software, R. Hooft, Nonius B.V., 1998). **Data reduction and cell refinement**: *Denzo* (Z. Otwinowski & W. Minor, *Methods in Enzymology* (1997) Vol. **276**: *Macromolecular Crystallography*, part A, pp. 307–326; C. W. Carter, Jr. & R. M. Sweet, Eds., Academic Press). **Absorption correction**: Sheldrick, G. M. SADABS - Bruker Nonius area detector scaling and absorption correction - V2.10 **Structure solution**: *SHELXS97* (G. M. Sheldrick, Acta Cryst. (1990) A**46** 467–473). **Structure refinement**: *SHELXL97* (G. M. Sheldrick (1997), University of Göttingen, Germany). **Graphics:** Cameron - A Molecular Graphics Package. (D. M. Watkin, L. Pearce and C. K. Prout, Chemical Crystallography Laboratory, University of Oxford, 1993).

Special details:. All hydrogen atoms were placed in idealised positions and refined using a riding model.

Table 2. Atomic coordinates [× 10^4], equivalent isotropic displacement parameters [Å^2 × 10^3] and site occupancy factors. U_{eq} is defined as one third of the trace of the orthogonalized U^{ij} tensor.

Atom	*x*	*y*	*z*	U_{eq}	*S.o.f.*
O1	11955(1)	4504(1)	13172(1)	55(1)	1
O2	9622(1)	2615(1)	7603(1)	43(1)	1
N1	16053(1)	2986(1)	12609(1)	34(1)	1
N2	13288(1)	3566(1)	12797(1)	36(1)	1
N3	11552(1)	2203(1)	8945(1)	36(1)	1
N4	13672(1)	1173(1)	10170(1)	33(1)	1
C1	18049(1)	2456(1)	11885(1)	44(1)	1
C2	17478(1)	2861(1)	12806(1)	37(1)	1
C3	18151(1)	3179(1)	13861(1)	40(1)	1
C4	19685(1)	3191(1)	14413(1)	52(1)	1
C5	17081(1)	3528(1)	14345(1)	38(1)	1
C6	17106(1)	3954(1)	15366(1)	45(1)	1
C7	15852(1)	4236(1)	15536(1)	47(1)	1
C8	14578(1)	4118(1)	14715(1)	43(1)	1
C9	14518(1)	3696(1)	13687(1)	35(1)	1
C10	15784(1)	3399(1)	13532(1)	33(1)	1
C11	12121(1)	3997(1)	12531(1)	39(1)	1
C12	11048(1)	3830(1)	11409(1)	38(1)	1
C13	9799(1)	4218(1)	11183(1)	47(1)	1
C14	8807(1)	4115(1)	10133(1)	51(1)	1
C15	9038(1)	3620(1)	9276(1)	44(1)	1

C16	10277(1)	3221(1)	9497(1)	37(1)	1
C17	11273(1)	3333(1)	10560(1)	38(1)	1
C18	10455(1)	2657(1)	8588(1)	35(1)	1
C19	11854(1)	1572(1)	8357(1)	33(1)	1
C20	11225(1)	1364(1)	7189(1)	38(1)	1
C21	11587(1)	705(1)	6718(1)	41(1)	1
C22	12567(1)	248(1)	7356(1)	37(1)	1
C23	13251(1)	454(1)	8534(1)	32(1)	1
C24	12884(1)	1103(1)	9015(1)	30(1)	1
C25	15051(1)	-568(1)	9326(1)	46(1)	1
C26	14322(1)	129(1)	9444(1)	34(1)	1
C27	14539(1)	585(1)	10418(1)	34(1)	1
C28	15528(1)	515(1)	11613(1)	43(1)	1
N5	16006(1)	1606(1)	16402(1)	38(1)	1
C29	15875(1)	2363(1)	16906(1)	42(1)	1
C30	15082(1)	2393(1)	17920(1)	54(1)	1
C31	14511(1)	3135(1)	18056(1)	70(1)	1
C32	13229(1)	3314(1)	17117(1)	90(1)	1
C33	16446(1)	1069(1)	17425(1)	45(1)	1
C34	17845(1)	1221(1)	18276(1)	45(1)	1
C35	18021(1)	754(1)	19399(1)	48(1)	1
C36	19435(1)	875(1)	20259(1)	56(1)	1
C37	17105(1)	1648(1)	15638(1)	36(1)	1
C38	17417(1)	938(1)	15110(1)	43(1)	1
C39	18410(1)	1017(1)	14265(1)	42(1)	1
C40	18822(1)	294(1)	13837(1)	55(1)	1
C41A	14614(1)	1361(1)	15767(1)	51(1)	0.50
C42A	13997(1)	1686(1)	14546(1)	51(1)	0.50
C43A	12545(1)	1351(1)	14072(1)	51(1)	0.50
C44A	11893(1)	1648(1)	12841(1)	51(1)	0.50
C41B	14629(1)	1360(1)	15607(1)	51(1)	0.50
C42B	14107(1)	1788(1)	14457(1)	51(1)	0.50
C43B	12559(1)	1657(1)	13883(1)	51(1)	0.50
C44B	12285(1)	930(1)	13302(1)	51(1)	0.50
F1	13807(1)	2438(1)	11178(1)	56(1)	1

3.7a CHLORIDE COMPLEX

Table 1. Crystal data and structure refinement details.

Empirical formula	$C_{43}H_{61}ClN_6O_2$	
Formula weight	729.43	
Temperature	120(2) K	
Wavelength	0.71073 Å	
Crystal system	Monoclinic	
Space group	$P2_1/n$	
Unit cell dimensions	a = 16.1573(3) Å	
	b = 15.3680(3) Å	β = 109.8590(10)°
	c = 17.4031(2) Å	
Volume	4064.30(12) Å^3	

Z	4
Density (calculated)	1.192 Mg / m^3
Absorption coefficient	0.137 mm^{-1}
F(000)	1576
Crystal	Block; Colourless
Crystal size	0.35 × 0.3 × 0.2 mm^3
θ range for data collection	2.93 – 27.48°
Index ranges	$-20 \le h \le 20$, $-19 \le k \le 19$, $-22 \le l \le 22$
Reflections collected	51747
Independent reflections	9289 [R_{int} = 0.0674]
Completeness to θ = 27.48°	99.8 %
Absorption correction	Semi–empirical from equivalents
Max. and min. transmission	0.9731 and 0.9436
Refinement method	Full-matrix least-squares on F^2
Data / restraints / parameters	9289 / 0 / 494
Goodness-of-fit on F^2	1.030
Final R indices [$F^2 > 2\sigma(F^2)$]	$R1$ = 0.0491, $wR2$ = 0.1124
R indices (all data)	$R1$ = 0.0811, $wR2$ = 0.1258
Extinction coefficient	0.0063(6)
Largest diff. peak and hole	0.349 and –0.350 e Å^{-3}

Diffractometer: *Nonius KappaCCD* area detector (ϕ scans and ω scans to fill *asymmetric unit*). **Cell determination:** DirAx (Duisenberg, A.J.M.(1992). J. Appl. Cryst. 25, 92-96.) **Data collection:** Collect (Collect: Data collection software, R. Hooft, Nonius B.V., 1998). **Data reduction and cell refinement**: *Denzo* (Z. Otwinowski & W. Minor, *Methods in Enzymology* (1997) Vol. **276**: *Macromolecular Crystallography*, part A, pp. 307–326; C. W. Carter, Jr. & R. M. Sweet, Eds., Academic Press). **Absorption correction**: Sheldrick, G. M. SADABS - Bruker Nonius area detector scaling and absorption correction - V2.10 **Structure solution**: *SHELXS97* (G. M. Sheldrick, Acta Cryst. (1990) A**46** 467–473). **Structure refinement**: *SHELXL97* (G. M. Sheldrick (1997), University of Göttingen, Germany). **Graphics:** Cameron - A Molecular Graphics Package. (D. M. Watkin, L. Pearce and C. K. Prout, Chemical Crystallography Laboratory, University of Oxford, 1993).

Special details: All hydrogen atoms were placed in idealised positions and refined using a riding model; NH hydrogens were freely refined.

Table 2. Atomic coordinates [× 10^4], equivalent isotropic displacement parameters [Å^2 × 10^3] and site occupancy factors. U_{eq} is defined as one third of the trace of the orthogonalized U^{ij} tensor.

Atom	*x*	*y*	*z*	U_{eq}	*S.o.f.*
Cl1	9771(1)	3663(1)	2232(1)	25(1)	1
N1	9380(1)	4072(1)	372(1)	23(1)	1
N2	8166(1)	5020(1)	1062(1)	24(1)	1
N3	8700(1)	5271(1)	2700(1)	21(1)	1
N4	10493(1)	5235(1)	3604(1)	23(1)	1
N5	11742(1)	3951(1)	3268(1)	26(1)	1
N6	14797(1)	6859(1)	694(1)	21(1)	1
O1	6725(1)	5032(1)	997(1)	26(1)	1
O2	10145(1)	5936(1)	4616(1)	28(1)	1
C1	10587(1)	3216(1)	154(1)	30(1)	1
C2	9777(1)	3759(1)	–165(1)	24(1)	1
C3	9313(1)	4036(1)	–940(1)	25(1)	1
C4	9536(1)	3899(1)	–1699(1)	33(1)	1

C5	8588(1)	4545(1)	−889(1)	23(1)	1
C6	7897(1)	4990(1)	−1464(1)	29(1)	1
C7	7302(1)	5433(1)	−1197(1)	29(1)	1
C8	7376(1)	5450(1)	−369(1)	27(1)	1
C9	8050(1)	5006(1)	213(1)	23(1)	1
C10	8654(1)	4557(1)	−57(1)	22(1)	1
C11	7521(1)	5049(1)	1391(1)	22(1)	1
C12	7840(1)	5121(1)	2310(1)	22(1)	1
C13	7231(1)	5051(1)	2713(1)	25(1)	1
C14	7520(1)	5142(1)	3554(1)	28(1)	1
C15	8401(1)	5301(1)	3962(1)	26(1)	1
C16	8970(1)	5355(1)	3516(1)	21(1)	1
C17	9927(1)	5538(1)	3964(1)	22(1)	1
C18	11426(1)	5322(1)	3918(1)	23(1)	1
C19	11849(1)	6020(1)	4405(1)	29(1)	1
C20	12768(1)	6065(1)	4728(1)	33(1)	1
C21	13293(1)	5423(1)	4585(1)	32(1)	1
C22	12892(1)	4724(1)	4074(1)	26(1)	1
C23	11963(1)	4689(1)	3743(1)	24(1)	1
C24	14169(1)	3709(2)	4008(1)	37(1)	1
C25	13221(1)	3973(1)	3779(1)	29(1)	1
C26	12508(1)	3532(1)	3282(1)	27(1)	1
C27	12455(1)	2719(1)	2792(1)	36(1)	1
C28	13960(1)	7404(1)	458(1)	24(1)	1
C29	13094(1)	6907(1)	194(1)	30(1)	1
C30	12344(1)	7499(1)	−316(1)	37(1)	1
C31	12310(2)	7569(2)	−1194(1)	49(1)	1
C32	14882(1)	6385(1)	−44(1)	21(1)	1
C33	15066(1)	6965(1)	−674(1)	27(1)	1
C34	15033(1)	6448(1)	−1429(1)	27(1)	1
C35	15344(1)	6999(1)	−2008(1)	35(1)	1
C36	15546(1)	7501(1)	1050(1)	23(1)	1
C37	16465(1)	7120(1)	1323(1)	27(1)	1
C38	17134(1)	7860(1)	1549(1)	33(1)	1
C39	18075(1)	7546(2)	1797(2)	51(1)	1
C40	14793(1)	6153(1)	1304(1)	24(1)	1
C41	14740(1)	6478(1)	2111(1)	35(1)	1
C42	14840(1)	5752(1)	2719(1)	33(1)	1
C43	14860(2)	6085(2)	3542(1)	48(1)	1

3.7b CHLORIDE COMPLEX

Table 1. Crystal data and structure refinement details.

Identification code	**2007sot0069 (Bensindole(Cl−))**
Empirical formula	$C_{44}H_{62}ClN_5O_2$
Formula weight	728.44
Temperature	120(2) K
Wavelength	0.71073 Å

Crystal system	Triclinic	
Space group	*P*–1	
Unit cell dimensions	a = 11.686 Å	α = 98.8110(10)°
	b = 13.0971(3) Å	β = 94.7230(10)°
	c = 14.2217(3) Å	γ =
101.2830(10)°		
Volume	2095.16(7) Å^3	
Z	2	
Density (calculated)	1.155 Mg / m^3	
Absorption coefficient	0.132 mm^{-1}	
F(000)	788	
Crystal	Block; Pale Yellow	
Crystal size	0.6 × 0.3 × 0.2 mm^3	
θ range for data collection	2.92 – 27.48°	
Index ranges	$-15 \le h \le 15$, $-16 \le k \le 17$, $-18 \le l \le 18$	
Reflections collected	28340	
Independent reflections	9550 [R_{int} = 0.0452]	
Completeness to θ = 27.48°	99.5 %	
Absorption correction	Semi–empirical from equivalents	
Max. and min. transmission	0.9740 and 0.9148	
Refinement method	Full-matrix least-squares on F^2	
Data / restraints / parameters	9550 / 20 / 473	
Goodness-of-fit on F^2	1.053	
Final *R* indices [$F^2 > 2\sigma(F^2)$]	*R1* = 0.0525, *wR2* = 0.1250	
R indices (all data)	*R1* = 0.0881, *wR2* = 0.1413	
Largest diff. peak and hole	0.717 and –0.682 e Å^{-3}	

Diffractometer: *Nonius KappaCCD* area detector (ϕ scans and ω scans to fill *asymmetric unit*). **Cell determination:** DirAx (Duisenberg, A.J.M.(1992). J. Appl. Cryst. 25, 92-96.) **Data collection:** Collect (Collect: Data collection software, R. Hooft, Nonius B.V., 1998). **Data reduction and cell refinement**: *Denzo* (Z. Otwinowski & W. Minor, *Methods in Enzymology* (1997) Vol. **276**: *Macromolecular Crystallography*, part A, pp. 307–326; C. W. Carter, Jr. & R. M. Sweet, Eds., Academic Press). **Absorption correction**: Sheldrick, G. M. SADABS - Bruker Nonius area detector scaling and absorption correction - V2.10 **Structure solution**: *SHELXS97* (G. M. Sheldrick, Acta Cryst. (1990) A**46** 467–473). **Structure refinement**: *SHELXL97* (G. M. Sheldrick (1997), University of Göttingen, Germany). **Graphics:** Cameron - A Molecular Graphics Package. (D. M. Watkin, L. Pearce and C. K. Prout, Chemical Crystallography Laboratory, University of Oxford, 1993).

Special details: All hydrogen atoms were placed in idealised positions and refined using a riding model.

Table 2. Atomic coordinates [× 10^4], equivalent isotropic displacement parameters [Å^2 × 10^3] and site occupancy factors. U_{eq} is defined as one third of the trace of the orthogonalized U^{ij} tensor.

Atom	*x*	*y*	*z*	U_{eq}	*S.o.f.*
Cl1	15818(1)	2075(1)	3582(1)	30(1)	1
C1	19358(2)	4018(2)	3755(2)	43(1)	1
C2	18825(2)	3888(2)	2741(2)	32(1)	1
C3	19234(2)	4321(2)	1987(2)	34(1)	1
C4	20377(2)	5085(2)	1987(2)	48(1)	1
C5	18364(2)	3910(2)	1175(2)	32(1)	1
C6	18305(2)	4035(2)	213(2)	37(1)	1

C7	17321(2)	3505(2)	−400(2)	37(1)	1
C8	16388(2)	2844(2)	−85(2)	32(1)	1
C9	16425(2)	2688(2)	861(2)	26(1)	1
C10	17428(2)	3231(2)	1485(2)	28(1)	1
C11	14599(2)	1283(2)	712(2)	26(1)	1
C12	13707(2)	786(2)	1297(1)	25(1)	1
C13	13138(2)	−265(2)	985(2)	29(1)	1
C14	12293(2)	−752(2)	1494(2)	31(1)	1
C15	12004(2)	−193(2)	2321(2)	30(1)	1
C16	12567(2)	859(2)	2644(2)	27(1)	1
C17	13411(2)	1346(2)	2124(1)	25(1)	1
C18	12213(2)	1434(2)	3535(2)	27(1)	1
C19	12977(2)	2887(2)	4928(2)	27(1)	1
C20	11925(2)	2945(2)	5304(2)	32(1)	1
C21	11909(2)	3639(2)	6160(2)	37(1)	1
C22	12917(2)	4282(2)	6658(2)	36(1)	1
C23	13989(2)	4243(2)	6298(2)	30(1)	1
C24	14001(2)	3551(2)	5430(2)	28(1)	1
C25	15566(3)	5570(2)	7524(2)	49(1)	1
C26	15178(2)	4779(2)	6619(2)	34(1)	1
C27	15861(2)	4423(2)	5959(2)	32(1)	1
C28	17150(2)	4699(2)	5907(2)	40(1)	1
C29	7897(1)	262(1)	1996(1)	32(1)	1
C30	9144(2)	501(2)	1743(2)	40(1)	1
C31	9294(2)	1362(2)	1136(2)	45(1)	1
C32	10499(3)	1659(3)	839(2)	85(1)	1
C33	8395(2)	−165(2)	3628(2)	32(1)	1
C34	8283(2)	897(2)	4168(2)	35(1)	1
C35	8886(2)	1076(2)	5190(2)	37(1)	1
C36	8778(2)	2124(2)	5768(2)	45(1)	1
C37A	6335(4)	−650(3)	2849(3)	38(1)	0.554(3)
C38A	5909(3)	−1262(3)	3645(3)	38(1)	0.554(3)
C39A	4575(3)	−1435(3)	3624(3)	38(1)	0.554(3)
C40A	3926(4)	−2264(3)	2789(3)	38(1)	0.554(3)
C37B	6353(1)	−681(2)	2689(2)	38(1)	0.446(3)
C38B	5834(4)	−1605(4)	3158(4)	38(1)	0.446(3)
C39B	4551(4)	−1593(4)	3291(4)	38(1)	0.446(3)
C40B	4328(2)	−734(1)	3984(1)	38(1)	0.446(3)
C41	7932(2)	−1594(2)	2254(2)	43(1)	1
C42	7266(3)	−2120(2)	1286(2)	66(1)	1
C43	7610(3)	−3152(2)	917(2)	55(1)	1
C44	6926(3)	−3661(2)	−52(2)	80(1)	1
N1	17730(2)	3220(1)	2441(1)	30(1)	1
N2	15510(2)	2030(1)	1224(1)	27(1)	1
N3	13073(2)	2210(1)	4068(1)	29(1)	1
N4	15149(2)	3676(1)	5236(1)	30(1)	1
N5	7642(2)	−539(1)	2664(1)	33(1)	1
O1	14492(1)	1023(1)	−165(1)	31(1)	1
O2	11209(1)	1195(1)	3751(1)	38(1)	1

DIMETHYLSULFOXIDE COMPLEX OF 3.9

Table 1. Crystal data and structure refinement details.

Empirical formula	$C_{24}H_{23}N_3O_3S$	
Formula weight	433.51	
Temperature	120(2) K	
Wavelength	0.71073 Å	
Crystal system	Triclinic	
Space group	*P*–1	
Unit cell dimensions	a = 7.6003(2) Å	α = 83.469(2)°
	b = 12.0848(4) Å	β = 78.876(2)°
	c = 12.5665(4) Å	γ = 71.766(2)°
Volume	1073.89(6) Å^3	
Z	2	
Density (calculated)	1.341 Mg / m^3	
Absorption coefficient	0.182 mm^{-1}	
F(000)	456	
Crystal	Block; Colourless	
Crystal size	0.08 × 0.07 × 0.02 mm^3	
θ range for data collection	3.02 – 27.48°	
Index ranges	$-9 \le h \le 9$, $-15 \le k \le 15$, $-15 \le l \le 16$	
Reflections collected	16956	
Independent reflections	4853 [R_{int} = 0.0369]	
Completeness to θ = 27.48°	98.5 %	
Absorption correction	Semi–empirical from equivalents	
Max. and min. transmission	0.9964 and 0.9756	
Refinement method	Full-matrix least-squares on F^2	
Data / restraints / parameters	4853 / 0 / 282	
Goodness-of-fit on F^2	1.036	
Final *R* indices [$F^2 > 2\sigma(F^2)$]	*R1* = 0.0585, *wR2* = 0.1195	
R indices (all data)	*R1* = 0.0782, *wR2* = 0.1322	
Largest diff. peak and hole	0.539 and –0.462 e Å^{-3}	

Diffractometer: *Nonius KappaCCD* area detector (ϕ scans and ω scans to fill *asymmetric unit*). **Cell determination:** DirAx (Duisenberg, A.J.M.(1992). J. Appl. Cryst. 25, 92-96.) **Data collection:** Collect (Collect: Data collection software, R. Hooft, Nonius B.V., 1998). **Data reduction and cell refinement**: *Denzo* (Z. Otwinowski & W. Minor, *Methods in Enzymology* (1997) Vol. **276**: *Macromolecular Crystallography*, part A, pp. 307–326; C. W. Carter, Jr. & R. M. Sweet, Eds., Academic Press). **Absorption correction**: Sheldrick, G. M. SADABS - Bruker Nonius area detector scaling and absorption correction - V2.10 **Structure solution**: *SHELXS97* (G. M. Sheldrick, Acta Cryst. (1990) A**46** 467–473). **Structure refinement**: *SHELXL97* (G. M. Sheldrick (1997), University of Göttingen, Germany). **Graphics:** Cameron - A Molecular Graphics Package. (D. M. Watkin, L. Pearce and C. K. Prout, Chemical Crystallography Laboratory, University of Oxford, 1993).

Special details: All hydrogen atoms were placed in idealised positions and refined using a riding model.

Table 2. Atomic coordinates [$\times 10^4$], equivalent isotropic displacement parameters [$Å^2 \times 10^3$] and site occupancy factors. U_{eq} is defined as one third of the trace of the orthogonalized U^{ij} tensor.

Atom	*x*	*y*	*z*	U_{eq}	*S.o.f.*
O1	5276(2)	2057(2)	4392(1)	26(1)	1
O2	−2594(2)	5078(1)	8521(1)	27(1)	1
N1	2816(3)	2125(2)	5770(1)	21(1)	1
N2	−720(2)	3968(2)	6615(1)	19(1)	1
N3	−4647(3)	6458(2)	7571(2)	21(1)	1
C1	7899(3)	1147(2)	5783(2)	25(1)	1
C2	9212(3)	531(2)	6430(2)	29(1)	1
C3	8659(3)	−46(2)	7390(2)	27(1)	1
C4	6788(3)	9(2)	7723(2)	27(1)	1
C5	5468(3)	624(2)	7078(2)	24(1)	1
C6	6016(3)	1196(2)	6105(2)	21(1)	1
C7	4677(3)	1833(2)	5346(2)	21(1)	1
C8	1356(3)	2661(2)	5153(2)	19(1)	1
C9	1436(3)	2363(2)	4114(2)	22(1)	1
C10	−7(3)	2946(2)	3511(2)	22(1)	1
C11	−1544(3)	3826(2)	3930(2)	22(1)	1
C12	−1684(3)	4131(2)	4998(2)	19(1)	1
C13	−250(3)	3525(2)	5608(2)	19(1)	1
C14	−3028(3)	4980(2)	5680(2)	21(1)	1
C15	−2399(3)	4850(2)	6655(2)	20(1)	1
C16	−3205(3)	5465(2)	7670(2)	20(1)	1
C17	−5681(3)	7199(2)	8418(2)	20(1)	1
C18	−6428(3)	8377(2)	8143(2)	24(1)	1
C19	−7465(3)	9142(2)	8942(2)	26(1)	1
C20	−7780(3)	8731(2)	10017(2)	27(1)	1
C21	−7069(4)	7557(2)	10284(2)	31(1)	1
C22	−6021(3)	6785(2)	9496(2)	27(1)	1
S1	2601(1)	2685(1)	8882(1)	32(1)	1
O3	1499(2)	2450(2)	8095(1)	30(1)	1
C23	3005(6)	4029(3)	8403(3)	66(1)	1
C24	916(5)	3202(4)	10060(3)	57(1)	1

DIMETHYLSULFOXIDE COMPLEX OF 3.10

Table 1. Crystal data and structure refinement details.

Empirical formula	$C_{25}H_{25}N_3O_3S$	
Formula weight	447.54	
Temperature	120(2) K	
Wavelength	0.71073 Å	
Crystal system	Triclinic	
Space group	*P*–1	
Unit cell dimensions	a = 9.8982(5) Å	α = 76.080(3)°
	b = 10.0741(4) Å	β = 88.484(2)°
	c = 11.5990(6) Å	γ = 87.099(2)°
Volume	1121.07(9) Å^3	
Z	2	
Density (calculated)	1.326 Mg / m^3	
Absorption coefficient	0.177 mm^{-1}	
F(000)	472	
Crystal	Slab; Colourless	
Crystal size	0.2 × 0.2 × 0.04 mm^3	
θ range for data collection	3.00 – 27.48°	
Index ranges	$-12 \le h \le 12$, $-13 \le k \le 13$, $-15 \le l \le 15$	
Reflections collected	21219	
Independent reflections	5119 [R_{int} = 0.0752]	
Completeness to θ = 27.48°	99.7 %	
Absorption correction	Semi–empirical from equivalents	
Max. and min. transmission	0.9930 and 0.9555	
Refinement method	Full-matrix least-squares on F^2	
Data / restraints / parameters	5119 / 0 / 291	
Goodness-of-fit on F^2	1.019	
Final *R* indices [$F^2 > 2\sigma(F^2)$]	*R1* = 0.0500, *wR2* = 0.0976	
R indices (all data)	*R1* = 0.1174, *wR2* = 0.1167	
Largest diff. peak and hole	0.243 and –0.493 e Å^{-3}	

Diffractometer: *Nonius KappaCCD* area detector (ϕ scans and ω scans to fill *asymmetric unit*). **Cell determination:** DirAx (Duisenberg, A.J.M.(1992). J. Appl. Cryst. 25, 92-96.) **Data collection:** Collect (Collect: Data collection software, R. Hooft, Nonius B.V., 1998). **Data reduction and cell refinement**: *Denzo* (Z. Otwinowski & W. Minor, *Methods in Enzymology* (1997) Vol. **276**: *Macromolecular Crystallography*, part A, pp. 307–326; C. W. Carter, Jr. & R. M. Sweet, Eds., Academic Press). **Absorption correction**: Sheldrick, G. M. SADABS - Bruker Nonius area detector scaling and absorption correction - V2.10 **Structure solution**: *SHELXS97* (G. M. Sheldrick, Acta Cryst. (1990) A**46** 467–473). **Structure refinement**: *SHELXL97* (G. M. Sheldrick (1997), University of Göttingen, Germany). **Graphics:** Cameron - A Molecular Graphics Package. (D. M. Watkin, L. Pearce and C. K. Prout, Chemical Crystallography Laboratory, University of Oxford, 1993).

Special details: All hydrogen atoms were placed in idealised positions and refined using a riding model.

Table 2. Atomic coordinates [× 10^4], equivalent isotropic displacement parameters [$Å^2$ × 10^3] and site occupancy factors. U_{eq} is defined as one third of the trace of the orthogonalized U^{ij} tensor.

Atom	*x*	*y*	*z*	U_{eq}	*S.o.f.*
C1	3758(2)	3509(2)	199(2)	27(1)	1
C2	4708(2)	2425(2)	355(2)	32(1)	1
C3	5471(2)	2078(2)	1371(2)	36(1)	1
C4	5276(2)	2802(2)	2235(2)	37(1)	1
C5	4329(2)	3884(2)	2072(2)	32(1)	1
C6	3560(2)	4257(2)	1047(2)	24(1)	1
C7	2547(2)	5463(2)	875(2)	29(1)	1
C8	1233(2)	5095(2)	1536(2)	24(1)	1
C9	−404(2)	5847(2)	2939(2)	22(1)	1
C10	−1556(2)	5235(2)	2721(2)	26(1)	1
C11	−2706(2)	5188(2)	3461(2)	30(1)	1
C12	−2748(2)	5750(2)	4431(2)	27(1)	1
C13	−1599(2)	6392(2)	4674(2)	22(1)	1
C14	−447(2)	6435(2)	3925(2)	21(1)	1
C15	−1265(2)	7079(2)	5569(2)	23(1)	1
C16	26(2)	7498(2)	5335(2)	23(1)	1
C17	888(2)	8285(2)	5919(2)	23(1)	1
C18	1075(2)	9018(2)	7800(2)	20(1)	1
C19	941(2)	8520(2)	9019(2)	24(1)	1
C20	1422(2)	9245(2)	9781(2)	29(1)	1
C21	2029(2)	10476(2)	9338(2)	28(1)	1
C22	2141(2)	10980(2)	8124(2)	25(1)	1
C23	1670(2)	10263(2)	7347(2)	23(1)	1
N1	794(2)	5933(2)	2240(2)	25(1)	1
N2	521(2)	7123(2)	4334(1)	22(1)	1
N3	526(2)	8257(2)	7063(1)	21(1)	1
O1	620(2)	4100(1)	1423(1)	30(1)	1
O2	1846(2)	8909(1)	5391(1)	32(1)	1
C24	2510(2)	10249(2)	2611(2)	30(1)	1
C25	4657(2)	8849(2)	3770(2)	34(1)	1
O3	2869(2)	7589(1)	2834(1)	34(1)	1
S1	3669(1)	8873(1)	2496(1)	29(1)	1

3.10 OBTAINED FROM ACETONITRILE

Table 1. Crystal data and structure refinement details.

Identification code	**2006sot1100**
Empirical formula	$C_{23}H_{19}N_3O_2$
Formula weight	369.41
Temperature	120(2) K
Wavelength	0.71073 Å

Crystal system	Monoclinic
Space group	*C*2/*c*
Unit cell dimensions	$a = 23.6704(5)$ Å
	$b = 9.3018(2)$ Å $\quad \beta = 98.9440(10)°$
	$c = 16.9937(3)$ Å
Volume	3696.13(13) Å^3
Z	8
Density (calculated)	1.328 Mg / m^3
Absorption coefficient	0.087 mm^{-1}
F(000)	1552
Crystal	Block; Colourless
Crystal size	0.3 × 0.2 × 0.1 mm^3
θ range for data collection	3.20 – 27.48°
Index ranges	$-30 \le h \le 30$, $-12 \le k \le 12$, $-22 \le l \le 21$
Reflections collected	26892
Independent reflections	4231 [$R_{int} = 0.0731$]
Completeness to $\theta = 27.48°$	99.8 %
Absorption correction	Semi–empirical from equivalents
Max. and min. transmission	0.9914 and 0.9645
Refinement method	Full-matrix least-squares on F^2
Data / restraints / parameters	4231 / 0 / 253
Goodness-of-fit on F^2	1.042
Final *R* indices [$F^2 > 2\sigma(F^2)$]	*R1* = 0.0507, *wR2* = 0.1134
R indices (all data)	*R1* = 0.0832, *wR2* = 0.1290
Largest diff. peak and hole	0.278 and –0.311 e Å^{-3}

Diffractometer: *Nonius KappaCCD* area detector (ϕ scans and ω scans to fill *asymmetric unit*). **Cell determination:** DirAx (Duisenberg, A.J.M.(1992). J. Appl. Cryst. 25, 92-96.) **Data collection:** Collect (Collect: Data collection software, R. Hooft, Nonius B.V., 1998). **Data reduction and cell refinement**: *Denzo* (Z. Otwinowski & W. Minor, *Methods in Enzymology* (1997) Vol. **276**: *Macromolecular Crystallography*, part A, pp. 307–326; C. W. Carter, Jr. & R. M. Sweet, Eds., Academic Press). **Absorption correction**: Sheldrick, G. M. SADABS - Bruker Nonius area detector scaling and absorption correction - V2.10 **Structure solution**: *SHELXS97* (G. M. Sheldrick, Acta Cryst. (1990) A**46** 467–473). **Structure refinement**: *SHELXL97* (G. M. Sheldrick (1997), University of Göttingen, Germany). **Graphics:** Cameron - A Molecular Graphics Package. (D. M. Watkin, L. Pearce and C. K. Prout, Chemical Crystallography Laboratory, University of Oxford, 1993).

Special details: All hydrogen atoms were placed in idealised positions and refined using a riding model.

Table 2. Atomic coordinates [× 10^4], equivalent isotropic displacement parameters [Å^2 × 10^3] and site occupancy factors. U_{eq} is defined as one third of the trace of the orthogonalized U^{ij} tensor.

Atom	*x*	*y*	*z*	U_{eq}	*S.o.f.*
C1	6511(1)	673(2)	4272(1)	33(1)	1
C2	6144(1)	–477(2)	4084(1)	39(1)	1
C3	5760(1)	–482(2)	3383(1)	38(1)	1
C4	5738(1)	684(2)	2878(1)	35(1)	1
C5	6092(1)	1855(2)	3078(1)	29(1)	1
C6	6486(1)	1856(2)	3770(1)	24(1)	1
C7	6876(1)	3131(2)	3987(1)	24(1)	1

C8	6648(1)	4035(2)	4611(1)	22(1)	1
C9	5919(1)	5898(2)	4758(1)	21(1)	1
C10	6139(1)	6493(2)	5484(1)	24(1)	1
C11	5806(1)	7412(2)	5884(1)	28(1)	1
C12	5253(1)	7763(2)	5578(1)	28(1)	1
C13	5018(1)	7175(2)	4837(1)	23(1)	1
C14	4471(1)	7265(2)	4353(1)	24(1)	1
C15	4492(1)	6427(2)	3694(1)	23(1)	1
C16	5354(1)	6257(2)	4435(1)	21(1)	1
C17	4052(1)	6080(2)	3011(1)	22(1)	1
C18	3020(1)	6088(2)	2538(1)	23(1)	1
C19	2985(1)	6711(2)	1790(1)	28(1)	1
C20	2501(1)	6466(2)	1228(1)	33(1)	1
C21	2059(1)	5631(2)	1414(1)	35(1)	1
C22	2093(1)	5039(2)	2165(1)	32(1)	1
C23	2573(1)	5268(2)	2731(1)	28(1)	1
N1	6231(1)	4974(2)	4318(1)	24(1)	1
N2	5027(1)	5827(2)	3737(1)	22(1)	1
N3	3509(1)	6320(2)	3127(1)	24(1)	1
O1	6822(1)	3863(2)	5326(1)	28(1)	1
O2	4182(1)	5578(1)	2385(1)	26(1)	1

DIMETHYLSULFOXIDE COMPLEX OF 3.12

Table 1. Crystal data and structure refinement details.

Empirical formula	$C_{24}H_{24}N_4O_3S$ $C_{22}H_{18}N_4O_2$, C_2H_6OS	
Formula weight	448.53	
Temperature	120(2) K	
Wavelength	0.71073 Å	
Crystal system	Triclinic	
Space group	*P*–1	
Unit cell dimensions	a = 8.3464(3) Å	α = 76.453(2)°
	b = 10.5112(3) Å	β = 85.668(2)°
	c = 13.0482(4) Å	γ = 84.522(2)°
Volume	1106.12(6) Å^3	
Z	2	
Density (calculated)	1.347 Mg / m^3	
Absorption coefficient	0.181 mm^{-1}	
F(000)	472	
Crystal	Block; Colourless	
Crystal size	0.2 × 0.2 × 0.06 mm^3	
θ range for data collection	3.04 – 27.48°	
Index ranges	$-10 \le h \le 10$, $-13 \le k \le 13$, $-16 \le l \le 16$	
Reflections collected	22815	

Independent reflections	5063 [R_{int} = 0.0612]
Completeness to θ = 27.48°	99.7 %
Absorption correction	Semi–empirical from equivalents
Max. and min. transmission	0.9892 and 0.9548
Refinement method	Full-matrix least-squares on F^2
Data / restraints / parameters	5063 / 0 / 307
Goodness-of-fit on F^2	1.038
Final R indices [$F^2 > 2\sigma(F^2)$]	$R1$ = 0.0476, $wR2$ = 0.1082
R indices (all data)	$R1$ = 0.0728, $wR2$ = 0.1215
Largest diff. peak and hole	0.218 and –0.496 e Å^{-3}

Diffractometer: *Nonius KappaCCD* area detector (ϕ scans and ω scans to fill *asymmetric unit*). **Cell determination:** DirAx (Duisenberg, A.J.M.(1992). J. Appl. Cryst. 25, 92-96.) **Data collection:** Collect (Collect: Data collection software, R. Hooft, Nonius B.V., 1998). **Data reduction and cell refinement**: *Denzo* (Z. Otwinowski & W. Minor, *Methods in Enzymology* (1997) Vol. **276**: *Macromolecular Crystallography*, part A, pp. 307–326; C. W. Carter, Jr. & R. M. Sweet, Eds., Academic Press). **Absorption correction**: Sheldrick, G. M. SADABS - Bruker Nonius area detector scaling and absorption correction - V2.10 **Structure solution**: *SHELXS97* (G. M. Sheldrick, Acta Cryst. (1990) A**46** 467–473). **Structure refinement**: *SHELXL97* (G. M. Sheldrick (1997), University of Göttingen, Germany). **Graphics:** Cameron - A Molecular Graphics Package. (D. M. Watkin, L. Pearce and C. K. Prout, Chemical Crystallography Laboratory, University of Oxford, 1993).

Special details: All hydrogen atoms were placed in idealised positions and refined using a riding model, except the NH's which were freely refined

Table 2. Atomic coordinates [× 10^4], equivalent isotropic displacement parameters [Å^2 × 10^3] and site occupancy factors. U_{eq} is defined as one third of the trace of the orthogonalized U^{ij} tensor.

Atom	*x*	*y*	*z*	U_{eq}	*S.o.f.*
O1	3283(2)	2628(1)	8118(1)	24(1)	1
O2	3393(2)	9181(1)	4652(1)	27(1)	1
N1	1400(2)	4277(2)	8386(1)	25(1)	1
N2	3928(2)	4774(2)	7729(1)	22(1)	1
N3	4598(2)	6704(1)	5738(1)	19(1)	1
N4	4977(2)	8965(2)	3180(1)	21(1)	1
C1	–1155(2)	4301(2)	9334(2)	27(1)	1
C2	–2431(2)	3687(2)	9929(2)	32(1)	1
C3	–2446(2)	2337(2)	10139(2)	33(1)	1
C4	–1203(2)	1618(2)	9719(2)	32(1)	1
C5	94(2)	2213(2)	9120(2)	26(1)	1
C6	126(2)	3565(2)	8944(1)	21(1)	1
C7	2897(2)	3793(2)	8076(1)	20(1)	1
C8	5348(2)	4638(2)	7080(1)	20(1)	1
C9	6539(2)	3635(2)	7316(1)	22(1)	1
C10	7878(2)	3533(2)	6606(2)	24(1)	1
C11	8073(2)	4443(2)	5667(2)	24(1)	1
C12	6918(2)	5523(2)	5428(1)	20(1)	1
C13	5563(2)	5602(2)	6140(1)	19(1)	1
C14	6711(2)	6649(2)	4572(1)	22(1)	1
C15	5294(2)	7341(2)	4785(1)	20(1)	1
C16	4463(2)	8578(2)	4211(1)	20(1)	1
C17	4382(2)	10119(2)	2468(1)	19(1)	1
C18	4178(2)	11327(2)	2741(1)	22(1)	1
C19	3661(2)	12440(2)	1997(2)	25(1)	1

C20	3359(2)	12358(2)	984(1)	23(1)	1
C21	3568(2)	11153(2)	715(1)	23(1)	1
C22	4080(2)	10035(2)	1450(1)	22(1)	1
S1	419(1)	8105(1)	7177(1)	28(1)	1
O3	1799(2)	7061(1)	7193(1)	32(1)	1
C23	-391(3)	8314(2)	5917(2)	36(1)	1
C24	1331(3)	9624(2)	6940(2)	38(1)	1

CHLORIDE COMPLEX OF 3.12

Table 1. Crystal data and refinement details for $3(C_{16}H_{36}N)^+$, $2(C_{22}H_{18}N_4O_2)$, H_2O, $3(Cl)^-$

Empirical formula	$C_{92}H_{146}Cl_3N_{11}O_5$
Formula weight	1592.55
Temperature	120(2) K
Wavelength	0.71073 Å
Crystal system	Monoclinic
Space group	$P2_1/n$
Unit cell dimensions	a = 8.2521(2) Å
	b = 26.0932(10) Å β = 92.152(2)°
	c = 42.7518(15) Å
Volume	9199.0(5) Å^3
Z	4
Density (calculated)	1.150 Mg / m^3
Absorption coefficient	0.155 mm^{-1}
F(000)	3464
Crystal	Rod; Colourless
Crystal size	0.55 × 0.1 × 0.07 mm^3
θ range for data collection	2.91 – 25.03°
Index ranges	$-9 \le h \le 9$, $-31 \le k \le 31$, $-48 \le l \le 50$
Reflections collected	44552
Independent reflections	15599 [R_{int} = 0.1138]
Completeness to θ = 25.03°	96.0 %
Absorption correction	Semi–empirical from equivalents
Max. and min. transmission	0.9892 and 0.9097
Refinement method	Full-matrix least-squares on F^2
Data / restraints / parameters	15599 / 2 / 1019
Goodness-of-fit on F^2	0.959
Final R indices [$F^2 > 2\sigma(F^2)$]	$R1$ = 0.0836, $wR2$ = 0.1909
R indices (all data)	$R1$ = 0.1833, $wR2$ = 0.2441
Extinction coefficient	0.0033(4)
Largest diff. peak and hole	0.475 and –0.401 e Å^{-3}

Diffractometer: *Nonius KappaCCD* area detector (ϕ scans and ω scans to fill *asymmetric unit*). **Cell determination:** DirAx (Duisenberg, A.J.M.(1992). J. Appl. Cryst. 25, 92-96.) **Data collection:** Collect (Collect: Data collection software, R. Hooft, Nonius B.V., 1998). **Data reduction and cell refinement**: *Denzo* (Z. Otwinowski & W. Minor, *Methods in Enzymology* (1997) Vol. **276**: *Macromolecular Crystallography*, part A, pp. 307–326; C. W. Carter, Jr. & R. M. Sweet, Eds., Academic Press). **Absorption**

correction: Sheldrick, G. M. SADABS - Bruker Nonius area detector scaling and absorption correction - V2.10 **Structure solution**: *SHELXS97* (G. M. Sheldrick, Acta Cryst. (1990) A**46** 467–473). **Structure refinement**: *SHELXL97* (G. M. Sheldrick (1997), University of Göttingen, Germany). **Graphics:** Cameron - A Molecular Graphics Package. (D. M. Watkin, L. Pearce and C. K. Prout, Chemical Crystallography Laboratory, University of Oxford, 1993).

Special details: All hydrogen atoms were placed in idealised positions and refined using a riding model, except those of the water which were refined using restraints.

Table 2. Atomic coordinates [$\times 10^4$], equivalent isotropic displacement parameters [$Å^2 \times 10^3$] and site occupancy factors. U_{eq} is defined as one third of the trace of the orthogonalized U^{ij} tensor.

Atom	*x*	*y*	*z*	U_{eq}	*S.o.f.*
O1	−69(4)	1236(1)	1134(1)	36(1)	1
O2	4196(4)	3527(1)	372(1)	42(1)	1
N1	478(4)	1968(1)	1419(1)	34(1)	1
N2	1181(4)	1924(1)	909(1)	33(1)	1
N3	2846(4)	2550(1)	439(1)	31(1)	1
N4	4887(4)	3351(1)	−131(1)	33(1)	1
C1	−737(5)	1355(2)	1785(1)	36(1)	1
C2	−1182(6)	1251(2)	2089(1)	41(1)	1
C3	−959(6)	1602(2)	2324(1)	44(1)	1
C4	−267(6)	2074(2)	2257(1)	45(1)	1
C5	184(5)	2186(2)	1959(1)	37(1)	1
C6	−35(5)	1827(2)	1718(1)	33(1)	1
C7	477(5)	1671(2)	1150(1)	31(1)	1
C8	1530(5)	1729(2)	614(1)	29(1)	1
C9	1149(5)	1238(2)	510(1)	35(1)	1
C10	1625(6)	1069(2)	212(1)	37(1)	1
C11	2435(6)	1375(2)	11(1)	37(1)	1
C12	2791(5)	1876(2)	111(1)	31(1)	1
C13	2342(5)	2047(2)	404(1)	28(1)	1
C14	3591(5)	2297(2)	−35(1)	35(1)	1
C15	3601(5)	2700(2)	171(1)	29(1)	1
C16	4261(5)	3227(2)	148(1)	33(1)	1
C17	5458(5)	3835(2)	−230(1)	34(1)	1
C18	5464(5)	3927(2)	−550(1)	36(1)	1
C19	6039(6)	4391(2)	−664(1)	44(1)	1
C20	6622(6)	4758(2)	−459(2)	51(2)	1
C21	6601(7)	4670(2)	−143(2)	58(2)	1
C22	6026(6)	4208(2)	−22(1)	47(1)	1
O3	−5303(4)	3614(1)	2261(1)	51(1)	1
O4	−1331(4)	4297(1)	3839(1)	43(1)	1
N5	−4785(5)	4450(2)	2409(1)	45(1)	1
N6	−4045(5)	3806(2)	2738(1)	40(1)	1
N7	−2439(4)	3682(2)	3359(1)	38(1)	1
N8	−267(4)	3618(1)	4120(1)	38(1)	1
C38	−1080(5)	3835(2)	3869(1)	36(1)	1
C23	−5097(6)	5259(2)	2156(1)	49(1)	1
C24	−5620(7)	5569(2)	1908(1)	58(2)	1
C25	−6349(7)	5350(2)	1642(2)	61(2)	1
C26	−6555(6)	4833(2)	1629(1)	57(2)	1
C27	−6054(6)	4510(2)	1877(1)	48(2)	1
C28	−5318(6)	4728(2)	2141(1)	43(1)	1

C29	−4759(6)	3925(2)	2452(1)	41(1)	1
C30	−3679(6)	3316(2)	2857(1)	36(1)	1
C31	−4014(6)	2856(2)	2712(1)	45(1)	1
C32	−3535(6)	2390(2)	2852(1)	49(1)	1
C33	−2720(6)	2367(2)	3136(1)	43(1)	1
C34	−2396(6)	2828(2)	3295(1)	37(1)	1
C35	−2887(5)	3295(2)	3159(1)	34(1)	1
C36	−1624(5)	2950(2)	3590(1)	37(1)	1
C37	−1659(5)	3471(2)	3622(1)	36(1)	1
C39	462(6)	3875(2)	4383(1)	37(1)	1
C40	254(6)	4390(2)	4442(1)	44(1)	1
C41	970(6)	4610(2)	4705(1)	49(2)	1
C42	1876(7)	4322(2)	4917(1)	53(2)	1
C43	2075(6)	3806(2)	4861(1)	47(1)	1
C44	1379(6)	3580(2)	4594(1)	43(1)	1
N9	2100(4)	5080(1)	3438(1)	38(1)	1
C45	2409(6)	5347(2)	3130(1)	44(1)	1
C46	920(6)	5409(2)	2906(1)	49(1)	1
C47	1433(6)	5613(2)	2595(1)	50(2)	1
C48	−6(7)	5766(2)	2383(1)	62(2)	1
C49	713(6)	5328(2)	3606(1)	38(1)	1
C50	964(5)	5886(2)	3696(1)	40(1)	1
C51	−509(6)	6097(2)	3857(1)	42(1)	1
C52	−788(6)	5870(2)	4179(1)	51(2)	1
C53	3686(6)	5118(2)	3632(1)	43(1)	1
C54	3671(6)	4905(2)	3961(1)	44(1)	1
C55	5396(6)	4922(2)	4108(1)	51(2)	1
C56	5479(6)	4734(2)	4445(1)	54(2)	1
C57	1636(6)	4520(2)	3387(1)	49(2)	1
C58	2943(7)	4175(2)	3248(2)	67(2)	1
C59	2311(6)	3615(2)	3219(2)	60(2)	1
C60	1220(8)	3572(2)	2931(2)	74(2)	1
N10	5020(4)	1737(2)	4054(1)	38(1)	1
C61	3411(5)	1774(2)	3868(1)	38(1)	1
C62	3498(6)	1964(2)	3534(1)	49(2)	1
C63	1805(6)	1995(2)	3383(1)	58(2)	1
C64	1822(7)	2093(2)	3038(1)	62(2)	1
C65	5712(6)	2276(2)	4116(1)	41(1)	1
C66	4800(6)	2605(2)	4342(1)	45(1)	1
C67	5312(6)	3159(2)	4300(1)	51(2)	1
C68	4616(6)	3412(2)	4001(1)	57(2)	1
C69	4696(6)	1462(2)	4356(1)	40(1)	1
C70	6191(6)	1355(2)	4566(1)	48(1)	1
C71	5743(6)	1090(2)	4872(1)	51(2)	1
C72	4879(7)	1449(2)	5085(1)	61(2)	1
C73	6271(5)	1458(2)	3865(1)	40(1)	1
C74	5810(6)	925(2)	3756(1)	45(1)	1
C75	7153(6)	684(2)	3572(1)	53(2)	1
N11	8035(4)	−1751(1)	3630(1)	36(1)	1
C76	6650(7)	175(2)	3426(1)	57(2)	1
C77	6556(5)	−1638(2)	3419(1)	40(1)	1
C78	6749(6)	−1233(2)	3169(1)	44(1)	1
C79	5167(6)	−1155(2)	2985(1)	59(2)	1
C80	5181(7)	−720(2)	2757(1)	60(2)	1

C81	8640(6)	−1272(2)	3798(1)	35(1)	1
C82	7455(6)	−1015(2)	4010(1)	44(1)	1
C83	8143(6)	−509(2)	4138(1)	47(2)	1
C84	6925(7)	−218(2)	4326(1)	60(2)	1
C85	7517(6)	−2154(2)	3864(1)	39(1)	1
C86	8820(5)	−2353(2)	4090(1)	38(1)	1
C87	8099(6)	−2733(2)	4318(1)	42(1)	1
C88	7018(6)	−2488(2)	4555(1)	49(2)	1
C89	9425(5)	−1944(2)	3437(1)	41(1)	1
C90	9123(5)	−2436(2)	3255(1)	40(1)	1
C91	10701(6)	−2626(2)	3128(1)	50(2)	1
C92	10490(7)	−3121(2)	2939(1)	54(2)	1
O5	2322(6)	4142(2)	801(1)	80(1)	1
Cl1	1834(1)	3062(1)	1125(1)	38(1)	1
Cl2	−3035(2)	4847(1)	3060(1)	43(1)	1
Cl3	5167(1)	2643(1)	−759(1)	38(1)	1

BENZOATE COMPLEX OF 3.13

Table 1. Crystal data and structure refinement details for $2(C_{16}H_{36}N)$, $C_{22}H_{18}N_4OS$, $2(C_7H_5O_2)$.

Identification code	**2006sot1361**	
Empirical formula	$C_{68}H_{100}N_6O_5S$	
Formula weight	1113.60	
Temperature	120(2) K	
Wavelength	0.71073 Å	
Crystal system	Triclinic	
Space group	*P*1	
Unit cell dimensions	a = 8.5044(2) Å	α = 91.9460(10)°
	b = 12.4661(4) Å	β = 99.404(2)°
	c = 16.0520(5) Å	γ = 109.096(2)°
Volume	1579.53(8) Å^3	
Z	1	
Density (calculated)	1.171 Mg / m^3	
Absorption coefficient	0.105 mm^{-1}	
F(000)	606	
Crystal	Block; Colourless	
Crystal size	0.3 × 0.2 × 0.2 mm^3	
θ range for data collection	2.98 – 27.48°	
Index ranges	$-11 \le h \le 11$, $-16 \le k \le 16$, $-20 \le l \le 20$	
Reflections collected	26382	
Independent reflections	12893 [R_{int} = 0.0466]	
Completeness to θ = 27.48°	99.7 %	
Absorption correction	Semi-empirical from equivalents	
Max. and min. transmission	0.9793 and 0.9592	

Refinement method	Full-matrix least-squares on F^2
Data / restraints / parameters	12893 / 3 / 730
Goodness-of-fit on F^2	1.049
Final R indices $[F^2 > 2\sigma(F^2)]$	$R1 = 0.0542$, $wR2 = 0.1176$
R indices (all data)	$R1 = 0.0842$, $wR2 = 0.1300$
Absolute structure parameter	0.00(7)
Extinction coefficient	0.049(2)
Largest diff. peak and hole	0.641 and −0.437 e Å^{-3}

Diffractometer: *Nonius KappaCCD* area detector (ϕ scans and ω scans to fill *asymmetric unit*). **Cell determination:** DirAx (Duisenberg, A.J.M.(1992). J. Appl. Cryst. 25, 92-96.) **Data collection:** Collect (Collect: Data collection software, R. Hooft, Nonius B.V., 1998). **Data reduction and cell refinement**: *Denzo* (Z. Otwinowski & W. Minor, *Methods in Enzymology* (1997) Vol. **276**: *Macromolecular Crystallography*, part A, pp. 307–326; C. W. Carter, Jr. & R. M. Sweet, Eds., Academic Press). **Absorption correction**: Sheldrick, G. M. SADABS - Bruker Nonius area detector scaling and absorption correction - V2.10 **Structure solution**: *SHELXS97* (G. M. Sheldrick, Acta Cryst. (1990) A**46** 467–473). **Structure refinement**: *SHELXL97* (G. M. Sheldrick (1997), University of Göttingen, Germany). **Graphics:** Cameron - A Molecular Graphics Package. (D. M. Watkin, L. Pearce and C. K. Prout, Chemical Crystallography Laboratory, University of Oxford, 1993).

Special details: All hydrogen atoms were placed in idealised positions and refined using a riding model.

Table 2. Atomic coordinates [× 10^4], equivalent isotropic displacement parameters [Å^2 × 10^3] and site occupancy factors. U_{eq} is defined as one third of the trace of the orthogonalized U^{ij} tensor.

Atom	*x*	*y*	*z*	U_{eq}	*S.o.f.*
C1	3116(4)	11278(3)	2716(2)	33(1)	1
C2	4108(4)	12136(3)	3353(2)	39(1)	1
C3	4126(4)	13241(3)	3323(2)	40(1)	1
C4	3161(4)	13511(3)	2639(2)	38(1)	1
C5	2157(3)	12676(2)	2003(2)	32(1)	1
C6	2120(3)	11557(2)	2037(2)	29(1)	1
C7	561(3)	9632(2)	1197(2)	25(1)	1
C8	−1215(3)	8186(2)	0(2)	21(1)	1
C9	−2149(3)	7293(2)	389(2)	27(1)	1
C10	−3069(4)	6229(2)	−64(2)	31(1)	1
C11	−3103(4)	6021(2)	−906(2)	30(1)	1
C12	−2183(3)	6910(2)	−1330(2)	23(1)	1
C13	−1255(3)	7979(2)	−868(2)	21(1)	1
C14	−1925(3)	7029(2)	−2182(2)	25(1)	1
C15	−906(3)	8120(2)	−2216(2)	23(1)	1
C16	−191(3)	8763(2)	−2900(2)	23(1)	1
C17	−380(3)	8701(2)	−4450(2)	24(1)	1
C18	988(4)	9682(2)	−4469(2)	30(1)	1
C19	1359(4)	10039(3)	−5246(2)	34(1)	1
C20	393(4)	9450(3)	−5998(2)	33(1)	1
C21	−954(4)	8470(2)	−5977(2)	32(1)	1
C22	−1335(3)	8085(2)	−5208(2)	27(1)	1
C23	−64(3)	11737(2)	−580(2)	22(1)	1
C24	−384(3)	12394(2)	−1312(2)	26(1)	1
C25	−923(3)	13318(2)	−1217(2)	32(1)	1
C26	−1282(4)	13885(3)	−1905(2)	41(1)	1
C27	−1120(4)	13534(3)	−2695(2)	44(1)	1

C28	−558(4)	12626(3)	−2804(2)	43(1)	1
C29	−192(4)	12055(2)	−2111(2)	32(1)	1
C37	6038(3)	9920(3)	553(2)	30(1)	1
C38	5360(4)	10064(3)	1347(2)	35(1)	1
C39	6813(4)	10472(3)	2102(2)	41(1)	1
C40	7794(5)	11734(3)	2162(2)	54(1)	1
C41	4068(3)	10617(2)	−448(2)	29(1)	1
C42	5373(4)	11734(2)	−570(2)	35(1)	1
C43	4638(4)	12686(2)	−592(2)	35(1)	1
C44	4334(5)	13047(3)	257(2)	46(1)	1
C45	5647(3)	9444(3)	−974(2)	31(1)	1
C46	4720(4)	9328(3)	−1875(2)	35(1)	1
C47	5821(4)	9165(3)	−2481(2)	45(1)	1
C48	5089(5)	9113(3)	−3405(2)	51(1)	1
C49	3224(3)	8604(2)	−220(2)	30(1)	1
C50	3597(4)	7539(2)	41(2)	34(1)	1
C51	1957(4)	6623(2)	148(2)	38(1)	1
C52	2239(5)	5542(3)	424(3)	66(1)	1
C53	2664(4)	6245(3)	4292(2)	35(1)	1
C54	2756(4)	7462(3)	4144(2)	45(1)	1
C55	4403(5)	8115(3)	3839(3)	66(1)	1
C56	4517(5)	7652(4)	2974(3)	75(1)	1
C57	−478(4)	5474(3)	3790(2)	33(1)	1
C58	−338(4)	5161(3)	2893(2)	41(1)	1
C59	−2041(5)	4896(3)	2291(2)	56(1)	1
C60	−2876(5)	5776(4)	2330(2)	59(1)	1
C61	1100(4)	4295(2)	4518(2)	32(1)	1
C62	−510(4)	3374(3)	4645(2)	36(1)	1
C63	−241(4)	2238(3)	4744(2)	39(1)	1
C64	−1874(4)	1292(3)	4789(2)	46(1)	1
C65	638(4)	5898(3)	5301(2)	32(1)	1
C66	1778(4)	5791(3)	6104(2)	32(1)	1
C67	1384(4)	6331(3)	6865(2)	36(1)	1
C68	2401(4)	6186(3)	7698(2)	42(1)	1
N1	1069(3)	10789(2)	1343(1)	28(1)	1
N2	−299(3)	9292(2)	385(1)	24(1)	1
N3	−477(3)	8698(2)	−1421(1)	23(1)	1
N4	−879(3)	8275(2)	−3696(1)	24(1)	1
N5	4747(3)	9642(2)	−271(2)	28(1)	1
N6	995(3)	5479(2)	4475(1)	29(1)	1
O1	956(2)	9686(2)	−2711(1)	30(1)	1
O2	−374(2)	11993(2)	124(1)	30(1)	1
O3	468(2)	10921(2)	−711(1)	28(1)	1
S1	922(1)	8732(1)	1887(1)	33(1)	1
C30	6063(3)	5345(2)	5559(2)	27(1)	1
C31	5330(3)	4303(2)	6019(2)	27(1)	1
C32	4684(3)	4403(2)	6748(2)	29(1)	1
C33	4005(4)	3446(3)	7159(2)	38(1)	1
C34	3986(4)	2391(3)	6864(2)	46(1)	1
C35	4650(4)	2296(3)	6148(2)	44(1)	1
C36	5307(4)	3237(3)	5721(2)	35(1)	1
O4	6132(2)	6292(2)	5902(1)	33(1)	1
O5	6526(3)	5194(2)	4883(1)	40(1)	1

STRUCUTRES FROM CHAPTER 4

CRYSTAL STRUCUTRE OF 4.6

Table 1. Crystal data and structure refinement details.

Empirical formula	$C_{30}H_{25}N_5O_2$	
Formula weight	487.55	
Temperature	120(2) K	
Wavelength	0.71073 Å	
Crystal system	Triclinic	
Space group	*P*–1	
Unit cell dimensions	a = 9.6907(3) Å	α = 87.119(2)°
	b = 10.9090(3) Å	β = 67.8340(10)°
	c = 12.3922(3) Å	γ = 77.531(2)°
Volume	1183.91(6) Å^3	
Z	2	
Density (calculated)	1.368 Mg / m^3	
Absorption coefficient	0.088 mm^{-1}	
F(000)	512	
Crystal	Block; Colourless	
Crystal size	0.2 × 0.15 × 0.08 mm^3	
θ range for data collection	3.28 – 27.48°	
Index ranges	$-12 \le h \le 12$, $-14 \le k \le 14$, $-16 \le l \le 15$	
Reflections collected	22295	
Independent reflections	5409 [R_{int} = 0.0467]	
Completeness to θ = 27.48°	99.6 %	
Absorption correction	Semi–empirical from equivalents	
Max. and min. transmission	0.9930 and 0.9725	
Refinement method	Full-matrix least-squares on F^2	
Data / restraints / parameters	5409 / 0 / 334	
Goodness-of-fit on F^2	1.020	
Final *R* indices [$F^2 > 2\sigma(F^2)$]	*R1* = 0.0483, *wR2* = 0.1059	
R indices (all data)	*R1* = 0.0627, *wR2* = 0.1129	
Largest diff. peak and hole	0.233 and –0.227 e Å^{-3}	

Diffractometer: *Nonius KappaCCD* area detector (ϕ scans and ω scans to fill *asymmetric unit*,). **Cell determination:** DirAx (Duisenberg, A.J.M.(1992). J. Appl. Cryst. 25, 92-96.) **Data collection:** Collect (Collect: Data collection software, R. Hooft, Nonius B.V., 1998). **Data reduction and cell refinement**: *Denzo* (Z. Otwinowski & W. Minor, *Methods in Enzymology* (1997) Vol. **276**: *Macromolecular Crystallography*, part A, pp. 307–326; C. W. Carter, Jr. & R. M. Sweet, Eds., Academic Press). **Absorption correction**: Sheldrick, G. M. SADABS - Bruker Nonius area detector scaling and absorption correction - V2.10 **Structure solution**: *SHELXS97* (G. M. Sheldrick, Acta Cryst. (1990) A**46** 467–473). **Structure refinement**: *SHELXL97* (G. M. Sheldrick (1997), University of Göttingen, Germany). **Graphics:** Cameron - A Molecular Graphics Package. (D. M. Watkin, L. Pearce and C. K. Prout, Chemical Crystallography Laboratory, University of Oxford, 1993).
Special details: All hydrogen atoms were placed in idealised positions and refined using a riding model.

Table 2. Atomic coordinates [$\times 10^4$], equivalent isotropic displacement parameters [$Å^2 \times 10^3$] and site occupancy factors. U_{eq} is defined as one third of the trace of the orthogonalized U^{ij} tensor.

Atom	*x*	*y*	*z*	U_{eq}	*S.o.f.*
C1	2260(2)	−2771(2)	133(2)	28(1)	1
C2	1535(2)	−3304(2)	−434(2)	28(1)	1
C3	953(2)	−2566(2)	−1172(2)	26(1)	1
C4	1128(2)	−1339(2)	−1317(1)	23(1)	1
C5	1896(2)	−884(2)	−727(1)	20(1)	1
C6	2194(2)	425(2)	−923(1)	22(1)	1
C7	2854(2)	1975(2)	39(1)	19(1)	1
C8	3266(2)	2274(1)	1012(1)	18(1)	1
C9	3193(2)	1705(1)	2056(1)	18(1)	1
C10	3782(2)	2436(1)	2630(1)	17(1)	1
C11	4164(2)	3441(1)	1918(1)	17(1)	1
C12	4748(2)	4565(1)	2011(1)	17(1)	1
C13	5737(2)	5725(1)	3104(1)	21(1)	1
C14	7239(2)	5272(1)	3255(1)	20(1)	1
C15	8574(2)	5582(2)	2480(1)	24(1)	1
C16	9909(2)	5166(2)	2680(2)	29(1)	1
C17	9869(2)	4463(2)	3642(2)	34(1)	1
C18	8494(2)	4193(2)	4354(2)	41(1)	1
C19	2570(2)	567(1)	2502(1)	17(1)	1
C20	3473(2)	−634(2)	2203(1)	21(1)	1
C21	2864(2)	−1692(2)	2571(2)	26(1)	1
C22	1331(2)	−1554(2)	3257(2)	26(1)	1
C23	412(2)	−365(2)	3580(1)	26(1)	1
C24	1029(2)	691(2)	3203(1)	21(1)	1
C25	3972(2)	2126(1)	3756(1)	17(1)	1
C26	2720(2)	2047(1)	4778(1)	20(1)	1
C27	2922(2)	1733(2)	5814(1)	23(1)	1
C28	4366(2)	1489(2)	5853(1)	24(1)	1
C29	5611(2)	1565(1)	4850(1)	23(1)	1
C30	5416(2)	1873(1)	3811(1)	19(1)	1
N1	2442(2)	−1578(1)	−2(1)	25(1)	1
N2	2649(2)	803(1)	−26(1)	21(1)	1
N3	3836(1)	3328(1)	957(1)	18(1)	1
N4	5114(2)	4676(1)	2935(1)	20(1)	1
N5	7188(2)	4577(2)	4182(1)	33(1)	1
O1	2720(1)	2764(1)	−680(1)	29(1)	1
O2	4860(1)	5353(1)	1249(1)	24(1)	1

CRYSTAL STRUCUTRE OF 4.8

Table 1. Crystal data and structure refinement details.

Empirical formula	$C_{30}H_{37}N_5O_4$	
Formula weight	531.65	
Temperature	120(2) K	
Wavelength	0.71073 Å	
Crystal system	Triclinic	
Space group	*P*–1	
Unit cell dimensions	a = 8.6927(3) Å	α = 95.971(2)°
	b = 10.7954(3) Å	β = 98.6220(10)°
	c = 15.8395(5) Å	γ = 107.604(2)°
Volume	1383.07(8) Å^3	
Z	2	
Density (calculated)	1.277 Mg / m^3	
Absorption coefficient	0.086 mm^{-1}	
F(000)	568	
Crystal	Block; Colourless	
Crystal size	0.2 × 0.2 × 0.06 mm^3	
θ range for data collection	3.03 – 27.48°	
Index ranges	$-11 \le h \le 11$, $-14 \le k \le 13$, $-20 \le l \le 20$	
Reflections collected	22645	
Independent reflections	6297 [R_{int} = 0.0500]	
Completeness to θ = 27.48°	99.5 %	
Absorption correction	Semi–empirical from equivalents	
Max. and min. transmission	0.9948 and 0.9730	
Refinement method	Full-matrix least-squares on F^2	
Data / restraints / parameters	6297 / 0 / 352	
Goodness-of-fit on F^2	1.033	
Final *R* indices [$F^2 > 2\sigma(F^2)$]	*R1* = 0.0489, *wR2* = 0.1086	
R indices (all data)	*R1* = 0.0689, *wR2* = 0.1179	
Largest diff. peak and hole	0.243 and –0.283 e Å^{-3}	

Diffractometer: *Nonius KappaCCD* area detector (ϕ scans and ω scans to fill *asymmetric unit*). **Cell determination:** DirAx (Duisenberg, A.J.M.(1992). J. Appl. Cryst. 25, 92-96.) **Data collection:** Collect (Collect: Data collection software, R. Hooft, Nonius B.V., 1998). **Data reduction and cell refinement**: *Denzo* (Z. Otwinowski & W. Minor, *Methods in Enzymology* (1997) Vol. **276**: *Macromolecular Crystallography*, part A, pp. 307–326; C. W. Carter, Jr. & R. M. Sweet, Eds., Academic Press). **Absorption correction**: Sheldrick, G. M. SADABS - Bruker Nonius area detector scaling and absorption correction - V2.10 **Structure solution**: *SHELXS97* (G. M. Sheldrick, Acta Cryst. (1990) A**46** 467–473). **Structure refinement**: *SHELXL97* (G. M. Sheldrick (1997), University of Göttingen, Germany). **Graphics:** Cameron - A Molecular Graphics Package. (D. M. Watkin, L. Pearce and C. K. Prout, Chemical Crystallography Laboratory, University of Oxford, 1993).

Special details: All hydrogen atoms were placed in idealised positions and refined using a riding model.

Table 2. Atomic coordinates [$\times 10^4$], equivalent isotropic displacement parameters [$Å^2 \times 10^3$] and site occupancy factors. U_{eq} is defined as one third of the trace of the orthogonalized U^{ij} tensor.

Atom	*x*	*y*	*z*	U_{eq}	*S.o.f.*
C1	2727(2)	2744(2)	1703(1)	24(1)	1
C2	1069(2)	1698(2)	1566(1)	27(1)	1
C3	−7(2)	3136(2)	2281(1)	28(1)	1
C4	1644(2)	4202(2)	2464(1)	25(1)	1
C5	4562(2)	4711(2)	2657(1)	24(1)	1
C6	6036(2)	4256(2)	2891(1)	23(1)	1
C7	7247(2)	3764(1)	4262(1)	18(1)	1
C8	6971(2)	3188(1)	5059(1)	17(1)	1
C9	5581(2)	2482(1)	5350(1)	17(1)	1
C10	6143(2)	2148(1)	6161(1)	17(1)	1
C11	7849(2)	2676(1)	6336(1)	17(1)	1
C12	9136(2)	2789(1)	7093(1)	19(1)	1
C13	9713(2)	2678(2)	8645(1)	28(1)	1
C14	8733(2)	1993(2)	9273(1)	31(1)	1
C15	6158(2)	1566(2)	9777(1)	30(1)	1
C16	4740(2)	2069(2)	9857(1)	34(1)	1
C17	6423(2)	4227(2)	9970(1)	32(1)	1
C18	7883(2)	3783(2)	9879(1)	27(1)	1
C19	3827(2)	2129(2)	4933(1)	17(1)	1
C20	2862(2)	817(2)	4652(1)	21(1)	1
C21	1208(2)	489(2)	4300(1)	24(1)	1
C22	484(2)	1472(2)	4238(1)	24(1)	1
C23	1422(2)	2778(2)	4520(1)	22(1)	1
C24	3080(2)	3104(2)	4864(1)	20(1)	1
C25	5055(2)	1374(1)	6695(1)	17(1)	1
C26	3703(2)	1717(2)	6890(1)	19(1)	1
C27	2701(2)	1009(2)	7395(1)	23(1)	1
C28	3014(2)	−55(2)	7714(1)	26(1)	1
C29	4329(2)	−421(2)	7510(1)	26(1)	1
C30	5336(2)	278(2)	7005(1)	22(1)	1
N1	2990(2)	3643(1)	2506(1)	19(1)	1
N2	5914(2)	3643(1)	3667(1)	21(1)	1
N3	8321(2)	3287(1)	5661(1)	17(1)	1
N4	8609(2)	2542(1)	7834(1)	23(1)	1
N5	7343(2)	2462(1)	9370(1)	25(1)	1
O1	−216(1)	2261(1)	1498(1)	25(1)	1
O2	8660(1)	4340(1)	4169(1)	22(1)	1
O3	10598(1)	3111(1)	7045(1)	27(1)	1
O4	5286(2)	3344(1)	10366(1)	33(1)	1

SULFURIC ACID COMPLEX OF 4.9

Table 1. Crystal data and structure refinement details.

Empirical formula	$C_{34}H_{41}N_7O_6S$	
Formula weight	675.80	
Temperature	120(2) K	
Wavelength	0.71073 Å	
Crystal system	Triclinic	
Space group	*P*–1	
Unit cell dimensions	a = 15.7033(4) Å	α = 65.8540(10)°
	b = 15.9794(4) Å	β = 83.729(2)°
	c = 16.6050(3) Å	γ = 61.1730(10)°
Volume	3310.72(13) Å^3	
Z	4	
Density (calculated)	1.356 Mg / m^3	
Absorption coefficient	0.155 mm^{-1}	
F(000)	1432	
Crystal	Rhombus; Colourless	
Crystal size	0.5 × 0.25 × 0.1 mm^3	
θ range for data collection	2.91 – 27.48°	
Index ranges	$-20 \le h \le 20$, $-20 \le k \le 20$, $-21 \le l \le 21$	
Reflections collected	52040	
Independent reflections	15085 [R_{int} = 0.0973]	
Completeness to θ = 27.48°	99.4 %	
Absorption correction	Semi–empirical from equivalents	
Max. and min. transmission	0.9908 and 0.9166	
Refinement method	Full-matrix least-squares on F^2	
Data / restraints / parameters	15085 / 3 / 869	
Goodness-of-fit on F^2	0.971	
Final *R* indices [$F^2 > 2\sigma(F^2)$]	*R1* = 0.0615, *wR2* = 0.1395	
R indices (all data)	*R1* = 0.1998, *wR2* = 0.2009	
Largest diff. peak and hole	1.218 and –0.614 e Å^{-3}	

Diffractometer: *Nonius KappaCCD* area detector (ϕ scans and ω scans to fill *asymmetric unit*). **Cell determination:** DirAx (Duisenberg, A.J.M.(1992). J. Appl. Cryst. 25, 92-96.) **Data collection:** Collect (Collect: Data collection software, R. Hooft, Nonius B.V., 1998). **Data reduction and cell refinement**: *Denzo* (Z. Otwinowski & W. Minor, *Methods in Enzymology* (1997) Vol. **276**: *Macromolecular Crystallography*, part A, pp. 307–326; C. W. Carter, Jr. & R. M. Sweet, Eds., Academic Press). **Absorption correction**: Sheldrick, G. M. SADABS - Bruker Nonius area detector scaling and absorption correction - V2.10 **Structure solution**: *SHELXS97* (G. M. Sheldrick, Acta Cryst. (1990) A**46** 467–473). **Structure refinement**: *SHELXL97* (G. M. Sheldrick (1997), University of Göttingen, Germany). **Graphics:** Cameron - A Molecular Graphics Package. (D. M. Watkin, L. Pearce and C. K. Prout, Chemical Crystallography Laboratory, University of Oxford, 1993).

Special details: All hydrogen atoms were placed in idealised positions and refined using a riding model.

Table 2. Atomic coordinates [× 10^4], equivalent isotropic displacement parameters [$Å^2 \times 10^3$] and site occupancy factors. U_{eq} is defined as one third of the trace of the orthogonalized U^{ij} tensor.

Atom	*x*	*y*	*z*	U_{eq}	*S.o.f.*
N1	51(2)	12987(2)	−2378(2)	22(1)	1
N2	43(2)	11917(2)	−1062(2)	21(1)	1
N3	2311(2)	11003(2)	−1189(2)	18(1)	1
N4	3361(2)	8893(2)	−1010(2)	17(1)	1
N5	3932(2)	6871(2)	431(2)	22(1)	1
C16	4825(2)	5490(3)	1877(2)	20(1)	1
C18	6221(3)	4818(3)	2670(2)	28(1)	1
O1	2375(2)	11505(2)	−2667(1)	24(1)	1
O2	4695(2)	6151(2)	−546(1)	24(1)	1
C1	1029(3)	13322(3)	−5427(2)	34(1)	1
C2	1043(3)	13537(3)	−4609(2)	29(1)	1
C3	420(3)	13220(3)	−3925(2)	25(1)	1
C4	383(3)	13552(3)	−3177(2)	26(1)	1
C5	−850(3)	13017(3)	−2340(2)	27(1)	1
C6	−847(2)	12348(3)	−1520(2)	25(1)	1
C7	581(2)	12318(3)	−1585(2)	19(1)	1
C8	1574(2)	12050(3)	−1285(2)	20(1)	1
C9	2644(2)	10817(3)	−1913(2)	18(1)	1
C10	3343(2)	9709(3)	−1751(2)	18(1)	1
C11	4037(2)	9312(3)	−2273(2)	18(1)	1
C12	4483(2)	8203(3)	−1831(2)	19(1)	1
C13	4041(2)	7973(3)	−1056(2)	18(1)	1
C14	4244(3)	6927(3)	−380(2)	20(1)	1
C15	4079(2)	5882(3)	1139(2)	22(1)	1
N6	4641(2)	5456(2)	2682(2)	25(1)	1
C17	5495(3)	5037(3)	3185(2)	29(1)	1
N7	5794(2)	5100(2)	1850(2)	23(1)	1
C19	6335(3)	4993(3)	1083(2)	25(1)	1
C20	7154(3)	3892(3)	1294(2)	28(1)	1
C21	7683(3)	3831(3)	478(2)	30(1)	1
C22	8347(3)	2723(3)	564(3)	42(1)	1
C23	4331(3)	9904(3)	−3092(2)	21(1)	1
C24	3720(3)	10550(3)	−3885(2)	28(1)	1
C25	4028(3)	11084(3)	−4642(2)	31(1)	1
C26	4939(3)	10993(3)	−4609(3)	40(1)	1
C27	5555(3)	10355(3)	−3830(3)	42(1)	1
C28	5255(3)	9811(3)	−3077(3)	34(1)	1
C29	5299(2)	7453(3)	−2138(2)	21(1)	1
C30	5157(3)	7355(3)	−2891(2)	34(1)	1
C31	5899(3)	6671(3)	−3192(3)	43(1)	1
C32	6812(3)	6067(3)	−2748(3)	41(1)	1
C33	6979(3)	6136(4)	−1983(3)	51(1)	1
C34	6223(3)	6825(3)	−1683(3)	43(1)	1
N8	15030(2)	1979(2)	−2612(2)	30(1)	1
N9	14964(2)	3085(2)	−3927(2)	21(1)	1
N10	12719(2)	3927(2)	−3735(2)	21(1)	1
N11	11621(2)	6044(2)	−3909(2)	19(1)	1
N12	11019(2)	8043(2)	−5347(2)	20(1)	1

N13	10318(2)	9450(2)	−7611(2)	22(1)	1
N14	9155(2)	9830(2)	−6793(2)	22(1)	1
O3	12677(2)	3426(2)	−2257(2)	26(1)	1
O4	10209(2)	8790(2)	−4398(1)	26(1)	1
C35	14011(4)	1682(4)	357(3)	81(2)	1
C36	13986(3)	1431(4)	−368(3)	58(2)	1
C37	14695(3)	1752(4)	−1063(2)	54(2)	1
C38	14739(3)	1395(3)	−1790(2)	50(1)	1
C39	15915(3)	1982(3)	−2681(2)	31(1)	1
C40	15871(3)	2680(3)	−3497(2)	28(1)	1
C41	14461(3)	2657(3)	−3387(2)	22(1)	1
C42	13466(2)	2893(3)	−3645(2)	26(1)	1
C43	12384(2)	4117(3)	−3011(2)	20(1)	1
C44	11667(2)	5207(3)	−3170(2)	19(1)	1
C45	10975(2)	5589(3)	−2640(2)	20(1)	1
C46	10506(2)	6694(3)	−3073(2)	19(1)	1
C47	10931(2)	6952(3)	−3854(2)	19(1)	1
C48	10695(2)	8001(3)	−4546(2)	21(1)	1
C49	10864(2)	9029(3)	−6065(2)	22(1)	1
C50	10127(3)	9424(3)	−6806(2)	20(1)	1
C51	9459(3)	9899(3)	−8127(2)	26(1)	1
C52	8732(3)	10132(3)	−7618(2)	26(1)	1
C53	8606(3)	9950(3)	−6035(2)	28(1)	1
C54	7866(3)	11073(3)	−6221(2)	29(1)	1
C55	7295(3)	11143(3)	−5425(2)	36(1)	1
C56	6656(3)	12253(4)	−5509(3)	51(1)	1
C57	10756(3)	4959(3)	−1781(2)	20(1)	1
C58	11369(3)	4471(3)	−1005(2)	31(1)	1
C59	11166(3)	3896(3)	−202(2)	36(1)	1
C60	10345(3)	3779(3)	−155(3)	37(1)	1
C61	9736(3)	4247(3)	−920(3)	36(1)	1
C62	9931(3)	4831(3)	−1720(2)	26(1)	1
C63	9690(3)	7422(3)	−2736(2)	22(1)	1
C64	9836(3)	7987(3)	−2367(2)	30(1)	1
C65	9103(3)	8603(3)	−2008(2)	32(1)	1
C66	8185(3)	8681(3)	−2012(2)	37(1)	1
C67	8030(3)	8122(3)	−2376(3)	40(1)	1
C68	8773(3)	7493(3)	−2731(2)	35(1)	1
S1	1952(1)	9458(1)	809(1)	21(1)	1
O5	940(2)	10320(2)	514(1)	28(1)	1
O6	2660(2)	9848(2)	634(1)	27(1)	1
O7	2183(2)	8779(2)	331(1)	26(1)	1
O8	2019(2)	8835(2)	1773(1)	26(1)	1
S2	2995(1)	5505(1)	4239(1)	21(1)	1
O9	2914(2)	6123(2)	3276(1)	28(1)	1
O10	2773(2)	6181(2)	4718(2)	28(1)	1
O11	2297(2)	5101(2)	4435(2)	32(1)	1
O12	4011(2)	4646(2)	4525(1)	29(1)	1

CRYSTAL STRUCUTRE OF 4.10

Table 1. Crystal data and structure refinement details.

Empirical formula	$C_{38}H_{57}N_5O_2$	
Formula weight	615.89	
Temperature	120(2) K	
Wavelength	0.71073 Å	
Crystal system	Triclinic	
Space group	*P*–1	
Unit cell dimensions	a = 9.5568(3) Å	α = 96.252(2)°
	b = 13.7997(5) Å	β = 91.957(2)°
	c = 27.4754(10) Å	γ = 95.650(2)°
Volume	3580.7(2) Å^3	
Z	4	
Density (calculated)	1.142 Mg / m^3	
Absorption coefficient	0.071 mm^{-1}	
F(000)	1344	
Crystal	Block; Colourless	
Crystal size	0.21 × 0.2 × 0.05 mm^3	
θ range for data collection	2.93 – 27.48°	
Index ranges	$-12 \le h \le 12$, $-17 \le k \le 17$, $-35 \le l \le 35$	
Reflections collected	54029	
Independent reflections	16331 [R_{int} = 0.0785]	
Completeness to θ = 27.48°	99.4 %	
Absorption correction	Semi–empirical from equivalents	
Max. and min. transmission	0.9965 and 0.9752	
Refinement method	Full-matrix least-squares on F^2	
Data / restraints / parameters	16331 / 0 / 819	
Goodness-of-fit on F^2	0.655	
Final *R* indices [$F^2 > 2\sigma(F^2)$]	*R1* = 0.0787, *wR2* = 0.2113	
R indices (all data)	*R1* = 0.1373, *wR2* = 0.2766	
Largest diff. peak and hole	1.178 and –0.508 e Å^{-3}	

Diffractometer: *Nonius KappaCCD* area detector (ϕ scans and ω scans to fill *asymmetric unit*). **Cell determination:** DirAx (Duisenberg, A.J.M.(1992). J. Appl. Cryst. 25, 92-96.) **Data collection:** Collect (Collect: Data collection software, R. Hooft, Nonius B.V., 1998). **Data reduction and cell refinement**: *Denzo* (Z. Otwinowski & W. Minor, *Methods in Enzymology* (1997) Vol. **276**: *Macromolecular Crystallography*, part A, pp. 307–326; C. W. Carter, Jr. & R. M. Sweet, Eds., Academic Press). **Absorption correction**: Sheldrick, G. M. SADABS - Bruker Nonius area detector scaling and absorption correction - V2.10 **Structure solution**: *SHELXS97* (G. M. Sheldrick, Acta Cryst. (1990) **A46** 467–473). **Structure refinement**: *SHELXL97* (G. M. Sheldrick (1997), University of Göttingen, Germany). **Graphics:** Cameron - A Molecular Graphics Package. (D. M. Watkin, L. Pearce and C. K. Prout, Chemical Crystallography Laboratory, University of Oxford, 1993).

Special details: All hydrogen atoms were placed in idealised positions and refined using a riding model.

Table 2. Atomic coordinates [$\times 10^4$], equivalent isotropic displacement parameters [$Å^2 \times 10^3$] and site occupancy factors. U_{eq} is defined as one third of the trace of the orthogonalized U^{ij} tensor.

Atom	*x*	*y*	*z*	U_{eq}	*S.o.f.*
C1	10258(5)	8841(4)	4373(2)	60(1)	1
C2	8725(5)	8855(4)	4516(2)	55(1)	1
C3	7993(5)	9684(3)	4340(2)	50(1)	1
C4	6485(5)	9645(3)	4469(2)	46(1)	1
C5	5821(9)	10022(4)	2606(2)	89(2)	1
C6	4824(6)	9600(4)	2952(2)	64(1)	1
C7	5635(6)	9439(4)	3419(2)	65(1)	1
C8	4768(6)	9099(4)	3808(2)	73(2)	1
C9	4546(4)	8400(3)	4557(2)	42(1)	1
C10	3987(4)	7358(3)	4378(2)	33(1)	1
C11	5237(3)	5871(2)	4379(1)	23(1)	1
C12	6565(3)	5454(2)	4255(1)	22(1)	1
C13	7486(3)	5599(2)	3881(1)	23(1)	1
C14	8669(3)	5093(2)	3972(1)	22(1)	1
C15	8413(3)	4643(2)	4395(1)	21(1)	1
C16	9170(3)	3972(2)	4668(1)	22(1)	1
C17	11182(3)	3057(2)	4753(1)	26(1)	1
C18	12596(3)	2956(3)	4526(1)	26(1)	1
C19	11862(4)	1708(2)	3851(1)	28(1)	1
C20	11524(4)	1459(3)	3306(1)	32(1)	1
C21	10661(4)	463(3)	3189(2)	39(1)	1
C22	10328(6)	178(3)	2645(2)	52(1)	1
C23	13806(3)	2979(2)	3767(1)	27(1)	1
C24	15052(4)	2427(3)	3894(1)	32(1)	1
C25	16365(4)	2737(3)	3626(1)	32(1)	1
C26	17641(4)	2228(3)	3763(2)	40(1)	1
C27	7228(3)	6134(2)	3451(1)	24(1)	1
C28	6006(4)	5879(3)	3152(1)	28(1)	1
C29	5734(4)	6384(3)	2758(1)	39(1)	1
C30	6679(5)	7140(3)	2649(2)	43(1)	1
C31	7904(4)	7388(3)	2931(2)	41(1)	1
C32	8187(4)	6885(3)	3330(1)	32(1)	1
C33	9863(3)	5021(2)	3646(1)	22(1)	1
C34	9644(4)	4550(3)	3173(1)	31(1)	1
C35	10741(4)	4509(3)	2856(1)	35(1)	1
C36	12072(4)	4940(3)	3012(1)	36(1)	1
C37	12304(3)	5404(3)	3480(1)	30(1)	1
C38	11215(3)	5453(2)	3802(1)	27(1)	1
N1	5568(4)	8804(2)	4227(1)	43(1)	1
N2	5162(3)	6791(2)	4270(1)	29(1)	1
N3	7132(3)	4864(2)	4555(1)	22(1)	1
N4	10440(3)	3761(2)	4519(1)	24(1)	1
N5	12474(3)	2720(2)	3993(1)	26(1)	1
O1	4291(2)	5400(2)	4576(1)	26(1)	1
O2	8626(2)	3613(2)	5017(1)	28(1)	1
C39	11837(5)	−2479(3)	2625(2)	50(1)	1
C40	11227(4)	−2922(3)	2133(2)	44(1)	1
C41	12119(4)	−2694(3)	1702(1)	36(1)	1
C42	12325(3)	−1617(3)	1621(1)	29(1)	1

C43	18046(4)	−1758(3)	1456(2)	42(1)	1
C44	16642(3)	−2169(3)	1189(1)	33(1)	1
C45	15429(3)	−1572(3)	1332(1)	32(1)	1
C46	14097(3)	−1914(2)	1008(1)	25(1)	1
C47	12982(3)	−416(2)	1059(1)	28(1)	1
C48	11575(3)	2(2)	1018(1)	27(1)	1
C49	9351(3)	−381(2)	555(1)	21(1)	1
C50	8410(3)	−1088(2)	222(1)	20(1)	1
C51	8491(3)	−2044(2)	11(1)	20(1)	1
C52	7180(3)	−2361(2)	−247(1)	20(1)	1
C53	6357(3)	−1583(2)	−186(1)	20(1)	1
C54	4950(3)	−1444(2)	−402(1)	20(1)	1
C55	3398(3)	−1827(3)	−1155(1)	26(1)	1
C56	3782(3)	−1907(2)	−1689(1)	26(1)	1
C57	5438(4)	−2646(3)	−2253(1)	30(1)	1
C58	6960(4)	−2876(3)	−2194(1)	28(1)	1
C59	7856(4)	−2105(3)	−1842(1)	32(1)	1
C60	9397(4)	−2287(3)	−1800(2)	37(1)	1
C61	4043(3)	−3667(2)	−1734(1)	27(1)	1
C62	2732(4)	−4069(3)	−2054(1)	34(1)	1
C63	2097(4)	−5059(3)	−1919(2)	37(1)	1
C64	1304(5)	−4987(3)	−1450(2)	47(1)	1
C65	9652(3)	−2666(2)	62(1)	20(1)	1
C66	9490(3)	−3449(2)	342(1)	25(1)	1
C67	10561(4)	−4051(2)	386(1)	28(1)	1
C68	11795(3)	−3881(2)	146(1)	26(1)	1
C69	11973(3)	−3100(2)	−130(1)	27(1)	1
C70	10907(3)	−2495(2)	−174(1)	24(1)	1
C71	6765(3)	−3347(2)	−513(1)	22(1)	1
C72	7595(3)	−3749(2)	−875(1)	24(1)	1
C73	7174(4)	−4660(2)	−1131(1)	27(1)	1
C74	5923(4)	−5180(2)	−1032(1)	29(1)	1
C75	5108(4)	−4805(2)	−666(1)	29(1)	1
C76	5526(3)	−3898(2)	−406(1)	25(1)	1
N6	12821(3)	−1451(2)	1135(1)	24(1)	1
N7	10638(3)	−621(2)	663(1)	26(1)	1
N8	7102(3)	−831(2)	102(1)	20(1)	1
N9	4678(3)	−1874(2)	−858(1)	25(1)	1
N10	4689(3)	−2689(2)	−1797(1)	25(1)	1
O3	8944(2)	402(2)	728(1)	27(1)	1
O4	4132(2)	−949(2)	−172(1)	24(1)	1

APPENDIX 2 - ^{1}H NMR TITRATION CURVES

CURVES FROM CHAPTER 2

Meso-octamethylcalix[4]pyrrole in dichloromethane-d_2

TBACl

K_a = 230

Error = 0.8 %

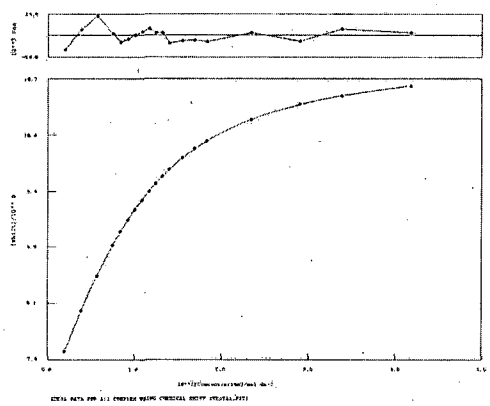

EMIMCl

K_a = 2240

Error = 12 %

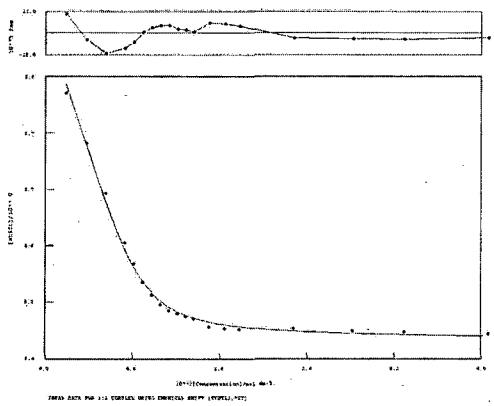

BMIMCl

K_a = 5960

Error = 7.6 %

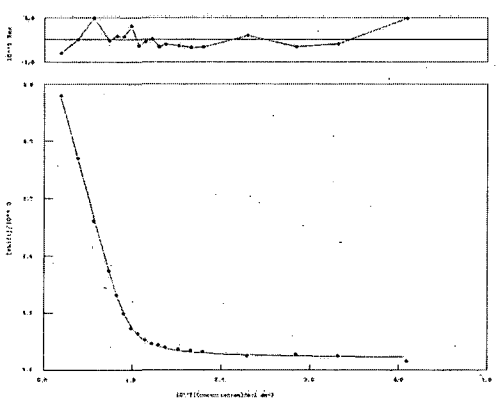

EtPyCl

K_a = 18,000

Error = 1 %

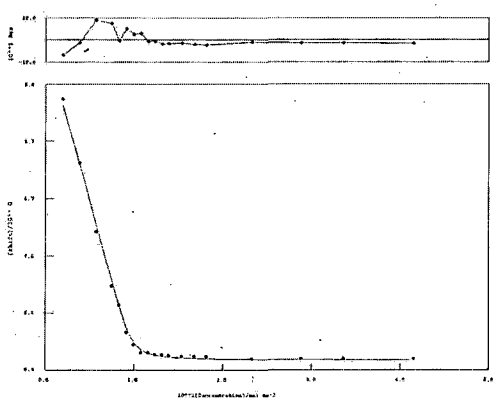

TBABr

K_a = <10

Error = 13.8 %

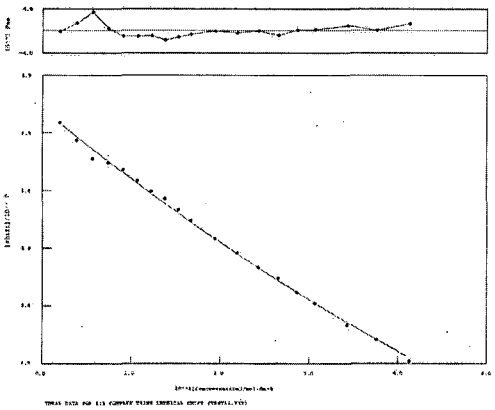

EMIMBr

K_a = 200

Error = 3.0 %

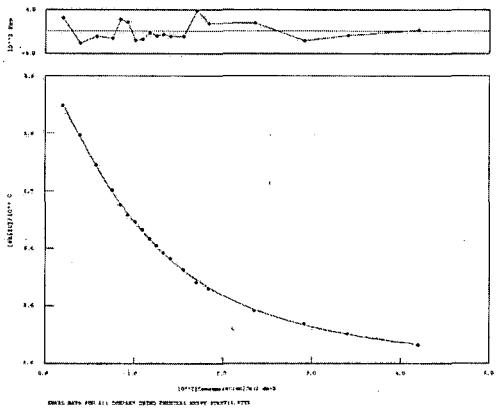

BMIMBr

K_a = 280

Error = 3.2 %

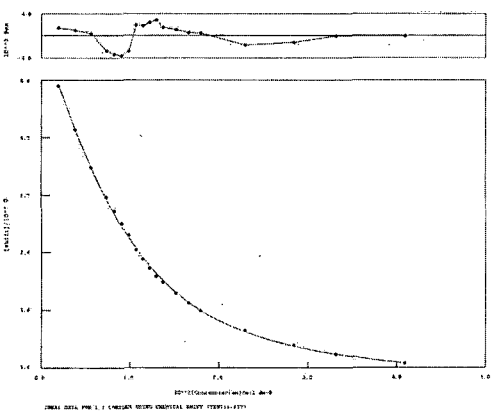

EtPyBr

K_a = 1180

Error = 5.2 %

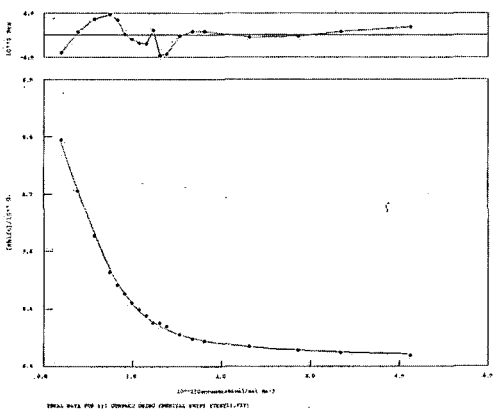

Meso-octamethylcalix[4]pyrrole in dimethylsulfoxide-d_6/0.5% water

TBACl

K_a = 980

Error = 4.3 %

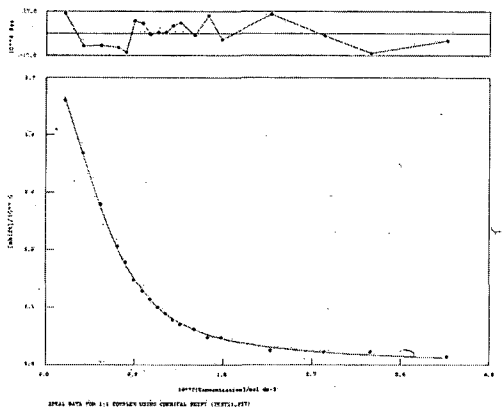

EMIMCl

K_a = 1250

Error = 1.4 %

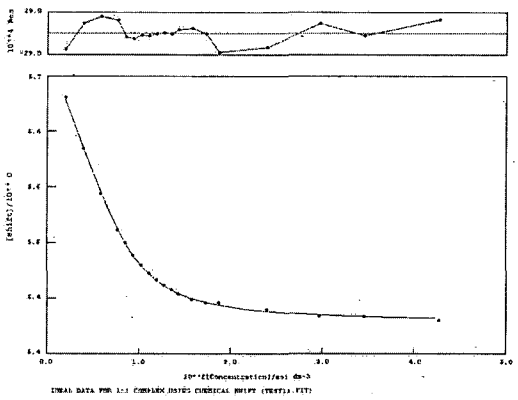

BMIMCl

K_a = 825

Error = 5.6 %

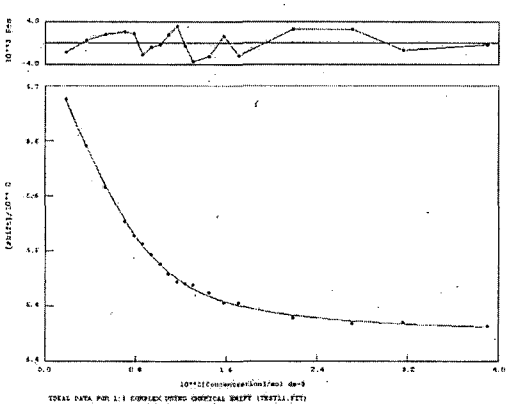

EtPyCl

K_a = 1100

Error = 2.2 %

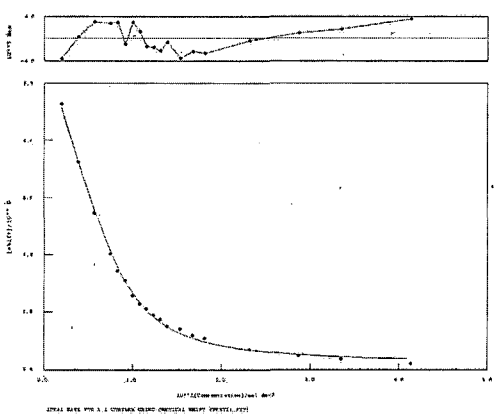

TBABr

K_a = 18

Error = 11 %

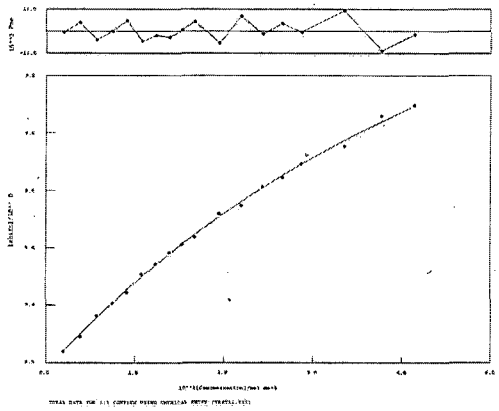

EMIMBr

K_a = <10

Error = 12 %

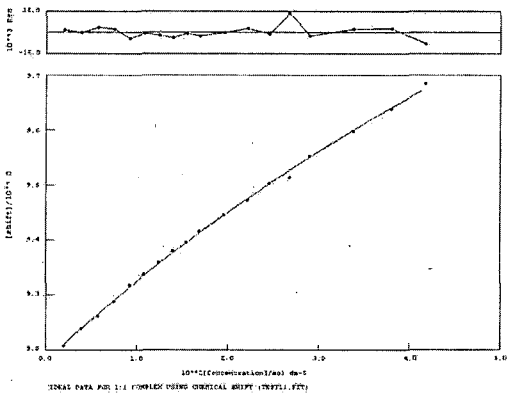

BMIMBr

K_a = 10

Error = 10 %

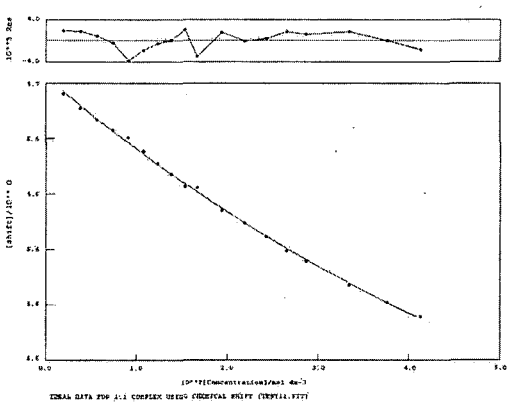

EtPyBr

K_a = 14

Error = 7.1 %

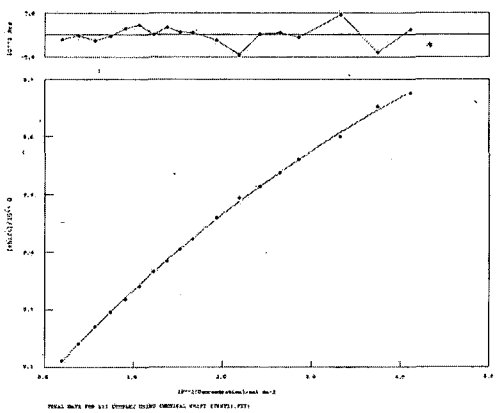

N-confused octamethylcalix[4]pyrrole in dichloromethane-d_2

TBACl

$K_a = 10$

Error = 13.2 %

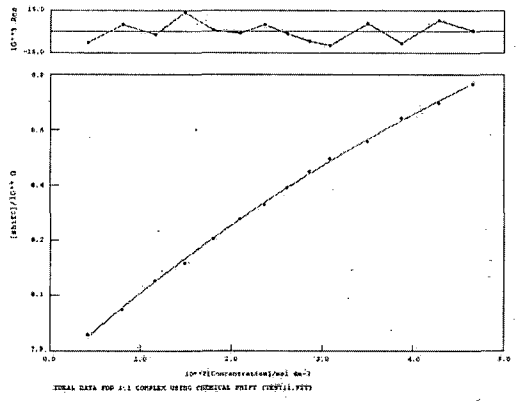

TEACl

$K_a = 36$

Error = 7.1 %

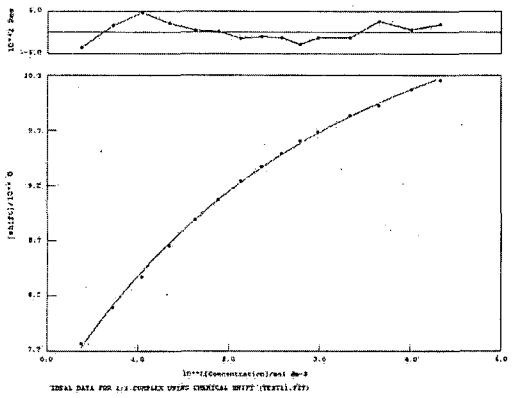

EMIMCl

$K_1 = 220$, $K_2 = 34$

$\beta = 7425$

Error - $K_1 = 30$ %, $K_2 = 17$ %

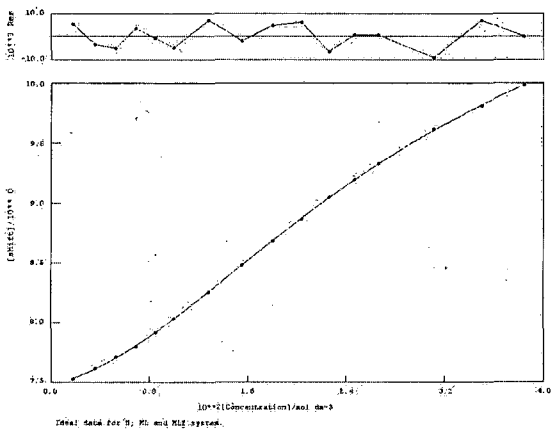

CURVES FROM CHAPTER 3

Pyridine-2,6-dicarboxylic acid bis-[(2,3-dimethyl-1*H*-indol-7-yl)-amide], 3.7a, in dimethylsulfoxide/0.5% water

TBA fluoride

K_a = 18, 775

Error = 14.8 %

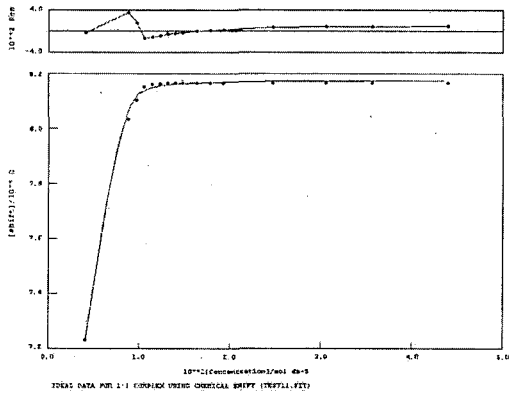

TBA acetate

K_a = 250

Error = 3.2 %

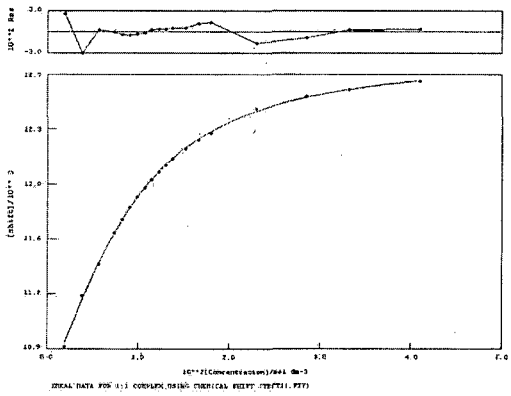

TBA dihydrogenphosphate

K_a = 70

Error = 7.0 %

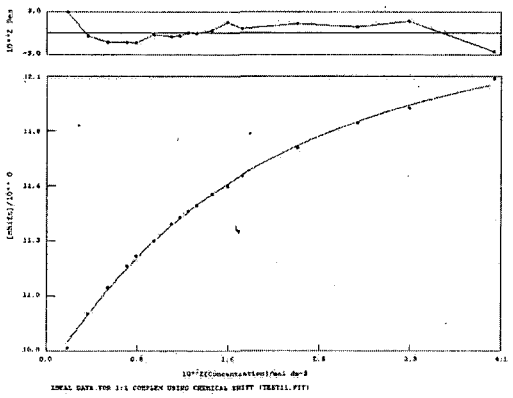

TBA benzoate

K_a = 17

Error = 3.4 %

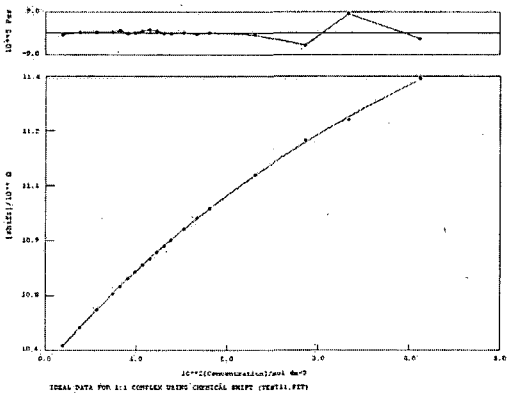

TBA chloride

$K_a = 5$

Error = 15 %

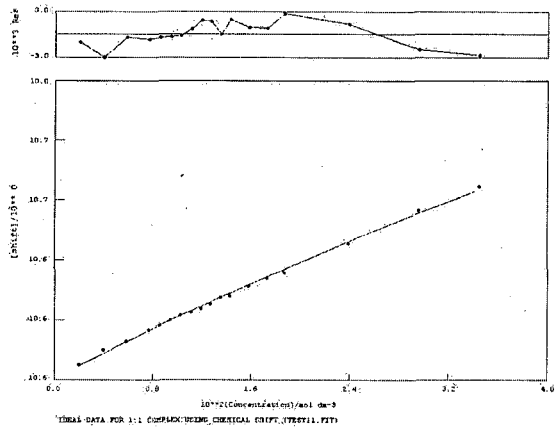

Pyridine-2,6-dicarboxylic acid bis-[(2,3-dimethyl-1*H*-indol-7-yl)-amide], 3.7a, in dimethylsulfoxide/5% water.

TBA fluoride

$K_a = 1360$

Error = 5.7 %

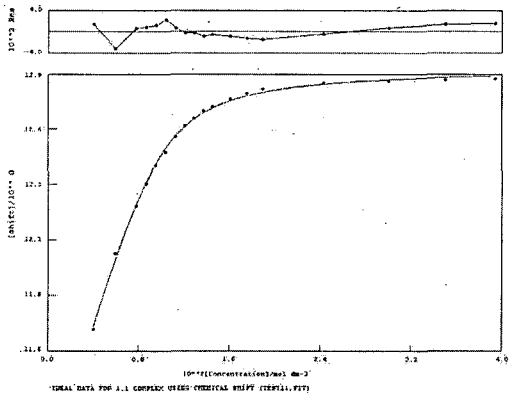

TBA acetate

$K_a = 14$

Error = 4.6 %

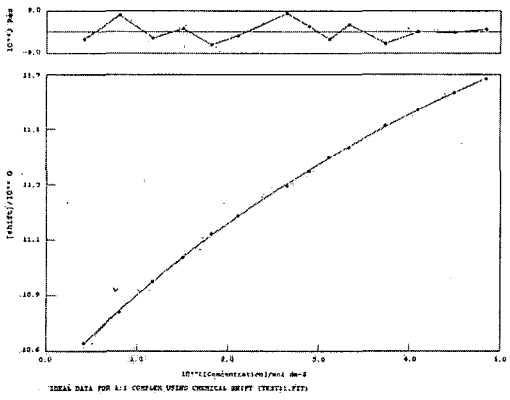

TBA dihydrogen phosphate

$K_a = 26$

Error = 6.2 %

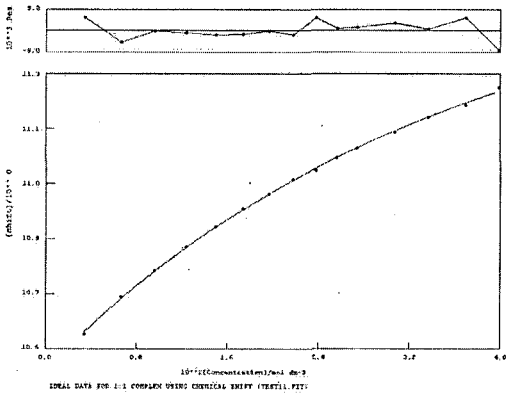

TBA benzoate

$K_a = 5$

Error = 15.2 %

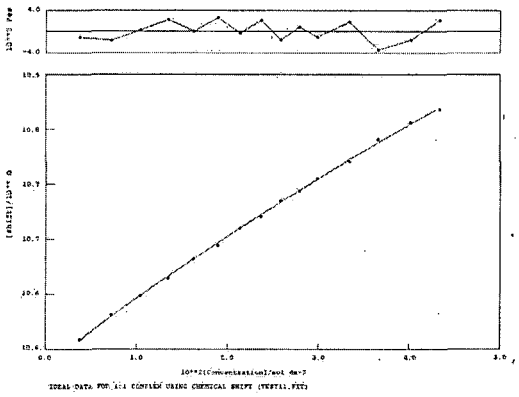

TBA chloride

$K_a = 6$

Error = 16.7 %

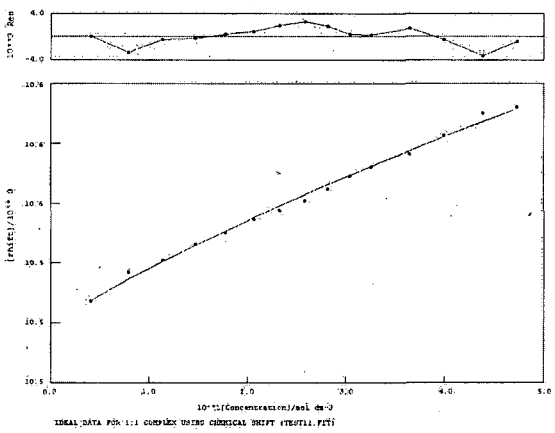

N,N'-Bis-(2,3-dimethyl-1H-indol-7-yl)-isophthalamide, 3.7b, in dimethylsuloxide-d_6/0.5% water

TBA acetate

K_a = 880

Error = 2.7 %

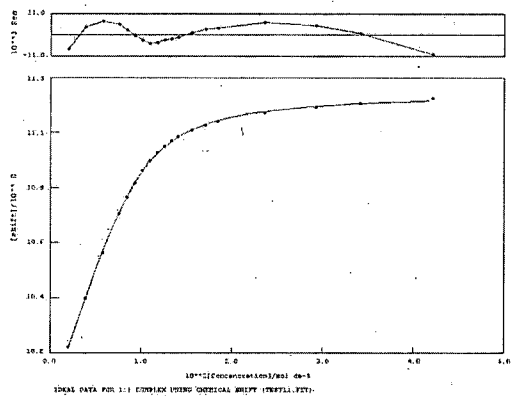

TBA dihydrogen phosphate

K_a = 1140

Error = 8.4 %

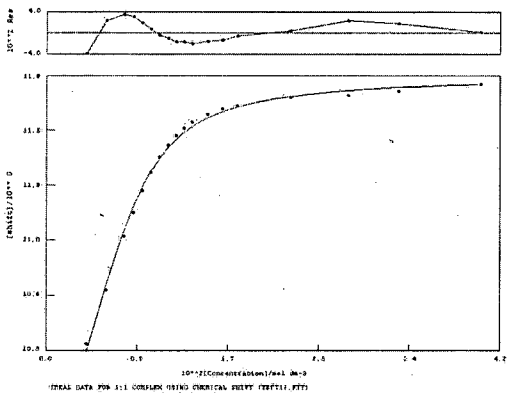

TBA benzoate

K_a = 120

Error = 1.4 %

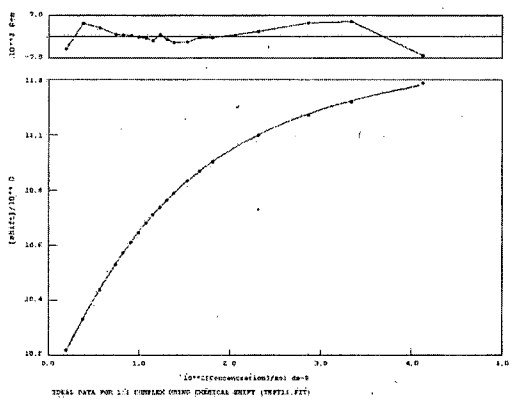

TBA chloride

K_a = 17

Error = 11.1 %

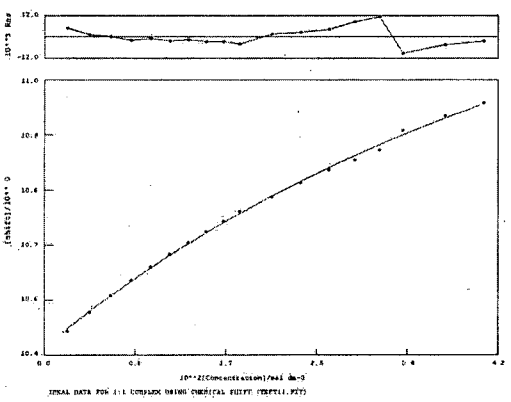

N,N'-Bis-(2,3-dimethyl-1*H*-indol-7-yl)-isophthalamide, 3.7b, in dimethylsuloxide-d_6/5% water

TBA fluoride

$K_1 = 940$, $K_2 = 21$

$\beta = 19{,}600$

Error – $K_1 = 10\%$, $K_2 = 7.2\ \%$

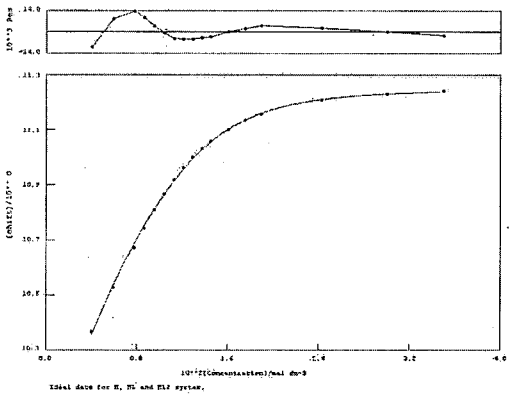

TBA acetate

$K_a = 110$

Error = 1.8 %

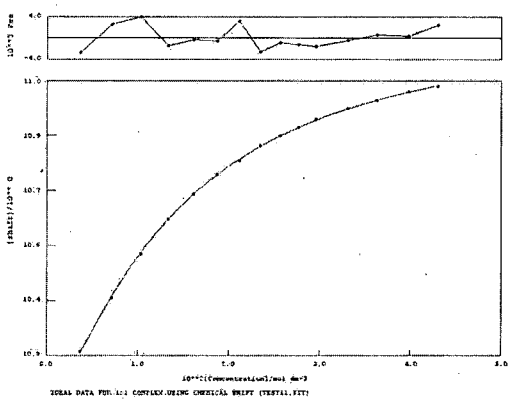

TBA dihydrogen phosphate

$K_a = 260$

Error = 5.3 %

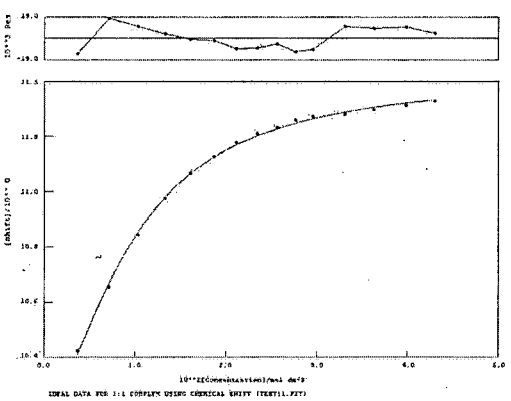

TBA bezoate

$K_a = 35$

Error = 2.9 %

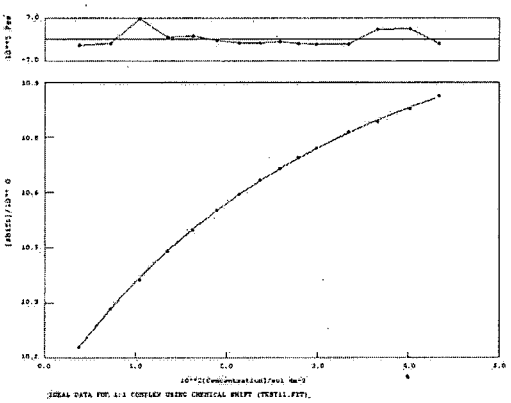

TBA chloride

K_a = 15

Error = 8.7 %

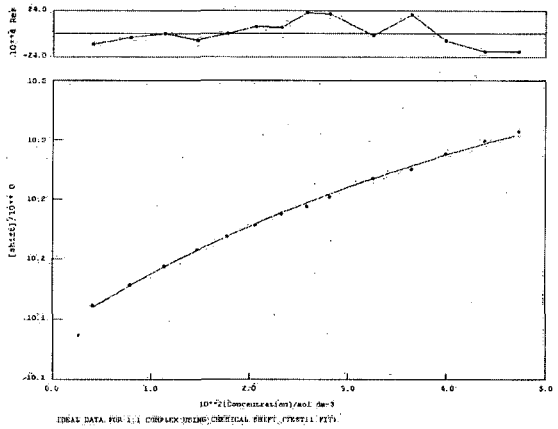

7-Pentanoylamino-1*H*-indole-2-carboxylic acid butylamide, 3.8, in dimethylsulfoxide-d_6/0.5% water

TBA acetate

K_a = 425

Error = 1.0 %

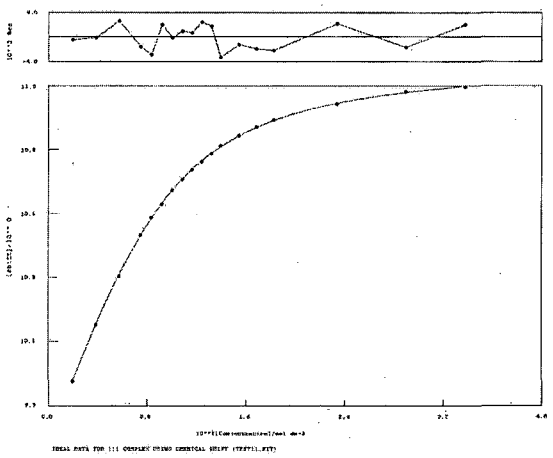

TBA dihydrogen phosphate

K_a = 390

Error = 3.6 %

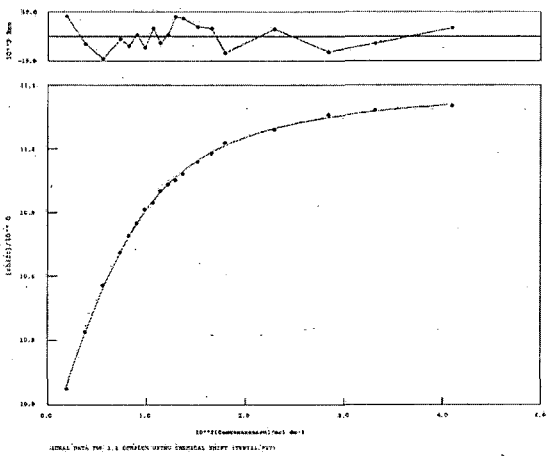

TBA benzoate

$K_a = 115$

Error = 1.1 %

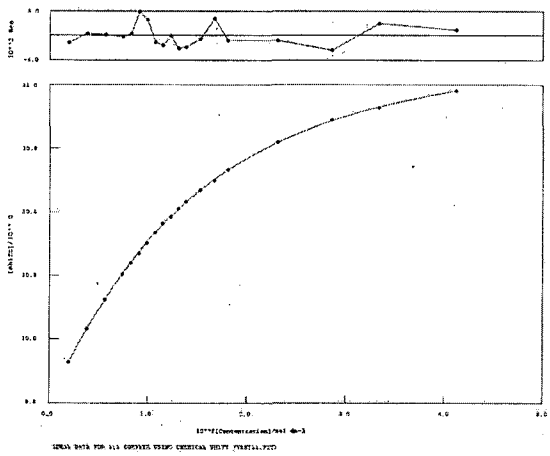

TBA chloride

$K_a = 4$

Error = 38 %

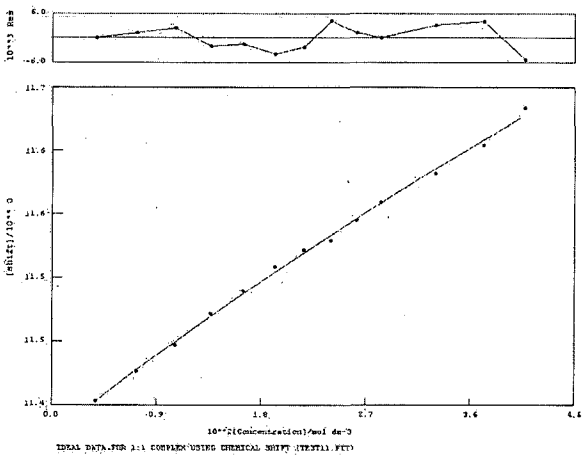

7-Benzoylamino-1*H*-indole-2-carboxylic acid phenylamide, 3.9, in dimethylsulfoxide-d_6/0.5% water

TBA acetate

$K_a = 650$

Error = 2.3 %

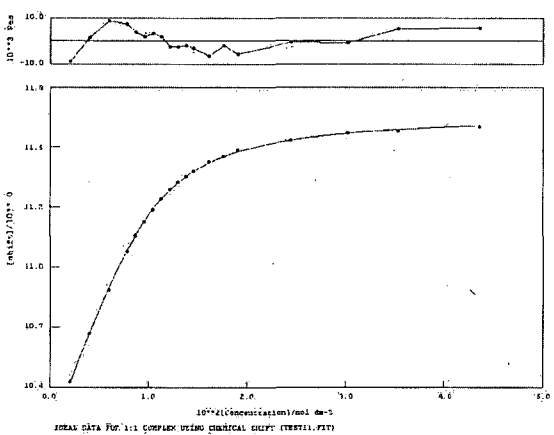

TBA dihydrogen phosphate

$K_a = 310$

Error = 3.5 %

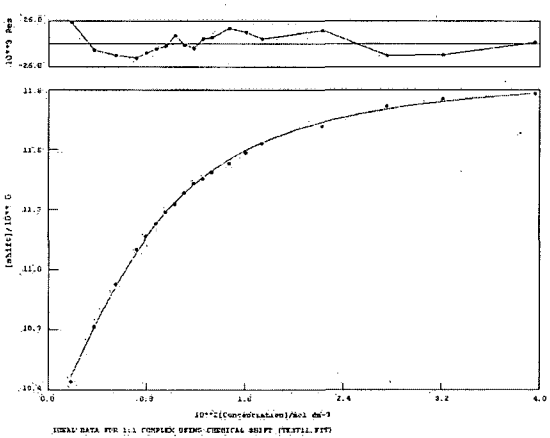

TBA benzoate

$K_a = 100$

Error = 0.7 %

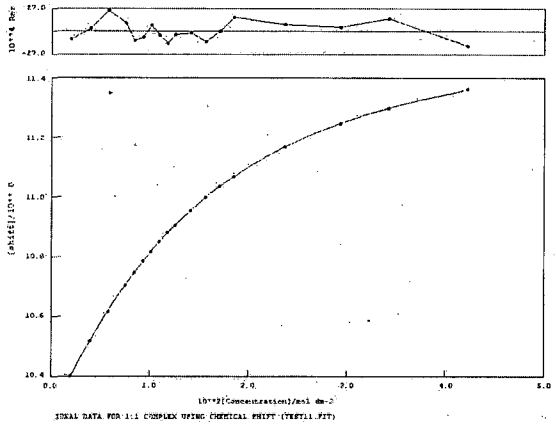

TBA chloride

$K_a = 7$

Error = 12 %

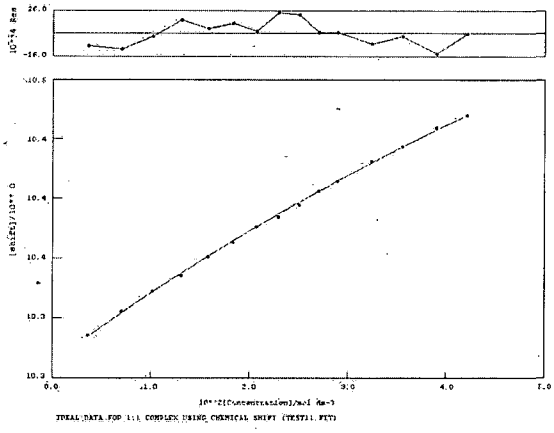

7-Phenylacetylamino-1*H*-indole-2-carboxylic acid phenylamide, 3.10, in dimethylsulfoxide-d_6/0.5% water

TBA acetate

$K_a = 900$

Error = 4.7 %

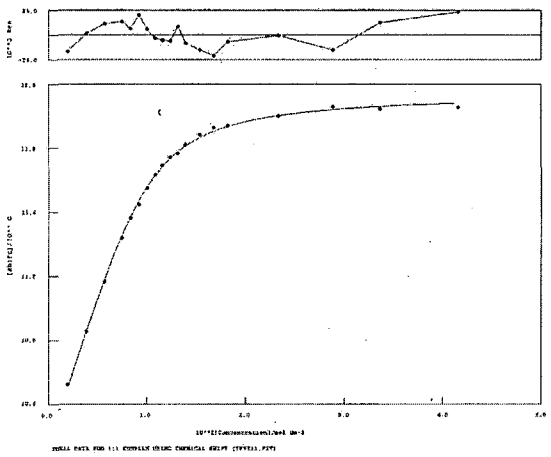

TBA dihydrogen phosphate

$K_a = 350$

Error = 4.8 %

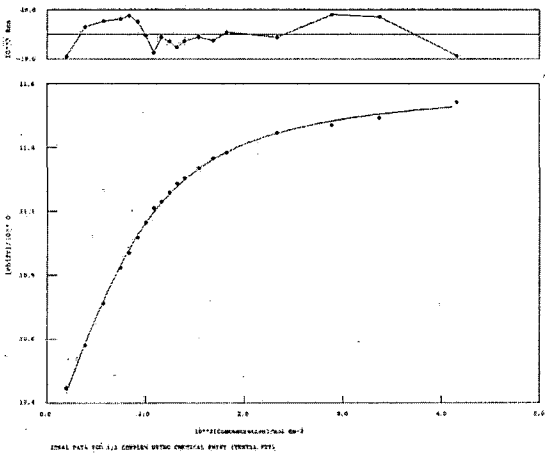

TBA benzoate

K_a = 140

Error = 1.9 %

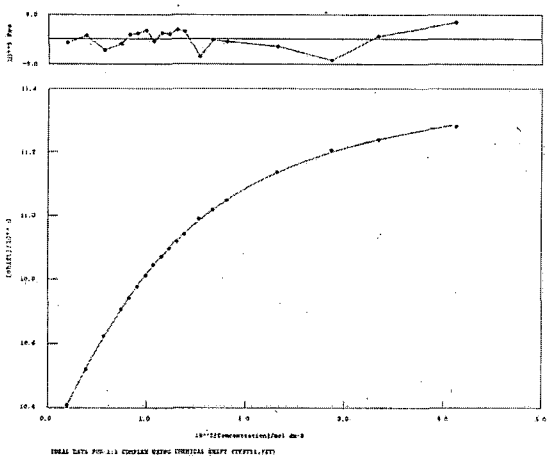

TBA chloride

K_a = 11

Error = 7.8 %

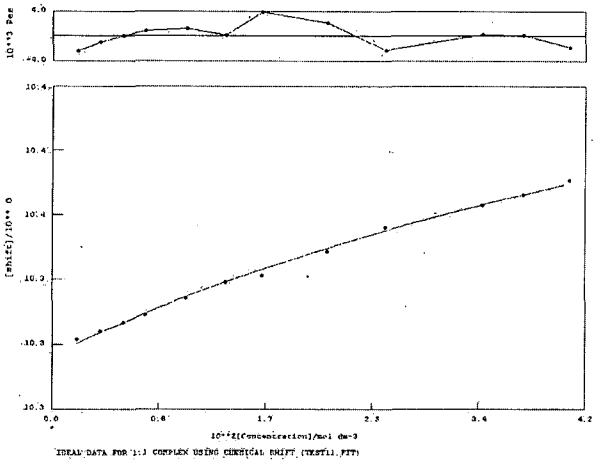

7-(3-Butyl-ureido)-1*H*-indole-2-carboxylic acid butylamide, 3.11, in dimethylsulfoxide-d_6/0.5% water

TBA acetate

K_a = 2060

Error = 6.9 %

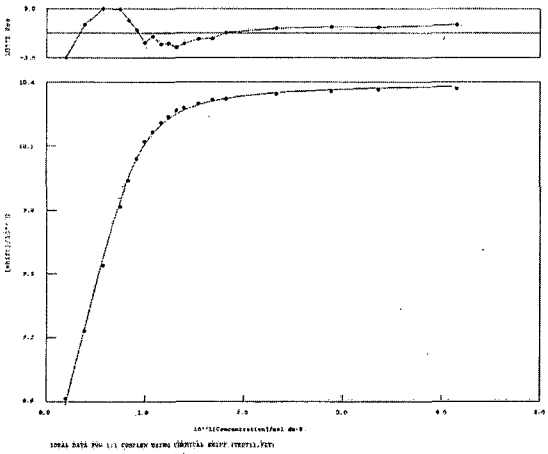

TBA dihydrogen phosphate

K_a = 940

Error = 9.6 %

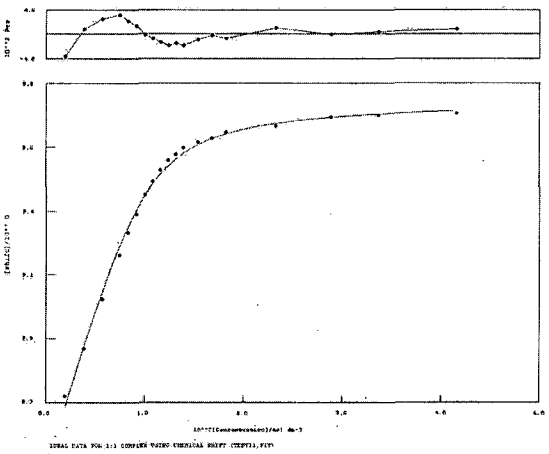

TBA benzoate

$K_a = 680$

Error = 5.7 %

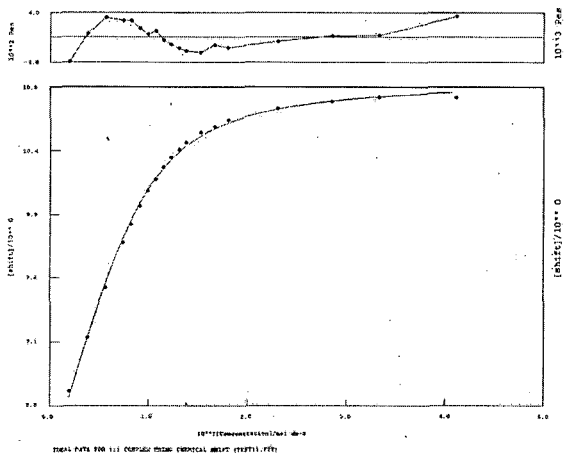

TBA chloride

$K_a = 20$

Error = 5.0 %

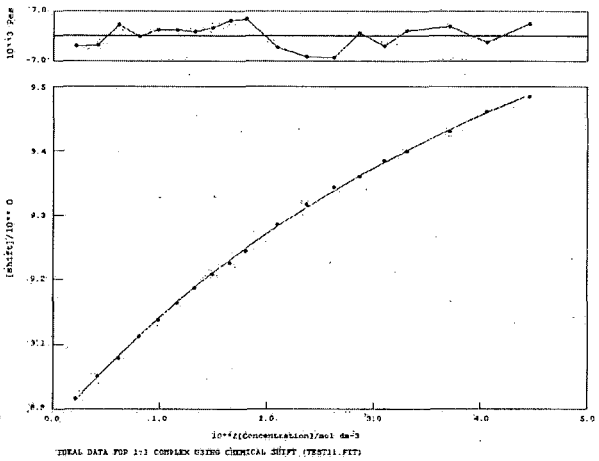

7-(3-Phenyl-ureido)-1*H*-indole-2-carboxylic acid phenylamide, 3.12, in dimethylsulfoxide-d_6/0.5% water

TBA acetate

$K_a = 10000$

Error = 7.2 %

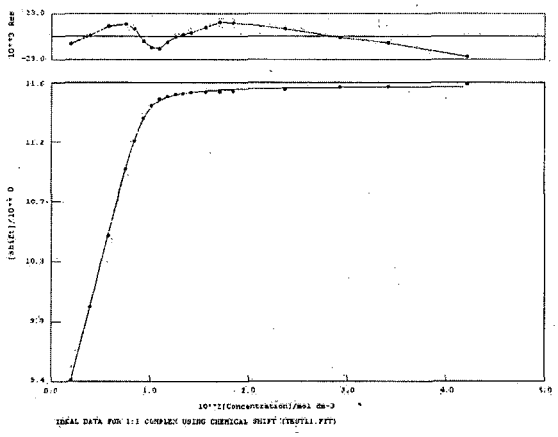

TBA dihydrogen phosphate

$K_a = 4950$

Error = 12 %

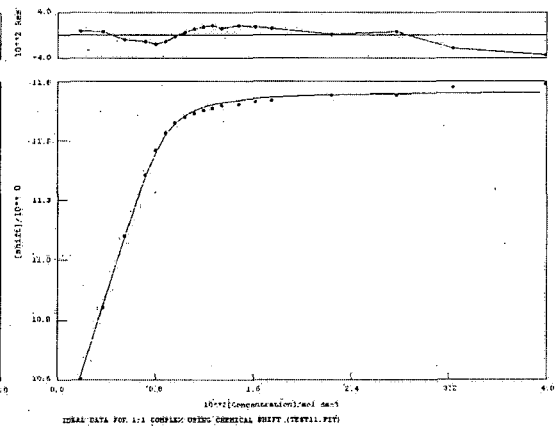

TBA benzoate

K_a = 4460

Error = 2.3 %

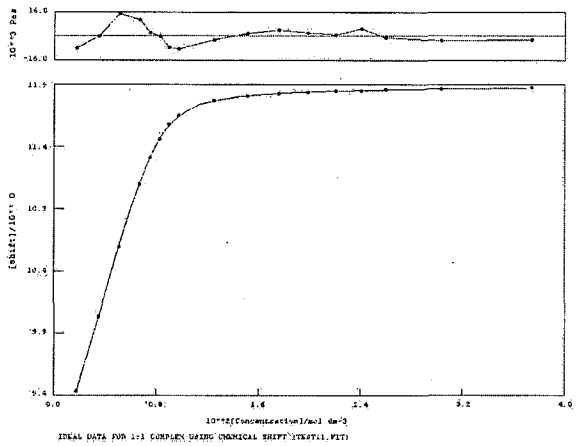

TBA chloride

K_a = 38

Error = 7.9 %

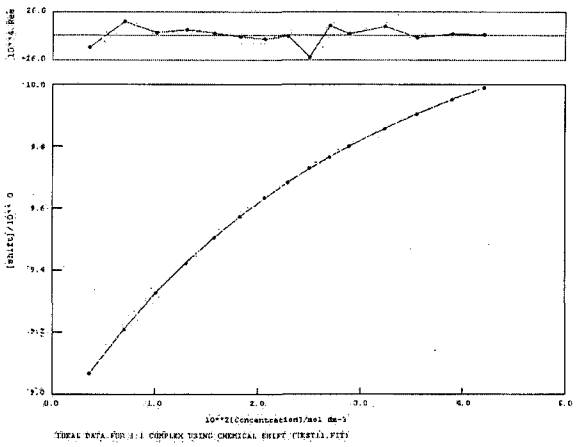

7-(3-Phenyl-thioureido)-1*H*-indole-2-carboxylic acid phenyl amide, 3.13, in dimethylsulfoxide-d_6/0.5% water

TBA dihydrogenphosphate

K_a = 1600

Error = 7.5 %

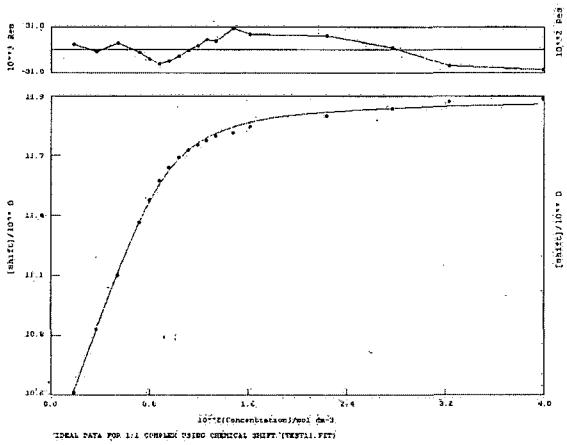

TBA benzoate

K_a = 780

Error = 7.6 %

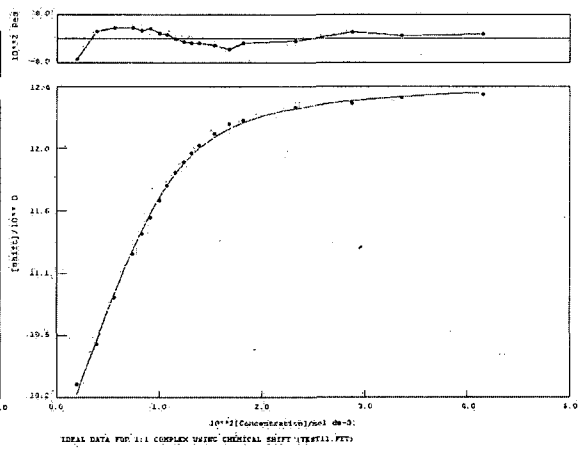

TBA chloride

$K_a = 16$

Error = 3.8 %

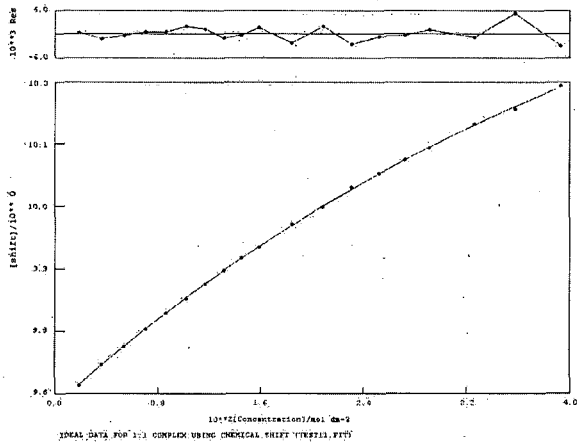

APPENDIX 3 - ICP-OES DATA

NICKEL EXTRACTION DATA WITH 4.11 ALONE

			mg/g
[pyrrole] in stock	mol/l	0.01002	=
[pyridine] in stock	mol/l	0.01026	
[benzene] in stock	mol/l	0.01007	
mass of 10ml BuOH	mg	8100	
butanol density @25C	g/l	810	
chloroform density @25C	g/l	1464.73	

Sample	pH	mass of org	vlm of soln	amt of Ni in icp sample	conc of Ni in 2 ml	% of total Ni
		g	l	mg/kg	mg/g	
1	1.224	2.9965	2.0458E-03	0	0.00E+00	0.0
2	1.519	3.0272	2.0667E-03	0	0.00E+00	0.0
3	1.853	3.0248	2.0651E-03	0	0.00E+00	0.0
4	2.046	3.2043	2.1876E-03	0	0.00E+00	0.0
5	2.292	3.1200	2.1301E-03	0	0.00E+00	0.0
6	2.528	3.1043	2.1194E-03	0	0.00E+00	0.0
8	2.732	3.0859	2.1068E-03	0	0.00E+00	0.0
9	3.047	3.1078	2.1218E-03	0	0.00E+00	0.0
10	3.172	3.1485	2.1495E-03	13.92	3.58E-02	13.4
11	3.565	3.1156	2.1271E-03	36.92	9.60E-02	36.0
12	3.747	3.1357	2.1408E-03	78.56	2.03E-01	76.2
13	4.795	3.0967	2.1142E-03	97.7	2.56E-01	95.9
14	6.272	3.1054	2.1201E-03	101.4	2.64E-01	99.3
		3.1254	2.1338E-03	102.8	2.66E-01	

ICP-OES DATA FOR DUAL HOST EXTRACTIONS

			mg/g
[4.10] in stock	mol/l	0.01002	=
[4.13] in stock	mol/l	0.01026	
[4.14] in stock	mol/l	0.01007	
ass of 10ml Bu(	mg	8100	
butanol density @25C	g/l	810	
chloroform density @25C	g/l	1464.73	

Sample	pH	mass of org	vlm of soln	amt of S in icp sample	amt of Ni in icp sample	amount of S in 2 ml	conc of Ni in 2 ml	100%S	% of total S	% of total Ni
4.10		g	l	mg/kg	mg/kg	mol/l	mg/g			
1	1.27	3.1011	2.1172E-03	97.49	0	6.7898E-04	0.00E+00	8.3825E+01	116.3	0.0
2	1.586	3.1167	2.1278E-03	100.6	0	6.8240E-04	0.00E+00	8.4246E+01	119.4	0.0
3	1.906	3.1120	2.1246E-03	101.3	0	6.8137E-04	0.00E+00	8.4119E+01	120.4	0.0
4	2.177	3.1005	2.1168E-03	99.19	0	6.7885E-04	0.00E+00	8.3809E+01	118.4	0.0
5	2.849	3.0885	2.1086E-03	97.02	34.22	6.7622E-04	8.97E-02	8.3484E+01	116.2	32.7
6	2.874	3.0778	2.1013E-03	95.51	35.55	6.7388E-04	9.36E-02	8.3195E+01	114.8	34.1
7	3.555	3.1054	2.1201E-03	96.32	61.35	6.7992E-04	1.60E-01	8.3941E+01	114.7	58.4
8	3.887	3.0466	2.0800E-03	92.46	83.27	6.6705E-04	2.21E-01	8.2352E+01	112.3	80.8
9	4.24	3.1180	2.1287E-03	83.24	93.72	6.8268E-04	2.43E-01	8.4282E+01	98.8	88.8
10	4.364	3.0846	2.1059E-03	76.17	96.34	6.7537E-04	2.53E-01	8.3379E+01	91.4	92.3
11	4.568	3.1325	2.1386E-03	53.85	96.18	6.8586E-04	2.49E-01	8.4673E+01	63.6	90.7
12	4.826	3.0847	2.1060E-03	27.3	99.44	6.7539E-04	2.61E-01	8.3381E+01	32.7	95.3
13	5.084	3.1122	2.1248E-03	13.01	104.3	6.8141E-04	2.71E-01	8.4125E+01	15.5	99.0
14	5.341	3.0660	2.0932E-03	1.432	101	6.7130E-04	2.67E-01	8.2876E+01	1.7	97.3
15	6.009	3.0982	2.1152E-03	0	101.6	6.7835E-04	2.66E-01	8.3746E+01	0.0	96.9
16	6.8	3.0379	2.0740E-03	0	109.6	6.6514E-04	2.92E-01	8.2116E+01	0.0	106.6
4.13									% of S	% of Ni
1	1.283	3.0602	2.0893E-03	83.94	0	6.7003E-04	0.00E+00	8.2719E+01	101.5	0.0

2	1.63	3.0514	2.0833E-03	84.91	0	6.6810E-04	0.00E+00	8.2481E+01	102.9	0.0
3	1.912	3.0968	2.1142E-03	91.19	0	6.7804E-04	0.00E+00	8.3708E+01	108.9	0.0
4	2.672	3.1150	2.1267E-03	91.97	0	6.8202E-04	0.00E+00	8.4200E+01	109.2	0.0
5	3.166	3.0713	2.0968E-03	89.1	4.873	6.7246E-04	1.29E-02	8.3019E+01	107.3	4.7
6	3.359	3.1285	2.1359E-03	86.68	7.369	6.8498E-04	1.91E-02	8.4565E+01	102.5	6.9
7	3.532	3.1136	2.1257E-03	90.09	14.44	6.8172E-04	3.76E-02	8.4163E+01	107.0	13.6
8	4.242	3.0927	2.1114E-03	87.1	32.95	6.7714E-04	8.63E-02	8.3598E+01	104.2	31.3
9	4.605	3.0671	2.0940E-03	81.06	72.55	6.7154E-04	1.92E-01	8.2906E+01	97.8	69.6
10	4.899	3.1188	2.1293E-03	68.04	89.31	6.8286E-04	2.32E-01	8.4303E+01	80.7	84.2
11	5.055	3.1302	2.1370E-03	39.17	89.72	6.8535E-04	2.32E-01	8.4611E+01	46.3	84.3
13	5.654	3.0862	2.1070E-03	6.996	100.4	6.7572E-04	2.64E-01	8.3422E+01	8.4	95.7
14	5.815	3.0354	2.0723E-03	4.46	103.5	6.6460E-04	2.76E-01	8.2049E+01	5.4	100.3
15	6.634	3.0853	2.1064E-03	0	111.4	6.7552E-04	2.92E-01	8.3398E+01	0.0	106.2
16	6.818	3.1378	2.1422E-03	0	105.9	6.8702E-04	2.73E-01	8.4817E+01	0.0	99.3
17	6.993	3.1100	2.1233E-03	0	106.7	6.8093E-04	2.78E-01	8.4065E+01	0.0	100.9
18	7.054	3.1146	2.1264E-03	0	111	6.8194E-04	2.89E-01	8.4190E+01	0.0	104.8
4.14									% of S	% 0f Ni
1	1.285	3.0884	2.1085E-03	78.3	0	6.7620E-04	0.00E+00	8.3481E+01	93.8	0.0
2	1.903	3.1161	2.1274E-03	89.22	0	6.8226E-04	0.00E+00	8.4230E+01	105.9	0.0
3	2.192	3.1006	2.1168E-03	81.13	0	6.7887E-04	0.00E+00	8.3811E+01	96.8	0.0
4	2.616	3.0949	2.1129E-03	88.58	0	6.7762E-04	0.00E+00	8.3657E+01	105.9	0.0
5	3.02	3.0784	2.1017E-03	83.74	6.821	6.7401E-04	1.79E-02	8.3211E+01	100.6	6.7
6	3.14	3.1117	2.1244E-03	88.25	24.25	6.8130E-04	6.31E-02	8.4111E+01	104.9	23.7
7	3.691	3.0932	2.1118E-03	86.97	49.7	6.7725E-04	1.30E-01	8.3611E+01	104.0	48.8
8	4.407	3.0354	2.0723E-03	87.76	76.52	6.6460E-04	2.04E-01	8.2049E+01	107.0	76.6
9	4.792	3.1031	2.1185E-03	78.51	89.85	6.7942E-04	2.35E-01	8.3879E+01	93.6	87.9
10	5.204	3.1145	2.1263E-03	60.22	98.36	6.8191E-04	2.56E-01	8.4187E+01	71.5	95.9
11	5.655	3.0985	2.1154E-03	28.36	99.7	6.7841E-04	2.61E-01	8.3754E+01	33.9	97.7
12	5.967	3.0919	2.1109E-03	12.31	100.3	6.7697E-04	2.63E-01	8.3576E+01	14.7	98.5
13	6.105	3.1069	2.1211E-03	2.813	101	6.8025E-04	2.63E-01	8.3982E+01	3.3	98.7
14	6.513	3.0879	2.1082E-03	0	102.4	6.7609E-04	2.69E-01	8.3468E+01	0.0	100.7
15	6.866	3.1209	2.1307E-03	0	104.1	6.8332E-04	2.70E-01	8.4360E+01	0.0	101.3
16	7.08	3.0943	2.1125E-03	0	103.1	6.7749E-04	2.70E-01	8.3641E+01	0.0	101.2
17	7.125	3.0877	2.1080E-03	0	102.5	6.7605E-04	2.69E-01	8.3463E+01	0.0	100.8
		3.0822	2.1043E-03	0	104.3	6.7484E-04	2.74E-01			
		3.1096	2.1230E-03	0	105.7	6.8084E-04	2.75E-01			

	3.0703	2.0962E-03	0	101.1	6.7224E-04	2.67E-01			

ICP-OES DATA FOR ANION ONLY EXTRACTIONS

			mg/g
[pyrrole] in stock	mol/l	0.01002	=
[pyridine] in stock	mol/l	0.0104	
[benzene] in stock	mol/l	0.0104	
mass of 10ml BuOH	mg	8100	
butanol density @25C	g/l	810	
chloroform density @25C	g/l	1464.73	

Sample	pH	mass of org	vlm of soln	amt of S in icp sample	amount of S in 2 ml	100%S		% of total S
Pyrrole		g	l	mg/kg	mol/l			
1	0.19		2.0000E-03	102.4	6.4140E-04	7.9185E+01		129.3
2	0.78		2.0000E-03	95.5	6.4140E-04	7.9185E+01		120.6
3	1.792	2.9826	2.0363E-03	87.47	6.5303E-04	8.0622E+01		108.5
4	2.006	2.9968	2.0460E-03	88.53	6.5614E-04	8.1005E+01		109.3
5	2.248	3.0559	2.0863E-03	90.25	6.6908E-04	8.2603E+01		109.3
6	2.45	2.8829	1.9682E-03	85.5	6.3121E-04	7.7927E+01		109.7
7	2.573	3.0981	2.1151E-03	91.48	6.7832E-04	8.3744E+01		109.2
8	2.822	3.1984	2.1836E-03	94.45	7.0028E-04	8.6455E+01		109.2
9	3.09	3.1111	2.1240E-03	91.09	6.8117E-04	8.4095E+01		108.3
10	3.482	3.1190	2.1294E-03	91.14	6.8290E-04	8.4309E+01		108.1
11	4.413	3.1055	2.1202E-03	67.47	6.7994E-04	8.3944E+01		80.4
12	4.67		2.0000E-03	50.6	6.4140E-04	7.9185E+01		63.9
13	5.16		2.0000E-03	14.3	6.4140E-04	7.9185E+01		18.1
14	5.4		2.0000E-03	7.5	6.4140E-04	7.9185E+01		9.5
15	5.6		2.0000E-03	1.7	6.4140E-04	7.9185E+01		2.1
16	6.03		2.0000E-03	0.7	6.4140E-04	7.9185E+01		0.9
17	6.67		2.0000E-03	0.008	6.4140E-04	7.9185E+01		0.0
Pyridine								% of S
1	1.802	3.1237	2.1326E-03	92.28	6.8393E-04	8.4436E+01		109.3
2	2.044	3.1363	2.1412E-03	91.5	6.8669E-04	8.4776E+01		107.9
3	2.29	3.1321	2.1383E-03	92.57	6.8577E-04	8.4663E+01		109.3
4	2.524	3.1273	2.1351E-03	91.01	6.8472E-04	8.4533E+01		107.7

5	2.924	3.1031	2.1185E-03	89.24	6.7942E-04	8.3879E+01	106.4
6	3.176	3.1582	2.1562E-03	93.46	6.9148E-04	8.5368E+01	109.5
7	3.294	3.1037	2.1190E-03	60.33	6.7955E-04	8.3895E+01	71.9
	4.049						106.1
	4.586						101.2
	4.799						91.3
8	4.886						77.11629512
	4.973						62.43339897
	5.069						52.67017698
9	5.098						46.35566449
10	5.212						36.20511988
11	7.522		0.0000E+00		0.0000E+00	0.0000E+00	2.1
12	7.85		0.0000E+00		0.0000E+00	0.0000E+00	2
13	7.903		0.0000E+00		0.0000E+00	0.0000E+00	1.6
Benzene							% of S
1	1.822	3.1214	2.1310E-03	97.07	6.8342E-04	8.4373E+01	115.0
2	2.042	3.1184	2.1290E-03	93.62	6.8277E-04	8.4292E+01	111.1
3	2.509	3.1190	2.1294E-03	92.09	6.8290E-04	8.4309E+01	109.2
4	2.907	3.1124	2.1249E-03	91.79	6.8145E-04	8.4130E+01	109.1
5	3.259	3.0936	2.1121E-03	92.56	6.7734E-04	8.3622E+01	110.7
7	5.087	3.1096	2.1230E-03	64.24	6.8084E-04	8.4054E+01	76.4
8	5.258						96.7
9	5.389						73.2
15	5.566						65.3
16	5.623						54.2
	5.706						45.1
	5.769						37.4
	5.789						32.73690756
	5.816						27.40787122
	7.54						0
	7.92						0

ICP-OES FOR EXTRACTION WITH 4.8 ALONE

Extraction with 4.8

pH	% of S
0.59	0.08
0.98	0.27
1.33	0.77
1.57	1.84
2.10	3.59
2.82	3.99
3.47	1.92
3.98	0.07
4.29	0.00
5.34	0.00
6.50	0.00
7.01	0.00